CHARLES UNIVERSITY IN PRAGUE

Faculty of Science

Ph.D. study program: Physiology

Mitochondria as a target for anti-cancer therapy by vitamin E analogues

Mgr. Katarína Kľučková

Ph.D. Thesis

Supervised by prof. Ing. Jiří Neužil, CSc

Institute of Biotechnology

Academy of Sciences of the Czech Republic

Praha, 2015

I hereby declare that I have written this thesis independently, and all the resources are employed and indicated. I further declare that I did not submit this thesis, or an essential part of it, to obtain other, or the same university degree.

Prague, March 2015 Katarína Kľučková

I would like to thank my supervisor J. Neužil for the guidance and support during my Ph.D. study as well as for creating friendly atmosphere in the laboratory. My sincere thanks also belongs to J. Rohlena for his exceptional help with the project. I also very much appreciated the collaboration and stimulating discussions with Z. Drahota and T. Mráček. I would also like to thank my colleagues from the Laboratory of Molecular Therapy for their help, useful discussions and advices.

KK

INDEX

ABSTRACT (EN)

Based on the promising results concerning the anti-cancer properties of redox-silent analogue vitamin E α-tocopheryl succinate (α-TOS), we prepared its mitochondrially targeted derivative MitoVES by attaching the positively charged triphenylphosphonium (TPP^+) tag to α-TOS molecule. We tested the hypothesis that 'sending' the drug directly to its cellular site of action, mitochondria, should enhance its anti-cancer properties, which would result in more effective anti-cancer agent while making it possible to reduce the effective concentration.

We provide evidence that, indeed, MitoVES is a highly effective anti-cancer compound, superior to untargeted α-TOS both *in vitro* and *in vivo*. We show that MitoVES exerts its anti-cancer effects by interfering with complex II (CII) activity specifically at the ubiquinone binding site (Q_p), where it blocks further electron transfer resulting in increased reactive oxygen species (ROS) production, which then leads to apoptosis induction via the intrinsic mitochondrial pathway, preferentially engaging the pro-apoptotic Bak protein causing mitochondrial membrane permeabilisation.

We further show that mitochondrial targeting on the basis of higher mitochondrial membrane potential (ΔΨ) is important for MitoVES pro-apoptotic activity. This feature endows the agent with selectivity for cancer cells, which have higher ΔΨ than normal cells, and as we found, high ΔΨ is also propensity of proliferating endothelial cells (ECs) in contrast to growth-arrested ECs. This provides MitoVES with yet another anti-cancer property, inhibition of angiogenesis in newly formed tumor.

Mutagenesis of CII Q_p site confirmed MitoVES interaction with this site and further corroborated the importance of ROS production for efficient cell death induction, as the Q_p site mutations conferred resistance to MitoVES treatment. This was reflected by less efficient inhibition of CII-derived respiration, lower ROS production and cell death. Interestingly, we found that another CII Q_p site inhibitor, TTFA, showed different efficiency in Q_p site inhibition than MitoVES, since the S68A mutant was more responsive to the drug than the wild-type cells and the other mutants. In this case, the potency of Q_p site inhibition again correlated with the extent of induced cell death. Surprisingly, we discovered that the high-affinity Q_p site inhibitor atpenin A5 did cause neither ROS generation nor cell death induction. We demonstrate that this is due to rapid accumulation of intracellular succinate, which is incompatible with ROS generation from CII.

Altogether, this work has established MitoVES as promising anti-cancer agent and defined mitochondrial CII as its target site. Moreover, CII Q_p site mutagenesis revealed a direct correlation between the efficacy of CII Q_p site inhibition, ensuing ROS production and the level of cell death induction, unless intracellular succinate is high.

ABSTRAKT (CZ)

Na základě slibných výsledků s protirakovinně působícím analogem vitaminu E bez redoxní aktivity α-tokoferyl sukcinátem (α-TOS) jsme připravili jeho mitochondriálně cílený derivát MitoVES, a to připojením skupiny TPP^+ k mateřské látce. Testovali jsme hypotézu, podle které by cílení látky přímo do jejího místa působení, mitochondrií, mělo zvýšit její protirakovinný účinek a vést k efektivnější protirakovinné látce s možností nižších účinných dávek.

Prokázali jsme, že MitoVES je vysoce efektivní protirakovinná látka, mnohonásobně účinnější než necílený α-TOS, a to *in vitro* i *in vivo*. Protirakovinné působení látky MitoVES je zajištěno jeho interakcí s komlexem II (CII) ve vazebném místě pro ubichinon (Q_p), čímž dojde k narušení funkce CII. MitoVES zde způsobí přerušení toku elektronů a následnou zvýšenou produkci reaktivních forem kyslíku (ROS), které poté indukují apoptózu. K té dochází mitochondriální drahou, a to preferenčně zapojením proapoptotického proteinu Bak, který způsobí permeabilizaci vnější mitochondriální membrány.

Z našich výsledků dále vyplývá, že pro apototickou funkci látky MitoVES je důležité jeho mitochondriální zacílení na základě vyššího mitochondriálního potenciálu ($\Delta\Psi$). Tato vlastnost zajišťuje, že MitoVES je selektivní pro rakovinné buňky, které mají vyšší $\Delta\Psi$ než buňky normální a také, jak jsme zjistili, proliferující endoteliální buňky disponují vyšším $\Delta\Psi$ než endoteliální buňky jejichž růst je zastaven. Z tohoto důvodu je MitoVES účinný také pro inhibici angiogeneze v rostoucím nádoru.

Mutageneze Q_p místa CII potvrdila interakci látky MitoVES s tímto místem a dále prokázala důležitost produkce ROS pro účinné vyvolání buněčné smrti, protože mutace v Q_p místě vedly k rezistenci k látce MitoVES. Toto se odrazilo v nižší účinnosti potlačení respirace přes CII, nižší produkci ROS a následné buněčné smrti. Zjistili jsme, že další inhibitor CII působící v Q_p místě, TTFA, inhibuje CII s jinou účinností než MitoVES, protože buňky s mutací S68A byly TTFA inhibovány více než ostatní mutanty a buňky bez mutace v Q_p místě. I v tomto případě účinnost inhibice CII korelovala s rozsahem buněčné smrti. Zajímavým poznatkem také je, že vysoce účinný inhibitor Q_p místa CII, atpenin A5, nevyvolal produkci ROS ani buněčnou smrt. Prokázali jsme, že toto je způsobeno rychlým nahromaděním sukcinátu, jenž zabraňuje produkci ROS z CII.

Tato práce ukázala, že MitoVES může být nadějným protirakovinným lékem a jako jeho cíl působení definovala mitochondriální CII. Dále, na základě studií s buňkami s mutacemi v Q_p místě CII byla zjištěna přímá korelace mezi účinností inhibice Q_p místa CII, následnou produkcí ROS a tím vyvolanou buněčnou smrtí za podmínek, kdy nedochází k nárůstu množství sukcinátu uvnitř buňky.

ABBREVIATIONS

ΔΨ	mitochondrial membrane potential
α-TOS	α-tocopheryl succinate
AIF	apoptosis-inducing factor
ADP	adenosine diphosphate
AMP	adenosine monophosphate
APL	acute promyelocytic leukemia
ATP	adenosine triphosphate
BH-3 domain	Bcl-2-homology-3 domain
BNE	blue native electrophoresis
CI	complex I, NADH-ubiquinone oxidoreductase
CII	complex II, succinate: ubiquinone oxidoreductase
CIII	complex III, ubiquinone-cytochrome c oxidoreductase
CIV	complex IV, cytochrome c oxidase
CV	complex V, ATP synthase
cyt c	cytochrome c
DHE	dihydroethidium
DR	death receptor
ETC	electron transport chain
$FADH_2$	reduced flavin adenine dinucleotide
FCCP	carbonyl cyanide-4-(trifluoromethoxy)phenylhydrazone
GPx	glutathione peroxiredoxin
GSH	glutathione
GTP	guanosine triphosphate
HIF	hypoxia-inducible factor
IMS	intramembrane space
JHMD	JmjC domain-containing histone demethylases
MAPK	mitogen-activated protein kinase
MIM	mitochondrial inner membrane
MitoVES	mitochondrially targeted vitamin E succinate
MOM	mitochondrial outer membrane

MOMP	mitochondrial outer membrane permeabilization
mtDNA	mitochondrial DNA
NADH	reduced nicotinamide adenine dinucleotide
NADPH	reduced nicotinamide adenine dinucleotide phosphate
NF-κB	nuclear factor-κB
OXPHOS	oxidative phosphorylation
P_i	inorganic phosphate
PCD	programmed cell death
PDK	pyruvate dehydrogenase kinase
PGL/PHEO	paraganglioma/pheochromocytoma
PHD	prolyl-hydroxylase
PP pathway	pentose phosphate pathway
Prx	peroxiredoxin
Q_p site	proximal ubiquinone binding site in complex II
RET	reverse electron transport
ROS	reactive oxygen species
SDH activity	succinate dehydrogenase activity
SMPs	small mitochondrial particles
SOD	superoxide dismutase
SQR	succinate quinone reductase activity
TCA cycle	tricarboxylic acid cycle
TET	ten-eleven translocation
TNF	tumour necrosis factor
TPP^+	triphenylphosphonium
TRAIL	tumour necrosis factor-related apoptosis-inducing ligand
TTFA	thenoyltrifluoroacetone
UbQ	ubiquinone
$UbQH_2$	reduced ubiquinone, ubiquinol
VDAC	voltage-dependent anion channel
VHL	von Hippel-Lindau

INTRODUCTION

MITOCHONDRIA

Mitochondria are small organelles that were observed in eukaryotic cells already in 1850s as small grains or thread like structures. The name mitochondria was used for the first time around the year 1898, coming from Greek words mitos - thread and chondros - grain. Already in 1913, German scientist Otto Warburg observed that mitochondria respire and in 1931 he was awarded Nobel Prize for the discovery and characterisation of mitochondrial respiratory complexes. Hans Krebs, who worked for some time in Warburg's laboratory as his assistant, was also awarded Nobel Prize for the discovery of tricarboxylic acid cycle (TCA, also known as Krebs cycle). Another Nobel Prize awarded breakthrough came in 1961, when British chemist Peter Mitchell proposed the missing link between mitochondrial respiration and energy production and described his chemiosmotic theory. Besides these ground-breaking milestone discoveries, mitochondrial role in energy production and metabolism includes β-oxidation of fatty acids and the urea cycle. These important discoveries firmly established mitochondrial role as the powerhouse of the cell. Metabolites generated in these catabolic reactions are precursors for biosynthetic pathways of various macromolecules such as lipids, carbohydrates, proteins and nucleotides. Further, generation of proteins that contain heme and porphyrin moieties also takes place in these organelles. Another discovery of paramount importance was made in 1963, being the first definitive evidence of DNA in mitochondria. This renewed the interest in the evolutionary origin of mitochondria. Today, the Endosymbiotic Theory of the origin of mitochondria is widely accepted, and their bacterial ancestor was traced to be related to α-proteobacteria [1].

Apart from already described biosynthetic and bioenergetic roles, mitochondria have many signalling functions [2], which became obvious during 1990s with the discoveries of mitochondrial release of cytochrome c during cell death [3] and mitochondrial reactive oxygen species (ROS) induced transcription, for example, during hypoxia [4].

Electron transport chain and oxidative phosphorylation

Electron transport chain (ETC) consists of four multiprotein complexes embedded in the mitochondrial inner membrane (MIM) (Fig.1). These are NADH-ubiquinone oxidoreductase, succinate: ubiquinone oxidoreductase, ubiquinone-cytochrome c oxidoreductase and cytochrome c oxidase, corresponding to complex I, II, III and IV (CI – CIV), respectively. These complexes acquire electrons from reduced

nicotinamid adenine dinucleotide (NADH) through CI or TCA cycle metabolite succinate via reduced flavin adenine dinucleotide ($FADH_2$) at CII, and transport them down the electric gradient through CIII to CIV, where they meet their final acceptor oxygen and reduce it to form water. CI, CIII and CIV function also as hydrogen proton (H^+) pumps. While the electrons are being transported, these three complexes simultaneously pump H^+ from mitochondrial matrix to the intramembrane space (IMS) and in this way create electrochemical gradient across the MIM in which energy is conserved. This energy is harvested by the fifth multimeric transmembrane complex (CV) with ATP synthase activity in a process of oxidative phosphorylation (OXPHOS). H^+ return back to mitochondrial matrix through CV and the energy from the H^+ gradient is used to create a chemical bond between inorganic phosphate (P_i) and adenosine diphosphate (ADP). In this way, energy stored in the adenosine triphosphate molecule (ATP) can be used where it is needed inside the cell.

The structure of individual complexes is created so that electrons can move within the complexes from places with lower potential to higher potential. This is sustained by the presence of certain cofactors like flavin adenine dinucleotide (FAD), various Fe-S centers and cytochromes, all of them organised in the direction of increasing potential. The electron transport between CI→CIII and CII→CIII is mediated by membrane soluble electron carrier ubiquinone (UbQ), which transports 2 electrons at a time, and between CIII→CIV cytochrome c (cyt c) transporting one electron at a time. For every 2 electrons extracted from NADH at CI, 6 H^+ are pumped to the IMS by CI, CIII and CIV, and they can be used for synthesis of 2 molecules of ATP at CV. In case that electrons are supplied from $FADH_2$ via CII, which does not span the IMM and transport H^+ to the IMS, only CIII and CIV pump 2 H^+ each, which lowers the ATP yield accordingly.

Considering that OXPHOS is fueled by the NADH via CI and succinate via CII, its function is critically dependent on the TCA cycle, a complex system of reactions in the mitochondrial matrix in which pyruvate imported into mitochondria from the glycolytic pathway is degraded, producing reduced NADH to fuel CI, and a GTP molecule. Succinate is produced during TCA cycle as an intermediate metabolite from α-ketoglutarate, and is converted to fumarate by the action of CII. The electrons extracted from succinate in the TCA cycle are channelled down the ETC to fuel ATP synthesis. Therefore, CII is common to both processes, i.e. the TCA cycle and the ETC.

To date, three models for organisation of the ETC have been proposed [5, 6]. The ‘fluid’ model describes individual complexes as randomly moving and colliding entities within the MIM, interconnected by the Q and cyt c mobile carriers. In the ‘solid’ model, respiratory complexes and mobile carriers are organised in supramolecular structures termed respirasomes. A very convincing support for this model was provided by Acin-Perez and colleagues, who were able to separate various respiratory supercomplexes by the technique of blue native electrophoresis (BNE) and showed that some

of them correspond to true respirasomes as they consumed oxygen when supplemented with NADH or succinate respiration substrates [7]. However, a third model has been proposed recently, involving dynamic adjustments of the supercomplex assembly [6]. Here the authors demonstrate existence of separate electron routes from NADH and $FADH_2$ substrates, which might enable cells to adapt to alterations in available carbon sources [6].

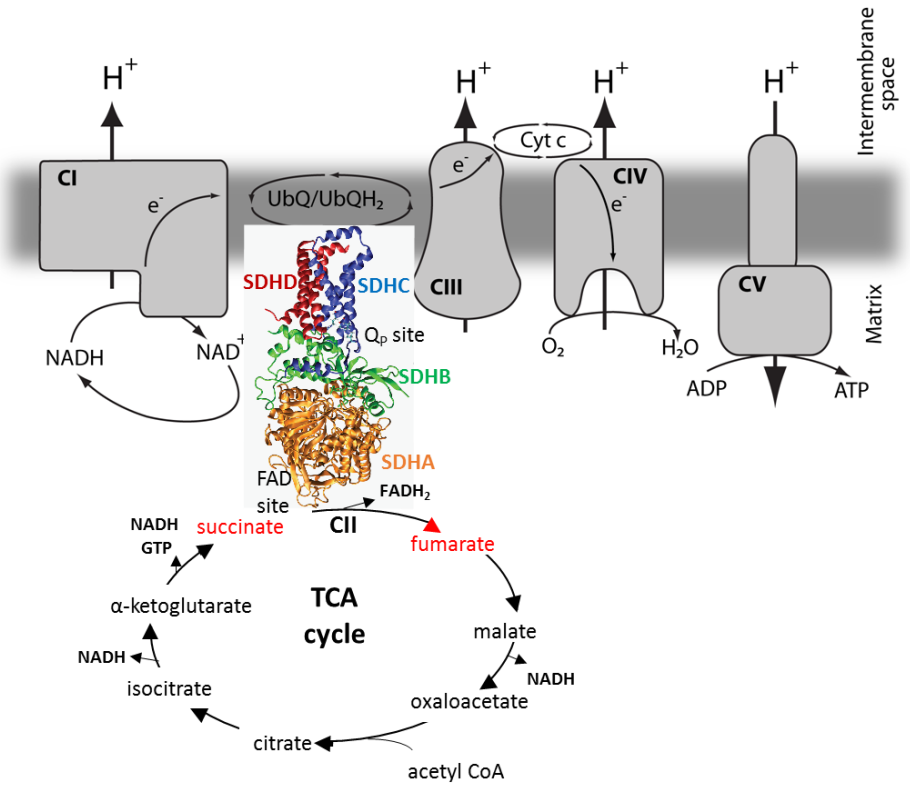

Fig. 1 Organisation of electron transport chain (ETC) and oxidative phosphorylation (OXPHOS) with tricarboxylic acid (TCA) cycle

CII (shown in colour) links both processes, OXPHOS in the MIM and TCA in mitochondrial matrix. Individual CII subunits are depicted in different colours in the CII protein structure. The reaction catalyzed by CII is shown in red. See text for details. Adapted from reference [95].

Complex II (CII)

As already mentioned, CII serves quite an exceptional role inside mitochondria, since it directly links OXPHOS with the TCA cycle without NADH used as intermediary (Fig1.). In contrast to the other OXPHOS complexes, CII is small and comprises only four different subunits (SDHA-D), which are all encoded in the nuclear DNA. All other OXPHOS complexes possess at least one subunit that is encoded in mitochondrial DNA (mtDNA). SDHA and SDHB subunits are in the mitochondrial matrix and are

anchored to the MIM by the other two subunits, SDHC and SDHD, which are buried in the MIM and comprise two UbQ-binding sites (Q sites) [8]. The largest subunit is the 70kDa SDHA and, together with the 30kDa SDHB, is responsible for the succinate dehydrogenase activity (SDH) of the enzyme, when SDHA accepts electrons from succinate by its flavin prosthetic group (FAD) at the dicarboxylate-binding site, and these electrons are then funneled through three iron sulphur centres in the SDHB subunit to the Q sites in SDHC/SDHD, where they reduce UbQ to $UbQH_2$ (ubiquinol). Of the two Q sites found in the crystal structure of porcine CII [8], only the proximal (Q_p) site closer to the mitochondrial matrix appears to be functional, whereas the distal site may be a non-functional pseudosite [9]. Until now, two assembly factors for CII have been identified; SDHAF1 is responsible for insertion of iron-sulphur centers in SDHB [10] and SDH5 or SDHAF2 is required for incorporation of the FAD cofactor in the SDHA subunit [11]. The assembly and enzymatic activity of CII is also probably dependent on the presence of the specific mitochondrial phospholipid cardiolipin [12]. CII activity can be further modulated by mutual interactions between complexes of the ETC [6] and directly via ROS-triggered phosphorylation of the SDHA subunit by Fgr tyrosine-kinase [13]. Interestingly, recent research shows that the SDHC subunit of CII might have another function besides its role in bioenergetics. In a yeast model, SDHC acts in the biogenesis and assembly of the TIMM22 protein translocase complex of the MIM, to which it is recruited by interaction with the Tim18 protein homologous to SDHD [14, 15].

CII couples two distinct chemical reactions in two separate active sites: oxidation of succinate, which is catalysed in the matrix domain (the SDH activity), and the reduction of UbQ, catalysed in the membrane domain (the succinate quinone reductase, SQR activity). Though these two active sites are structurally separated, chemical reactions between them are coupled, since electrons extracted from succinate that are the product of the SDH reaction become the substrate of the second reaction where they reduce UbQ to $UbQH_2$ [16]. CII's SDH and SQR activities can be dissociated *in vitro* and separately assessed in colorimetric enzymatic assays using different artificial electron acceptors [17]. If this happens also *in vivo* is questionable. The dissociation of the two CII activities has been suggested to be involved in CII-mediated cell death, when it was found that during cell death the SQR activity was specifically impaired without affecting the SDH activity [18]. Further, similar situation was observed in the absence of cardiolipin, which resulted in a defect of CII assembly and lack of SQR, but robust SDH activity. This was first shown in experiments performed with CII enzymes reconstituted into nanoscale lipid bilayers [12], but later also shown to be true in cell culture experiments [19]. On the other hand, SDH activity seems to be impaired in rare types of cancers, where mutations in CII membrane subunits result in dysfunctional CII [20].

Reactive oxygen species (ROS)

Mitochondria are considered highly significant, if not the main, source of ROS in the cell [21-23]. There are at least 10 known sites capable of ROS generation in mitochondria, including the ETC. Other important sites are the electron transfer flavoprotein: UbQ oxidoreductase on the matrix surface of the MIM, glycerol-3-phosphate dehydrogenase on the outer surface of the MIM, dihydrolipoyl dehydrogenase-containing enzymes such as α-ketoglutarate dehydrogenase and pyruvate dehydrogenase, and NADH-UbQ oxidoreductases other than CI [21, 22]. The term free radicals and ROS are very often used in an interchangeable manner. A free radical is any atom or molecule with an unpaired electron in its outermost shell, and the term ROS is usually used to describe any oxygen-containing molecule capable of initiating oxidative reactions [22]. ROS include the superoxide anion, hydrogen peroxide, hydroxyl radical, peroxyl radical, alkoxyl radical, hydroperoxyl radical, hypochlorous acid and singlet oxygen [22].

Superoxide is the primary ROS in mitochondria. Due to its negative charge, superoxide cannot pass across the mitochondrial membrane, although it has been shown that the voltage-dependent anion channel (VDAC) can facilitate its release from mitochondria to the cytosol [24]. However, superoxide is relatively reactive and, inside the mitochondria, rapidly converted to hydrogen peroxide by mitochondrial superoxide dismutase or superoxide dismutase-2 (SOD2), after which it can easily cross the mitochondrial membranes [21].

ROS are believed to be responsible for oxidative damage in many pathologies including neurodegenerative diseases and cancer [25], as well as in the aging process [26]. Mitochondrial theory of aging proposes, that mitochondria with its ETC as a major ROS producer are extremely vulnerable to oxidative damage because of the close proximity of mtDNA, which codes for essential genes of the ETC components. Faulty products of damaged mtDNA would in turn lead to even higher ROS production, which will accumulate with aging [27]. Numerous correlative data have been gathered in support to this half-century old hypothesis [26]. However, in disagreement with a direct role of oxidative stress in the aging process, a model of mouse which accumulated mtDNA mutations in a linear manner was utilized to demonstrate that these substantial mtDNA mutations, though indeed leading to premature aging phenotypes, did not affect the amount of ROS produced in tissues from these mice [28].

Nevertheless, besides the negative aspects of their action, ROS participate in essential functions including killing of bacteria by cells of the immune system and redox signalling to the cytosol and nucleus, in particular important in promotion of mitotic signalling in cancer [29].

Because of their deleterious but also signalling effects, ROS production needs to be tightly controlled and this is ensured by highly elaborated antioxidant defense system. This includes several enzymes specialised in the removal of superoxide, hydrogen peroxide and organic hydroperoxides, in most cases

ubiquitously present in all mammalian cells (though their levels might exhibit some tissue and species specifity) [23]. As already mentioned, SOD2 converts mitochondrial superoxide to hydrogen peroxide, which is then eliminated by the action of various peroxiredoxins (Prx3 and Prx5 in mitochondria), glutathione peroxidases (GPx1 and GPx4 in mitochondria) and catalase (in peroxisomes) [23, 30]. There are three known isoforms of SOD, which differ in their spatial localisation inside the cell. SOD1 is cytosolic and also found in the IMS, SOD2 resides in mitochondrial matrix and SOD3 is tethered to the extracellular matrix [30]. Most of these enzymes use nicotinamide adenine dinucleotide phosphate (NADPH) or glutathione (GSH) as reducing equivalents which, particularly in mitochondria reach milimolar concentrations [23]. Because of this, short bursts of ROS would be expected to be neutralised effectively but the prolonged exposure to high levels of ROS will depend on the supply of NADPH and GSH from the corresponding regenerating reactions [23]. Another, particularly interesting system capable of superoxide scavenging is cyt c plus CIV. Cyt c can be alternatively reduced by the respiratory chain or superoxide and oxidised by CIV, and this reaction then supports production of ATP due to contribution to the H^+ gradient [23].

ROS implication in cancer will be discussed in greater detail later. In the next part, special focus is put on the role of CII in ROS production, and then ROS involvement in the context of programmed cell death is discussed.

ROS production from CII

Until recently, ROS production from CII has been very much underestimated (or dismissed) with most studies on ROS-producing capabilities of CI and CIII [21, 22]. Although CII's role in high ROS production was recognized and appreciated very soon, the contribution of CII was assumed only to extract electrons from succinate and transfer them to the UbQ pool. These then fuel proton-pumping activities of CIII and CIV and serve to establish high H^+ gradient across the MIM. After the system becomes highly reduced, a 'backflow' of electrons from the reduced UbQ pool to CI results in high ROS production from the matrix-exposed flavin site in CI. This situation is referred to as reverse electron transport (RET) and occurs in the presence of high levels of succinate as an OXPHOS substrate. It is inhibited by the inhibitor of the Q site of CI rotenone. RET is known to produce the highest rates of ROS in isolated mitochondria [21, 22] and recently has been shown to occur *in vivo* during ischemia-reperfusion injury in murine models of heart-attack and stroke [31].

Functional studies of OXPHOS complexes, including respirometry measurements and assessment of ROS production, are usually performed at highly saturating substrate concentrations, meaning that excessive and non-physiological concentrations of succinate are added (5-10 mM) [32]. This might be the reason, why the CII capability of ROS generation has been considered negligible in comparison to

the levels of ROS observed to be formed at CI and CIII. Very few studies have been performed in the presence of low succinate either with bacterial CII containing membranes [33], isolated rat mitochondria [34] or bovine sub-mitochondrial particles (SMPs) [35]; they demonstrate that CII generates ROS directly from its dicarboxylate succinate-binding site in the SDHA subunit, and this is prevented by addition of malonate, an inhibitor of this site. In the case of the *E.coli* and SMPs studies, ROS production peaked at 100 μM succinate, while in rat mitochondria 400 μM succinate was found to be optimal. As stated by the authors, at this concentration the supply of electrons from succinate was high enough to reduce the system and low enough not to interfere with ROS generation. In *E.coli* CII produced exclusively superoxide [33] while in the eukaryotic models, superoxide and hydrogen peroxide production was detected, the latter at higher amounts than the former [34, 35]. Importantly, it was shown in the study with rat mitochondria that when CI and CIII are inhibited, CII-produced ROS approach or exceed the maximum rates observed for CI or CIII under conditions, which the authors found to maximise ROS production from these two sites [34]. This study proposed that the higher succinate concentration at the active dicarboxylate site in SDHA can hinder access of oxygen and thus suppress ROS formation from $FADH_2$. This model was further elaborated in the study with SMPs, where the authors definitively confirmed that ROS are produced from CII only if the dicarboxylate site in SDHA is unoccupied, as was shown not only for the CII substrate succinate but also for other TCA cycle dicarboxylates that structurally resemble succinate including fumarate, oxaloacetate, malate and, to lesser level citrate [35] (Fig.2). Importantly, this study revealed that the redox state of the UbQ pool and the activity of other OXPHOS complexes had very little effect on ROS generation induced by the highly specific Q-site inhibitor atpenin A5 [35, 36].

The possibility of CII contribution to ROS generation has been further studied in several models of CII dysfunction due to mutations in genes coding for its subunits, implicating CII in oxidative stress in various experimental models such as the nematode *C. elegans* [37], the yeast *S.cerevisae* [38, 39], the plant *Arabidopsis* [40] and mammalian cells [41-43]. The *mev-1* mutant of *C.elegans* has a mutation in a subunit of CII, which is homologous to human SDHC, and impaires its ability to catalyse the electron transport. This results in hypersensitivity to increased oxygen levels, which negatively affect its lifespan [37]. The authors were able to reproduce the ROS-overproducing phenotype of this mutation in the mouse fibroblast NIH3T3 cell line [43] and also in a conditional transgenic mouse [44]. Reports on increased oxidative stress in the Chinese hamster fibroblast cell line B9 with a mutation in the *SDHC* gene resulting in premature translation termination [45] showed contrasting results [41, 46]. In the genetic screen for an *Arabidopsis* mutant lacking early stress-responsive gene GSTF8, a CII mutant with significantly reduced CII activity was isolated. This mutant showed increased susceptibility to specific pathogens and had problems to mount appropriate ROS-mediated defense responses [40].

A role for CII in ROS generation in melanoma cells was very recently described. Here the authors found a positive correlation between CII activity and melanin pigment content and suggested that hyperpigmentation could be a protective mechanism in response to CII-mediated ROS production [47]. Increased CII activity and expression was found to be increased and associated with higher ROS production also in a rat model of heart failure, but it was concluded that these ROS were released from CIII [48].

CII-derived ROS production is further suspected to occur in specific cancer syndromes due to inactivating mutations in CII subunits [49] and has been documented in studies on anti-cancer properties of CII inhibitors [50].

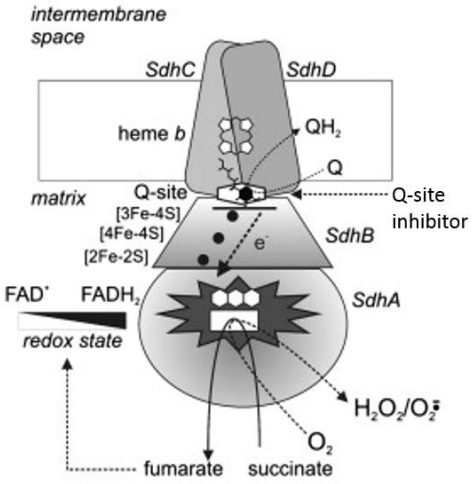

Fig. 2 Proposed model for reactive oxygen species (ROS) production from complex II (CII).

SdhA–D indicate the 4 subunits of complex II. The relative positions of the prosthetic groups and functional sites are indicated as black circles ([Fe-S] clusters), a tricyclic structure (FAD), a stretched white hexagon (Q_p site) and a white rectangle (dicarboxylate binding site). Upon binding of inhibitor to the Q_p site, transfer of electrons is blocked and upstream redox-groups including the FAD become reduced. ROS can be only produced from $FADH_2$ if the dicarbocylate site is unoccupied. Adapted from reference [35].

Programmed cell death (PCD)

According to the Nomenclature Committee on Cell Death, there are two criteria on how to identify dead cells [51]. These are cells that exhibit considerable plasma membrane permeabilisation and have undergone complete fragmentation. Previously, the engulfment of cell by professional phagocytes or other cells with phagocytic activity was included as the third criterion, but recently it was recognised to be faulty, as it was reported that engulfed cells can be under some circumstances released from phagosomes as they preserve their viability [51]. Cell death can be either accidental or regulated. Accidental cell death is caused by severe physicochemical or mechanical insults, which do not involve a specific molecular machinery and cannot be prevented or manipulated. Regulated cell death, on the contrary, involves a genetically encoded molecular machinery, and its progress can be modulated by means of pharmacologic and/or genetic interventions. Regulated cell death that occurs as part of a

development or to preserve physiologic tissue homeostasis is referred to as PCD and is often initiated in the context of unsuccessful responses to perturbations of intracellular or extracellular homeostasis [51].

A predominant form of PCD is apoptosis, which is necessary for proper development and tissue homeostasis in all multicellular organisms and its deregulation contributes to various diseases such as neurodegeneration and cancer [29]. Apoptosis can be initiated by intracellular or extracellular stimuli and, accordingly we distinguish intrinsic and extrinsic apoptotic pathways (Fig. 3) [51].

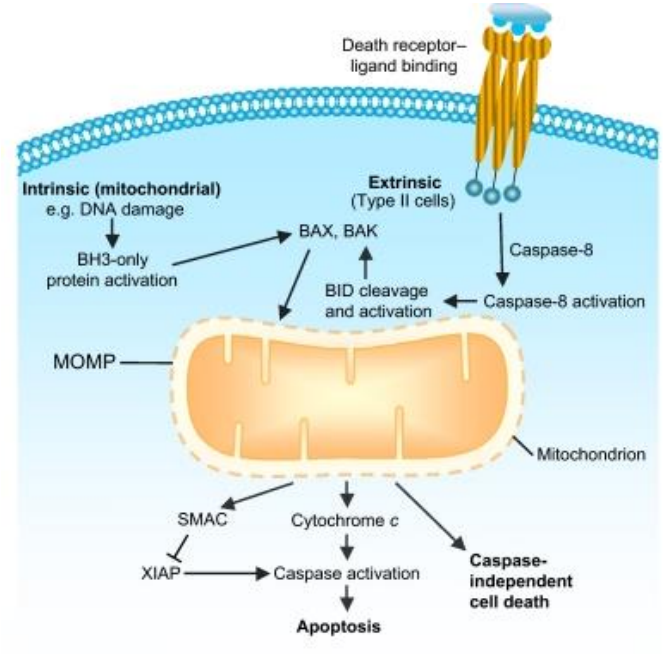

Fig. 3 Mitochondrial apoptotic pathways

In the intrinsic pathway of apoptosis, pro-apoptotic stimuli activate BH3-only proteins that then activate Bak and Bax, which cause mitochondrial outer membrane permeabilisation (MOMP), leading to release of proteins from the intermembrane space , including cytochrome *c* and Smac, which then activate specific proteases caspases. In the extrinsic pathway, activation of death receptors leads to activation of the initiator caspase-8, which then cleaves and activates the BH3-only protein Bid, leading to Bax and Bak activation and MOMP. Adapted from reference [29].

Mitochondria actively participate in apoptotic program in both cases, particularly in the intrinsic pathway, where they are required to mount the proper downstream response [29]. In this pathway, apoptotic stimuli such as DNA damage or viral infection lead to activation of Bid and Bim, activator pro-apoptotic Bcl-2-homology-3 (BH3) domain-only proteins from a large Bcl-2 family of apoptosis-regulating proteins, that, in turn, activate multi-domain pro-apoptotic members from the Bcl-2 family, Bax and Bak, which subsequently oligomerise and form pores in the mitochondrial outer membrane (MOM) [52, 53]. This results in mitochondrial outer membrane permeabilisation (MOMP) leading to release of proteins from IMS, including cyt c and Smac, which then activate specific proteases called caspases. Smac activates caspases indirectly by inhibiting XIAP family of caspase inhibitors. Cyt c, once in the cytosol, activates the initiator caspase-9 by way of forming a complex known as apoptosome, which then cleaves and activates effector caspases [29, 52].

The extrinsic apoptotic pathway is induced by death receptor-ligand binding at cells surface and proceeds via activation of the initiator caspase-8 directly at the intracellular part of the receptor-ligand complex [29]. Activated caspase-8 can then either activate effector caspases directly or it requires

mitochondria for effective apoptosis execution. In this scenario, caspase-8 cleaves and activates the pro-apoptotic BH3-only protein Bid which, in turn, activates Bax and Bak as in the case of the intrinsic pathway [29].

The function of pro-apoptotic Bcl-2 proteins is held in check by group of anti-apoptotic proteins of the same family, which directly interact with and inhibit the pro-apoptotic members. Bcl-2 family proteins share up to four Bcl-2 homology domains (BH1-4) in their structure, with BH3 domain being the domain shared by all members and making their mutual interaction possible [52]. The multi-domain pro-survival anti-apoptotic members are Bcl-2 itself, plus Bcl-x_L, Bcl-w, A1 and Mcl1 [51, 52]. Pro-apoptotic BH3 only proteins include Bim and Bid proteins, which activate Bax/Bak directly, and sensitizer BH3-only proteins such as Puma, Bad, Bmf, Bik and Noxa, that inhibit the pro-survival Bcl-2 family proteins, but cannot activate Bax and Bak directly [52]. However, a possibility that Puma, Bmf and Noxa can also directly activate Bax/Bak might exist [54]. Pro-apoptotic Bax and Bak are indispensable for MOMP formation in the mitochondria-mediated intrinsic pathway, as cells doubly deficient in Bax and Bak are resistant to multiple apoptotic stimuli acting through disruption of mitochondrial function, such as staurosporine, UV irradiation and the endoplasmic reticulum stress [55]. Although under some circumstances MOMP can be involved in non-lethal signalling function [29], its formation is generally considered as a point of no return, which results in cell death commitment via release of multiple caspase-dependent and -independent death effectors and the loss of essential mitochondrial functions [56].

Caspase-independent apoptotic proteins released from the IMS during MOMP include the apoptosis-inducing factor (AIF), serine protease Omi/Htra2 and endonuclease EndoG. AIF and EndoG subsequently translocate from the cytosol to the nucleus, where they cause DNA fragmentation and condensation, resulting in typical DNA morphology observed in TUNEL assays used for apoptosis detection. Another key apoptotic phenotype is exposure of phosphatidyl serine (PS) on the outer surface of plasma membrane, which was found to precede the nuclear changes and the loss of membrane integrity [57] and which constitutes a general signal for recognition of apoptotic cells by phagocytes being sufficient as an “eat me” signal [57, 58]. Recently, the phospholipid flippase responsible for PS exposure was recognised as a direct caspase substrate during apoptosis [58]. The notion of PS externalisation also resulted in establishment of a practical assay to detect apoptosis, based on affinity of annexin V for PS, evaluated by flow cytometry [57, 59].

Loss of mitochondrial function during apoptosis is usually linked to loss of mitochondrial transmembrane potential ($\Delta\Psi$) and dysfunction of the ETC and OXPHOS with increased ROS production. Direct link between these three processes was shown to be mediated by activation of caspase-3, which disrupted CI and CII function and electron transport with ensuing loss of $\Delta\Psi$ and

increased ROS generation. In the case of CI, the 75kDa NDUFS1 subunit was identified to be cleaved by caspase-3 [60, 61]. Inhibition of CI function during apoptosis was also shown in the case of tumour necrosis factor (TNF)-induced apoptosis [62]. However, here the authors observed CI inhibition prior to cyt c release and mitochondrial permeabilisation and they concluded that TNF-induced CI inhibition was the cause of the cyt c release and subsequent caspase activation and mitochondrial permeabilisation [62]. A model for specific role of CII during apoptosis was suggested by the Grimm group. First, they found that CII-deficient cells became resistant to many apoptosis-inducing cytostatic drugs including cisplatin, menadione, etoposide, arsenic trioxide and doxorubicin [63]. In the follow-up work they showed that during apoptosis, CII disintegrates in a specific way, so that the SDHA plus SDHB subunits dissociate from the membrane anchor, and this sub-complex retaining its SDH activity is then responsible for increased ROS generation, as the electrons cannot be transferred to the Q site comprised in the SDHC/SDHD membrane subunits. This would be consistent with partial inhibition of CII's SQR activity without any impairment of the SDH activity as observed in their model [18]. This specific CII disintegration was ascribed to pH changes and excessive calcium influx into mitochondria during apoptosis [18, 19]. Mitochondrial ROS production has been shown to promote apoptosis through oxidation of the mitochondria-specific phospholipid cardiolipin that, upon oxidation, loses its affinity for cyt c and its oxidation products (mostly cardiolipin hydroperoxides) that accumulate in mitochondria lead to the release of pro-apoptotic factors into the cytosol [64]. Another direct role of ROS in apoptosis has been provided via their effect on Bax activation involving oxidation of its cysteine residues, which resulted in conformational change and Bax oligomerisation for permeabilisation of mitochondria [65, 66].

A study performed on transmitochondrial cybrid cells harboring diverse pathogenic mtDNA mutations affecting different components of ETC and OXPHOS showed that cells that cannot generate electron flow but still possess the respiratory complexes were protected against apoptosis induced by staurosporine and etoposide, known to engage the mitochondrial apoptotic pathway. On the contrary, cells with a partial reduction in electron flow showed increased apoptosis, and cells lacking the respiratory chain (ρ^0 cells) were resistant [67]. Interestingly, the authors also observed that cells defective in respiratory chain components and cells with impaired electron flow showed dysregulated expression of mitochondrial levels of anti-apoptotic proteins [67]. Overal, all these studies implicate mitochondrial ETC and OXPHOS in apoptosis modulation and propagation.

Owing to the crosstalk between metabolism and cell death, existence of several "metabolic checkpoints" to regulate cell death has been suggested recently [68]. These were proposed to react to metabolic imbalance such as alterations in the ratios of ATP/ADP, acetyl-coenzyme A/coenzyme A, NAD^+/NADH, $NADP^+$/NADPH, as well as to ROS amounts. As the first reaction, the cells induce an

adaptive response to re-establish cellular homeostasis; however in case these metabolic perturbations are too severe or persistent, metabolic checkpoints then initiate cell death [68].

Besides apoptosis, mitochondria might have a role in other forms of PCD such as autophagic and necroptotic cellular demise. Autophagy functions as an adaptive response to stressful conditions including nutrient depletion when cells form cytoplasmic, double-layered membranes known as phagophores, which mature into autophagosomes and engulf long-lived proteins and damaged cytoplasmic organelles to provide building blocks and cellular energy for biosynthesis [29]. However, under conditions of extreme or prolonged stress, cells undergo autophagic cell death [29]. Necroptosis is a regulated form of necrotic cell death pathway, which in contrast to apoptosis and autophagy was previously thought to be an uncontrolled accidental form of cell death. However, it is now established that necroptosis is also a form of PCD initiated by death receptors and proceeding via controlled series of events [51, 69]. Mitochondrial implication in both described cell death modes was proposed since they share certain proteins and signalling pathways ultimately converging on mitochondrial function/dysfunction [29, 69, 70], though recently mitochondrial role in necroptosis was challenged [71]. Interestingly, a selective autophagic degradation of mitochondria has been described and termed mitophagy. This process mediates clearance of damaged mitochondria to maintain a healthy population of mitochondria and is involved in the removal of mitochondria from maturing erythrocytes and eliminating sperm mitochondria after fertilisation [72].

CANCER

As originally proposed and defined by Hanahan and Weinberg [73, 74], cancer is characterized by eight major hallmarks. These are sustaining proliferative signalling, evading growth suppressors, resisting cell death, enabling replicative immortality, inducing angiogenesis, activating evasion and metastasis, evading immune destruction and reprogramming of energy metabolism. First six of them were recognized in 2000 [73], last two were added decade later [74]. Besides the two new hallmarks, additional so called ‘enabling characteristics’ crucial to the acquisition of the hallmarks were included in the list: tumour-promoting inflammation and genome instability and mutations [74].

Altered metabolism in cancer cells

Without any doubt, the most and longest studied metabolic alteration in cancer cells is the upregulation of the glycolytic pathway. Increased glycolysis in tumour cells was first observed by Otto Warburg and at first ascribed to defects in mitochondrial respiration and energy production machinery in cancer, because high glycolytic rates were observed even in the presence of high levels of oxygen. This high glycolysis and lactate production under aerobic conditions was termed Warburg effect [75]. Nowadays,

it is well recognized that Warburg effect arises not because of damaged respiration in cancer cells but a damage to the regulation of the glycolytic pathway [75, 76].

Cancer cells increase expression of glucose transporters, which enable glucose uptake into the cell, and upregulate expression of most enzymes participating in glycolysis. Further, the mitochondrial respiration is often suppressed to certain level. Upregulation of glycolysis confers cancer progression at various levels. On one hand, it supplies energy in the form of ATP, but what is even more important, increased glucose flux through glycolysis and its diversion towards the pentose phosphate (PP) pathway provides important building blocks for protein and nucleotide biosynthesis needed for rapid cell division [77]. Cancer cells demonstrate increased glutamine uptake and utilization, which is used for non-essential amino acids synthesis and/or to fuel the TCA cycle through α-ketoglutarate. α-Ketoglutarate can then support the forward TCA cycle reaction or can be converted to citrate in a process known as reductive carboxylation and exported to the cytosol to support lipid synthesis via acetyl-CoA or amino acid synthesis via oxaloacetate production [77-79]. The PP pathway also results in the production of NADPH, which is essential for various biosynthetic reactions such as fatty acid synthesis, and contributes to proper redox control. The described diversions from normal metabolism are outcomes of regulation by various oncogenes and tumour-suppressor genes that work as transcription factors, including Myc and hypoxia-inducible factor (HIF) oncogenes and the tumour-suppresor p53 [78]. These metabolic alterations allow cancer cells to survive also under hypoxic conditions, which are encountered regularly as tumour mass grows and the oxygen in the tumour environment becomes scarce. Under these conditions, cancer cells rely particularly on increased glycolysis with the PP pathway and TCA cycle replenishment by way of reductive carboxylation and increased glutamine uptake [79]. Though some of these metabolic pathways present normal physiological response to lower oxygen levels, in cancer cells these can be activated constitutively and contribute to enhanced tumour survival and growth. Also, these alterations make them addicted to increased uptake of glucose/glutamine and vulnerable to their interruptions, and exploited for cancer therapy [80-82].

Increased metabolic flux is accompanied by an increase in oxidative intermediates and altered redox environment inside the cell with elevated ROS levels. On one hand, high ROS levels can be advantageous for cancer cells as they contribute to genomic instability, metastatic behavior, HIF stabilization, Akt activation and stimulation of proliferation [25]. On the other hand, excessive oxidative stress can induce oxidative damage and cell death, and be selectively targeted as anti-cancer intervention because of high ROS levels in cancer cells [25, 78, 83, 84]. Very recently, an interesting and readily available possibility of how to treat cancer by way of increasing ROS production was suggested by Harris and colleagues. They discovered that combined inhibition of GSH and the thioredoxin anti-

oxidant pathways by inhibitors that are already used in the clinic results in cancer cell death and limits tumour initiation and progression *in vitro* and *in vivo* [85].

Cell death evasion in cancer cells

Cancer cells possess large variety of strategies how to limit or evade apoptosis. Probably the most prominent one is the imbalance in the level of Bcl-2-family proteins in favor of anti-apoptotic proteins and deregulation of the DNA-damage sensor p53 pathway [74]. The Bcl-2 protein was first described in the chromosomal translocations in follicular B-lymphoma cancer cells, from which its name is derived. The resulting fusion gene is deregulated and leads to over-expression of Bcl-2, which is classified as an oncogene. Other anti-apoptotic Bcl-2 family members are also known to be over-expressed in a wide variety of cancers contributing to tumour progression and resistance to anti-cancer therapy [86]. This can occur via oncogenic signalling involving the PI3K/Akt pathway, Ras/Raf/mitogen-activated protein kinase (MAPK) pathway or the transcription factor Myc [86]. The tumour-suppressor p53, which is often found 'lost' in tumours, induces apoptosis by transcriptional induction of the pro-apoptotic Bax protein and the BH3-only proteins Puma and Noxa or via direct activation of Bax/Bak as well as inhibition of the anti-apoptotic Bcl-x_L and Bcl-2 proteins [83, 86].

Another way, how cancer cells can acquire resistance to cell death is via alteration of their metabolism. In this context, upregulation of the glycolytic pathway seems to play role in their resistance to mitochondrial membrane permeabilisation, which is one of the critical events in apoptosis. Cancer cells upregulate hexokinase that binds directly to mitochondria, where it associates with VDAC. This interaction facilitates immediate glucose phosphorylation by hexokinase for its utilization in glycolysis and also keeps VDAC in conformation that counteracts its proposed role in mitochondrial permeabilisation [80, 83]. The shift from mitochondrial metabolism towards glycolysis might be responsible for mitochondrial hyperpolarization, which has been observed in cancer but not in non-cancerous cells [87]. High $\Delta\Psi$ in malignant cells has been shown to confer apoptosis resistance [87, 88], and this phenotype was reversed by the pyruvate dehydrogenase kinase (PDK) inhibitor dichloroacetate (DCA), which redirected metabolism from glycolysis to mitochondria [87].

CII in cancer

SDHA, SDHB, SDHC, SDHD plus the CII assembly factor SDHAF2 have been found mutated in certain hereditary cancer types of neuroendocrine origin, in particular paraganglioma and pheochromocytoma (PGL/PHEO) [49]. Besides mutations in CII genes, mutations in other distinct genes are associates with PGL/PHEO including kinase receptor and signalling regulators RET and NF1, the transcription factor Max, the *TMEM127* gene involved in endosomal signalling as well as regulators

of the response to hypoxia, such as von Hippel-Lindau (VHL) and HIF2A. PGL/PHEO carry the highest degree of heritability (around 40%) of all human tumours. These neoplasias are predominantly benign, but approximately 10-15% of them can become metastatic [89]. In addition to PGL/PHEO, mutations in CII genes were identified in gastrointestinal stromal tumours, renal tumours, thyroid tumours, testicular seminoma and neuroblastomas [49].

The molecular mechanism underlying tumorigenicity of CII mutations is still a matter of debate and various possibilities have been proposed. A predominant feature of these tumours is diminished expression of CII subunits and reduction in CII activity. There are two possible scenarios that could lead to tumour transformation due to malfunctional CII: succinate accumulation and an increase in ROS. Both options are supported by published studies, but the role of high succinate seems more probable also because it has strong support from robust clinical data [90, 91], while ROS detection in CII-dysfunctional cells has been somewhat controversial [89]. Increased succinate stabilizes the oncogenic HIF transcription factor through product inhibition of prolyl-hydroxylase (PHD) enzymes which under conditions of normal oxygen levels hydroxylate HIFα subunit in reaction dependent on oxygen and α-ketoglutarate, providing a signal for proteasomal degradation of HIF mediated by VHL. This state of hypoxia due to defect in HIF degradation at normal oxygen levels is termed pseudohypoxia and is now considered a possible mechanism of tumorigenesis in both CII- and VHL-derived tumours. PHD enzymes controlling HIF are not the only α-ketoglutarate-dependent, succinate-producing enzymes present in cells. The large family of α-ketoglutarate dependent oxygenase includes the JmjC domain-containing histone demethylases (JHMD), which modulate the epigenome by removing methyl residues from specific lysines of histones, and ten-eleven translocation (TET) DNA hydroxylases, which demethylate genomic DNA [92]. Thus, accumulation of succinate can in this way easily affect the whole epigenome, and recently published investigations underscore this intriguing possibility [90, 91].

MITOCANS

Mitocans represent a variety of compounds identified to act upon and destabilize mitochondria to cause cell death, which is in some cases specific for malignant cells. The acronym mitocan stands for ‘mitochondrially targeted, apoptosis-inducing anticancer compound’ or ‘mitochondria and cancer’. Mitocans were proposed to encompass several classes based on their particular mitochondrial target site [93, 94]. These are: hexokinase inhibitors (3-bromopyruvate, 2-deoxyglucose), compounds targeting Bcl-2 family proteins (gossypol, α-tocopheryl succinate), thiol redox inhibitors (isothiocyanates, arsenic trioxide), VDAC/ANT targeting drugs (lonidamine, arsenites), ETC-targeting drugs (tamoxifen, α-tocopheryl succinate), lipophilic cations targeting inner membrane (rhodamine-123, F16), drugs targeting the TCA cycle (dichloroacetate, 3-bromopyruvate) and drugs targeting mtDNA (vitamin K3,

fialuridine). In several cases targets of mitocans overlap, such as for 3-bromopyruvate and α-tocopheryl succinate (α-TOS). In this work, focus is placed on class five mitocans, i.e. ETC-targeting drugs, particularly on the vitamin E analogue α-TOS as discussed further in greater detail.

ETC-targeting drugs

This class of mitocans comprises a group of compounds targeted to the individual complexes of mitochondrial ETC, and it includes compounds often highly selective for cancer cells, some of them already undergoing clinical trials. Although some of these compounds have also other known (and possibly presently unknown) targets and modes of cell death induction, their inhibition of particular ETC complexes, resulting in increased ROS production, is one of the major reasons for their application [93-96]. Unfortunately, as mitochondrial ETC is the most important site for energy production in large majority of cells, some of these agents show undesirable toxic side effect, being particularly neurotoxic, while some of these mitocans are selective for cancer cells and therefore present intriguing possibilities in anti-cancer therapy [95, 96].

Potentially clinicaly relevant CI inhibitors for cancer treatment are presented by the antagonist of the estrogen receptor tamoxifen, the biguanidine compound metformin as well as deguelin, an analogue of rotenone. Although tamoxifen is used in the clinic for treatment of hormone-dependent breast cancer, it has shown anti-proliferative effects against cells lacking the estrogen receptor as well as against prostate cancer, and was reported to inhibit CI [97]. Metformin, an activator of AMP-activated protein kinase used in the clinic to treat type-2 diabetes, was shown to block CI derived respiration, and displays anti-tumour effects *in* vivo. Patients given metformin present with reduced incidence of cancer and increased susceptibility to chemotherapy treatment. In contrast to the first two described drugs, deguelin is not yet used in the clinic, but has shown promise in experimental cancer and xenograft models [95].

In the case of CII inhibition, the 'redox-silent' analogue of vitamin E α-TOS has been shown to effectively kill cancer cells *in vitro* as well as *in vivo* in experimental mouse models, and this will be discussed in greater detail in separate chapter. Of the other CII inhibitors, a Q site inhibitor thenoyltrifluoroacetone (TTFA) and two compounds that inhibit the dicarboxylate site in SDHA subunit, malonate and 3-nitropropionic acid, exhibit toxic properties also in noncancerous cells [98] and cannot be considered for use in the clinic. An anti-diabetic and anti-inflammatory CII inhibitor, troglitazone was withdrawn from the clinic due to liver toxicity [95]. The aforementioned facts would leave, so far, α-TOS and other vitamin E analogues as the sole representatives of the CII-targeting drugs as possible options for anti-cancer treatment.

An interesting group of CIII-targeting compounds are plant-derived polyphenols, such as resveratrol and xanthohumol, which induce apoptosis and that have been shown to be effective in various pre-clinical

cancer models. Besides CIII, both agents also inhibit CI. Another natural compound that inhibits CIII in cancer cells and initiates ROS-mediated apoptosis is benzyl isothiocyanate (BITC), which is able to suppress angiogenesis and xenograft tumour growth in experimental cancer models [95, 96].

Latest research suggests that inhibitors of mitochondrial respiration might be particularly useful for treatment of resistant cancer [99]. As shown for melanoma, cells that acquired resistance against vemurafenib, a selective inhibitor of mutant BRAF, display high rates of mitochondrial respiration and OXPHOS and are sensitive to inhibition of these mitochondrial pathways [100, 101]. Elesclomol, a pro-oxidant agent currently undergoing clinical trials, induced increased intracellular ROS generation and melanoma cell death [100]. The mechanism by which elesclomol leads to enhanced ROS production was ascribed to its ability to greatly increase copper amount in cells [102], which then mediates ROS generation possibly through interaction with ETC [103].

Vitamin E analogues

The term vitamin E is used for a family of eight naturally occurring phenolic compounds. These are divided in tocopherols and tocotrienols, the difference being the presence of either saturated lipophilic phytyl side chain in case of tocopherols or poly-unsaturated side chain in tocotrienols. Each group includes four isoforms, α-, β-, γ-, δ- tocopherols and tocotrienols, which differ by the number and position of methyl group at the chromanol ring. All of them display wide-range of anti-oxidant related activities. α-Tocopherol is the first vitamin E form discovered in the nature and later synthetized. Since then, several compounds with various substitutions in the original structure of vitamin E were prepared and are known as vitamin E analogues. Their structure can be divided into three distinct domains. The hydrophobic domain represented by the lipophilic side chain, the middle signaling domain with the chromanol ring and the functional domain, which is the group attached at C6 of the chromanol ring. This group determines whether the molecule behaves as a redox-active or a redox-silent compound. The anti-oxidants of vitamin E family have at this place the redox-active hydroxyl group which can donate its hydrogen to free radicals and in this way terminate their damaging oxidative properties. Redox-silent analogues, in which the hydroxyl group was replaced by ether-linked acetic acid or ester-linked succinyl group do not possess the anti-oxidant properties, but were recognized as pro-apoptotic and anti-neoplastic agents [104]. The most prominent and highly studied derivative of these redox-silent vitamin E analogues is the dicarboxylic ester with succinyl group at the chromanol ring, α-TOS (Fig. 4).

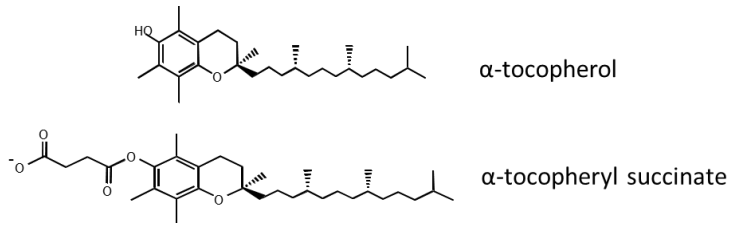

Fig. 4 Structure of α-tocopherol (a form of vitamin E) and α-tocopheryl succinate (α-TOS)

α-TOS

α-TOS shares characteristics of two mitocan classes. It acts as a BH3 mimetic [105] and impairs CII activity of mitochondrial ETC [106]. In the context of being a BH3 mimetic, it was suggested that α-TOS can disrupt the association of the pro-apoptotic Bak protein with anti-apoptotic Bcl-x_L and Bcl-2 proteins, leading to caspase-dependent apoptosis in prostate cancer cells [105]. Moreover, in the same study, the authors observed that treatment with α-TOS resulted in decreased expression of Bad, a member of the BH3-only Bcl-2 family [105]. α-TOS further affects interactions between pro-apoptotic and anti-apoptotic members of the Bcl-2-family proteins by upregulating the pro-apoptotic BH3-only protein Noxa [107] by way of engaging the Mst1-FoxO1-Noxa pathway, whose activation was recapitulated after hydrogen peroxide treatment, suggestive of ROS involvement [108]. α-TOS properties as BH3-mimetic might be important for its reported function as a sensitizer of apoptosis induction by the tumour necrosis factor-related apoptosis-inducing ligand (TRAIL) [109, 110], paclitaxel [111, 112] and etoposide [113]. Surprisingly, co-treatment with α-TOS and cisplatin led to decreased levels of apoptosis than when cells were exposed to cisplatin only [113]. In the case of sensitization to TRAIL, increased expression of death receptors DR4 and DR5 was suggested to play a role [110] and this was also proposed for nuclear factor-κB (NF-κB) activation [109]. In the paclitaxel co-treatment study, enhanced activation of caspase-8 was found along with down-regulation of anti-apoptotic Bcl-x_L protein expression [111].

Our laboratory identified CII as a molecular target for α-TOS. In two subsequent publications, it was shown that CII-deficient cells and xenografts in mice derived from them were significantly less responsive to α-TOS treatment [114]; ROS generation in response to exposure to α-TOS was suppressed in the CII-deficient cells [106]. The Q_p site of CII was proposed as the target of α-TOS pro-apoptotic action, as α-TOS inhibited CII activity in a similar manner to TTFA, a well known Q_p site inhibitor. Further molecular modelling revealed strong binding of α-TOS to the Q_p site in CII, with only slightly lower binding energy than that of UbQ, which suggests that α-TOS could be considered as a competitive inhibitor of the Q_p site in CII [106]. Displacing UbQ from its binding site would then cause ROS generation with ensuing induction of apoptosis. Enhanced ROS levels observed after treatment with α-

TOS [106, 114-119] are instrumental for apoptosis induction, since the use of antioxidants prevented α-TOS induced cell death [106, 114, 115, 119]. Besides CII, also CI [116] and CIII [117] inhibition by α-TOS was suggested to play a role in ROS production after α-TOS exposure. Though in SMPs CII activity was inhibited at much lower α-TOS doses than CIII activity (42 μM vs 315 μM) [117], in rat liver isolated mitochondria and permeabilised acute promyelocytic leukemia (APL) cells, CI was inhibited with higher efficacy than CII [116].

Apoptosis induced by α-TOS engages the intrinsic mitochondrial pathway, as α-TOS leads to MOMP formation through formation of Bax channels [120] and/or, preferentially, Bak channels [107] (but these two types of channels are not mutually exclusive and can work together), and this results in relocalisation of the pro-apoptotic Smac and cyt c to the cytosol [118-121] and activation of caspase-9 and -3 [116, 118, 120]. Morphological changes following exposure to α-TOS are highly reminiscent of apoptosis with characteristic ultrastructural features like condensation of chromatin, appearance of numerous autophagic vacuoles, convolution of nuclear membrane with fragmentation into nuclear bodies as well as convolution of cell membrane resulting in formation of cellular blebs and final fragmentation of the cell into apoptotic bodies [118].

α-TOS kills selectively cancer cells [122] including the Her2/erbB2-overexpressing breast cancer cells [119] and cells deficient in the p53 tumour suppressor [107, 122]. Its selectivity for cancer cells was confirmed *in vivo* in several pre-clinical models, including mice with xenografts of colon [123], breast [106] and lung cancer [124] as well as mesothelioma [125], and spontaneous erbB2-high breast carcinomas in FVB/N *c-neu* transgenic mice [106, 115] and in a murine syngeneic transplantation model of leukemia [116]. Importantly, α-TOS also inhibits formation of new blood vessels essential for tumour progression, as shown in a mouse cancer model by ultrasound imaging fitted with the Power Doppler function [115].

Selectivity of α-TOS for cancer cells was ascribed to its ester bond between the functional succinyl group and the rest of the molecule, which cleavage due to high levels of esterases in normal cells will result in its conversion to vitamin E in non-cancerous cells, while the pro-apoptotic activity of the ester will be maintained in cancer cells. Further, it is possible that α-TOS preferentially kills cancer cells because of the acidic nature of tumour interstitium, which would protonate the α-TOS molecule, which can then easily diffuse into cancer cells [126]. Another important reason, why α-TOS is more effective in cancer cells, stems from the nature of the molecular mechanism by which it leads to cell death, the accumulation of ROS. Cancer cells generally feature higher levels of ROS and saturated antioxidant defense systems, so that further increase of ROS can provoke their demise [95, 127, 128].

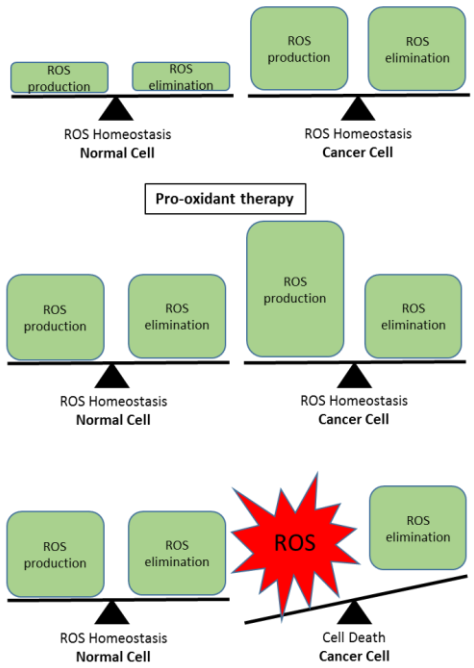

Fig. 5 Targeting cancer cells by increasing ROS levels

In normal cells and cancer cells, ROS levels are kept in balance through ROS production and ROS elimination. In cancer cells both processes occur at an increased rate compared to normal cells, so that further increase of ROS by pro-oxidant therapy can provoke the selective demise of cancer cells. Adapted from reference [127].

AIMS OF THE STUDY

The main focus of this thesis was to evaluate the pro-apoptotic and anti-cancer properties of mitochondrially targeted vitamin E succinate (MitoVES), which represents a novel compound that could be potentially used in anti-cancer therapy. To fulfill this task, specific goals were set at the beginning and during the study:

1. To examine the efficacy and selectivity of MitoVES in apoptosis induction in cancer cells and compare it to its parental untargeted compound, α-TOS.
2. To investigate the mechanism by which MitoVES kills cancer cells and define its cellular target.
3. To prepare and characterise a proper cellular model for the detailed study of MitoVES interaction with mitochondrial CII.
4. To verify CII as a direct target for cell death initiation.
5. To help elucidate the role of CII in mitochondrial ROS production.

DISCUSSION

The importance of mitochondria for cancer cells, and therefore their consideration as a potential target in anti-cancer treatment, has been neglected for the large part of the last century. This was partly due to the misinterpretation of Otto Warburg‘s data when it was reasoned that respiration in cancer cells must be compromised because of the high glycolytic activity even in the presence of high levels of oxygen [75], the other reason being the discovery of oncogenes and tumour-suppressor genes in the 1980‘s as the cause of cancer development and progression, which was a major focus of scientists for quite some time. Nevertheless, Warburg‘s observation of high glycolytic activity in cancer was correct, indeed, and it was thoroughly studied particularly in last 20 years, so that we can today recognise that the cause for the ‘Warburg effect’ in cancer cells is not damaged mitochondria or dysfunctional OXPHOS but the dysregulation of glycolysis itself [75, 129]. Besides glycolysis, many other metabolic pathways were found to be altered in cancer cells [129], either resulting from mutations in oncogenes and tumour-suppressor genes or the availability of metabolic substrates, the ultimate goal of the cells being to survive and proliferate. High proliferation rate costs cancer cells their redox homeostasis with increase in oxidative intermediates and excessive ROS production [25, 78]. Higher levels of ROS can on one hand stimulate cell growth and promote genetic instability, what is advantageous for cancer cells, but on the other hand, this very feature of cancer can also be exploited for anti-cancer therapy [25, 78, 84, 127]. In cells, there are many sources contributing to oxidative stress, and mitochondria with its electron transport chain and several other sites capable of generating ROS are of high importance [21, 30, 83].

Mitochondrially produced superoxide is a normal physiological by-product of cellular respiration, and together with hydrogen peroxide, which is the product of its dismutation by SOD2, has various signalling roles within the cell [21]. The rate of superoxide production from ETC can increase under certain pathological conditions or using specific compounds that inhibit the electron flow between the respiratory complexes, and it may cause premature recombination of free electron with oxygen molecule.

Earlier work of our group documented that α-TOS, a redox-silent analogue of vitamin E, could be used as an effective anti-cancer agent in this context. α-TOS kills selectively cancer cells [122] by way of apoptosis induction via the mitochondrial pathway [118] and has been shown to be effective also *in vivo* in various mouse models [114, 115, 123]. Although α-TOS has been reported to induce apoptosis in cancer cells by various means (reviewed in [130]), its main target has been reported to be mitochondrial CII, since cells lacking CII as well as mice with xenografts derived from these cells are resistant to the agent [106, 114].

Due to its hydrophobic structure, α-TOS easily penetrates biological membranes and, once inside the cell, indiscriminately localises to any membranous compartment. This means that only a relatively small portion of the drug is really available in mitochondria to perform its action. It therefore appears highly plausible that 'sending' α-TOS to mitochondria should boost its ROS producing efficacy and anti-cancer activity while making it possible to reduce the effective concentration. We therefore decided to investigate whether targeting the drug to mitochondria would result in more effective anti-cancer agent. We employed here the approach introduced by Murphy and Smiths, which they have successfully used in the case of mitochondrially targeted UbQ (MitoQ) [131, 132]. Based on the differences in electrical gradients across biological membranes, they tagged UbQ with the delocalised cationic triphenylphosphonium (TPP^+) group. They found that this modified UbQ localised to mitochondria and was able to cycle between its oxidised and reduced forms by exchanging electrons with the respiratory chain [131]. Cellular uptake of TPP^+ tagged compounds is driven by the plasma membrane potential (30-60 mV) and its mitochondrial localisation by the $\Delta\Psi$ (150-180 mV). Therefore, the final level of such agents in mitochondria can be 100-500 fold higher than outside the cell [132].

We modified the α-TOS molecule to generate a compound referred to as MitoVES (mitochondrially targeted vitamin E succinate) in which an 11 carbons chain links the positively charged TPP^+ group and the functional tocopheryl succinyl group, and in two subsequent publications showed that, indeed, mitochondrial targeting considerably enhanced the pro-apoptotic and anti-cancer activity of α-TOS [133, 134]. The pro-apoptotic activity of MitoVES was some 20-50 fold higher compared to that of α-TOS as shown for Jurkat cells [133]. Importantly, MitoVES still kept its selectivity towards malignant cells as documented by much less effective killing of non-malignant cells and very low toxicity for experimental

animals [134]. Furthermore, cell lines defective in the tumour-suppressor p53 were efficiently killed by MitoVES [134]. This is particularly important in the context of cancer treatment, as in many cancers, p53 is mutated and therefore tumour cells are resistant to p53-mediated cell death pathways [135].

MitoVES-induced cell death was ROS-dependent, as either co-treatment with PEG-SOD or pre-treatment with MitoQ [131], two antioxidants, diminished MitoVES-induced ROS generation and the ensuing cell death [134]. ROS production after MitoVES addition occurred within 5 min, as documented using cells transiently transfected with pHyPer-dMito, whose product, the redox-sensitive OxyR, leads to increase in fluorescence if hydrogen peroxide is present [134]. This high and very rapid ROS production most likely stems from interaction of MitoVES with CII of the mitochondrial ETC, as functional CII was required for generation of ROS and induction of cell death [133].

Cell death pathway via which MitoVES kills cancer cells was, as in the case of the parental compound α-TOS, dependent on mitochondrial (intrinsic) pro-apoptotic signalling [134]. This was recognised after showing that MitoVES treatment leads to cytosolic translocation of cyt c and Smac and to formation of Bak and Bax oligomers in mitochondria [134]. Further, an inhibitor of caspase-9, but not a caspase-8, resulted in suppression of MitoVES-induced apoptosis [134]. The pro-apoptotic proteins Bak and Bax can either work together to permeabilise mitochondrial membrane or, in some cases, there could be either redundancy in their pore-forming activity or a preference for one of them. We found, that in the case of MitoVES, a conformational change in the Bak protein causing its activation precedes that of Bax. In fact, Bax was found dispensable for MitoVES pro-apoptotic activity since the agent killed Jurkat cells lacking only Bax as effectively as it killed parental cells, while cells with silenced Bak, were relatively resistant to MitoVES, particularly at lower concentrations of the drug [134].

If mitochondrial targeting of MitoVES is the underlying cause of its substantially higher killing efficiency compared to the untargeted α-TOS, then interfering with MitoVES accumulation in mitochondria should result in decreased apoptosis. Targeting of MitoVES to mitochondria is due to the presence of the TPP^+ group and high $\Delta\Psi$. Therefore dissipation of $\Delta\Psi$ with the uncoupler carbonyl cyanide-4-(trifluoromethoxy)phenylhydrazone (FCCP) should be expected to lower the level of apoptotic response in the case of MitoVES but not for the non-targeted α-TOS. This, indeed, was the case and provided the evidence, that $\Delta\Psi$ is important for high MitoVES pro-apoptotic activity [133]. Delocalised lipophilic cations, such as compounds with TPP^+, show selectivity for mitochondria of carcinoma cells [136], and this is ascribed to higher plasma membrane and mitochondrial membrane potential of carcinoma cells compared to normal epithelial cells [87, 136]. The reason for this could be the altered metabolism of cancer cells resulting in metabolic remodelling due to down-regulation of K^+ channels [87]. Mitochondrial hyperpolarisation is very important feature of cancer cells [87, 137] and is predominantly perceived in negative context, as it confers apoptosis resistance [87, 88]. However,

conversely, this is beneficial for killing of cancercells selectively and efficiently by MitoVES. Indeed, using a fluorescently labelled MitoVES administered to mice, we found high level of fluorescence in tumours and not in heart, kidney or liver, which demonstrates that MitoVES is selectively taken up by cancer cells also *in vivo* [138].

Further, we studied MitoVES anti-angiogenic potential on proliferating and confluent endothelial-like EAhy926 cells and showed that the drug was much more effective in induction of ROS production and apoptosis in proliferating cells [139]. Importantly, we found, that the resistance of the confluent growth arrested endothelial-like cells could be ascribed to their lower $\Delta\Psi$ compared to their proliferating counterparts, which was about three-fold lower [139]. Again, experiments with the mitochondrial uncoupler FCCP confirmed that MitoVES is preferentially taken up by mitochondria with higher $\Delta\Psi$ [139].

We also studied a mechanism by which cancer cells could potentially acquire resistance to α-TOS and if this could be overcome by the application of the mitochondrially targeted derivative. Exposure of two different lung cancer cell lines to escalating doses of α-TOS made them resistant to the agent. We found this to be the result of upregulation of the ABCA1 protein from the family of ABC transporters associated with multidrug resistance. On the other hand, MitoVES which is taken up on the basis of plasma membrane potential and quickly accumulates in mitochondria, bypassed the increased level of ABCA1 transporter and efficiently killed the cells resistant to α-TOS [140]. This finding may have clinical implications as shown in a single patient with malignant mesothelioma. This patient was treated by transdermal application of α-TOS. Over several years, the tumour did not progress and even started to recede. However, the tumour then started to grow quickly and the patient passed away. While we have no evidence at this stage, it is possible that the patient developed resistance to the drug. We believe that this could be in the future overcome by the application of MitoVES.

After defining MitoVES superiority over parental α-TOS and, importantly, showing its effectivity and safety *in vivo*, we turned our attention to its target site within mitochondria, CII of the ETC, and to the mechanism by which its inhibition leads to ROS production. This issue needed further clarification for two reasons. First, although we have shown that CII Q_p site is important for ROS production using several experimental approaches that employed B9 cells lacking fully functional CII [45, 133] as well as cells with a mutation in the Q_p site, these are only circumstantial proofs, because the mutant has not been further characterised and the mutation at the Q_p site can as well lead to another CII dysfunctional model, such as the parental B9 cells. Further, the actual target of MitoVES could be upstream of CII, and CII could only serve here as an amplifier of the signal as it has been suggested before that CII works as a sensor and modulator of apoptosis [141], disintegrating after the mitochondrial calcium influx [19] and pH changes during apoptosis [18] whereby enhancing ROS generation [18, 19]. Second, a reason to

study in more detail interaction of MitoVES with CII is due to the fact that this complex has been rather neglected as a site for ROS formation within the ETC, which has been ascribed largely to CI and CIII [21, 22]. This attitude towards CII has just begun to change due to several recent reports indicating that ROS production directly from CII is occurring in mammalian cells [34, 35, 47], nematodes [142] and plants [40].

To elucidate these questions, we employed again the CII-deficient B9 cells. This cell line was described by Scheffler's group to lack functional CII due to a premature stop codon in the gene coding for the SDHC subunit [45]. SDHC and SDHD subunit comprise the Q_p site of CII, and several amino acid residues of SDHC were predicted to stabilise the functional succinyl group of α-TOS [106], which α-TOS shares with MitoVES [133]. For this reason, the B9 cells lacking the SDHC protein present a great model, into which we could insert *SDHC* with desired changes, in our case mutations resulting in substitutions of amino acids possibly interacting with MitoVES or flanking the cavity in the protein at which bottom is the UbQ and presumably, too, α-TOS/MitoVES-binding site. Alhough the B9 cell line is of Chinese hamster origin and the *SDHC* gene sequence used for mutagenesis and transfections was human, it was previously shown, that human *SDHC* gene can reconstitute the CII activity in these cells [45, 46]. Since human cell lines would be better to work with, we tried to knock out *SDHC* using the zinc-finger nuclease approach for MCF-7 and HEK293 cells. Regardless of numerous attempts, we failed to achieve this goal, therefore used B9 cells.

We reconstituted CII activity with wild-type (WT) and mutated *SDHC* gene. While B9 cells with WT *SDHC* underwent efficient apoptosis when challenged with MitoVES, all three mutant lines were significantly more resistant to the agent [143]. We then assesed the impact of the mutations on CII assembly and function by various methods employing either isolated mitochondria (subjected to BNE and SQR and SDH in gel activity evaluation), permeabilised cells (assessed for respiration using the oxygraph) or intact cells (evaluated for the level of succinate by mass spectrometry). This thorough characterisation revealed that neither of the mutations affected CII assembly, but electron transporting capacity of CII was almost completely suppressed in the R72C variant cells. We found a subtle defect in respiration after uncoupling of mitochondria in the S68A variant cells, where we observed no rise in succinate-dependent oxygen consumption after addition of FCCP as was the case of the WT and I56F variant cells [143]. In mitochondria, CII converts succinate to fumarate; in case this activity is impaired, higher succinate concentrations are detected in affected cells and tissues [144, 145]. Therefore, the evaluation of intracellular succinate levels was very important for elucidating the real impact of individual mutations on CII activity under physiological conditions in intact cells. This showed that intracellular succinate levels in S68A variant cells were as low as in WT and I56F cells, while succinate

levels in parental B9 and R72C cells were much higher [143]. This suggests that the uncoupling defect in S68A cells may be of little significance in intact cells.

The finding that I56F and S68A mutations did not lead to impaired CII activity was of importance. The reason is that, as discussed above, there would be no direct proof of CII interaction with MitoVES without functional CII with intact electron flow and the mutant cells would just reciprocate the phenotype of parental B9 cells. Detailed respirometry studies confirmed that MitoVES inhibitory effect on CII is lower in both CII-variant cell lines, i.e. I56F and S68A [143]. To verify the effect of the mutations on the Q_p site in CII, we performed the same experiments with malonate, an inhibitor of succinate-binding site in CII, and TTFA, which inhibits CII at the Q_p site. These experiments confirmed that the mutations affected only the Q_p site, as there was no difference in the inhibition with malonate, while TTFA proved to be much stronger inhibitor of CII in the S68A variant than in the WT and I56F cells. The more potent inhibition of CII with TTFA correlated with higher level of apoptosis induced by this inhibitor and provided strong support for direct involvement of CII in cell death induction [143].

Further, utilising the recently developed fluorescence module together with the Oroboros Oxygraph-2k, we could show with isolated mitochondria that inhibition of CII-dependent respiration with either MitoVES or TTFA leads to ROS production. In agreement with the observations by others [33-35], we could only observe ROS production in the presence of low, in our case 500 μM succinate, and only after substantial CII respiration was blocked by the CII inhibitor [35]. It was suggested that high (5-10 mM) succinate concentrations, usually used in respirometry studies [32], block the access of molecular oxygen to electrons at the FAD site, so that superoxide is not produced [35]. Importantly, the increase in ROS production in these experiments followed the pattern of susceptibility to apoptosis and was confirmed in flow cytometry assays with the fluorescent probe DHE in intact cells. The only exception was the R72C variant, where very low residual CII activity sufficed to support some ROS production in the presence of low succinate (particularly with TTFA), but the cells showed very low apoptosis and ROS production with both inhibitors [143]. Though apparently surprising, this observation is rather interesting and could be easily explained by the model of superoxide production from CII mentioned above [35]. Due to severely impaired CII activity, these cells accumulate high levels of succinate, that will block superoxide production from CII in intact cells. This effect would not be present in the case of fluorescence respiratory measurements done with isolated mitochondria in the presence of low succinate, so the rise in ROS production after addition of the inhibitor could be observed.

When analysing our observations of the effect of MitoVES on the different CII-variant cell lines, another aspect of MitoVES action on mitochondria should be discussed. It has been reported that MitoVES at very low doses acts as an uncoupler and collapses $\Delta\Psi$ to stimulate oxygen uptake [146]. We also observed this uncoupling effect of MitoVES in our inhibitory studies. High $\Delta\Psi$ was very often

accepted as a prerequisite for increased ROS production from mitochondrial ETC [23, 147] because if ΔΨ across the inner membrane of mitochondria becomes too high, CI, CIII and CIV, which also work as proton pumps, start to have difficulties to pump protons against the high ΔΨ. Electrons in the ETC thus become stalled and easily escape into the extra-membrane environment, where they can recombine with molecular oxygen to form superoxide [148]. In this context, reverse electron transport from reduced $UbQH_2$ to CI (see Introduction) is usually considered responsible, and such ROS production can be suppressed with the CI inhibitor rotenone [22]. Here it could be argued that the MitoVES uncoupling propensity works against the idea of reverse electron transport being responsible for ROS generation by this compound. However, data presented in this thesis and in detailed studies by Moreno-Sanchez and colleagues who showed that rotenone had no effect on ROS production with MitoVES in various models of isolated mitochondria and that reverse electron transport does not contribute to elevated ROS when MitoVES is used as a CII inhibitor [149].

Quinlan and colleagues recently observed that CII can generate ROS at rates comparable to those of CI and CIII, and in the absence of protonmotive force [34]. Moreover, our results suggest that the initial dissipation of ΔΨ with MitoVES could even result in higher ROS production in comparison with non-uncoupling CII inhibitors, as the proton pumps in the ETC do not have to work against high electro-chemical gradient. Movement of electrons and their 'leak' can be in such case rather rapid. In our experiments, we observed that MitoVES led to higher ROS production than TTFA, and the reason for this could be the uncoupling property of MitoVES. In this context, the S68A CII variant, whose partial defect results in the failure to 'uncouple', offers an interesting model. This mild defect, which has possibly no impact under coupled conditions, might be one of the reasons why ROS generation in these cells is lower and why they are more resistant to MitoVES. Nevertheless, the inhibitory curve obtained with MitoVES also points to diminished binding of the drug in the Q_p site compromised by the S68A mutation.

To further support our findings that increased ROS production links the inhibition of CII and cell death induction, we over-expressed catalase in WT and S68A variant cells and found that this additional ROS detoxifying mechanism lowered the apoptotic response. For this experiment, we chose these two cell lines, since they represent the high and low responders to both inhibitors used [143].

When we tried to correlate the inhibition of CII with yet another widely used inhibitor of CII, Atpenin V [36], we found, that this inhibitor, though extremely potent (IC_{50} 15-20 nM in B9 derived CII variant cell lines), did not induce apoptosis nor ROS production in either cell line tested [143]. We suspect, that the reason for this could be the strong inhibition of CII, resulting in quick build-up in succinate levels, which would subsequently block ROS production from CII. Indeed, results from measurement of intracellular succinate after addition of each of the inhibitors tested show that, in contrast to MitoVES

and TTFA, 30 min incubation with Atpenin A5 increased succinate levels 5-fold [143]. These findings demonstrate that CII inhibition results in cell death only when intracellular succinate accumulation is not too rapid and ROS can be efficiently formed, and further help to elucidate the controversial role of CII in superoxide production and cell death induction.

We further found that MitoVES exerts its anti-cancer effects not only at doses leading to cell death but also at sub-apoptotic levels. Under these conditions, MitoVES inhibits cell proliferation by way of suppression of the mitochondrial transcription factor TFAM, resulting in inhibition of mtDNA transcription, which was showed to occur both *in vitro* and *in vivo*. In a transgenic mouse model of breast cancer, MitoVES lowered levels of mtDNA transcripts in cancer cells but not in normal tissue. We proposed an involvement of CII-derived ROS in this process as cells lacking functional CII, where MitoVES cannot produce ROS, did not undergo cell growth arrest upon MitoVES treatment [138].

In the context of CII mutations and ROS production, it might be interesting to mention the role of CII in certain rare cancers, such as paraganglioma and pheochromocytoma. Here CII plays a role of classical tumour-suppressor, because its inactivating mutations lead to a tumorigenic phenotype through accumulation of succinate and/or increased ROS production. Considering the fact that neither we, nor others [33, 35] have observed increased ROS production from CII at higher succinate levels, which occur in these tumours [144], we would conclude that higher succinate is a more plausible cause of the tumorigenic transformation. And if higher levels of ROS are observed within these tumours and cell models, they are probably not of CII origin. Here, it cannot be excluded that if $\Delta\Psi$ is kept high, increased succinate concentrations in these tumours may favour the reverse electron flow from CI as was recently shown to be the case in ischemia/reperfusion injury [31].

Most part of this work has focused on defining the role of CII and subsequent increase in ROS production in cell death induced by MitoVES, and this was performed using cell culture models. However, experiments where MitoVES was shown to suppress growth of spontaneous breast carcinoma in transgenic FVB/N *c-neu* mice [134, 139] as well as xenografts in Balb-c *nu/nu* mice derived from colorectal HCT116 cells [134] provide strong support for its potential anti-cancer effect *in vivo*, with very low adverse toxicity. The use of mitochondrial inhibitors in the clinic is only now coming to attention and as emphasized in a recent paper by Wolf, suggesting that the main benefit of drugs inhibiting OXPHOS might lie in their combinations with other established anti-cancer agents blocking proliferation of cancer cells [99]. Further, due to high heterogeneity of cells even within the same tumour, CII offers an interesting and invariant target. Importantly, it only rarely mutates, which is often not the case for other metabolic targets.

Targeting the ETC could be also interesting in the context of our recently published findings (a publication not included in this thesis) that cancer cells without mtDNA show delayed tumour growth

and to restore their metabolic capacities, they acquire functional mitochondria from the host, which enables them to form tumours [150]. This work corroborates the notion of high level of tumour plasticity and reveals an essential requirement for CII and OXPHOS in tumor progression.

In conclusion, this work has established MitoVES as a promising anti-cancer agent and defined mitochondrial CII as its target site. Moreover, the CII Q_P site mutagenesis revealed a direct correlation between the efficacy of inhibition of the CII Q_P site, the ensuing ROS production and the extent of cell death induction, which may be counteracted by high levels of intracellular succinate.

CONCLUSIONS

1. We have shown that mitochondrially targeted MitoVES is superior to non-targeted α-TOS in its anti-cancer efficiency and that this could be, in large part, ascribed to its mitochondrial localisation and high $\Delta\Psi$.

2. MitoVES kills cancer cells via the intrinsic apoptotic pathway, preferentially engaging the Bak protein for permeabilisation of MOM.

3. Detailed study of MitoVES interaction with the Q_p site of CII confirmed that MitoVES binding to this site is necessary for stimulation of ROS production and efficient cell death induction.

4. Upon CII Q_p site inhibition, ROS are produced directly from the CII dicarboxylate site and this production correlates with the level of CII inhibition and cell death induction, unless intracellular

succinate is high, which validates the Q_p site of CII as a target for cell death induction with relevance to anti-cancer therapy.

LIST OF PUBLICATIONS

Dong LF, Jameson VJ, Tilly D, Cerny J, Mahdavian E, Marín-Hernández A, Hernández-Esquivel L, Rodríguez-Enríquez S, Stursa J, Witting PK, Stantic B, Rohlena J, Truksa J, **Kluckova K**, Dyason JC, Ledvina M, Salvatore BA, Moreno-Sánchez R, Coster MJ, Ralph SJ, Smith RA, Neuzil J. **Mitochondrial targeting of vitamin E succinate enhances its pro-apoptotic and anti-cancer activity via mitochondrial complex II.** J Biol Chem. 2011 Feb 4;286(5):3717-28. **IF = 4.60**

Dong LF, Jameson VJ, Tilly D, Prochazka L, Rohlena J, Valis K, Truksa J, Zobalova R, Mahdavian E, **Kluckova K**, Stantic M, Stursa J, Freeman R, Witting PK, Norberg E, Goodwin J, Salvatore BA, Novotna J, Turanek J, Ledvina M, Hozak P, Zhivotovsky B, Coster MJ, Ralph SJ, Smith RA, Neuzil J. **Mitochondrial targeting of α-tocopheryl succinate enhances its pro-apoptotic efficacy: A new paradigm for effective cancer therapy.** Free Radic Biol Med. 2011 Jun 1;50(11):1546-55. **IF = 5.71**

Rohlena J, Dong LF, **Kluckova K**, Zobalova R, Goodwin J, Tilly D, Stursa J, Pecinova A, Philimonenko A, Hozak P, Banerjee J, Ledvina M, Sen CK, Houstek J, Coster MJ, Neuzil J. **Mitochondrially targeted α-tocopheryl succinate is antiangiogenic: Potential benefit against tumor angiogenesis but caution against wound healing.** Antioxid Redox Signal. 2011 Dec 15;15(12):2923-35. **IF = 7.67**

Prochazka L, Koudelka S, Dong LF, Stursa J, Goodwin J, Neca J, Slavik J, Ciganek M, Masek J, **Kluckova K**, Nguyen M, Turanek J, Neuzil J.
Mitochondrial targeting overcomes ABCA1-dependent resistance of lung carcinoma to α-tocopheryl succinate. Apoptosis. 2013 Mar;18(3):286-99. **IF = 3.61**

Kluckova K, Bezawork-Geleta A, Rohlena J, Dong L, Neuzil J.
Mitochondrial complex II, a novel target for anti-cancer agents. Biochim Biophys Acta. 2013 May;1827(5):552-64. **IF = 4.83**

Truksa J, Dong LF, Rohlena J, Stursa J, Vondrusova M, Goodwin J, Nguyen M, **Kluckova K**, Rychtarcikova Z, Lettlova S, Spacilova J, Stapelberg M, Zoratti M, Neuzil J.
Mitochondrially Targeted Vitamin E Succinate Modulates Expression of Mitochondrial DNA Transcripts and Mitochondrial Biogenesis. Antioxid Redox Signal. 2015 Feb 25. **IF = 7.67**

Kluckova K, Dong LF, Bajzikova M, Rohlena J, Neuzil J.
Evaluation of respiration of mitochondria in cancer cells exposed to mitochondria-targeted agents. Methods Mol Biol. 2015;1265:181-94. **Without IF, but PubMed and WOS listed.**

Kluckova K, Sticha M, Cerny J, Mracek T, Dong L, Drahota Z, Gottlieb E, Neuzil J and Rohlena J.
Ubiquinone-binding site mutagenesis reveals the role of mitochondrial complex II in cell death initiation. Accepted for publication in Cell Death Dis. **IF = 5.17**

REFERENCES

[1] I. Scheffler, Mitochondria, Second edition, John Wiley & Sons, Inc., Hoboken, New Jersey, USA, 2008.
[2] N.S. Chandel, Mitochondria as signaling organelles, BMC Biol., 12 (2014) 34.
[3] X. Liu, C.N. Kim, J. Yang, R. Jemmerson, X. Wang, Induction of apoptotic program in cell-free extracts: requirement for dATP and cytochrome c, Cell, 86 (1996) 147-157.
[4] N.S. Chandel, E. Maltepe, E. Goldwasser, C.E. Mathieu, M.C. Simon, P.T. Schumacker, Mitochondrial reactive oxygen species trigger hypoxia-induced transcription, Proc. Natl. Acad. Sci. U. S. A., 95 (1998) 11715-11720.
[5] E.J. Boekema, H.P. Braun, Supramolecular structure of the mitochondrial oxidative phosphorylation system, J. Biol. Chem., 282 (2007) 1-4.
[6] E. Lapuente-Brun, R. Moreno-Loshuertos, R. Acin-Perez, A. Latorre-Pellicer, C. Colas, E. Balsa, E. Perales-Clemente, P.M. Quiros, E. Calvo, M.A. Rodriguez-Hernandez, P. Navas, R. Cruz, A. Carracedo, C. Lopez-Otin, A. Perez-Martos, P. Fernandez-Silva, E. Fernandez-Vizarra, J.A. Enriquez, Supercomplex assembly determines electron flux in the mitochondrial electron transport chain, Science, 340 (2013) 1567-1570.
[7] R. Acin-Perez, P. Fernandez-Silva, M.L. Peleato, A. Perez-Martos, J.A. Enriquez, Respiratory active mitochondrial supercomplexes, Mol. Cell, 32 (2008) 529-539.
[8] F. Sun, X. Huo, Y. Zhai, A. Wang, J. Xu, D. Su, M. Bartlam, Z. Rao, Crystal structure of mitochondrial respiratory membrane protein complex II, Cell, 121 (2005) 1043-1057.

[9] E. Maklashina, G. Cecchini, The quinone-binding and catalytic site of complex II, Biochim. Biophys. Acta, 1797 (2010) 1877-1882.
[10] D. Ghezzi, P. Goffrini, G. Uziel, R. Horvath, T. Klopstock, H. Lochmuller, P. D'Adamo, P. Gasparini, T.M. Strom, H. Prokisch, F. Invernizzi, I. Ferrero, M. Zeviani, SDHAF1, encoding a LYR complex-II specific assembly factor, is mutated in SDH-defective infantile leukoencephalopathy, Nat. Genet., 41 (2009) 654-656.
[11] H.X. Hao, O. Khalimonchuk, M. Schraders, N. Dephoure, J.P. Bayley, H. Kunst, P. Devilee, C.W. Cremers, J.D. Schiffman, B.G. Bentz, S.P. Gygi, D.R. Winge, H. Kremer, J. Rutter, SDH5, a gene required for flavination of succinate dehydrogenase, is mutated in paraganglioma, Science, 325 (2009) 1139-1142.
[12] C.T. Schwall, V.L. Greenwood, N.N. Alder, The stability and activity of respiratory Complex II is cardiolipin-dependent, Biochim. Biophys. Acta, 1817 (2012) 1588-1596.
[13] R. Acin-Perez, I. Carrascoso, F. Baixauli, M. Roche-Molina, A. Latorre-Pellicer, P. Fernandez-Silva, M. Mittelbrunn, F. Sanchez-Madrid, A. Perez-Martos, C.A. Lowell, G. Manfredi, J.A. Enriquez, ROS-triggered phosphorylation of complex II by Fgr kinase regulates cellular adaptation to fuel use, Cell Metab, 19 (2014) 1020-1033.
[14] N. Gebert, M. Gebert, S. Oeljeklaus, K. von der Malsburg, D.A. Stroud, B. Kulawiak, C. Wirth, R.P. Zahedi, P. Dolezal, S. Wiese, O. Simon, A. Schulze-Specking, K.N. Truscott, A. Sickmann, P. Rehling, B. Guiard, C. Hunte, B. Warscheid, M. van der Laan, N. Pfanner, N. Wiedemann, Dual function of Sdh3 in the respiratory chain and TIM22 protein translocase of the mitochondrial inner membrane, Mol. Cell, 44 (2011) 811-818.
[15] B. Kulawiak, J. Hopker, M. Gebert, B. Guiard, N. Wiedemann, N. Gebert, The mitochondrial protein import machinery has multiple connections to the respiratory chain, Biochim. Biophys. Acta, 1827 (2013) 612-626.
[16] T.M. Iverson, Catalytic mechanisms of complex II enzymes: a structural perspective, Biochim. Biophys. Acta, 1827 (2013) 648-657.
[17] A. Lemarie, S. Grimm, Mutations in the heme b-binding residue of SDHC inhibit assembly of respiratory chain complex II in mammalian cells, Mitochondrion, 9 (2009) 254-260.
[18] A. Lemarie, L. Huc, E. Pazarentzos, A.L. Mahul-Mellier, S. Grimm, Specific disintegration of complex II succinate:ubiquinone oxidoreductase links pH changes to oxidative stress for apoptosis induction, Cell Death Differ., 18 (2011) 338-349.
[19] M.S. Hwang, C.T. Schwall, E. Pazarentzos, C. Datler, N.N. Alder, S. Grimm, Mitochondrial Ca(2+) influx targets cardiolipin to disintegrate respiratory chain complex II for cell death induction, Cell Death Differ., 21 (2014) 1733-1745.
[20] A.P. Gimenez-Roqueplo, J. Favier, P. Rustin, J.J. Mourad, P.F. Plouin, P. Corvol, A. Rotig, X. Jeunemaitre, The R22X mutation of the SDHD gene in hereditary paraganglioma abolishes the enzymatic activity of complex II in the mitochondrial respiratory chain and activates the hypoxia pathway, Am. J. Hum. Genet., 69 (2001) 1186-1197.
[21] M.P. Murphy, How mitochondria produce reactive oxygen species, Biochem. J., 417 (2009) 1-13.
[22] A.J. Lambert, M.D. Brand, Reactive oxygen species production by mitochondria, Methods Mol. Biol., 554 (2009) 165-181.
[23] A.A. Starkov, The role of mitochondria in reactive oxygen species metabolism and signaling, Ann. N. Y. Acad. Sci., 1147 (2008) 37-52.
[24] D. Han, F. Antunes, R. Canali, D. Rettori, E. Cadenas, Voltage-dependent anion channels control the release of the superoxide anion from mitochondria to cytosol, J. Biol. Chem., 278 (2003) 5557-5563.
[25] S.S. Sabharwal, P.T. Schumacker, Mitochondrial ROS in cancer: initiators, amplifiers or an Achilles' heel?, Nat. Rev. Cancer, 14 (2014) 709-721.

[26] R.S. Balaban, S. Nemoto, T. Finkel, Mitochondria, oxidants, and aging, Cell, 120 (2005) 483-495.
[27] D. Harman, The biologic clock: the mitochondria?, J. Am. Geriatr. Soc., 20 (1972) 145-147.
[28] A. Trifunovic, A. Hansson, A. Wredenberg, A.T. Rovio, E. Dufour, I. Khvorostov, J.N. Spelbrink, R. Wibom, H.T. Jacobs, N.G. Larsson, Somatic mtDNA mutations cause aging phenotypes without affecting reactive oxygen species production, Proc. Natl. Acad. Sci. U. S. A., 102 (2005) 17993-17998.
[29] S.W. Tait, D.R. Green, Mitochondria and cell signalling, J. Cell Sci., 125 (2012) 807-815.
[30] L.A. Sena, N.S. Chandel, Physiological roles of mitochondrial reactive oxygen species, Mol. Cell, 48 (2012) 158-167.
[31] E.T. Chouchani, V.R. Pell, E. Gaude, D. Aksentijevic, S.Y. Sundier, E.L. Robb, A. Logan, S.M. Nadtochiy, E.N. Ord, A.C. Smith, F. Eyassu, R. Shirley, C.H. Hu, A.J. Dare, A.M. James, S. Rogatti, R.C. Hartley, S. Eaton, A.S. Costa, P.S. Brookes, S.M. Davidson, M.R. Duchen, K. Saeb-Parsy, M.J. Shattock, A.J. Robinson, L.M. Work, C. Frezza, T. Krieg, M.P. Murphy, Ischaemic accumulation of succinate controls reperfusion injury through mitochondrial ROS, Nature, 515 (2014) 431-435.
[32] D. Pesta, E. Gnaiger, High-resolution respirometry: OXPHOS protocols for human cells and permeabilized fibers from small biopsies of human muscle, Methods Mol. Biol., 810 (2012) 25-58.
[33] K.R. Messner, J.A. Imlay, Mechanism of superoxide and hydrogen peroxide formation by fumarate reductase, succinate dehydrogenase, and aspartate oxidase, J. Biol. Chem., 277 (2002) 42563-42571.
[34] C.L. Quinlan, A.L. Orr, I.V. Perevoshchikova, J.R. Treberg, B.A. Ackrell, M.D. Brand, Mitochondrial complex II can generate reactive oxygen species at high rates in both the forward and reverse reactions, J. Biol. Chem., 287 (2012) 27255-27264.
[35] I. Siebels, S. Drose, Q-site inhibitor induced ROS production of mitochondrial complex II is attenuated by TCA cycle dicarboxylates, Biochim. Biophys. Acta, 1827 (2013) 1156-1164.
[36] H. Miyadera, K. Shiomi, H. Ui, Y. Yamaguchi, R. Masuma, H. Tomoda, H. Miyoshi, A. Osanai, K. Kita, S. Omura, Atpenins, potent and specific inhibitors of mitochondrial complex II (succinate-ubiquinone oxidoreductase), Proc. Natl. Acad. Sci. U. S. A., 100 (2003) 473-477.
[37] N. Ishii, M. Fujii, P.S. Hartman, M. Tsuda, K. Yasuda, N. Senoo-Matsuda, S. Yanase, D. Ayusawa, K. Suzuki, A mutation in succinate dehydrogenase cytochrome b causes oxidative stress and ageing in nematodes, Nature, 394 (1998) 694-697.
[38] S.S. Szeto, S.N. Reinke, B.D. Sykes, B.D. Lemire, Ubiquinone-binding site mutations in the Saccharomyces cerevisiae succinate dehydrogenase generate superoxide and lead to the accumulation of succinate, J. Biol. Chem., 282 (2007) 27518-27526.
[39] J. Guo, B.D. Lemire, The ubiquinone-binding site of the Saccharomyces cerevisiae succinate-ubiquinone oxidoreductase is a source of superoxide, J. Biol. Chem., 278 (2003) 47629-47635.
[40] C. Gleason, S. Huang, L.F. Thatcher, R.C. Foley, C.R. Anderson, A.J. Carroll, A.H. Millar, K.B. Singh, Mitochondrial complex II has a key role in mitochondrial-derived reactive oxygen species influence on plant stress gene regulation and defense, Proc. Natl. Acad. Sci. U. S. A., 108 (2011) 10768-10773.
[41] B.G. Slane, N. Aykin-Burns, B.J. Smith, A.L. Kalen, P.C. Goswami, F.E. Domann, D.R. Spitz, Mutation of succinate dehydrogenase subunit C results in increased O2.-, oxidative stress, and genomic instability, Cancer Res., 66 (2006) 7615-7620.
[42] K.M. Owens, N. Aykin-Burns, D. Dayal, M.C. Coleman, F.E. Domann, D.R. Spitz, Genomic instability induced by mutant succinate dehydrogenase subunit D (SDHD) is mediated by O2(-*) and H2O2, Free Radic. Biol. Med., 52 (2012) 160-166.
[43] T. Ishii, K. Yasuda, A. Akatsuka, O. Hino, P.S. Hartman, N. Ishii, A mutation in the SDHC gene of complex II increases oxidative stress, resulting in apoptosis and tumorigenesis, Cancer Res., 65 (2005) 203-209.
[44] T. Ishii, M. Miyazawa, A. Onodera, K. Yasuda, N. Kawabe, M. Kirinashizawa, S. Yoshimura, N. Maruyama, P.S. Hartman, N. Ishii, Mitochondrial reactive oxygen species generation by the SDHC V69E mutation causes low birth weight and neonatal growth retardation, Mitochondrion, 11 (2011) 155-165.

[45] F.G. Oostveen, H.C. Au, P.J. Meijer, I.E. Scheffler, A Chinese hamster mutant cell line with a defect in the integral membrane protein CII-3 of complex II of the mitochondrial electron transport chain, J. Biol. Chem., 270 (1995) 26104-26108.
[46] M.A. Selak, R.V. Duran, E. Gottlieb, Redox stress is not essential for the pseudo-hypoxic phenotype of succinate dehydrogenase deficient cells, Biochim. Biophys. Acta, 1757 (2006) 567-572.
[47] S.J. Boulton, M.A. Birch-Machin, Impact of hyperpigmentation on superoxide flux and melanoma cell metabolism at mitochondrial complex II, FASEB J., 29 (2015) 346-353.
[48] E.M. Redout, M.J. Wagner, M.J. Zuidwijk, C. Boer, R.J. Musters, C. van Hardeveld, W.J. Paulus, W.S. Simonides, Right-ventricular failure is associated with increased mitochondrial complex II activity and production of reactive oxygen species, Cardiovasc. Res., 75 (2007) 770-781.
[49] C. Bardella, P.J. Pollard, I. Tomlinson, SDH mutations in cancer, Biochim. Biophys. Acta, 1807 (2011) 1432-1443.
[50] K. Kluckova, A. Bezawork-Geleta, J. Rohlena, L. Dong, J. Neuzil, Mitochondrial complex II, a novel target for anti-cancer agents, Biochim. Biophys. Acta, 1827 (2013) 552-564.
[51] L. Galluzzi, J.M. Bravo-San Pedro, I. Vitale, S.A. Aaronson, J.M. Abrams, D. Adam, E.S. Alnemri, L. Altucci, D. Andrews, M. Annicchiarico-Petruzzelli, E.H. Baehrecke, N.G. Bazan, M.J. Bertrand, K. Bianchi, M.V. Blagosklonny, K. Blomgren, C. Borner, D.E. Bredesen, C. Brenner, M. Campanella, E. Candi, F. Cecconi, F.K. Chan, N.S. Chandel, E.H. Cheng, J.E. Chipuk, J.A. Cidlowski, A. Ciechanover, T.M. Dawson, V.L. Dawson, V. De Laurenzi, R. De Maria, K.M. Debatin, N. Di Daniele, V.M. Dixit, B.D. Dynlacht, W.S. El-Deiry, G.M. Fimia, R.A. Flavell, S. Fulda, C. Garrido, M.L. Gougeon, D.R. Green, H. Gronemeyer, G. Hajnoczky, J.M. Hardwick, M.O. Hengartner, H. Ichijo, B. Joseph, P.J. Jost, T. Kaufmann, O. Kepp, D.J. Klionsky, R.A. Knight, S. Kumar, J.J. Lemasters, B. Levine, A. Linkermann, S.A. Lipton, R.A. Lockshin, C. Lopez-Otin, E. Lugli, F. Madeo, W. Malorni, J.C. Marine, S.J. Martin, J.C. Martinou, J.P. Medema, P. Meier, S. Melino, N. Mizushima, U. Moll, C. Munoz-Pinedo, G. Nunez, A. Oberst, T. Panaretakis, J.M. Penninger, M.E. Peter, M. Piacentini, P. Pinton, J.H. Prehn, H. Puthalakath, G.A. Rabinovich, K.S. Ravichandran, R. Rizzuto, C.M. Rodrigues, D.C. Rubinsztein, T. Rudel, Y. Shi, H.U. Simon, B.R. Stockwell, G. Szabadkai, S.W. Tait, H.L. Tang, N. Tavernarakis, Y. Tsujimoto, T. Vanden Berghe, P. Vandenabeele, A. Villunger, E.F. Wagner, H. Walczak, E. White, W.G. Wood, J. Yuan, Z. Zakeri, B. Zhivotovsky, G. Melino, G. Kroemer, Essential versus accessory aspects of cell death: recommendations of the NCCD 2015, Cell Death Differ., 22 (2015) 58-73.
[52] L.A. Gillies, T. Kuwana, Apoptosis regulation at the mitochondrial outer membrane, J. Cell. Biochem., 115 (2014) 632-640.
[53] D. Westphal, G. Dewson, P.E. Czabotar, R.M. Kluck, Molecular biology of Bax and Bak activation and action, Biochim. Biophys. Acta, 1813 (2011) 521-531.
[54] H. Du, J. Wolf, B. Schafer, T. Moldoveanu, J.E. Chipuk, T. Kuwana, BH3 domains other than Bim and Bid can directly activate Bax/Bak, J. Biol. Chem., 286 (2011) 491-501.
[55] M.C. Wei, W.X. Zong, E.H. Cheng, T. Lindsten, V. Panoutsakopoulou, A.J. Ross, K.A. Roth, G.R. MacGregor, C.B. Thompson, S.J. Korsmeyer, Proapoptotic BAX and BAK: a requisite gateway to mitochondrial dysfunction and death, Science, 292 (2001) 727-730.
[56] D.R. Green, G. Kroemer, The pathophysiology of mitochondrial cell death, Science, 305 (2004) 626-629.
[57] S.J. Martin, C.P. Reutelingsperger, A.J. McGahon, J.A. Rader, R.C. van Schie, D.M. LaFace, D.R. Green, Early redistribution of plasma membrane phosphatidylserine is a general feature of apoptosis regardless of the initiating stimulus: inhibition by overexpression of Bcl-2 and Abl, J. Exp. Med., 182 (1995) 1545-1556.
[58] K. Segawa, S. Kurata, Y. Yanagihashi, T.R. Brummelkamp, F. Matsuda, S. Nagata, Caspase-mediated cleavage of phospholipid flippase for apoptotic phosphatidylserine exposure, Science, 344 (2014) 1164-1168.

[59] G. Kroemer, L. Galluzzi, P. Vandenabeele, J. Abrams, E.S. Alnemri, E.H. Baehrecke, M.V. Blagosklonny, W.S. El-Deiry, P. Golstein, D.R. Green, M. Hengartner, R.A. Knight, S. Kumar, S.A. Lipton, W. Malorni, G. Nunez, M.E. Peter, J. Tschopp, J. Yuan, M. Piacentini, B. Zhivotovsky, G. Melino, D. Nomenclature Committee on Cell, Classification of cell death: recommendations of the Nomenclature Committee on Cell Death 2009, Cell Death Differ., 16 (2009) 3-11.
[60] J.E. Ricci, R.A. Gottlieb, D.R. Green, Caspase-mediated loss of mitochondrial function and generation of reactive oxygen species during apoptosis, J. Cell Biol., 160 (2003) 65-75.
[61] J.E. Ricci, C. Munoz-Pinedo, P. Fitzgerald, B. Bailly-Maitre, G.A. Perkins, N. Yadava, I.E. Scheffler, M.H. Ellisman, D.R. Green, Disruption of mitochondrial function during apoptosis is mediated by caspase cleavage of the p75 subunit of complex I of the electron transport chain, Cell, 117 (2004) 773-786.
[62] M. Higuchi, R.J. Proske, E.T. Yeh, Inhibition of mitochondrial respiratory chain complex I by TNF results in cytochrome c release, membrane permeability transition, and apoptosis, Oncogene, 17 (1998) 2515-2524.
[63] T. Albayrak, V. Scherhammer, N. Schoenfeld, E. Braziulis, T. Mund, M.K. Bauer, I.E. Scheffler, S. Grimm, The tumor suppressor cybL, a component of the respiratory chain, mediates apoptosis induction, Mol. Biol. Cell, 14 (2003) 3082-3096.
[64] H. Bayir, V.E. Kagan, Bench-to-bedside review: Mitochondrial injury, oxidative stress and apoptosis--there is nothing more practical than a good theory, Crit. Care, 12 (2008) 206.
[65] M. D'Alessio, M. De Nicola, S. Coppola, G. Gualandi, L. Pugliese, C. Cerella, S. Cristofanon, P. Civitareale, M.R. Ciriolo, A. Bergamaschi, A. Magrini, L. Ghibelli, Oxidative Bax dimerization promotes its translocation to mitochondria independently of apoptosis, FASEB J., 19 (2005) 1504-1506.
[66] C. Nie, C. Tian, L. Zhao, P.X. Petit, M. Mehrpour, Q. Chen, Cysteine 62 of Bax is critical for its conformational activation and its proapoptotic activity in response to H2O2-induced apoptosis, J. Biol. Chem., 283 (2008) 15359-15369.
[67] J.Q. Kwong, M.S. Henning, A.A. Starkov, G. Manfredi, The mitochondrial respiratory chain is a modulator of apoptosis, J. Cell Biol., 179 (2007) 1163-1177.
[68] D.R. Green, L. Galluzzi, G. Kroemer, Cell biology. Metabolic control of cell death, Science, 345 (2014) 1250256.
[69] K.D. Marshall, C.P. Baines, Necroptosis: is there a role for mitochondria?, Front. Physiol., 5 (2014) 323.
[70] S. Mukhopadhyay, P.K. Panda, N. Sinha, D.N. Das, S.K. Bhutia, Autophagy and apoptosis: where do they meet?, Apoptosis, 19 (2014) 555-566.
[71] S.W. Tait, A. Oberst, G. Quarato, S. Milasta, M. Haller, R. Wang, M. Karvela, G. Ichim, N. Yatim, M.L. Albert, G. Kidd, R. Wakefield, S. Frase, S. Krautwald, A. Linkermann, D.R. Green, Widespread mitochondrial depletion via mitophagy does not compromise necroptosis, Cell Rep, 5 (2013) 878-885.
[72] G. Ashrafi, T.L. Schwarz, The pathways of mitophagy for quality control and clearance of mitochondria, Cell Death Differ., 20 (2013) 31-42.
[73] D. Hanahan, R.A. Weinberg, The hallmarks of cancer, Cell, 100 (2000) 57-70.
[74] D. Hanahan, R.A. Weinberg, Hallmarks of cancer: the next generation, Cell, 144 (2011) 646-674.
[75] W.H. Koppenol, P.L. Bounds, C.V. Dang, Otto Warburg's contributions to current concepts of cancer metabolism, Nat. Rev. Cancer, 11 (2011) 325-337.
[76] R. Moreno-Sanchez, S. Rodriguez-Enriquez, A. Marin-Hernandez, E. Saavedra, Energy metabolism in tumor cells, FEBS J., 274 (2007) 1393-1418.
[77] M.G. Vander Heiden, L.C. Cantley, C.B. Thompson, Understanding the Warburg effect: the metabolic requirements of cell proliferation, Science, 324 (2009) 1029-1033.
[78] A.J. Levine, A.M. Puzio-Kuter, The control of the metabolic switch in cancers by oncogenes and tumor suppressor genes, Science, 330 (2010) 1340-1344.

[79] A.R. Mullen, W.W. Wheaton, E.S. Jin, P.H. Chen, L.B. Sullivan, T. Cheng, Y. Yang, W.M. Linehan, N.S. Chandel, R.J. DeBerardinis, Reductive carboxylation supports growth in tumour cells with defective mitochondria, Nature, 481 (2012) 385-388.
[80] G. Kroemer, J. Pouyssegur, Tumor cell metabolism: cancer's Achilles' heel, Cancer Cell, 13 (2008) 472-482.
[81] H. Pelicano, D.S. Martin, R.H. Xu, P. Huang, Glycolysis inhibition for anticancer treatment, Oncogene, 25 (2006) 4633-4646.
[82] J.B. Wang, J.W. Erickson, R. Fuji, S. Ramachandran, P. Gao, R. Dinavahi, K.F. Wilson, A.L. Ambrosio, S.M. Dias, C.V. Dang, R.A. Cerione, Targeting mitochondrial glutaminase activity inhibits oncogenic transformation, Cancer Cell, 18 (2010) 207-219.
[83] V. Gogvadze, S. Orrenius, B. Zhivotovsky, Mitochondria in cancer cells: what is so special about them?, Trends Cell Biol., 18 (2008) 165-173.
[84] D. Trachootham, J. Alexandre, P. Huang, Targeting cancer cells by ROS-mediated mechanisms: a radical therapeutic approach?, Nat. Rev. Drug Discov., 8 (2009) 579-591.
[85] I.S. Harris, A.E. Treloar, S. Inoue, M. Sasaki, C. Gorrini, K.C. Lee, K.Y. Yung, D. Brenner, C.B. Knobbe-Thomsen, M.A. Cox, A. Elia, T. Berger, D.W. Cescon, A. Adeoye, A. Brustle, S.D. Molyneux, J.M. Mason, W.Y. Li, K. Yamamoto, A. Wakeham, H.K. Berman, R. Khokha, S.J. Done, T.J. Kavanagh, C.W. Lam, T.W. Mak, Glutathione and thioredoxin antioxidant pathways synergize to drive cancer initiation and progression, Cancer Cell, 27 (2015) 211-222.
[86] R. Elkholi, T.T. Renault, M.N. Serasinghe, J.E. Chipuk, Putting the pieces together: How is the mitochondrial pathway of apoptosis regulated in cancer and chemotherapy?, Cancer Metab, 2 (2014) 16.
[87] S. Bonnet, S.L. Archer, J. Allalunis-Turner, A. Haromy, C. Beaulieu, R. Thompson, C.T. Lee, G.D. Lopaschuk, L. Puttagunta, S. Bonnet, G. Harry, K. Hashimoto, C.J. Porter, M.A. Andrade, B. Thebaud, E.D. Michelakis, A mitochondria-K+ channel axis is suppressed in cancer and its normalization promotes apoptosis and inhibits cancer growth, Cancer Cell, 11 (2007) 37-51.
[88] M. Kulawiec, K.M. Owens, K.K. Singh, Cancer cell mitochondria confer apoptosis resistance and promote metastasis, Cancer Biol. Ther., 8 (2009) 1378-1385.
[89] P.L. Dahia, Pheochromocytoma and paraganglioma pathogenesis: learning from genetic heterogeneity, Nat. Rev. Cancer, 14 (2014) 108-119.
[90] J.K. Killian, S.Y. Kim, M. Miettinen, C. Smith, M. Merino, M. Tsokos, M. Quezado, W.I. Smith, Jr., M.S. Jahromi, P. Xekouki, E. Szarek, R.L. Walker, J. Lasota, M. Raffeld, B. Klotzle, Z. Wang, L. Jones, Y. Zhu, Y. Wang, J.J. Waterfall, M.J. O'Sullivan, M. Bibikova, K. Pacak, C. Stratakis, K.A. Janeway, J.D. Schiffman, J.B. Fan, L. Helman, P.S. Meltzer, Succinate dehydrogenase mutation underlies global epigenomic divergence in gastrointestinal stromal tumor, Cancer Discov., 3 (2013) 648-657.
[91] E. Letouze, C. Martinelli, C. Loriot, N. Burnichon, N. Abermil, C. Ottolenghi, M. Janin, M. Menara, A.T. Nguyen, P. Benit, A. Buffet, C. Marcaillou, J. Bertherat, L. Amar, P. Rustin, A. De Reynies, A.P. Gimenez-Roqueplo, J. Favier, SDH mutations establish a hypermethylator phenotype in paraganglioma, Cancer Cell, 23 (2013) 739-752.
[92] N.J. Kluckova K, Rohlena J, Mitochondrial Complex II in cancer, in: Mitochondria: The Anti-cancer Target for the Third Millennium, Springer Science+Business Media, Dordrecht, Netherland, 2014, pp. 81-104.
[93] S.J. Ralph, J. Neuzil, Mitochondria as targets for cancer therapy, Mol. Nutr. Food Res., 53 (2009) 9-28.
[94] J. Neuzil, L.F. Dong, J. Rohlena, J. Truksa, S.J. Ralph, Classification of mitocans, anti-cancer drugs acting on mitochondria, Mitochondrion, 13 (2013) 199-208.
[95] J. Rohlena, L.F. Dong, S.J. Ralph, J. Neuzil, Anticancer drugs targeting the mitochondrial electron transport chain, Antioxid. Redox Signal., 15 (2011) 2951-2974.

[96] J. Rohlena, L.F. Dong, J. Neuzil, Targeting the mitochondrial electron transport chain complexes for the induction of apoptosis and cancer treatment, Curr. Pharm. Biotechnol., 14 (2013) 377-389.
[97] P.I. Moreira, J. Custodio, A. Moreno, C.R. Oliveira, M.S. Santos, Tamoxifen and estradiol interact with the flavin mononucleotide site of complex I leading to mitochondrial failure, J. Biol. Chem., 281 (2006) 10143-10152.
[98] G. Liot, B. Bossy, S. Lubitz, Y. Kushnareva, N. Sejbuk, E. Bossy-Wetzel, Complex II inhibition by 3-NP causes mitochondrial fragmentation and neuronal cell death via an NMDA- and ROS-dependent pathway, Cell Death Differ., 16 (2009) 899-909.
[99] D.A. Wolf, Is Reliance on Mitochondrial Respiration a "Chink in the Armor" of Therapy-Resistant Cancer?, Cancer Cell, 26 (2014) 788-795.
[100] P. Corazao-Rozas, P. Guerreschi, M. Jendoubi, F. Andre, A. Jonneaux, C. Scalbert, G. Garcon, M. Malet-Martino, S. Balayssac, S. Rocchi, A. Savina, P. Formstecher, L. Mortier, J. Kluza, P. Marchetti, Mitochondrial oxidative stress is the Achille's heel of melanoma cells resistant to Braf-mutant inhibitor, Oncotarget, 4 (2013) 1986-1998.
[101] A. Roesch, A. Vultur, I. Bogeski, H. Wang, K.M. Zimmermann, D. Speicher, C. Korbel, M.W. Laschke, P.A. Gimotty, S.E. Philipp, E. Krause, S. Patzold, J. Villanueva, C. Krepler, M. Fukunaga-Kalabis, M. Hoth, B.C. Bastian, T. Vogt, M. Herlyn, Overcoming intrinsic multidrug resistance in melanoma by blocking the mitochondrial respiratory chain of slow-cycling JARID1B(high) cells, Cancer Cell, 23 (2013) 811-825.
[102] M. Nagai, N.H. Vo, L. Shin Ogawa, D. Chimmanamada, T. Inoue, J. Chu, B.C. Beaudette-Zlatanova, R. Lu, R.K. Blackman, J. Barsoum, K. Koya, Y. Wada, The oncology drug elesclomol selectively transports copper to the mitochondria to induce oxidative stress in cancer cells, Free Radic. Biol. Med., 52 (2012) 2142-2150.
[103] R.K. Blackman, K. Cheung-Ong, M. Gebbia, D.A. Proia, S. He, J. Kepros, A. Jonneaux, P. Marchetti, J. Kluza, P.E. Rao, Y. Wada, G. Giaever, C. Nislow, Mitochondrial electron transport is the cellular target of the oncology drug elesclomol, PLoS One, 7 (2012) e29798.
[104] D.L.a.N. J, Vitamin E Analogues as Prototypic Mitochondria-Targeting Anti-cancer Agents, in: Mitochondria: The Anti-cancer Target for the Third Millennium, Springer Science+Business Media, Dordrecht, Nedherland, 2014, pp. 151-181.
[105] C.W. Shiau, J.W. Huang, D.S. Wang, J.R. Weng, C.C. Yang, C.H. Lin, C. Li, C.S. Chen, alpha-Tocopheryl succinate induces apoptosis in prostate cancer cells in part through inhibition of Bcl-xL/Bcl-2 function, J. Biol. Chem., 281 (2006) 11819-11825.
[106] L.F. Dong, P. Low, J.C. Dyason, X.F. Wang, L. Prochazka, P.K. Witting, R. Freeman, E. Swettenham, K. Valis, J. Liu, R. Zobalova, J. Turanek, D.R. Spitz, F.E. Domann, I.E. Scheffler, S.J. Ralph, J. Neuzil, Alpha-tocopheryl succinate induces apoptosis by targeting ubiquinone-binding sites in mitochondrial respiratory complex II, Oncogene, 27 (2008) 4324-4335.
[107] L. Prochazka, L.F. Dong, K. Valis, R. Freeman, S.J. Ralph, J. Turanek, J. Neuzil, alpha-Tocopheryl succinate causes mitochondrial permeabilization by preferential formation of Bak channels, Apoptosis, 15 (2010) 782-794.
[108] K. Valis, L. Prochazka, E. Boura, J. Chladova, T. Obsil, J. Rohlena, J. Truksa, L.F. Dong, S.J. Ralph, J. Neuzil, Hippo/Mst1 stimulates transcription of the proapoptotic mediator NOXA in a FoxO1-dependent manner, Cancer Res., 71 (2011) 946-954.
[109] H. Dalen, J. Neuzil, Alpha-tocopheryl succinate sensitises a T lymphoma cell line to TRAIL-induced apoptosis by suppressing NF-kappaB activation, Br. J. Cancer, 88 (2003) 153-158.
[110] M. Tomasetti, L. Andera, R. Alleva, B. Borghi, J. Neuzil, A. Procopio, Alpha-tocopheryl succinate induces DR4 and DR5 expression by a p53-dependent route: implication for sensitisation of resistant cancer cells to TRAIL apoptosis, FEBS Lett., 580 (2006) 1925-1931.

[111] S.J. Lim, M.K. Choi, M.J. Kim, J.K. Kim, Alpha-tocopheryl succinate potentiates the paclitaxel-induced apoptosis through enforced caspase 8 activation in human H460 lung cancer cells, Exp. Mol. Med., 41 (2009) 737-745.
[112] K. Kanai, E. Kikuchi, S. Mikami, E. Suzuki, Y. Uchida, K. Kodaira, A. Miyajima, T. Ohigashi, J. Nakashima, M. Oya, Vitamin E succinate induced apoptosis and enhanced chemosensitivity to paclitaxel in human bladder cancer cells in vitro and in vivo, Cancer Sci., 101 (2010) 216-223.
[113] B. Kruspig, B. Zhivotovsky, V. Gogvadze, Contrasting effects of alpha-tocopheryl succinate on cisplatin- and etoposide-induced apoptosis, Mitochondrion, 13 (2013) 533-538.
[114] L.F. Dong, R. Freeman, J. Liu, R. Zobalova, A. Marin-Hernandez, M. Stantic, J. Rohlena, K. Valis, S. Rodriguez-Enriquez, B. Butcher, J. Goodwin, U.T. Brunk, P.K. Witting, R. Moreno-Sanchez, I.E. Scheffler, S.J. Ralph, J. Neuzil, Suppression of tumor growth in vivo by the mitocan alpha-tocopheryl succinate requires respiratory complex II, Clin. Cancer. Res., 15 (2009) 1593-1600.
[115] L.F. Dong, E. Swettenham, J. Eliasson, X.F. Wang, M. Gold, Y. Medunic, M. Stantic, P. Low, L. Prochazka, P.K. Witting, J. Turanek, E.T. Akporiaye, S.J. Ralph, J. Neuzil, Vitamin E analogues inhibit angiogenesis by selective induction of apoptosis in proliferating endothelial cells: the role of oxidative stress, Cancer Res., 67 (2007) 11906-11913.
[116] G.A. dos Santos, R.S. Abreu e Lima, C.R. Pestana, A.S. Lima, P.S. Scheucher, C.H. Thome, H.L. Gimenes-Teixeira, B.A. Santana-Lemos, A.R. Lucena-Araujo, F.P. Rodrigues, R. Nasr, S.A. Uyemura, R.P. Falcao, H. de The, P.P. Pandolfi, C. Curti, E.M. Rego, (+)alpha-Tocopheryl succinate inhibits the mitochondrial respiratory chain complex I and is as effective as arsenic trioxide or ATRA against acute promyelocytic leukemia in vivo, Leukemia, 26 (2012) 451-460.
[117] J. Gruber, K. Staniek, C. Krewenka, R. Moldzio, A. Patel, S. Bohmdorfer, T. Rosenau, L. Gille, Tocopheramine succinate and tocopheryl succinate: mechanism of mitochondrial inhibition and superoxide radical production, Bioorg. Med. Chem., 22 (2014) 684-691.
[118] T. Weber, H. Dalen, L. Andera, A. Negre-Salvayre, N. Auge, M. Sticha, A. Lloret, A. Terman, P.K. Witting, M. Higuchi, M. Plasilova, J. Zivny, N. Gellert, C. Weber, J. Neuzil, Mitochondria play a central role in apoptosis induced by alpha-tocopheryl succinate, an agent with antineoplastic activity: comparison with receptor-mediated pro-apoptotic signaling, Biochemistry, 42 (2003) 4277-4291.
[119] X.F. Wang, P.K. Witting, B.A. Salvatore, J. Neuzil, Vitamin E analogs trigger apoptosis in HER2/erbB2-overexpressing breast cancer cells by signaling via the mitochondrial pathway, Biochem. Biophys. Res. Commun., 326 (2005) 282-289.
[120] W. Yu, B.G. Sanders, K. Kline, RRR-alpha-tocopheryl succinate-induced apoptosis of human breast cancer cells involves Bax translocation to mitochondria, Cancer Res., 63 (2003) 2483-2491.
[121] V. Gogvadze, E. Norberg, S. Orrenius, B. Zhivotovsky, Involvement of Ca2+ and ROS in alpha-tocopheryl succinate-induced mitochondrial permeabilization, Int. J. Cancer, 127 (2010) 1823-1832.
[122] J. Neuzil, T. Weber, N. Gellert, C. Weber, Selective cancer cell killing by alpha-tocopheryl succinate, Br. J. Cancer, 84 (2001) 87-89.
[123] J. Neuzil, T. Weber, A. Schroder, M. Lu, G. Ostermann, N. Gellert, G.C. Mayne, B. Olejnicka, A. Negre-Salvayre, M. Sticha, R.J. Coffey, C. Weber, Induction of cancer cell apoptosis by alpha-tocopheryl succinate: molecular pathways and structural requirements, FASEB J., 15 (2001) 403-415.
[124] J. Quin, D. Engle, A. Litwiller, E. Peralta, A. Grasch, T. Boley, S. Hazelrigg, Vitamin E succinate decreases lung cancer tumor growth in mice, J. Surg. Res., 127 (2005) 139-143.
[125] M. Tomasetti, N. Gellert, A. Procopio, J. Neuzil, A vitamin E analogue suppresses malignant mesothelioma in a preclinical model: a future drug against a fatal neoplastic disease?, Int. J. Cancer, 109 (2004) 641-642.
[126] J. Neuzil, Alpha-tocopheryl succinate epitomizes a compound with a shift in biological activity due to pro-vitamin-to-vitamin conversion, Biochem. Biophys. Res. Commun., 293 (2002) 1309-1313.

[127] A. Glasauer, N.S. Chandel, Targeting antioxidants for cancer therapy, Biochem. Pharmacol., 92 (2014) 90-101.
[128] C. Gorrini, I.S. Harris, T.W. Mak, Modulation of oxidative stress as an anticancer strategy, Nat. Rev. Drug Discov., 12 (2013) 931-947.
[129] M. Sciacovelli, E. Gaude, M. Hilvo, C. Frezza, The metabolic alterations of cancer cells, Methods Enzymol., 542 (2014) 1-23.
[130] J. Neuzil, L.F. Dong, L. Ramanathapuram, T. Hahn, M. Chladova, X.F. Wang, R. Zobalova, L. Prochazka, M. Gold, R. Freeman, J. Turanek, E.T. Akporiaye, J.C. Dyason, S.J. Ralph, Vitamin E analogues as a novel group of mitocans: anti-cancer agents that act by targeting mitochondria, Mol. Aspects Med., 28 (2007) 607-645.
[131] G.F. Kelso, C.M. Porteous, C.V. Coulter, G. Hughes, W.K. Porteous, E.C. Ledgerwood, R.A. Smith, M.P. Murphy, Selective targeting of a redox-active ubiquinone to mitochondria within cells: antioxidant and antiapoptotic properties, J. Biol. Chem., 276 (2001) 4588-4596.
[132] M.P. Murphy, Targeting lipophilic cations to mitochondria, Biochim. Biophys. Acta, 1777 (2008) 1028-1031.
[133] L.F. Dong, V.J. Jameson, D. Tilly, J. Cerny, E. Mahdavian, A. Marin-Hernandez, L. Hernandez-Esquivel, S. Rodriguez-Enriquez, J. Stursa, P.K. Witting, B. Stantic, J. Rohlena, J. Truksa, K. Kluckova, J.C. Dyason, M. Ledvina, B.A. Salvatore, R. Moreno-Sanchez, M.J. Coster, S.J. Ralph, R.A. Smith, J. Neuzil, Mitochondrial targeting of vitamin E succinate enhances its pro-apoptotic and anti-cancer activity via mitochondrial complex II, J. Biol. Chem., 286 (2011) 3717-3728.
[134] L.F. Dong, V.J. Jameson, D. Tilly, L. Prochazka, J. Rohlena, K. Valis, J. Truksa, R. Zobalova, E. Mahdavian, K. Kluckova, M. Stantic, J. Stursa, R. Freeman, P.K. Witting, E. Norberg, J. Goodwin, B.A. Salvatore, J. Novotna, J. Turanek, M. Ledvina, P. Hozak, B. Zhivotovsky, M.J. Coster, S.J. Ralph, R.A. Smith, J. Neuzil, Mitochondrial targeting of alpha-tocopheryl succinate enhances its pro-apoptotic efficacy: a new paradigm for effective cancer therapy, Free Radic. Biol. Med., 50 (2011) 1546-1555.
[135] A.J. Levine, M. Oren, The first 30 years of p53: growing ever more complex, Nat. Rev. Cancer, 9 (2009) 749-758.
[136] J.S. Modica-Napolitano, J.R. Aprille, Delocalized lipophilic cations selectively target the mitochondria of carcinoma cells, Adv Drug Deliv Rev, 49 (2001) 63-70.
[137] L.B. Chen, Mitochondrial membrane potential in living cells, Annu. Rev. Cell Biol., 4 (1988) 155-181.
[138] J. Truksa, L. Dong, J. Rohlena, J. Stursa, M. Vondrusova, J. Goodwin, M. Nguyen, K. Kluckova, Z. Rychtarcikova, S. Lettlova, J. Spacilova, M. Stapelberg, M. Zoratti, J. Neuzil, Mitochondrially targeted vitamin E succinate modulates expression of mitochondrial DNA transcripts and mitochondrial biogenesis, Antioxid. Redox Signal., (2015).
[139] J. Rohlena, L.F. Dong, K. Kluckova, R. Zobalova, J. Goodwin, D. Tilly, J. Stursa, A. Pecinova, A. Philimonenko, P. Hozak, J. Banerjee, M. Ledvina, C.K. Sen, J. Houstek, M.J. Coster, J. Neuzil, Mitochondrially targeted alpha-tocopheryl succinate is antiangiogenic: potential benefit against tumor angiogenesis but caution against wound healing, Antioxid. Redox Signal., 15 (2011) 2923-2935.
[140] L. Prochazka, S. Koudelka, L.F. Dong, J. Stursa, J. Goodwin, J. Neca, J. Slavik, M. Ciganek, J. Masek, K. Kluckova, M. Nguyen, J. Turanek, J. Neuzil, Mitochondrial targeting overcomes ABCA1-dependent resistance of lung carcinoma to alpha-tocopheryl succinate, Apoptosis, 18 (2013) 286-299.
[141] S. Grimm, Respiratory chain complex II as general sensor for apoptosis, Biochim. Biophys. Acta, 1827 (2013) 565-572.
[142] M.P. Paranagama, K. Sakamoto, H. Amino, M. Awano, H. Miyoshi, K. Kita, Contribution of the FAD and quinone binding sites to the production of reactive oxygen species from Ascaris suum mitochondrial complex II, Mitochondrion, 10 (2010) 158-165.

[143] S.M. Kluckova K, Cerny J, Mracek T, Dong L, Drahota Z, Gottlieb E, Neuzil J and Rohlena J, Ubiquinone-binding site mutagenesis reveals the role of mitochondrial complex II in cell death initiation, Cell Death Dis., Accepted for publication.
[144] P.J. Pollard, J.J. Briere, N.A. Alam, J. Barwell, E. Barclay, N.C. Wortham, T. Hunt, M. Mitchell, S. Olpin, S.J. Moat, I.P. Hargreaves, S.J. Heales, Y.L. Chung, J.R. Griffiths, A. Dalgleish, J.A. McGrath, M.J. Gleeson, S.V. Hodgson, R. Poulsom, P. Rustin, I.P. Tomlinson, Accumulation of Krebs cycle intermediates and over-expression of HIF1alpha in tumours which result from germline FH and SDH mutations, Hum. Mol. Genet., 14 (2005) 2231-2239.
[145] M.A. Selak, S.M. Armour, E.D. MacKenzie, H. Boulahbel, D.G. Watson, K.D. Mansfield, Y. Pan, M.C. Simon, C.B. Thompson, E. Gottlieb, Succinate links TCA cycle dysfunction to oncogenesis by inhibiting HIF-alpha prolyl hydroxylase, Cancer Cell, 7 (2005) 77-85.
[146] S. Rodriguez-Enriquez, L. Hernandez-Esquivel, A. Marin-Hernandez, L.F. Dong, E.T. Akporiaye, J. Neuzil, S.J. Ralph, R. Moreno-Sanchez, Molecular mechanism for the selective impairment of cancer mitochondrial function by a mitochondrially targeted vitamin E analogue, Biochim. Biophys. Acta, 1817 (2012) 1597-1607.
[147] M. Huttemann, I. Lee, A. Pecinova, P. Pecina, K. Przyklenk, J.W. Doan, Regulation of oxidative phosphorylation, the mitochondrial membrane potential, and their role in human disease, J. Bioenerg. Biomembr., 40 (2008) 445-456.
[148] S.S. Korshunov, V.P. Skulachev, A.A. Starkov, High protonic potential actuates a mechanism of production of reactive oxygen species in mitochondria, FEBS Lett., 416 (1997) 15-18.
[149] R. Moreno-Sanchez, L. Hernandez-Esquivel, N.A. Rivero-Segura, A. Marin-Hernandez, J. Neuzil, S.J. Ralph, S. Rodriguez-Enriquez, Reactive oxygen species are generated by the respiratory complex II--evidence for lack of contribution of the reverse electron flow in complex I, FEBS J., 280 (2013) 927-938.
[150] A.S. Tan, J.W. Baty, L.F. Dong, A. Bezawork-Geleta, B. Endaya, J. Goodwin, M. Bajzikova, J. Kovarova, M. Peterka, B. Yan, E.A. Pesdar, M. Sobol, A. Filimonenko, S. Stuart, M. Vondrusova, K. Kluckova, K. Sachaphibulkij, J. Rohlena, P. Hozak, J. Truksa, D. Eccles, L.M. Haupt, L.R. Griffiths, J. Neuzil, M.V. Berridge, Mitochondrial genome acquisition restores respiratory function and tumorigenic potential of cancer cells without mitochondrial DNA, Cell Metab, 21 (2015) 81-94.

APPENDIX

Publications that are part of the thesis:

THE JOURNAL OF BIOLOGICAL CHEMISTRY VOL. 286, NO. 5, pp. 3717–3728, February 4, 2011

Mitochondrial Targeting of Vitamin E Succinate Enhances Its Pro-apoptotic and Anti-cancer Activity via Mitochondrial Complex II*[S]

Received for publication, September 20, 2010, and in revised form, October 28, 2010 Published, JBC Papers in Press, November 8, 2010, DOI 10.1074/jbc.M110.186643

Lan-Feng Dong,[a] Victoria J. A. Jameson,[b] David Tilly,[c] Jiri Cerny,[d] Elahe Mahdavian,[e] Alvaro Marín-Hernández,[f] Luz Hernández-Esquivel,[f] Sara Rodríguez-Enríquez,[f] Jan Stursa,[g] Paul K. Witting,[h] Bela Stantic,[i] Jakub Rohlena,[d] Jaroslav Truksa,[d] Katarina Kluckova,[d] Jeffrey C. Dyason,[j] Miroslav Ledvina,[g] Brian A. Salvatore,[e] Rafael Moreno-Sánchez,[f] Mark J. Coster,[c] Stephen J. Ralph,[a] Robin A. J. Smith,[b] and Jiri Neuzil[a,j1]

From the [a]School of Medical Science, [i]Institute for Integrated and Intelligent Systems, and [j]Institute for Glycomics, Griffith University, Southport 4222, Queensland, Australia, the [b]Department of Chemistry, University of Otago, Dunedin 9016, New Zealand, the [c]Eskitis Institute for Cell and Molecular Therapies, Griffith University, Nathan 4111, Queensland, Australia, the [d]Institute of Biotechnology and [g]Institute of Organic Chemistry and Biochemistry, Academy of Sciences of the Czech Republic, Prague 14220, Czech Republic, the [e]Department of Chemistry and Physics, Louisiana State University, Shreveport, Louisiana 71115, the [f]Department of Biochemistry, National Institute of Cardiology, Mexico City 14080, Mexico, and the [h]Discipline of Pathology, Bosch Research Institute, Sydney Medical School, University of Sydney, Sydney 2006, New South Wales, Australia

Mitochondrial complex II (CII) has been recently identified as a novel target for anti-cancer drugs. Mitochondrially targeted vitamin E succinate (MitoVES) is modified so that it is preferentially localized to mitochondria, greatly enhancing its pro-apoptotic and anti-cancer activity. Using genetically manipulated cells, MitoVES caused apoptosis and generation of reactive oxygen species (ROS) in CII-proficient malignant cells but not their CII-dysfunctional counterparts. MitoVES inhibited the succinate dehydrogenase (SDH) activity of CII with IC_{50} of 80 μM, whereas the electron transfer from CII to CIII was inhibited with IC_{50} of 1.5 μM. The agent had no effect either on the enzymatic activity of CI or on electron transfer from CI to CIII. Over 24 h, MitoVES caused stabilization of the oxygen-dependent destruction domain of HIF1α fused to GFP, indicating promotion of the state of pseudohypoxia. Molecular modeling predicted the succinyl group anchored into the proximal CII ubiquinone (UbQ)-binding site and successively reduced interaction energies for serially shorter phytyl chain homologs of MitoVES correlated with their lower effects on apoptosis induction, ROS generation, and SDH activity. Mutation of the UbQ-binding Ser^{68} within the proximal site of the CII SDHC subunit (S68A or S68L) suppressed both ROS generation and apoptosis induction by MitoVES. *In vivo* studies indicated that MitoVES also acts by causing pseudohypoxia in the context of tumor suppression. We propose that mitochondrial targeting of VES with an 11-carbon chain localizes the agent into an ideal position across the interface of the mitochondrial inner membrane and matrix, optimizing its biological effects as an anti-cancer drug.

Mitochondria are emerging as targets for a variety of anti-cancer drugs (1–5) that belong to a group of compounds termed "mitocans" (6, 7). Of these agents, we and others have been studying the group of vitamin E (VE)[2] analogs, epitomized by the "redox-silent" α-tocopheryl succinate (α-TOS) and α-tocopheryl acetyl ether (8). Both of these agents proved to be selective inducers of apoptosis in cancer cells and efficient suppressors of tumors in experimental models (9–16).

VE analogs with anti-cancer activity have been classified as mitocans (*i.e.* small anti-cancer agents that act by selectively destabilizing mitochondria in cancer cells) (6–8). Of the several groups of mitocans, the anti-cancer VE analogs belong to both the class of BH3 mimetics, which includes compounds interfering with the interactions of the Bcl-2 family proteins (17), as well as to the class of agents that interfere with the mitochondrial electron redox chain. The latter activity is probably the main reason for the strong apoptogenic efficacy of agents like α-TOS (18). More specifically, α-TOS interferes

* This work was supported by grants from the Australian Research Council, the Cancer Council Queensland, the National Breast Cancer Foundation, Grant Agency of the Czech Republic Grants 204/08/0811 and P301/10/1937, Grant Agency of the Academy of Sciences of the Czech Republic Grants IAA500520702, KJB500970904, and KAN200520703) (to J. N.), the Griffith Health Institute (to L.-F. D.), the Otago University Research Grants Committee (to R. A. J. S.), Consejo Nacional de Ciencia y Tecnologia-México Grants 80534 and 20675 (to R. M.-S. and S. R.-E.), and National Institutes of Health, NCRR, Grant P20RR016456 (to E. M. and B. A. S.).

[S] The on-line version of this article (available at http://www.jbc.org) contains supplemental material describing the synthesis of VE analogs.

[1] To whom correspondence should be addressed: Apoptosis Research Group, School of Medical Science, Griffith Health Institute, Griffith University Gold Coast Campus, Parklands Ave., Southport, Queensland 4222, Australia. Tel.: 61-2-555-29109; Fax: 61-2-555-28804; E-mail: j.neuzil@griffith.edu.au.

[2] The abbreviations used are: VE, vitamin E; CI, CII, and CIII, complex I, II, and III, respectively; FCCP, carbonyl cyanide *p*-(trifluoromethoxy) phenylhydrazone; MIM, mitochondrial inner membrane; MitoQ, mitochondrially targeted coenzyme Q; MitoVES, mitochondrially targeted vitamin E succinate; MitoVE_nS, MitoVES homologue with *n* carbons linking the tocopheryl headgroup and the triphenyphosphonium group; ODD, oxygen-dependent destruction; POPE, phosphatidylethanolamine; ROS, reactive oxygen species; SDH, succinate dehydrogenase; SMP, submitochondrial particle; α-TOS, α-tocopheryl succinate; TPP^+, triphenylphosphonium; UbQ, ubiquinone; USI, ultrasound imaging; VES, vitamin E succinate; $\Delta\Psi_{m,i}$, mitochondrial inner transmembrane potential; Q_P, proximal UbQ site; Q_D, distal UbQ site; qPCR, quantitative PCR; mtDNA, mitochondrial DNA.

with the ubiquinone (UbQ)-binding site(s) of the mitochondrial complex II (CII), an event that results in generation of reactive oxygen species (ROS), in turn causing apoptosis induction (19). Moreover, CII has also been shown to be important for the anti-tumor efficacy of α-TOS (20).

Although α-TOS acts on mitochondria, it does not discriminate between the different membranous compartments within the cell. Therefore, we decided to generate a variant of the agent that would be targeted to mitochondria, anticipating that by doing so, its apoptogenic activity would be increased. This reasoning was based on the work from the group of Murphy and Smith, who prepared a series of mitochondrially targeted antioxidants by tagging them with the positively charged triphenylphosphonium group (TPP^+) (21), producing very efficient redox-active compounds (22–24). Further, we assumed that the TPP^+ group will be advantageous for the cancer cell specificity of the agents because cancer cell mitochondria feature greater mitochondrial inner membrane potential ($\Delta\Psi_{m,i}$) than normal cells (25–27). Our recent work[3] documents that the prototypic compound of such a targeted VE analog (*i.e.* mitochondrially targeted vitamin E succinate (MitoVES)) indeed is some 1–2 orders of magnitude more apoptogenic than the untargeted, parental compound.

Molecular modeling and theoretical considerations suggest that tagging a hydrophobic compound with a cationic group, such as in the case of MitoVES, will dictate its position at the interface of the mitochondrial inner membrane (MIM) and the mitochondrial matrix. Therefore, we expect that it will be juxtapositioned to preferentially interact with CII more than the untargeted VE analog, such that its apoptogenic activity would be much greater. In this paper, we show that, indeed, MitoVES interacts with the proximal UbQ-binding (Q_p) site of CII, which endows it with greater activity for inducing cancer cell apoptosis.

EXPERIMENTAL PROCEDURES

Cell Culture—Human T lymphoma Jurkat cells were grown in RPMI medium supplemented with 10% FCS and antibiotics. Chinese hamster lung fibroblasts with a dysfunctional CII (B9 cells) as well as the parental cells (B1 cells) (28) were grown in DMEM with 10% FCS, antibiotics, 10 mg/ml glucose, and 1% non-essential amino acids. The cells were transformed to malignancy by transfection with an *H-RAS* vector (29), and CII in the B9 cells was reconstituted as reported elsewhere (20, 30). The human colon cancer cells $HCT116_{ODD\text{-}GFP}$ were cultured in DMEM with 10% FCS plus antibiotics; this subline was prepared by stable transfection of HCT116 cells using a plasmid coding for the oxygen-dependent destruction (ODD) domain of the HIF1α protein fused with GFP (31, 32).

Preparation of Submitochondrial Particles (SMPs)—Coupled bovine heart SMPs were obtained from frozen mitochondria (20–30 mg of protein/ml) incubated in the SHE medium (250 mM sucrose, 10 mM HEPES, 1 mM EGTA, pH 7.2) supplemented with 3 mM $MgCl_2$, 3 mM ATP, and 20 mM succinate. The mitochondrial suspensions were sonicated three times in aliquots of 20 ml on ice for 15 s, with a 5-mm diameter probe tip using a Branson Sonifier 450 sonicator. The suspensions were diluted in the SHE medium and centrifuged twice at 17,370 $\times$ *g* for 5 min at 4 °C. The supernatant was then centrifuged at 105,000 $\times$ *g* for 40 min at 4 °C. The pellet was resuspended in the SHE medium plus 1% (w/v) fatty acid-free BSA and stored at −70 °C until use (33).

Synthesis of VE Analogs—The synthesis of the prototypic, racemic $MitoVE_{11}S$ (**2**), an agent with an 11-C chain linking the TPP and the tocopheryl succinyl group, and its shorter chain homologs $MitoVE_9S$ (**3**), $MitoVE_7S$ (**4**), and $MitoVE_5S$ (**5**), as well as its stereoisomers *S*-$MitoVE_{11}S$ (**6**) and *R*-$MitoVE_{11}S$ (**7**), is shown in the supplemental material.

Assessment of Apoptosis, ROS Generation, and Mitochondrial Potential—Apoptosis levels were assessed using the annexin V/propidium iodide method (19). Cellular ROS levels were detected using dihydroethidium (Molecular Probes) and flow cytometry and expressed as mean fluorescence intensity or by trapping with 5,5-dimethyl-1-pyrroline *N*-oxide (Sigma) using EPR spectroscopy (19) and expressed in arbitrary units/mg of cellular protein. $\Delta\Psi_{m,i}$ was assessed using the fluorescent probe tetramethylrhodamine methyl ester and flow cytometry according to a standard protocol.

Assessment of CI, CII, and CIII Activity—In whole cells, succinate dehydrogenase (SDH) activity was estimated using a short term (1 h) modified MTT assay with succinate as the sole source of electrons driving the respiratory system, specifically via CII, as described (18). For SMPs, CI and CII dehydrogenase activities were determined at 37 °C in 1 ml of the SHE medium that also contained 0.075–0.1 mM 2,6-dichlorophenol indophenol and 0.025 mg/ml protein. The reaction was started after a 15-min preincubation with $MitoVE_{11}S$ by adding succinate (0.25–2 mM) or NADH (0.1–1 mM) as CII or CI substrates, respectively. The rate of 2,6-dichlorophenol indophenol reduction was determined by measuring the absorbance change at 600 nm and using the extinction coefficient of 21.3 $mM^{-1}\ cm^{-1}$. The CII dehydrogenase activity (SDH) was completely inhibited by malonate.

The activities of both succinate-cytochrome *c* oxidoreductase (complex II + III) and NADH-cytochrome *c* oxidoreductase (complex I + III) were determined at 37 °C in 1 ml of 50 mM Hepes, pH 7.2, 1 mM cyanide, 50 μM cytochrome *c* (from horse heart) and SMPs at 25 μg of protein. The reaction was started after a 15-min preincubation with $MitoVE_{11}S$ by adding succinate (0.25–2 mM) or NADH (0.1–1 mM). The activity was determined in a dual wavelength spectrophotometer by measuring the reduction of oxidized cytochrome *c* over time from the absorbance difference at 550 and 540 nm and by using the extinction coefficient of 19.1 $mM^{-1}\ cm^{-1}$ (34). The CII oxidoreductase activity was fully blocked by malonate or antimycin, whereas the CI oxidoreductase activity was 88% inhibited by 20 μM rotenone.

[3] L.-F. Dong, V. J. A. Jameson, D. Tilly, L. Prochazka, J. Rohlena, K. Valis, J. Truksa, R. Zobalova, E. Mahdavian, K. Kluckova, M. Stantic, J. Stursa, X.-F. Wang, R. Freeman, P. K. Witting, E. Norberg, J. Goodwin, B. A. Salvatore, J. Novotna, J. Turanek, M. Ledvina, P. Hozak, B. Zhivotovsky, M. J. Coster, S. J. Ralph, R. A. J. Smith, and J. Neuzil, submitted for publication.

TABLE 1
Primers used for qPCR and RT-PCR

Gene	Primers	
	Forward	Reverse
ND1	5′-ATA CCC ATG GCC AAC CTC CT-3′	5′-GGG CCT TTG CGT AGT TGT AT-3′
ND2	5′-GGC CCA ACC CGT CAT CTA CT3′	5′-GAT GCG GTT GCT TGC GTG AG-3′
ND3	5′-CCG CGT CCC TTT CTC CAT AA-3′	5′-GGT AGG GGT AAA AGG AGG GC-3′
ND4	5′-ACT ACT CAC TCT CAC TGC CC-3′	5′-AGT GGA GTC CGT AAA GAG GT-3′
ND4L	5′-AAC CCT CAA CAC CCA CTC CC-3′	5′-TAG GCC CAC CGC TGC TTC GC-3′
ND5	5′-AAC AGA GTG GTG ATA GCG CC-3′	5′-CCC TAC TCC ACT CAA GCA CT-3′
ND6	5′-CCT ACC TCC ATC GCT AAC CC-3′	5′-AGG GGG AAT GAT GGT TGT CT-3′
CYTB	5′-GAA ACT TCG GCT CAC TCC TT-3′	5′-GGC GAT TGA TGA AAA GGC GG-3′
COX1	5′-GCC TCC GTA GAC CTA ACC AT-3′	5′-GTT ATG GCA GGG GGT TTT AT-3′
COX2	5′-AGT CCT GTA TGC CCT TTT CC-3′	5′-GCG ATG AGG ACT AGG ATG AT-3′
COX3	5′-CCC ACC AAT CAC ATG CCT AT-3′	5′-TAG GCC GGA GGT CAT TAG GA-3′
ATP6	5′-CTG TTC GCT TCA TTC ATT GC-3′	5′-GAT TAG TCA TTG TTG GGT GG-3′
ATP8	5′-TGC CCC AAC TAA ATA CTA CC-3′	5′-CTT TGG TGA GGG AGG TAG GT-3′
P0	5′-TCG ACA ATG GCA GCA TCT AC-3′	5′-ATC CGT CTC CAC AGA CAA GG-3′

Isolation of Mitochondria and Gel Filtration Chromatography—Cells (1.2×10^8) were treated with $MitoVE_{11}S$ for different periods and harvested. The pellet was resuspended in 0.5 ml of ice-cold hypotonic fractionation buffer (25 mM Tris at pH 7.4, 2 mM EDTA, 5 mM $MgCl_2$, 10 mM KCl, 125 mM sucrose, 1 mM PMSF plus a protease inhibitor mixture) and left on ice for 10 min. The swollen cells were lysed using a glass homogenizer (Kontes Glass Co.). The isotonicity of each sample was achieved by the addition of 250 μl of ice-cold hypertonic fractionation buffer with 0.5 M sucrose. Organelles and unbroken cells were centrifuged at 900 $\times$ *g* for 10 min, followed by centrifugation of the supernatant at 1,700 $\times$ *g* for 5 min. The remaining supernatant was then centrifuged at 15,000 $\times$ *g* for 10 min, and the mitochondrial pellet was lysed in a buffer comprising 25 mM HEPES, pH 7.5, 0.3 M NaCl, and 2% CHAPS. The mitochondrial lysates were centrifuged at 19,000 $\times$ *g* for 5 min and loaded onto a Superdex-200 10/300 preparation grade column (separation range 10 to ~600 kDa; Amersham Biosciences) equilibrated with the 2% CHAPS lysis buffer (see above). Proteins were eluted at 0.3 ml/min, and fractions of 0.5 ml were collected and mixed with 3× Laemmli reducing sample buffer and boiled. The samples were then analyzed by SDS-PAGE and Western blotting for subunits of CI, CII, and CIII.

Western Blotting—Proteins in whole cell lysates or mitochondrial fractions were separated using SDS-PAGE before Western blotting was performed according to a standard protocol using the antibody to the CI 39-kDa subunit (clone 20C11), the CIII core-2 subunit (clone 16D10; both from Invitrogen), and the CII SDHC subunit (clone M01; Santa Cruz Biotechnology, Inc. (Santa Cruz, CA)).

RT-PCR and qPCR—The amount of target mRNA was assessed by RT-PCR and qPCR. Total RNA was isolated using the Aurum RNA total minikit, including the DNase treatment step (Bio-Rad), and reverse transcribed by the Revertaid First Strand cDNA synthesis kit (Fermentas) according to the manufacturer's instructions (1–5 μg of total RNA per 20 μl of reaction mixture). RT-PCR was carried out using the standard procedure. For qPCR, cDNA corresponding to 12 ng of starting total RNA was diluted with water into 4.5 μl, 0.5 μl of the combined 10 μM forward and reverse primers were added, and, finally, 5 μl of 2× SYBR Green JumpStart Taq ready mix (Sigma) was added, and the reaction was carried out on a Bio-Rad CFX96 real-time thermal cycler using three-step PCR (98 °C for 5 s, 60 °C for 15 s, and 72 °C for 25 s) for 40 cycles followed by melting curve analysis. Primers were designed on the intron/exon boundaries to prevent DNA amplification and are listed in Table 1.

Site-directed Mutagenesis—The S68A and S68L substitutions were introduced by site-directed mutagenesis of human WT *SDHC* cDNA in the *pEF-IRES-PURO* expression vector using the QuikChange Lightning mutagenesis kit (Stratagene) and the following primers: S68A, 5′-TCC CAT GGC GAT GGC CAT CTG CCA CCG-3′ (forward) and 5′-CGG TGG CAG ATG GCC ATC GCC ATG GGA-3′ (reverse); S68L, 5′-CTT CCC ATG GCG ATG TTA ATC TGC CAC CGT GGC A-3′ (forward) and 5′-TGC CAC GGT GGC AGA TTA ACA TCG CCA TGG GAA G-3′ (reverse). The constructs were confirmed by sequencing and used to transfect the SDHC-deficient B9 fibroblasts using the Superfect reagent (Qiagen), followed by incubation with 2–4 μg/ml puromycin (Sigma) for 2 weeks. Clones were analyzed for the expression of human *SDHC* by RT-PCR, and those selected were then transformed using the *pEGFP-C3-H-Ras* vector as described previously (20). Total RNA was collected, and the presence of the S68A or S68L mutation was verified by cDNA sequencing.

Confocal Microscopy—$HCT116_{ODD\text{-}GFP}$ cells were cultured on coverslips, exposed to $MitoVE_{11}S$, mounted with DAPI-containing Vectashield (Vector Laboratories), and inspected in a confocal microscope. Sections from paraffin-embedded tumors derived from control or $MitoVE_{11}S$-treated mice were processed as above for the cultured cells.

Mouse Tumor Experiments—Tumors were established in immunocompromised, athymic (BALB/c *nu*/*nu*) mice by injecting $HCT116_{ODD\text{-}GFP}$ cells subcutaneously at 5×10^6 cells/animal. Mice were regularly checked by ultrasound imaging (USI) using the Vevo770 USI apparatus equipped with the 30-μm resolution RMV708 scan head (VisualSonics) as detailed elsewhere (18, 20, 35, 36). As soon as tumors reached ~40 mm^3, the animals were treated by intraperitoneal injection of 1–2 μmol of $MitoVE_{11}S$ or 15 μmol of α-TOS in corn oil containing 4% EtOH every 3–4 days. Control mice were injected with an equal volume (100 μl) of the vehicle only. Progression of tumor growth was assessed using USI, which enables three-dimensional reconstruction of tumors and precise quantification of their volume. All animal experimenta-

tion was performed according to the guidelines of the Australian and New Zealand Council for the Care and Use of Animals in Research and Teaching and was approved by the Griffith University Animal Ethics Committee.

Molecular Modeling—The binding of different MitoVE$_{11}$S compounds to the mitochondrial respiratory CII protein was analyzed by means of empirical force field molecular modeling/molecular dynamics. The initial geometry of the protein was taken from the available crystal structure of the porcine heart CII (Protein Data Bank code 1ZOY). As ligands, we selected both *R*- and *S*-stereoisomeric forms of MitoVE$_{11}$S as well as a series of compounds with 9, 7, and 5 carbons in the aliphatic chain.

To make the simulations feasible, the extended structure of CII was partitioned accordingly to allow closer examination of the regions of interest. The properties of the membrane-bound part of the protein and the membrane itself were analyzed by placing the hydrophobic chains (C and D) into the bilayer of phosphatidylethanolamine (POPE). For the MitoVE$_{11}$S binding site study, the residues found within 10 Å from the Q_p site were included. The protein/membrane study was initiated using a pre-equilibrated 6.7-nm rectangular patch of the POPE bilayer. The C and D chains of the protein were inserted into the center of the bilayer, and the overlapping POPE molecules were removed, resulting in the complex containing 76 POPE molecules.

For the MitoVE$_{11}$S complexes, the protein residues within 10 Å from the Q_p site were first selected. In those situations where only one to two residues were missing between consecutive residues, these residues were also added into the selection. Terminal residues of the selection were capped with acetamide and *N*-methyl groups.

The molecular dynamics study was performed employing the AMBER force field. The parm99 force field (37) was used for the standard protein residues, whereas for the MitoVES molecules, the general AMBER force field (GAFF) (38) parameters were used. The MitoVE$_{11}$S point charges were determined by a restrained fit to the electrostatic potential according to recommended procedures (39).

The modeled complexes were placed in a periodic rectangular box 1 nm larger than the complex along all three axes. For the study of the interaction of the hydrophobic chains (C and D) of the protein with the membrane, a 1-nm extension of the box size was used only in the "out of plane" coordinate, resulting in periodic lipid bilayer slabs. The box was filled with TIP3P water molecules. Chlorine ions were added to neutralize the system, placed at the positions with the lowest electrostatic potential. A molecular dynamics simulation was then conducted employing the GROMACS suite of programs (40). The equilibration procedure used consists of heating the water molecules separately to 300 K during 20 ps with the system held at 10 K, followed by a 20-ps heating of the whole system to 300 K while applying position restraints on the heavy atoms of the solute. After heating, the position restraints only on the carbonyl carbons of protein were used (allowing for side chain rearrangement while keeping the backbone fixed), and the 2-ns simulation at constant temperature of 300 K and constant pressure of 1 atm was performed. A time step of 2 fs with van der Waals and electrostatic cut-offs of 1 nm were used throughout the simulations.

For calculating interaction energies, the energy groups were introduced, the periodic conditions were removed while increasing the cut-offs to 3 nm, and the energies were calculated using the rerun switch of the mdrun program operating on the previously obtained trajectories. The group energies were collected for the (equilibrated) second half of the trajectories and analyzed with the g_analyze program.

For assessment of changes in the structure of CII upon replacing Ser^{68} with Leu, the original geometry of the protein was taken from the available crystal structure (Protein Data Bank code 1ZOY). Modeling of the three-dimensional structure was performed by Asmara version 8.12.26 (41). The cell boundaries were defined as 80 × 80 × 120 Å, which were filled with a water density of 1.0 g/ml, and the AMBER99 force field was then applied. When modeling of the three-dimensional structure was completed, structural alignment to establish equivalences between the original structure 1ZOY and the structure with the mutated residue, based on their shape and three-dimensional conformation, was carried out. It is common for structural alignment methods to use only the backbone atoms included in the peptide bond. For simplicity and efficiency, only the C_α positions were considered because the peptide bond has a minimally variant planar conformation. The root mean square deviation is the measure of the average distance between the backbones of superimposed proteins. In the study of globular protein conformations, one customarily measures the similarity of the three-dimensional structure by the root mean square deviation of the C_α atomic coordinates after optimal rigid body superposition (42).

Statistics—All data shown are mean values of three independent experiments (unless stated otherwise) ± S.D. Statistical significance was assessed using Student's *t* test, and differences were considered significant at $p < 0.05$.

RESULTS

Induction of Apoptosis by MitoVE$_{11}$S Is Dependent on Mitochondrial Potential and Complex II—We recently found that the mitochondrially targeted vitamin E analog, MitoVE$_{11}$S, is some 20–50-fold more efficient than the untargeted α-TOS,[3] as documented in Fig. 2*A* for Jurkat cells. This is in good agreement with the IC_{50} value of ~0.5 μM for MitoVES for apoptosis induction in Jurkat cells, which was ~20 μM for α-TOS. Mitochondrial accumulation of MitoVE$_{11}$S can be ascribed to the TPP^+ tag and the high $\Delta\Psi_{m,i}$. To prove this, we carried out experiments in which Jurkat cells were exposed to MitoVE$_{11}$S or α-TOS in the absence or presence of the mitochondrial uncoupler carbonyl cyanide *p*-(trifluoromethoxy) phenylhydrazone (FCCP) and assessed for apoptosis. Fig. 2*B* documents that FCCP considerably lowered apoptosis induced by MitoVE$_{11}$S but not by α-TOS, documenting that $\Delta\Psi_{m,i}$ is important for high biological activity of the mitochondrially targeted vitamin E analog, which is not the case for α-TOS lacking the TPP^+ tag.

Due to the superior activity of MitoVE$_{11}$S, we investigated its molecular target. Given the fact that α-TOS, which lacks specific mitochondrial targeting, was shown to cause apopto-

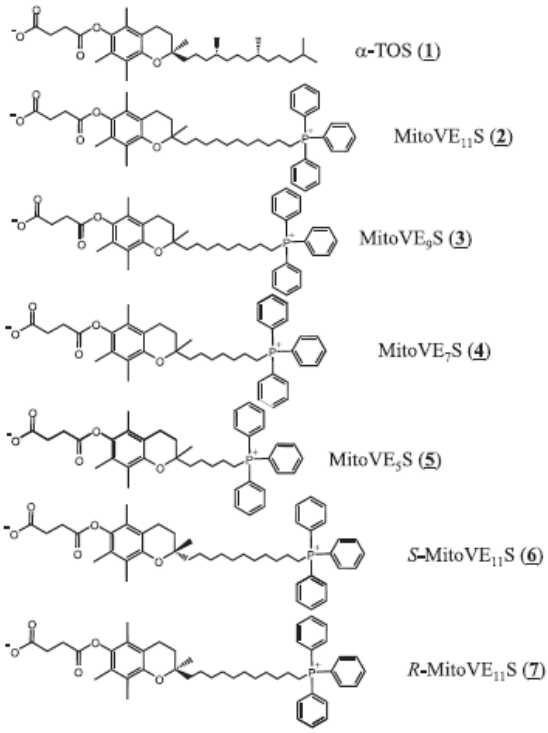

FIGURE 1. **Structures of the compounds used in this study.**

sis by interacting with CII lying at the interphase of the MIM and the mitochondrial matrix (18), it was reasoned that MitoVE$_{11}$S (compound 2 in Fig. 1, where it is referred to as MitoVE$_{11}$S due to the 11-C chain spanning the TPP$^+$ and the tocopheryl succinyl headgroup) would be more ideally located to induce apoptosis due to its accumulation in close proximity to the target. Therefore, the capacity of MitoVE$_{11}$S to induce apoptosis in parental, CII-dysfunctional and CII-reconstituted B1$_{Ras}$, B9$_{Ras}$, and B9$_{Ras\text{-}SDHC}$ cells, respectively, was tested (20). Fig. 2*C* documents that the parental as well as CII-reconstituted cells were susceptible to MitoVE$_{11}$S, whereas the CII-dysfunctional cells were resistant. Notably, the capacity of the three cell lines to generate radicals in response to MitoVE$_{11}$S exposure correlated with their susceptibility to apoptosis, as shown by EPR spectroscopy using a radical trap and flow cytometry using a fluorescent probe (Fig. 2, *C–E*).

We next tested whether the generation of radicals was due to an effect of MitoVE$_{11}$S on the integrity of the mitochondrial electron transport complexes. This was particularly important given that CI-CIII are considered to be major sources of mitochondrially derived ROS (43). To ascertain this point, Jurkat cells, which are very sensitive to MitoVE$_{11}$S,[3] were used. The cells were treated with 5 μM MitoVE$_{11}$S for 6 h before mitochondria were isolated, and their extracts were separated by size exclusion chromatography, followed by Western blotting of the individual fractions for subunits of CI, CII, and CIII. Fig. 2*G* documents virtually no effect of the agent on the integrity of any of the three complexes. We did, however, observe a slight shift toward higher molecular weight for CI and CII. Further, it was examined whether MitoVE$_{11}$S affects the expression of any of the 13 proteins coded by mtDNA as subunits of mitochondrial electron redox chain complexes. A 6-h exposure of Jurkat cells to 5 μM MitoVE$_{11}$S followed by RT-PCR revealed a very small, if any, effect on expression of the mtDNA-coded genes at the level of mRNA, with a mild effect on *ND3*, *ND6*, *COX1*, and *COX2* (Fig. 2*G*). Analysis by qPCR confirmed this mild effect (data not shown). This indicates that generation of ROS in cancer cells exposed to MitoVE$_{11}$S is not due to an effect of the agent on the levels or integrity of the mitochondrial complexes.

MitoVE$_{11}$S Inhibits the Oxidoreductase Activity of Complex II—Next, the effects of MitoVE$_{11}$S on the enzymatic and oxidoreductase activities of CI and CII were examined. For these studies, heart tissue-derived mitochondrial preparations as SMPs were used because of their ready availability and because they would be directly accessible to drug testing on the function of the respiratory chain. MitoVE$_{11}$S was examined for its capacity to disrupt the electron transfer between CI and CIII, and between CII and CIII. Fig. 3*A* reveals that the oxidoreductase activity of CII (transfer of electrons from CII to CIII) was very sensitive to low levels of the compound (IC$_{50}$ values of 1.5 and 10 μM at high and low levels of succinate, respectively) (Table 2), whereas no effect was evident on the electron transfer activity from CI to CIII (Fig. 3*A*). This suggests that MitoVE$_{11}$S preferentially binds to the fully active CII. At low succinate, the addition of detergent to the reaction mixture only minimally affected the MitoVE$_{11}$S IC$_{50}$ value, whereas at high succinate, the detergent's effects became more pronounced, revealing the importance of the natural and fully active conformation of the CII tetramer to allow for maximal effects of MitoVE$_{11}$S (Table 2). The SDH enzymatic activity of CII, on the other hand, was only inhibited by high MitoVE$_{11}$S concentrations (Fig. 3*A*) (IC$_{50}$ values for conversion of succinate to fumarate by CII were 80 μM at high and 76 μM at low succinate; Table 2), whereas the NADH dehydrogenase (*NDH*) activity of CI was not affected (Fig. 3*A*).

Inhibition of SDH can cause the state of pseudohypoxia, leading to activation of prolyl hydroxylase that modifies two proline residues flanking the ODD domain of HIF1α, resulting in the accumulation of this transcription factor (31). To find out whether this process was invoked by MitoVE$_{11}$S, HCT116 cells stably transfected with *ODD-GFP* were used. Prolonged exposure of the cells under normoxia to MitoVE$_{11}$S at 1–5 μM resulted in the expression of the ODD-GFP fusion protein (Fig. 3, *B* and *C*). This indicates that even at relatively low drug levels, sufficient SDH inhibition can occur over the long term to enable succinate levels to accumulate that activate the pseudohypoxic state and further documents the role for CII as a target for MitoVE$_{11}$S. In support of this premise, we have recently found that exposure of cancer cells to vitamin E analogs results in succinate accumulation.[4]

MitoVE$_{11}$S Targets the Proximal UbQ-binding Site of Complex II—In order to characterize the interaction of MitoVE$_{11}$S with CII in more detail, computer modeling was used, based

[4] J. Rohlena and J. Neuzil, unpublished data.

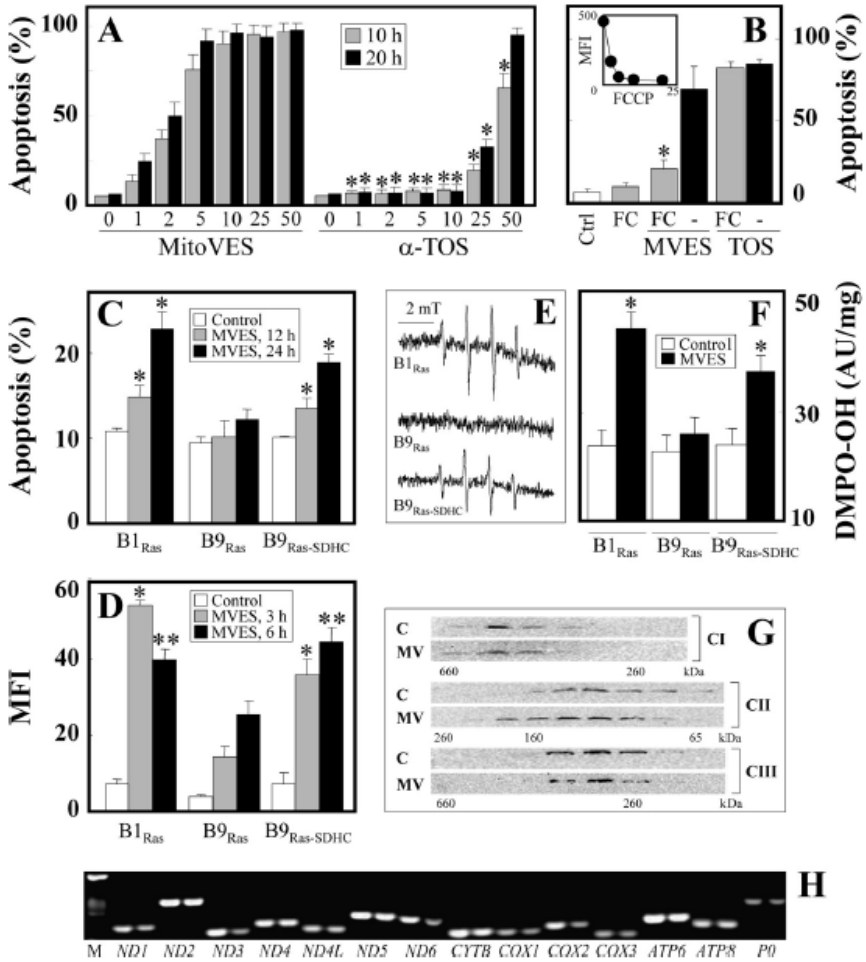

FIGURE 2. **MitoVE$_{11}$S is superior to α-TOS, requires high $\Delta\Psi_{m,i}$, and acts by targeting the mitochondrial respiratory CII.** *A*, Jurkat cells were exposed to MitoVE$_{11}$S or α-TOS at the concentrations shown (μM) for 10 or 20 h and assessed for apoptosis by flow cytometry. *B*, Jurkat cells were exposed to 4 μM MitoVE$_{11}$S (*MVES*) for 4 h or 100 μM α-TOS (*TOS*) for 6 h in the presence or absence of 5 μM FCCP (*FC*) and assessed for apoptosis. The *inset* shows that exposure of Jurkat cells to increasing doses (μM) of FCCP for 6 h results in dissipation of $\Delta\Psi_{m,i}$, as assessed using the fluorescent probe tetramethylrhodamine methyl ester and flow cytometry (mean fluorescence intensity (*MFI*)). B1$_{Ras}$, B9$_{Ras}$, and B9$_{Ras\text{-}SDHC}$ cells were exposed to 5 μM MitoVE$_{11}$S for the times shown (*C* and *D*) or for 2 h (*E* and *F*) and assessed for apoptosis induction (*C*) and ROS accumulation by flow cytometry (*D*) and EPR spectroscopy (*E*, EPR spectra; *F*, double integration evaluation of the signal; *AU*, arbitrary units). *G*, Jurkat cells were exposed to 5 μM MitoVE$_{11}$S (*MV*) for 6 h, their mitochondria were lysed, and the lysates were fractionated using size exclusion chromatography. Individual fractions were probed by Western blotting for the presence of CI–CIII using specific antibodies. *H*, Jurkat cells were exposed to 5 μM MitoVE$_{11}$S for 6 h, and mRNA levels of the mtDNA genes coding subunits of mitochondrial complexes were assessed using RT-PCR (*left lanes*, control; *right lanes*, MitoVE$_{11}$S; *M*, markers). The data shown are mean ± S.D. (*error bars*) ($n = 3$); the *images* are representative of three independent experiments. * (*A*), statistically significant differences between corresponding treatments with MitoVE$_{11}$S and α-TOS; * (*B*), statistically significant differences between treatments in the absence and presence of FCCP; * and ** (*C–F*), significant differences between B1$_{Ras}$ or B9$_{Ras\text{-}SDHC}$ cells and B9$_{Ras}$ cells treated with MitoVE$_{11}$S for 3 and 6 h, respectively ($p < 0.05$).

on the published crystal structure of CII (44), which we inserted within a POPE bilayer simulating the environment of the MIM. Our model predicts that the TPP^+ group of MitoVE$_{11}$S is located at the matrix interface of the MIM, whereas the active succinyl group of the drug is buried within the membrane, interacting with the Q_p site of CII (Fig. 4). This requires the aliphatic linker separating the chromanol succinate and TPP^+ moieties to be of a certain length. Indeed, when serially shorter linkers were used in the simulation, the model-derived binding energies of these MitoVES homologs were correspondingly successively reduced (Table 3). Experimental results confirmed these predictions. Reducing the length of the linker lowered the biological activity of the MitoVES homologs, and the shortest variant, MitoVE$_5$S (compound 5), lost most of its activity, as shown by low levels of apoptosis in Jurkat cells (Fig. 5*A*) as well as in HCT116$_{ODD\text{-}GFP}$ cells examined for SDH activity inhibition, ROS accumulation, apoptosis induction, and ODD-GFP stabilization (Fig. 5, *B–E*). Similar results were obtained for the reduction of CII oxidoreductase activity in isolated SMPs, thereby excluding the possibility of a reduction in cellular uptake of the shorter MitoVES homologs (Table 2).

The model also predicted that the *R* enantiomer of MitoVE$_{11}$S (compound 7 in Fig. 1) would bind CII ~20% more efficiently than the *S* enantiomer (compound 6) (Fig. 6*A* and Table 3). In support of this, the *R* enantiomer induced

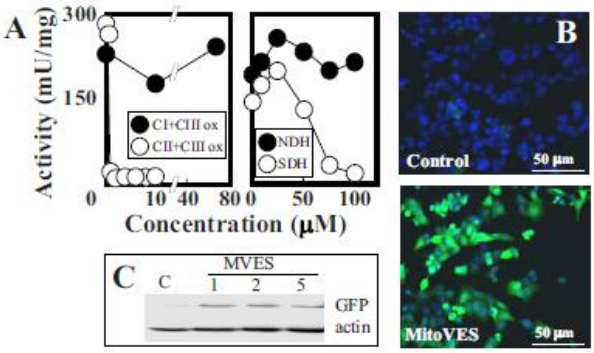

FIGURE 3. **MitoVE$_{11}$S efficiently inhibits the oxidoreductase activity of CII.** *A*, SMPs were assessed for the transfer of electrons from CI to CIII and from CII to CIII (*left*) and the activity of CI (*NDH*) and CII (*SDH*) (*right*) in the presence of MitoVE$_{11}$S. HCT116$_{ODD\text{-}GFP}$ cells were assessed for stabilization of GFP by Western blotting after exposure to MitoVE$_{11}$S at the levels shown (μM) for 24 h by Western blotting (*B*) or by fluorescence microscopy following 24-h exposure to 5 μM MitoVE$_{11}$S (*C*). The data in *A* are average values from two independent experiments; the *images* are representative of three independent experiments.

TABLE 2
IC$_{50}$ values of MitoVE$_{11}$S for CII activities

Compound	Activity	Tween	IC$_{50}$[a] 0.25 mM succinate	IC$_{50}$[a] 2 mM succinate
			μM	
MitoVE$_{11}$S	SDH[b]		76	80
MitoVE$_{11}$S	e$^-$ transfer[c]	−	10	1.5
MitoVE$_{11}$S	e$^-$ transfer[c]	+	20	18.5
MitoVE$_5$S	e$^-$ transfer	−	35	24

[a] The IC$_{50}$ values are given in μM and are average values of two independent experiments with the individual values differing by not more than 10%.
[b] The SDH activity refers to conversion of succinate to fumarate.
[c] The electron transfer activity refers to transfer of e$^-$ from CII to CIII.

apoptosis more efficiently in Jurkat cells than the *S* enantiomer, with the results for the racemic mixture of MitoVE$_{11}$S between the two (Fig. 6*B*). This difference in the apoptotic efficacy of the stereoisomers was apparent at relatively low levels of MitoVE$_{11}$S (*e.g.* the concentration of 2.5 μM shown in Fig. 6*B*), and it was lost at 5 μM MitoVE$_{11}$S (data not shown).

Mutation of the CII UbQ-binding Ser^{68} in the Q$_P$ Site Causes Resistance to MitoVE$_{11}$S—In order to verify the significance of the Q$_p$ site for the biological activity of MitoVE$_{11}$S, we reconstituted the SDHC-deficient B9 cells with SDHC variants mutated at Ser^{68}, a residue important for UbQ binding (44) (Ser^{27} in *E. coli* (45)). Substitution of Ser^{68} by either Ala or Leu, which according to the model should cause only minor shifts within the binding site (the root mean square deviation being 44 Å for S68A and 52 Å for S68L) abrogated the capacity of MitoVE$_{11}$S to induce ROS production and apoptosis (Fig. 7, *A* and *B*), confirming the importance of the Q$_p$ site and, more specifically, the UbQ-binding S68 of SDHC for the activity of MitoVE$_{11}$S.

MitoVE$_{11}$S Suppresses Tumor Progression and Causes Pseudohypoxia in Tumor Cells—To assess the effect of MitoVE$_{11}$S on tumors and obtain insight into the molecular mechanism of its anti-cancer effects, nude mice with xenografts derived from the HCT116$_{ODD\text{-}GFP}$ cells were used. Once palpable tumors appeared (volume of ~40 mm^3), the

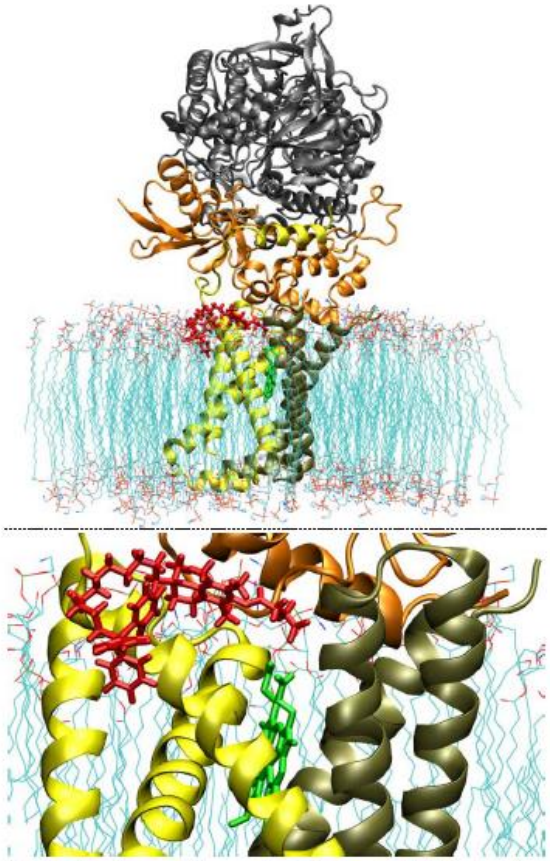

FIGURE 4. **Molecular modeling predicts binding of MitoVE$_{11}$S at the Q$_P$ site.** The CII model was refined by the addition of POPE molecules simulating the MIM. The position of the heme group is indicated in *green*, and the predicted position of MitoVE$_{11}$S is shown in *red*. The *bottom panel* shows the detail of the interaction of MitoVE$_{11}$S with CII.

TABLE 3
Relative interaction energies for MitoVES homologues and MitoQ binding the Q$_p$ site of CII

Compound	Relative interaction energy
	%
R-MitoVE$_{11}$S[a]	100[b]
S-MitoVE$_{11}$S	79.5
R-MitoVE$_9$S	79.3
R-MitoVE$_7$S	70.5
R-MitoVE$_5$S	58.6
MitoQ	51.2

[a] Except for *S*-MitoVE$_{11}$S, all other homologues used for calculations of their relative interaction energies with Q$_p$ of CII were in the *R* conformation.
[b] The calculated interaction energy of *R*-MitoVE$_{11}$S was set as 100%.

animals were treated by intraperitoneal administration of either MitoVE$_{11}$S at 1–2 μmol or α-TOS at 15 μmol. Fig. 8*A* shows that MitoVE$_{11}$S, applied at 10-fold lower concentration than the untargeted α-TOS, suppressed the growth of colorectal carcinomas and was, therefore, much more efficient. At the end of the experiment, the mice were sacrificed, and the isolated tumors were used for preparation of paraffin-embedded sections, which were inspected by light microscopy for their morphology and by confocal microscopy for the appearance of the ODD-GFP green fluorescence (Fig. 8*B*). Unlike

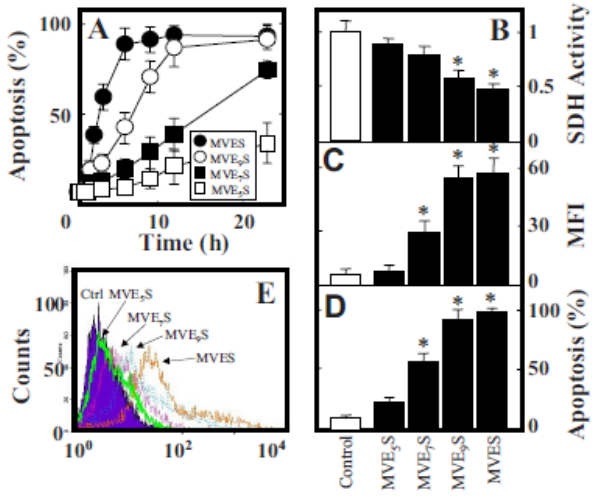

FIGURE 5. **Shortening the aliphatic chain of MitoVE$_{11}$S successively reduces its cancer cell cytotoxic activity.** *A*, Jurkat cells were exposed to homologs of MitoVES at 5 μM and evaluated for the level of apoptosis. HCT116$_{ODD\text{-}GFP}$ cells were exposed to MitoVES homologs at 5 μM for 3 h and assessed for SDH activity (*B*) and ROS accumulation (*C*) or exposed for 12 h and assessed for the level of apoptosis (*D*) and expression of GFP (*E*). The data in *A–D* are mean ± S.D. (*error bars*) ($n = 3$), and data in *E* are representative of three independent experiments. *, significant difference ($p < 0.05$) between control cells and cells treated with different MitoVES homologs.

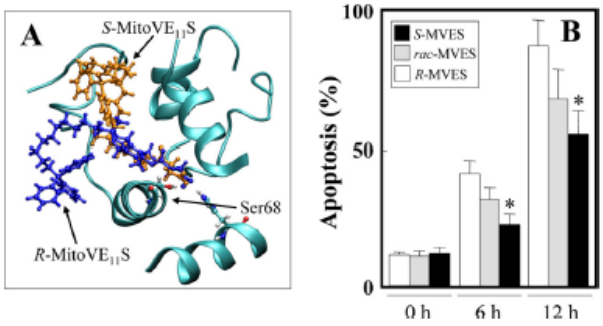

FIGURE 6. **Apoptogenic efficacy of MitoVE$_{11}$S depends on its chirality.** *A*, molecular modeling documents the predicted interaction of *R*- (*blue*) and *S*-MitoV$_{11}$ES (*brown*) with the UbQ-interacting Ser^{68} in the Q_p site of SDHC. *B*, Jurkat cells were exposed to *rac*-, *R*-, or *S*-MitoVE$_{11}$S at 2.5 μM for the times shown and assessed for apoptosis induction. The data are mean ± S.D. (*error bars*) ($n = 3$). *, significant difference ($p < 0.05$) between cells treated with *S*- and *R*-MitoVE$_{11}$S.

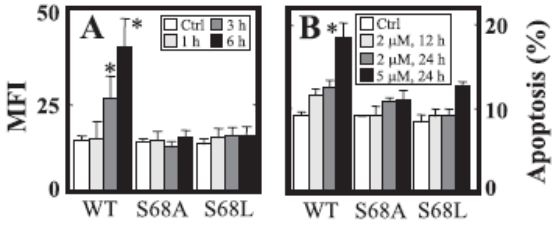

FIGURE 7. **The UbQ-binding Ser^{68} in the Q_p site of CII is important for the effect of MitoVE$_{11}$S.** B9$_{Ras\text{-}SDHC}$ (WT), B9$_{Ras\text{-}SDHCS68A}$ (S68A), or B9$_{Ras\text{-}SDHCS68L}$ cells (S68L) were exposed to MitoVE$_{11}$S at 2 μM for the times shown and assessed for ROS accumulation (*A*) and apoptosis levels (*B*). The data are mean ± S.D. (*error bars*) ($n = 3$). *, significant difference ($p < 0.05$) between MitoVE$_{11}$S-treated B9$_{Ras}$ cells stably transfected with WT SDHC or with S68A or C68L mutant SDHC.

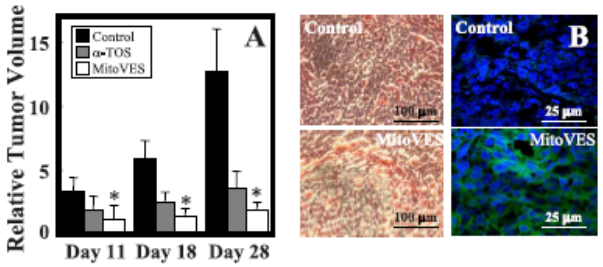

FIGURE 8. **MitoVE$_{11}$S suppresses tumor progression and causes the state of pseudohypoxia.** *A*, BALB/c *nu/nu* mice with xenografts derived from HCT116$_{ODD\text{-}GFP}$ cells were treated by intraperitoneal injection of 1–2 μmol of MitoVE$_{11}$S or 15 μmol of α-TOS per mouse every 3–4 days, and tumors were visualized and their volume was quantified using USI on days 11, 18, and 28. *B*, tumors were paraffin-embedded, sectioned, and stained with H&E and photographed in a light microscope (*left images*) or mounted in DAPI-containing Vectashield and imaged using a confocal microscope (*right images*). The data are mean ± S.D. (*error bars*) ($n = 6–7$). *, significant difference between corresponding control and MitoVE$_{11}$S-treated animals ($p < 0.05$).

tumors from the control mice, tumors from the MitoVE$_{11}$S-treated animals showed abundant green fluorescence in the tumor cell cytoplasm, documenting the stable expression of the *ODD-GFP* transgene. This result suggests that the molecular mechanism by which MitoVE$_{11}$S induces apoptosis in cultured tumor cells and in experimental tumors to suppress their growth involves targeting of CII, resulting in generation of ROS, and culminates in the state of cell pseudohypoxia.

DISCUSSION

In this paper, we present data on the molecular mechanism of generation of ROS in cancer cells exposed to the novel VE analog, MitoVE$_{11}$S. We show that (i) MitoVE$_{11}$S requires a functional CII for ROS generation and apoptosis induction; (ii) MitoVE$_{11}$S very efficiently suppresses electron transfer from CII to CIII while only mildly inhibiting the SDH headgroup enzymatic activity of CII; (iii) the length of the hydrophobic chain of MitoVE$_{11}$S is critical to allow the biologically active succinate moiety of the agent to reach the Q_p of CII; (iv) the UbQ-interacting Ser^{68} of the Q_P is important for the biological activity of MitoVE$_{11}$S; and (v) the molecular mechanism by which MitoVE$_{11}$S triggers apoptosis in cultured cells *in vitro* and suppresses tumor progression *in vivo* can be closely correlated to involve the CII Q_p binding and downstream effects. These major findings document that MitoVE$_{11}$S, as an efficient anti-cancer agent, has the propensity to interact with CII, which plays a role in the pro-apoptotic activity of several anti-cancer drugs (46) and has been proposed as a novel target for mitocans from the group of VE analogs (18, 20).

Although CII has only now been identified as a target for anti-cancer drugs, its subunits *SDHB*, *SDHC*, and *SDHD* have been reported as tumor suppressor genes (47–49), whose mutations give rise to relatively rare neoplastic diseases, including familial paragangliomas and pheochromocytomas (50, 51). The molecular mechanism of tumorigenicity arising from mutations in *SDHB*, *SDHC*, or *SDHD* is not completely clear at present, although it has been suggested that mutations resulting in impaired expression of the protein(s), imperfect

assembly, or lack of binding of UbQ may give rise to slightly increased generation of ROS, probably promoting the malignant transformation (30, 52, 54–57). In light of these findings, it is interesting that CII can also serve as a target for anti-cancer drugs, an intriguing paradigm corroborated by the notion that CII mutates mostly in relatively benign neoplastic diseases, whereas, for example, only one of 1 million breast cancer patients is positive for a mutation in a CII subunit (51).

Our recent finding of CII as a target for anti-cancer drugs comes from experiments with α-TOS, which showed that a mutation in the *SDHC* gene, whereby the protein is not expressed, renders the cells resistant to the VE analog. Because CII appears to be a highly intriguing, invariant target (mutating very rarely in major carcinomas), especially considering the findings that cancers are extremely promiscuous and feature different sets of mutations even within the same type of the disease (58), our aim was to maximize the efficacy of CII-targeting agents. To achieve this, the strategy of Murphy and Smith (21), used previously to deliver antioxidants to the mitochondria of cultured cells and tissues *in vivo* was adapted here. For their studies, a lipophilic cationic group was used to tag and modify antioxidants (21, 59), thereby endowing them with profound biological activity (60, 61) while not jeopardizing the normal mitochondrial physiology (62). Further, incorporation of lipophilic cationic compounds inside tumor mitochondria is favored by the inherent nature of their much greater electrochemical gradient (by 20–60 mV *versus* normal cell mitochondria). This promotes increased lipophilic cation accumulation at the matrix face of the MIM, imparting higher selectivity for such modified drugs to target cancer cells (63). The premise that $\Delta\Psi_{m,i}$ is greater in cancer cells when compared with their non-malignant counterparts (25–27) would also indicate that TPP^+-tagged compounds would be selective for cancer cells. Indeed, we found that the IC_{50} for killing of cancer cells by MitoVES is ~0.5–3 μM for cancer cells and ~20–60 μM for non-malignant cells,[3] further supporting the intriguing nature of such compounds.

We therefore synthesized analogs of anti-cancer agents, with the mitochondrially targeted vitamin E succinate, $MitoVE_{11}S$, as the prototypic compound by tagging VES with the TPP^+ group (*cf.* Fig. 1) because such a modification is expected to cause preferential compartmentalization of the compounds in mitochondria, enhancing their bioactivity (64). We have shown that, indeed, $MitoVE_{11}S$ causes a greater level of apoptosis in cancer cells, some 1–2 log greater than does α-TOS, and that it does partition to mitochondria while retaining the cancer cell selectivity of the untargeted α-TOS.[3] Due to the structure of $MitoVE_{11}S$ and the data shown for the mitochondrially targeted UbQ (MitoQ) (21, 23, 24), we reasoned that $MitoVE_{11}S$ would be positioned so that its TPP^+ group is at the matrix face of the MIM and the tocopheryl succinyl group buried in the MIM, potentially in the vicinity or inside the Q_P site of CII. To test whether $MitoVE_{11}S$ induces ROS generation and apoptosis via CII, we used the parental, CII-dysfunctional and CII-reconstituted, *RAS*-transformed, Chinese hamster lung fibroblasts (20) and found that the agent was relatively inefficient in inducing the two processes in the CII-dysfunctional cells compared with cells with normal SDH activity.

The role of CII as a target for $MitoVE_{11}S$ is further documented by the stabilization of the ODD-GFP protein expressed in $HCT116_{ODD\text{-}GFP}$ cells when exposed to the agent. This is because inhibiting SDH, even with low levels of the drug over extended periods, probably results in an increase in the succinate/fumarate ratio, diffusion of succinate to the cytosol, and inhibition of prolyl hydroxylases, invoking the state of pseudohypoxia (31, 32). This, in turn, stabilizes the ODD domain of the HIF1α, which in the *ODD-GFP* construct regulates the stability of GFP. Because we did not observe GFP fluorescence in $HCT116_{ODD\text{-}GFP}$ cells exposed to $MitoVE_{11}S$ in less than 6 h (data not shown), whereas significant ROS accumulation occurred within relatively short periods, the pseudohypoxic state is probably secondary to the importance of ROS in promoting the onset of apoptosis in cancer cells exposed to $MitoVE_{11}S$. To corroborate this premise, using live confocal microscopy and cells transfected with the *pHyPer-dMito* plasmid coding for the redox sensor OxyR (65), we observed generation of ROS in cancer cells as early as in 5 min following the addition of $MitoVE_{11}S$.[3] This further supports the primary role of the CII UbQ-binding site in the molecular action of the agent and is consistent with the notion that inhibition of CII can result in HIF1α stabilization (31, 32, 66, 67).

$MitoVE_{11}S$-induced ROS did not significantly affect the expression of individual mtDNA-encoded subunits examined or the stability of the CI–CIII assemblies, although some shift toward the higher molecular weight was observed for CII and CIII (*cf.* Fig. 2*E*). It is unlikely that this has a direct effect, such as on the generation of ROS, because this is observed within minutes after the addition of $MitoVE_{11}S$ (see above). It is likely that the observed increase in the molecular weight of CI and CII is a consequence of the early ROS generation and the ensuing apoptosis. Most importantly, generation of ROS is not a result of destabilization of the mitochondrial complexes. However, $MitoVE_{11}S$ did specifically affect CII, inhibiting the conversion of succinate to fumarate and transfer of electrons from CII to CIII, which is normally accomplished by the endogenous UbQ of CII. The IC_{50} values for the two activities indicate a much stronger inhibition of electron transfer than that of the SDH enzymatic activity (1.5 *versus* 80 μM, respectively). Because $MitoVE_{11}S$ very efficiently blocks electron transfer from CII to CIII, electrons will be redirected to produce superoxide anion radicals, triggering the apoptotic pathway (68). At the same time, the relatively mild inhibition of the SDH activity of CII allows for succinate conversion to fumarate, resulting in generation of electrons to form superoxide levels high enough for apoptosis induction.

Because TPP^+ acts as a charged anchor excluded from the lipid bilayer, it cannot be incorporated into the MIM (23, 24, 69). Shortening the aliphatic chain of $MitoVE_{11}S$ is proposed to restrict the access of the tocopheryl succinate headgroup penetrating down into the bilayer, causing loss of CII binding and apoptotic activity. Consistent with this premise, the short chain $MitoVE_{11}S$ homologs were much less efficient in ROS generation and apoptosis induction. In addition, the shorter

chain compounds were less effective in causing GFP stabilization in the $HCT116_{ODD\text{-}GFP}$ cells and in inhibiting the electron transfer from CII to CIII. Hence, the data are consistent with the molecular mechanism of $MitoVE_{11}S$ with its biologically active moiety most likely binding into the Q_P site, thereby affecting the function of UbQ. This is consistent with a report on MitoQ, a TPP-tagged analog of UbQ with a 10-C hydrophobic chain, whose quinone headgroup interacts with CII but not CI or CIII, such that it becomes the acceptor of electrons coming from the conversion of succinate to fumarate. The authors also showed that shortening the hydrophobic chain resulted in a lower level of its reduction by CII (23, 24).

The above findings were verified by molecular modeling, which was based on the published crystal structure of mammalian CII (44). Phospholipids were introduced to mimic the MIM in which the SDHC and SDHD subunits of CII are buried, enabling calculations of the interaction energies. MitoVES homologs with TPP^+ at the surface of the mitochondrial face of the MIM and succinate lying at the Q_P site showed affinities paralleling their relative activities in killing cancer cells as well as in causing ROS accumulation. The results of the modeling were also consistent with the higher apoptogenic activity obtained for *R*-$MitoVE_{11}S$ over the *S*-isomer. The data for the calculated affinity of $MitoVE_{11}S$ binding in the Q_P site were supported by the results of an experiment in which we used SDHC-deficient cells transfected with the WT *SDHC* gene (18, 20) or with an *SDHC* gene in which the UbQ-binding Ser^{68} (44) was replaced with Ala or Leu. Cells expressing mutant SDHC showed greater resistance to ROS generation and apoptosis induction in response to $MitoVE_{11}S$, supporting the importance of the UbQ-binding of Ser^{68} in the Q_P site for the biological activity of the agent.

Finally, we assessed the effect of $MitoVE_{11}S$ on a preclinical model of cancer, based on nude mice with $HCT116_{ODD\text{-}GFP}$ cell-derived xenografts. Although $MitoVE_{11}S$ was >10-fold more efficient than the non-targeted α-TOS, it caused stabilization of GFP in the tumors, as revealed by their sectioning followed by confocal microscopy. This result suggests that the molecular basis for induction of apoptosis by $MitoVE_{11}S$ in cultured cells, involving the state of pseudohypoxia, is also operational in suppression of tumor growth in preclinical, experimental carcinomas.

We propose that the molecular mechanism by which $MitoVE_{11}S$ affects cancer cells is based on its strong interaction with the binding of UbQ to the CII Q_P site. Consequently, the agent very efficiently blocks transfer of electrons from CII to CIII while only mildly suppressing the SDH activity of CII, which is important for generation of electrons from conversion of succinate to fumarate at the CII SDHA. Because the electrons are blocked from transfer to CIII, they then recombine with molecular oxygen to give rise to the apoptosis-inducing ROS. Further, it has been shown that the mammalian CII comprises two UbQ sites, the proximal (Q_P) and the distal (Q_D) sites (44). We suggested earlier that α-TOS is likely to interact with both Q_P and Q_D because it is not restricted in dissolving in the MIM (18). $MitoVE_{11}S$, on the other hand, can only reach the Q_P site. The molecular mechanism for its effect on CII is indicated in Fig. 9, which depicts

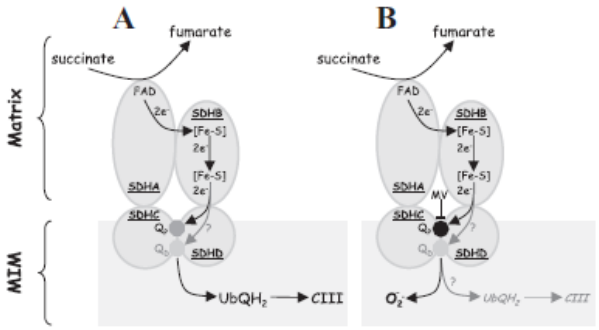

FIGURE 9. **Model for the molecular mechanism of action of $MitoVE_{11}S$ on CII.** *A*, in unstimulated cells, electrons generated from the conversion of succinate to fumarate at SDHA move via a series of Fe-S clusters down SDHB to the Q_P and, possibly, Q_D made up by amino acid residues of SDHC and SDHD. UbQ undergoes a two-electron reduction, when its affinity for the Q site(s) of CII is low, and it directs the two electrons to CIII, where it reoxidizes and shuttles back to CII. *B*, in the presence of $MitoVE_{11}S$, the SDH activity of CII is only mildly reduced (IC_{50} ~80 μM). Therefore, electrons are formed by conversion of succinate to fumarate, moving to the Q_P (and possibly Q_D) within the MIM. However, $MitoVE_{11}S$, which is positioned so that its TPP^+ group lies at the matrix face of the MIM and the tocopheryl succinyl group, interacts with the Q_P, displacing access to UbQ and very efficiently suppresses transfer of electrons from Q_P of CII to CIII (IC_{50} ~1.5 μM). Consequently, this situation is highly unstable and gives rise to generation of superoxide as a by-product.

that $MitoVE_{11}S$ interferes with the Q_P site, blocking the movement of electrons from CII to CIII, which yields superoxide that acts as a signal triggering apoptosis. It is possible that in the presence of $MitoVE_{11}S$, some electrons may proceed to CIII via the Q_D site. However, because this site is less well defined than Q_P and because its biological relevance is not defined, the potential flow of electrons via the Q_D is questionable at this stage.

Present $MitoVE_{11}S$ results provide very strong evidence for mitochondrial CII as a *bona fide* target for potential cancer treatment and considerably extend our previous data obtained with α-TOS (18, 20). We conclude that mitochondrial targeting, achieved by tagging hydrophobic compounds with cationic groups, epitomized by VES modified with the TPP^+ group, endows such agents with superior efficacy in apoptosis induction, translating into efficient anti-cancer activity, while retaining selectivity for malignant cells. Given the bleak outlook for cancer management (70, 71), finding novel, highly efficient, and selective drugs is of the utmost importance. Our proposal to target drugs that relay their activity by interfering with the mitochondrial function (mitocans) (1–5, 53) to these organelles to increase their concentration at their molecular target is a highly intriguing paradigm that has great potential for clinical benefit.

Acknowledgments—We thank I. Scheffler for B1 and B9 cells, E. Gottlieb for $HCT116_{ODD\text{-}GFP}$ cells, D. Spitz and F. Domann for pCR3.1-SDHC, and J. Hancock for pEGFP-C3-H-Ras.

REFERENCES

1. Fantin, V. R., and Leder, P. (2006) *Oncogene* **25,** 4787–4797
2. Moreno-Sánchez, R., Rodríguez-Enríquez, S., Marín-Hernández, A., and Saavedra, E. (2007) *FEBS J.* **274,** 1393–1418
3. Gogvadze, V., Orrenius, S., and Zhivotovsky, B. (2008) *Trends Cell Biol.*

18, 165–173
4. Trachootham, D., Alexandre, J., and Huang, P. (2009) *Nat. Rev. Drug Discov.* **8,** 579–591
5. Fulda, S., Galluzzi, L., and Kroemer, G. (2010) *Nat. Rev. Drug Discov.* **9,** 447–464
6. Neuzil, J., Wang, X. F., Dong, L. F., Low, P., and Ralph, S. J. (2006) *FEBS Lett.* **580,** 5125–5129
7. Neuzil, J., Dong, L. F., Ramanathapuram, L., Hahn, T., Chladova, M., Wang, X. F., Zobalova, R., Prochazka, L., Gold, M., Freeman, R., Turanek, J., Akporiaye, E. T., Dyason, J. C., and Ralph, S. J. (2007) *Mol. Aspects Med.* **28,** 607–645
8. Neuzil, J., Tomasetti, M., Zhao, Y., Dong, L. F., Birringer, M., Wang, X. F., Low, P., Wu, K., Salvatore, B. A., and Ralph, S. J. (2007) *Mol. Pharmacol.* **71,** 1185–1199
9. Neuzil, J., Weber, T., Gellert, N., and Weber, C. (2001) *Br. J. Cancer* **84,** 87–89
10. Neuzil, J., Weber, T., Schröder, A., Lu, M., Ostermann, G., Gellert, N., Mayne, G. C., Olejnicka, B., Nègre-Salvayre, A., Stícha, M., Coffey, R. J., and Weber, C. (2001) *FASEB J.* **15,** 403–415
11. Weber, T., Lu, M., Andera, L., Lahm, H., Gellert, N., Fariss, M. W., Korinek, V., Sattler, W., Ucker, D. S., Terman, A., Schröder, A., Erl, W., Brunk, U. T., Coffey, R. J., Weber, C., and Neuzil, J. (2002) *Clin. Cancer Res.* **8,** 863–869
12. Malafa, M. P., Fokum, F. D., Mowlavi, A., Abusief, M., and King, M. (2002) *Surgery* **131,** 85–91
13. Yu, W., Sanders, B. G., and Kline, K. (2003) *Cancer Res.* **63,** 2483–2491
14. Stapelberg, M., Gellert, N., Swettenham, E., Tomasetti, M., Witting, P. K., Procopio, A., and Neuzil, J. (2005) *J. Biol. Chem.* **280,** 25369–25376
15. Lawson, K. A., Anderson, K., Menchaca, M., Atkinson, J., Sun, L., Knight, V., Gilbert, B. E., Conti, C., Sanders, B. G., and Kline, K. (2003) *Mol. Cancer Ther.* **2,** 437–444
16. Hahn, T., Szabo, L., Gold, M., Ramanathapuram, L., Hurley, L. H., and Akporiaye, E. T. (2006) *Cancer Res.* **66,** 9374–9378
17. Shiau, C. W., Huang, J. W., Wang, D. S., Weng, J. R., Yang, C. C., Lin, C. H., Li, C., and Chen, C. S. (2006) *J. Biol. Chem.* **281,** 11819–11825
18. Dong, L. F., Low, P., Dyason, J. C., Wang, X. F., Prochazka, L., Witting, P. K., Freeman, R., Swettenham, E., Valis, K., Liu, J., Zobalova, R., Turanek, J., Spitz, D. R., Domann, F. E., Scheffler, I. E., Ralph, S. J., and Neuzil, J. (2008) *Oncogene* **27,** 4324–4335
19. Weber, T., Dalen, H., Andera, L., Nègre-Salvayre, A., Augé, N., Sticha, M., Lloret, A., Terman, A., Witting, P. K., Higuchi, M., Plasilova, M., Zivny, J., Gellert, N., Weber, C., and Neuzil, J. (2003) *Biochemistry* **42,** 4277–4291
20. Dong, L. F., Freeman, R., Liu, J., Zobalova, R., Marin-Hernandez, A., Stantic, M., Rohlena, J., Valis, K., Rodriguez-Enriquez, S., Butcher, B., Goodwin, J., Brunk, U. T., Witting, P. K., Moreno-Sanchez, R., Scheffler, I. E., Ralph, S. J., and Neuzil, J. (2009) *Clin. Cancer Res.* **15,** 1593–1600
21. Murphy, M. P., and Smith, R. A. (2007) *Annu. Rev. Pharmacol. Toxicol.* **47,** 629–656
22. Kelso, G. F., Porteous, C. M., Coulter, C. V., Hughes, G., Porteous, W. K., Ledgerwood, E. C., Smith, R. A., and Murphy, M. P. (2001) *J. Biol. Chem.* **276,** 4588–45896
23. James, A. M., Cochemé, H. M., Smith, R. A., and Murphy, M. P. (2005) *J. Biol. Chem.* **280,** 21295–21312
24. James, A. M., Sharpley, M. S., Manas, A. R., Frerman, F. E., Hirst, J., Smith, R. A., and Murphy, M. P. (2007) *J. Biol. Chem.* **282,** 14708–14718
25. Davis, S., Weiss, M. J., Wong, J. R., Lampidis, T. J., and Chen, L. B. (1985) *J. Biol. Chem.* **260,** 13844–13850
26. Modica-Napolitano, J. S., and Aprille, J. R. (2001) *Adv. Drug Deliv. Rev.* **49,** 63–70
27. Fantin, V. R., Berardi, M. J., Scorrano, L., Korsmeyer, S. J., and Leder, P. (2002) *Cancer Cell* **2,** 29–42
28. Oostveen, F. G., Au, H. C., Meijer, P. J., and Scheffler, I. E. (1995) *J. Biol. Chem.* **270,** 26104–26108
29. Prior, I. A., Harding, A., Yan, J., Sluimer, J., Parton, R. G., and Hancock, J. F. (2001) *Nat. Cell Biol.* **3,** 368–375
30. Slane, B. G., Aykin-Burns, N., Smith, B. J., Kalen, A. L., Goswami, P. C., Domann, F. E., and Spitz, D. R. (2006) *Cancer Res.* **66,** 7615–7620
31. Selak, M. A., Armour, S. M., MacKenzie, E. D., Boulahbel, H., Watson, D. G., Mansfield, K. D., Pan, Y., Simon, M. C., Thompson, C. B., and Gottlieb, E. (2005) *Cancer Cell* **7,** 77–85
32. MacKenzie, E. D., Selak, M. A., Tennant, D. A., Payne, L. J., Crosby, S., Frederiksen, C. M., Watson, D. G., and Gottlieb, E. (2007) *Mol. Cell. Biol.* **27,** 3282–3289
33. Jasso-Chávez, R., Torres-Márquez, M. E., and Moreno-Sánchez, R. (2001) *Arch. Biochem. Biophys.* **390,** 295–303
34. Covián, R., and Moreno-Sánchez, R. (2001) *Eur. J. Biochem.* **268,** 5783–5790
35. Dong, L. F., Swettenham, E., Eliasson, J., Wang, X. F., Gold, M., Medunic, Y., Stantic, M., Low, P., Prochazka, L., Witting, P. K., Turanek, J., Akporiaye, E. T., Ralph, S. J., and Neuzil, J. (2007) *Cancer Res.* **67,** 11906–11913
36. Wang, X. F., Birringer, M., Dong, L. F., Veprek, P., Low, P., Swettenham, E., Stantic, M., Yuan, L. H., Zobalova, R., Wu, K., Ledvina, M., Ralph, S. J., and Neuzil, J. (2007) *Cancer Res.* **67,** 3337–3344
37. Wang, J. M., Cieplak, P., and Kollman, P. A. (2000) *J. Comput. Chem.* **21,** 1049–1074
38. Wang, J., Wolf, R. M., Caldwell, J. W., Kollman, P. A., and Case, D. A. (2004) *J. Comput. Chem.* **25,** 1157–1174
39. Bayly, C. I., Cieplak, P., Cornell, W. D., and Kollman, P. A. (1993) *J. Phys. Chem.* **97,** 10269–10280
40. Van Der Spoel, D., Lindahl, E., Hess, B., Groenhof, G., Mark, A. E., and Berendsen, H. J. (2005) *J. Comput. Chem.* **26,** 1701–1718
41. Krieger, E., Koraimann, G., and Vriend, G. (2002) *Proteins* **47,** 393–402
42. Maiorov, V. N., and Crippen, G. M. (1994) *J. Mol. Biol.* **235,** 625–634
43. Adam-Vizi, V., and Chinopoulos, C. (2006) *Trends Pharmacol. Sci.* **27,** 639–645
44. Sun, F., Huo, X., Zhai, Y., Wang, A., Xu, J., Su, D., Bartlam, M., and Rao, Z. (2005) *Cell* **121,** 1043–1057
45. Yang, X., Yu, L., He, D., and Yu, C. A. (1998) *J. Biol. Chem.* **273,** 31916–31923
46. Albayrak, T., Scherhammer, V., Schoenfeld, N., Braziulis, E., Mund, T., Bauer, M. K., Scheffler, I. E., and Grimm, S. (2003) *Mol. Biol. Cell* **14,** 3082–3096
47. Eng, C., Kiuru, M., Fernandez, M. J., and Aaltonen, L. A. (2003) *Nat. Rev. Cancer* **3,** 193–202
48. Gottlieb, E., and Tomlinson, I. P. (2005) *Nat. Rev. Cancer* **5,** 857–866
49. King, A., Selak, M. A., and Gottlieb, E. (2006) *Oncogene* **25,** 4675–4682
50. Schiavi, F., Boedeker, C. C., Bausch, B., Peçzkowska, M., Gomez, C. F., Strassburg, T., Pawlu, C., Buchta, M., Salzmann, M., Hoffmann, M. M., Berlis, A., Brink, I., Cybulla, M., Muresan, M., Walter, M. A., Forrer, F., Välimäki, M., Kawecki, A., Szutkowski, Z., Schipper, J., Walz, M. K., Pigny, P., Bauters, C., Willet-Brozick, J. E., Baysal, B. E., Januszewicz, A., Eng, C., Opocher, G., and Neumann, H. P. (2005) *JAMA* **294,** 2057–2063
51. Peczkowska, M., Cascon, A., Prejbisz, A., Kubaszek, A., Cwikła, B. J., Furmanek, M., Erlic, Z., Eng, C., Januszewicz, A., and Neumann, H. P. (2008) *Nat. Clin. Pract. Endocrinol. Metab.* **4,** 111–115
52. Ishii, T., Yasuda, K., Akatsuka, A., Hino, O., Hartman, P. S., and Ishii, N. (2005) *Cancer Res.* **65,** 203–209
53. Galluzzi, L., Morselli, E., Kepp, O., Vitale, I., Rigoni, A., Vacchelli, E., Michaud, M., Zischka, H., Castedo, M., and Kroemer, G. (2010) *Mol. Aspects Med.* **31,** 1–20
54. Szeto, S. S., Reinke, S. N., Sykes, B. D., and Lemire, B. D. (2007) *J. Biol. Chem.* **282,** 27518–27526
55. Cervera, A. M., Apostolova, N., Crespo, F. L., Mata, M., and McCreath, K. J. (2008) *Cancer Res.* **68,** 4058–4067
56. Guzy, R. D., Sharma, B., Bell, E., Chandel, N. S., and Schumacker, P. T. (2008) *Mol. Cell. Biol.* **28,** 718–731
57. Lemarie, A., and Grimm, S. (2009) *Mitochondrion* **9,** 254–260
58. Hayden, E. C. (2008) *Nature* **455,** 158
59. Smith, R. A., Porteous, C. M., Gane, A. M., and Murphy, M. P. (2003) *Proc. Natl. Acad. Sci. U.S.A.* **100,** 5407–5412
60. Adlam, V. J., Harrison, J. C., Porteous, C. M., James, A. M., Smith, R. A., Murphy, M. P., and Sammut, I. A. (2005) *FASEB J.* **19,** 1088–1095

61. Neuzil, J., Widén, C., Gellert, N., Swettenham, E., Zobalova, R., Dong, L. F., Wang, X. F., Lidebjer, C., Dalen, H., Headrick, J. P., and Witting, P. K. (2007) *Redox Rep.* **12,** 148–162
62. Rodriguez-Cuenca, S., Cochemé, H. M., Logan, A., Abakumova, I., Prime, T. A., Rose, C., Vidal-Puig, A., Smith, A. C., Rubinsztein, D. C., Fearnley, I. M., Jones, B. A., Pope, S., Heales, S. J., Lam, B. Y., Neogi, S. G., McFarlane, I., James, A. M., Smith, R. A., and Murphy, M. P. (2010) *Free Radic. Biol. Med.* **48,** 161–172
63. Rodríguez-Enríquez, S., Marín-Hernández, A., Gallardo-Pérez, J. C., Carreño-Fuentes, L., and Moreno-Sánchez, R. (2009) *Mol. Nutr. Food Res.* **53,** 29–48
64. Biassutto, L., Dong, L. F., Neuzil, J., and Zoratti, M. (2010) *Mitochondrion*, in press
65. Belousov, V. V., Fradkov, A. F., Lukyanov, K. A., Staroverov, D. B., Shakhbazov, K. S., Terskikh, A. V., and Lukyanov, S. (2006) *Nat. Methods* 3 281–286
66. Piantadosi, C. A., and Suliman, H. B. (2008) *J. Biol. Chem.* **283,** 10967–10977
67. Hawkins, B. J., Levin, M. D., Doonan, P. J., Petrenko, N. B., Davis, C. W. Patel, V. V., and Madesh, M. (2010) *J. Biol. Chem.* **285,** 26494–26505
68. Prochazka, L., Dong, L. F., Valis, K., Freeman, R., Ralph, S. J., Turanek, J and Neuzil, J. (2010) *Apoptosis* **15,** 782–794
69. Biasutto, L., Sassi, N., Mattarei, A., Marotta, E., Cattelan, P., Toninello, A., Garbisa, S., Zoratti, M., and Paradisi, C. (2010) *Biochim. Biophys. Acta* **1797,** 189–196
70. Twombly, R. (2005) *J. Natl. Cancer Inst.* **97,** 330–331
71. Jemal, A., Siegel, R., Xu, J., and Ward, E. (2010) *CA Cancer J. Clin.* **60,** 277–300

Contents lists available at ScienceDirect

Free Radical Biology & Medicine

journal homepage: www.elsevier.com/locate/freeradbiomed

Original Contribution

Mitochondrial targeting of α-tocopheryl succinate enhances its pro-apoptotic efficacy: A new paradigm for effective cancer therapy

Lan-Feng Dong [a,*], Victoria J.A. Jameson [b], David Tilly [c], Lubomir Prochazka [d], Jakub Rohlena [e], Karel Valis [e], Jaroslav Truksa [e], Renata Zobalova [a,e], Elahe Mahdavian [f], Katarina Kluckova [e], Marina Stantic [a], Jan Stursa [g], Ruth Freeman [a], Paul K. Witting [h], Erik Norberg [i], Jacob Goodwin [a], Brian A. Salvatore [f], Jana Novotna [e], Jaroslav Turanek [d], Miroslav Ledvina [g], Pavel Hozak [j], Boris Zhivotovsky [i], Mark J. Coster [c], Stephen J. Ralph [a], Robin A.J. Smith [b], Jiri Neuzil [a,e,*]

[a] School of Medical Science, Griffith University, Southport, QLD 4222, Australia
[b] Department of Chemistry, University of Otago, Dunedin, New Zealand
[c] Eskitis Institute for Cell and Molecular Therapies, Griffith University, Nathan, QLD, Australia
[d] Veterinary Research Institute, Brno, Czech Republic
[e] Institute of Biotechnology, Academy of Sciences of the Czech Republic, Prague, Czech Republic
[f] Department of Chemistry and Physics, Louisiana State University Shreveport, Shreveport, LA 71115, USA
[g] Institute of Biochemistry and Organic Chemistry, Academy of Sciences of the Czech Republic, Prague, Czech Republic
[h] Discipline of Pathology, Bosch Research Institute, Sydney Medical School, University of Sydney, Sydney, NSW, Australia
[i] Institute of Environmental Medicine, Karolinska Institute, Stockholm, Sweden
[j] Institute of Molecular Genetics, Academy of Sciences of the Czech Republic, Prague, Czech Republic

ARTICLE INFO

Article history:
Received 30 December 2010
Revised 16 February 2011
Accepted 25 February 2011
Available online 12 March 2011

Keywords:
Mitochondrial targeting
Triphenyl phosphonium
Reactive oxygen species
Apoptosis, Anti-cancer agents
Free radicals

ABSTRACT

Mitochondria are emerging as intriguing targets for anti-cancer agents. We tested here a novel approach, whereby the mitochondrially targeted delivery of anti-cancer drugs is enhanced by the addition of a triphenylphosphonium group (TPP^+). A mitochondrially targeted analog of vitamin E succinate (MitoVES), modified by tagging the parental compound with TPP^+, induced considerably more robust apoptosis in cancer cells with a 1–2 log gain in anti-cancer activity compared to the unmodified counterpart, while maintaining selectivity for malignant cells. This is because MitoVES associates with mitochondria and causes fast generation of reactive oxygen species that then trigger mitochondria-dependent apoptosis, involving transcriptional modulation of the Bcl-2 family proteins. MitoVES proved superior in suppression of experimental tumors compared to the untargeted analog. We propose that mitochondrially targeted delivery of anti-cancer agents offers a new paradigm for increasing the efficacy of compounds with anti-cancer activity.

Mitochondria have become a focus of research as emerging targets for anti-cancer drugs [1–5]. We recently proposed the term "mitocans" for small compounds with anti-cancer activity that destabilize mitochondria, which results in apoptosis induction, often selectively affecting cancer cells, and classified them into several groups according to their molecular targets and mechanism of action [6].

Mitocans from the vitamin E (VE) group, epitomized by the redox-silent α-tocopheryl succinate (α-TOS), selectively induce apoptosis in cancer cells [6–9] and suppress the growth of many types of carcinomas in preclinical models [10–14]. At the molecular level, α-TOS acts as a Bcl-2 homology domain 3 (BH3) mimetic [15], effectively sensitizing cancer cells to other drugs. More importantly, α-TOS and other apoptogenic VE analogs induce apoptosis by affecting the mitochondrial complex II (CII). The VE analogs interfere with the function of ubiquinone (UbQ) [16] as the natural acceptor for electrons generated by the succinate dehydrogenase activity of CII during conversion of succinate to fumarate [17].

Previous reports showed that adding a triphenylphosphonium (TPP^+) group onto antioxidant compounds further enhanced their

Abbreviations: BH3, Bcl-2 homology domain 3; CII, complex II; ChIP, chromatin immunoprecipitation; DHE, dihydroethidium; DMPO, 5,5-dimethyl-1-pyrroline *N*-oxide; EPR, electron paramagnetic resonance; MIM, mitochondrial inner membrane; MitoQ, mitochondrially targeted coenzyme Q; MitoVES, mitochondrially targeted vitamin E succinate; MOM, mitochondrial outer membrane; NS, nonsilencing; ROS, reactive oxygen species; SOD, superoxide dismutase; TEM, transmission electron microscopy; α-TOS, α-tocopheryl succinate; TPP^+, triphenylphosphonium; UbQ, ubiquinone; USI, ultrasound imaging; VE, vitamin E; VES, vitamin E succinate.

* Corresponding authors at: School of Medical Science, Griffith University, Southport, QLD 4222, Australia. Fax: +61 2 555 28804.
E-mail addresses: l.dong@griffith.edu.au (L.-F. Dong), j.neuzil@griffith.edu.au (J. Neuzil).

activity by promoting their selective mitochondrial uptake driven by the mitochondrial membrane potential [18,19]. Therefore, we decided to modify mitocans, exemplified by VE succinate (VES), in a similar manner, anticipating that tagged agents accumulate in the mitochondrial inner membrane (MIM), providing a greater apoptogenic efficacy than the prototypic, untargeted α-TOS. Here we show that TPP^+ tagging of the hydrophobic chain of apoptogenic VE analogs indeed significantly increased their efficacy in killing cancer cells, while maintaining their selectivity for malignant cells, translating into their superior anti-cancer effect. We propose this as a new paradigm of efficient cancer therapy.

Materials and methods

Cell culture and treatment

The following cell lines used in this study were obtained from the ATCC, unless specified otherwise: human T lymphoma Jurkat, Bax^- Jurkat, and Bax^-/Bak^- Jurkat cells [20]; human mesothelioma cells Meso2, Ist-Mes, Ist-Mes-2, and MM-BI [21]; human breast cancer cells MCF7 (erbB2-low) and MDA-MB-453 (erbB2-high) and $MCF7_{DD9}$ cells with transcriptionally inactive p53 [22]; human colorectal cells HCT116; human neuroblastoma TetN21 cells [23]; human non-small-cell lung carcinoma cells H1299; human cervical cancer cells HeLa; mouse mesothelioma cells AE17 [24]; human nonmalignant mesothelial cells Met-5A; human fibroblasts A014578; rat ventricular myocyte-like cells HL1 [25]; and mouse atrial myocyte-like cells H9c2. The murine breast cancer cells NeuTL were prepared from breast carcinomas of transgenic FVB/N *c-neu* mice [26]. Jurkat cells deficient in Bak were prepared by stable transfection of parental Jurkat cells with a plasmid coding for *BAK* short-hairpin RNA (shRNA), and the lack of expression of Bak was verified by Western blotting (not shown). Jurkat cells were grown in the RPMI medium, and DMEM was used for other malignant and nonmalignant cell lines unless specified otherwise, supplemented with 10% fetal calf serum and antibiotics. HL1 cells, maintained in fibronectin/gelatin-coated dishes, were grown in Claycomb medium supplemented with noradrenalin [25]. The cells were exposed to mitochondrially targeted vitamin E succinate (MitoVES) and other agents prepared as will be published elsewhere.

Assessment of IC_{50}, apoptosis, and reactive oxygen species (ROS) generation

Toxicity of the various analogs toward cancer and nonmalignant cells was assessed on the basis of IC_{50} values determined using the standard MTT assay. Apoptosis level was assessed using the annexin V/propidium iodide method [27]. Cell death was, in some cases, assessed using the crystal violet method, as follows: cells were placed into 96-well plates at 10,000 cells per well. The next day the medium was replaced with fresh medium containing increasing concentrations of MitoVES. The crystal violet staining was performed after 24 h by fixing the cells with 2% paraformaldehyde for 30 min, washing three times with PBS, staining with 0.05% crystal violet, washing three times with PBS, and subsequently solubilizing in 1% SDS. The final absorbance measurement was determined at 595 nm using the Tecan Infinity plate reader.

Cellular ROS were detected with the probe dihydroethidium (DHE; Molecular Probes) by flow cytometry or by trapping with 5,5-dimethyl-1-pyrroline *N*-oxide (DMPO; Sigma) using electron paramagnetic resonance (EPR) spectroscopy [27]. ROS generation was also assessed using the TetN21 cells transiently transfected with pHyPer-dMito (Evrogen), a plasmid coding for the mitochondrially targeted redox sensor OxyR, which shifts its fluorescence at increased levels of hydrogen peroxide [28]. Formation of hydrogen peroxide was assessed by time-lapse analysis using confocal microscopy.

Isolation of mitochondria and gel filtration chromatography

Cells (1.2×10^8) were treated with MitoVES for various periods and harvested. The pellet was resuspended in 0.5 ml of ice-cold hypotonic fractionation buffer (25 mM Tris at pH 7.4, 2 mM EDTA, 5 mM $MgCl_2$, 10 mM KCl, 125 mM sucrose, 1 mM phenylmethylsulfonyl fluoride, plus a protease inhibitor cocktail) and left on ice for 10 min. The swollen cells were lysed using a glass homogenizer (Kontes Glass). The isotonicity of each sample was achieved by addition of 250 μl of ice-cold hypertonic fractionation buffer with 0.5 M sucrose. Organelles and unbroken cells were centrifuged at 900 *g* for 10 min, followed by centrifugation of the supernatant at 1700 *g* for 5 min. The remaining supernatant was then centrifuged at 15,000 *g* for 10 min and the mitochondrial pellet lysed in a buffer comprising 25 mM Hepes, pH 7.5, 0.3 M NaCl, and 2% Chaps. The mitochondrial lysate was centrifuged at 19,000 *g* for 5 min and loaded onto the Superdex-200 10/300 preparation grade column (separation range ~600–10 kDa; Amersham Biosciences) equilibrated with the 2% Chaps lysis buffer (see above). Proteins were eluted at 0.3 ml/min and fractions of 0.5 ml collected and mixed with 3× Laemmli reducing sample buffer and boiled. The samples were then analyzed by SDS–PAGE followed by Western blotting for Bax and Bak.

RT-PCR and qPCR

The amount of target mRNA was assessed by RT-PCR and qPCR. Total RNA was isolated using the Aurum RNA Total Mini Kit including the DNase treatment step (Bio-Rad) and reverse-transcribed using the Revertaid First Strand cDNA Synthesis Kit (Fermentas) according to the manufacturer's instructions (1–5 μg total RNA per 20 μl reaction mixture). RT-PCR was carried out using the standard procedure. For qPCR, cDNA corresponding to 12 ng starting total RNA was diluted

Table 1
Primers used for qPCR and RT-PCR.

Gene	Primers	
	Forward	Reverse
BCL-2	5′-GGTCATGTGTGTGGAGAGCG-3′	5′-GGGGCCGTACAGTTCCACAA-3′
BCL-X_L	5′-GGGATGGGGTAAACTGGGGT-3′	5′CAAAAGTATCCCAGCCGCCG-3′
MCL-1	5′-TAAGGACAAAACGGGACTGG-3′	5′-ACCAGCTCCTACTCCAGCAA-3′
BAX	5′-TCCCCGATGCGCTTGAGACA-3′	5′-CGGGGTTTCATCCAGGATCG-3′
BAK	5′-GCTATGACTCAGAGTTCCAGACCA-3′	5′-CAATTGATGCCACTCTCAAACAG-3′
BAD	5′-CAACCAGCAGCAGCCATCAT-3′	5′-AAACTCGTCACTCATCCTCCGG-3′
BID1	5′-AGCTCAGGAACACCAGCCGGT-3′	5′-GACATCACGGAGCAAGGACG-3′
BID2	5′-GATGAGCTGCAGACTGATGG-3′	5′-CACTGTCGCAGCTCCATGAA-3′
BIM	5′-GCACATTTCCCTCTGGCCTG-3′	5′-CCCACGGGAGGCATACTTTCTG-3′
NOXA	5′-TGTAGTTGGCATCTCCGCGC-3′	5′-CTCGACTTCCAGCTCTGCTG-3′
PUMA	5′-CCAAACGTGACCACTAGCCT-3′	5′-ACAGGATTCACAGTCTGGGC-3′
P0	5′-TCGACAATGGCAGCATCTAC-3′	5′-ATCCGTCTCCACAGACAAGG-3′

with water to 4.5 µl, 0.5 µl of the combined 10 µM forward and reverse primers was added, and, finally, 5 µl of 2× SYBR Green JumpStart Taq Ready Mix (Sigma) was added, and the reaction was carried out on a Bio-Rad CFX96 real-time thermal cycler using three-step PCR (98 °C for 5 s, 60 °C for 15 s, 72 °C for 25 s) for 40 cycles followed by melting curve analysis. Primers were designed on the intron/exon boundaries to prevent DNA amplification and are listed in Table 1. *P0* was used as the housekeeping gene.

Western blotting

Proteins in whole-cell lysates and cytosolic, nuclear, and mitochondrial fractions, prepared by standard methods, were separated using SDS–polyacrylamide gel electrophoresis before Western blotting was performed. Antibodies for the following proteins were used: Cyt *c*, Smac/Diablo, Bax, Bcl-x_L, Bim L, Bim EL, Puma, Cox4, FoxO1, Mst1, phospho-Mst1 (Thr183) (Cell Signaling), AIF, Bcl-2, p53, $p21^{Waf1/Cip1}$ (Santa Cruz Biotechnology), Mcl-1 (BD Pharmingen), Bak (Upstate Biotechnology), and Noxa (Alexis). Anti-actin IgG or anti-lamin IgG (both Sigma) was used as a loading control.

Analysis of Bak and Bax conformational changes

MitoVES-induced exposure of the N-terminus of Bak was assessed using the epitope-specific antibody directed against the amino acid sequence 1–57 of the Bak protein (clone Ab-1; Calbiochem) [29]. The active conformation of Bax was estimated using anti-Bax IgG (clone 6A7; Sigma) directed against amino acids 12–24 [30]. Cells grown in a six-well plate were exposed to MitoVES, harvested, fixed with 0.25% paraformaldehyde, incubated with the primary antibody diluted 1:50 in digitonin (100 µg/ml in PBS) and with FITC-labeled secondary antibody diluted 1:75 in digitonin–PBS, and analyzed by flow cytometry using "live gating" to exclude cellular debris.

Chromatin immunoprecipitation (ChIP) analysis

The ChIP assay was performed using a ChIP kit with enzymatic shearing (Active Motif). Briefly, nuclei isolated from 4×10^7 MitoVES-treated or control Jurkat cells were sheared for 10 min using the Enzymatic Shearing Cocktail, precleared by incubation with protein G beads to reduce the nonspecific background (10 µl of precleared chromatin was saved as input), and incubated overnight at 4 °C on a rotator with anti-FoxO1 IgG or a nonspecific rabbit IgG (both from Santa Cruz Biotechnology) as a negative control. In the next step, the antibody complexes were precipitated by incubation with protein G beads and after several washes eluted by a solution of SDS and $NaHCO_3$. Nucleoprotein complexes were then de-cross-linked by an overnight incubation at 65 °C and treatment with RNase A and proteinase K. The resulting DNA molecules were purified using the DNA purification minicolumns. Five microliters of purified DNA was used for RT-PCR and qPCR analysis with the following *NOXA* primers: forward 5′-TGTAGTTGGCATCTCCGCGC-3′, reverse 5′-CTCGACTTC-CAGCTCTGCTG-3′.

Knockdown of Bak and Mst1

The Bak protein was knocked down stably using shRNA. In brief, Jurkat cells were electroporated (10^7 cells with 40 µg DNA; 1 pulse of 325 V for 15 ms; ECM830 square electroporator from BTX) in the presence of a plasmid carrying *BAK* or nonsilencing (NS) shRNA (SureSilencing shRNA plasmid; SA Biosystems). Four different shRNA plasmids were used. Before transfection, the plasmid's original puromycin resistance was replaced with Geneticin resistance. The cells were selected for ~1 month in the presence of 1 mg/ml G418, tested by Western blotting, and used in experiments.

MCF7 cells were transfected using the FUGENE transfection reagent and the anti-human *Mst1* Mission shRNA cloned into the pLKO.1-puro vector, clone NM_006282.2-829s1c1 (Sigma). The shRNA sequence was CCGGCCAGAGCTATGGTCAGATAACCTCGAGGT-TATCTGACCATAGCTCTGGTTTTTTG. Cells were selected with 0.5 µg/ml puromycin for 2 weeks and individual clones chosen on the basis of diminished expression of *Mst1* assessed by qPCR and Western blotting.

Confocal microscopy

For acquisition of images with the fluorescently labeled MitoVES (MitoVES-F), NeuTL cells were grown on coverslips, stained with MitoTracker red (Molecular Probes), incubated with 10 µM $MitoVE_{11}$-S-F for 30 min, counterstained with Hoechst 33342, and inspected in a confocal microscope.

Transmission electron microscopy (TEM)

Cells were subjected to TEM after being processed as described [27].

Mouse tumor experiments

The FVB/N *c-neu* mice carrying the rat *HER-2/neu* proto-oncogene driven by the MMTV promoter on the H-2^q FVB/N background [18] were used in this study. The animals form spontaneous ductal breast carcinomas at the age of 7–9 months. Tumors were also established in immunocompromised, athymic (Balb c *nu/nu*) mice by injecting HCT116 cells subcutaneously at 5×10^6 cells per animal.

Animals were regularly checked by ultrasound imaging (USI) using the Vevo770 USI apparatus equipped with the 30-µm resolution RMV708 scan head (VisualSonics) as detailed elsewhere [16,31–33]. As soon as tumors reached ~40 mm^3, the animals were treated by ip injection of 1–2 µmol MitoVES or 10–15 µmol α-TOS in corn oil containing 4% EtOH every 3–4 days. Control mice were injected with an equal volume (100 µl) of the excipient only. Progression of tumor growth was assessed every 3–4 days using USI, which enables three-dimensional reconstruction of tumors and precise quantification of their volume.

All animal experimentation was performed according to the guidelines of the Australian and New Zealand Council for the Care and Use of Animals in Research and Teaching and was approved by the Griffith University Animal Ethics Committee.

Statistics

All data shown are mean values of three independent experiments (unless stated otherwise) ±SD. Statistical significance was assessed using Student's *t* test and differences were considered significant at $p<0.05$.

Results

We synthesized and tested several compounds derived from VE by the addition of the TPP^+ group (Fig. 1). MitoVES, the prototypic mitochondrially targeted racemic VES with an 11-carbon linker between the chromanol and the TPP^+ group induced >90% apoptosis at 50 µM within 3–10 h in various cancer cell lines and was still apoptogenic at 1 µM (Fig. 2A). Equimolar α-TOS or VES (an analog of α-TOS lacking methyl groups in the aliphatic chain) was significantly less efficient than MitoVES (Fig. 2B). Addition of TPP^+ to the succinyl moiety of α-TOS via a four-carbon spacer (VES4TPP) did not enhance the activity of the parental agent (Fig. 2B), suggesting that in this case TPP^+, while mediating mitochondrial delivery, masked the free carboxyl group essential for the apoptogenic activity of the compound

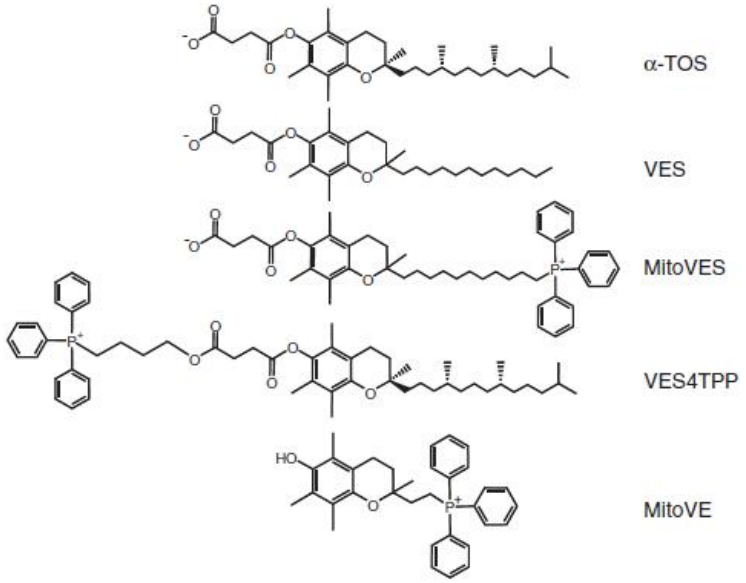

Fig. 1. Structures of compounds used in the study.

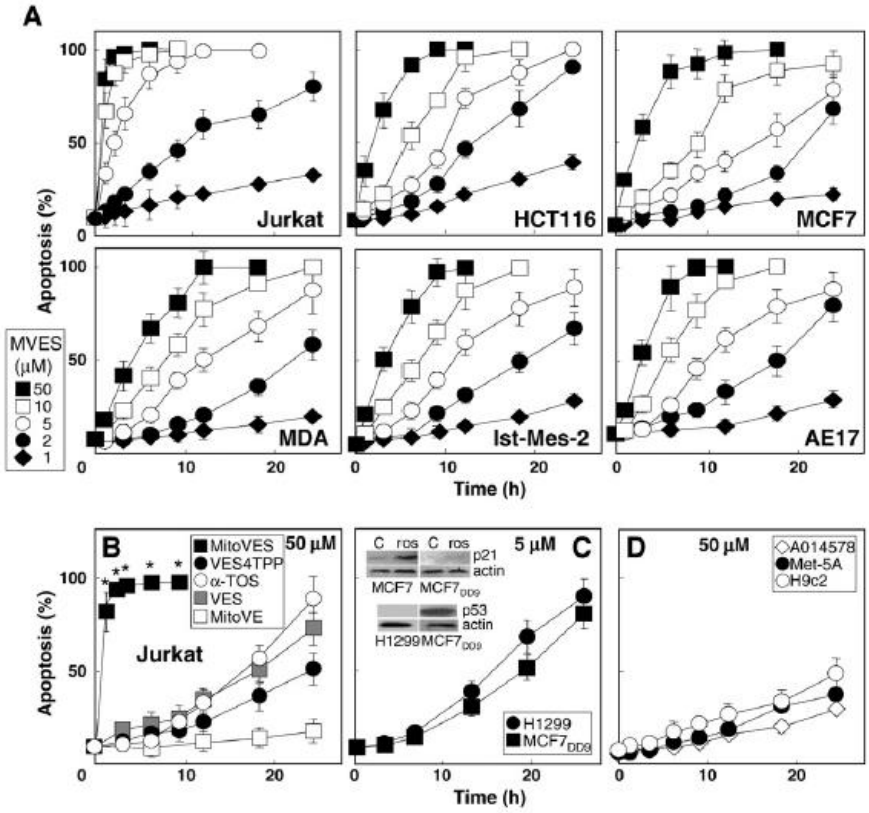

Fig. 2. MitoVES causes efficient apoptosis selectively in malignant cells. (A) The malignant Jurkat, HCT116, MCF7, MDA-MB-453 (MDA), Ist-Mes-2, and AE17 cells were exposed to MitoVES at the concentrations shown. (B) Jurkat cells were exposed to 50 μM MitoVES, VES4TPP, α-TOS, VES, or MitoVE. (C) H1299 and MCF-7_{DD9} cells were exposed to 5 μM MitoVES. (D) Fibroblasts A014578, the nonmalignant mesothelial cells Met5A, and the cardiomyoblasts H9c2 were exposed to 50 μM MitoVES. In all cases, the cells were evaluated for apoptosis level. The inset in (C) shows the expression of p21 in MCF7 and $MCF7_{DD9}$ cells, after exposure to roscovitine (ros; a drug promoting p53 stability), and p53 in H1299 and $MCF7_{DD9}$ cells. The data shown are mean values ± SD ($n = 3$), the images are representative of three independent experiments. *$p < 0.05$, significant difference between cells treated with MitoVES and cells treated with the other agents.

Table 2
IC_{50} values of VE analogs for apoptosis in various malignant and nonmalignant cell lines.

Cell type[a]	MitoVES	α-TOS	VES4TPP
Jurkat	0.48 ± 0.1	18 ± 3[b]	21 ± 5
MM-BI	1.4 ± 0.3	26 ± 4	n.d.[c]
Meso2	2.4 ± 0.5	29 ± 5	28 ± 6
Ist-Mes	2.2 ± 0.3	24 ± 5	n.d.
Ist-Mes-2	1.1 ± 0.25	21 ± 3	n.d.
AE17	3.1 ± 0.7	33 ± 5	n.d.
MCF7	1.9 ± 0.5	22 ± 4	19 ± 3
$MCF7_{DD9}$	2.8 ± 0.9	25 ± 6	n.d.
MDA-MB-453	3.3 ± 0.7	28 ± 5	n.d.
NeuTL	2.1 ± 0.5	65 ± 8	n.d.
HCT116	2.8 ± 0.8	31 ± 6	n.d.
H1299	4.9 ± 1.1	39 ± 6	n.d.
Hela	0.44 ± 0.07	69 ± 7.5	n.d.
A014578	67 ± 10.4	>100	>100
H9c2	54 ± 8.3	>100	>100
HL1	48 ± 6.2	>100	>100
Met5A	21 ± 4.5	69 ± 8	n.d.

[a] Jurkat cells were treated at 0.5×10^6/ml, other cell lines were treated at ~60% confluency.
[b] The IC_{50} values were derived from viability curves using the MTT viability assay and are expressed in micromolar.
[c] n.d., not determined.

[12,34]. VE with a short aliphatic chain, modified by addition of TPP^+ to its phytyl chain (MitoVE) [18], did not show any effect (Fig. 2B). The data for MitoVES and α-TOS showed similar trends in the IC_{50} values, with MitoVES more effective (>10- to 30-fold) than its untagged counterpart (Table 2). MitoVES efficiently killed lung cancer cells deficient in p53 (line H1299) as well as breast cancer cells with transcriptionally inactive p53 (line $MCF7_{DD9}$) (Fig. 2C), demonstrating p53 independence of apoptosis induced by the agent. Compared to cancer cells, MitoVES was much less effective in inducing apoptosis in nonmalignant cells, such as fibroblasts, cardiomyoblasts, and non-malignant mesothelial cells (Fig. 2D). The IC_{50} values of MitoVES for nonmalignant cell types were 1–2 orders of magnitude greater than those determined for the cancer cells (Table 2). Collectively, these results demonstrate considerably greater potency of MitoVES for killing in a range of cancer cell types compared to α-TOS without loss of selectivity.

Mitochondrial ROS production is emerging as an important mechanism in the mitocan-induced activation of apoptosis to kill cancer cells [35]. EPR spectroscopy and flow cytometry revealed ROS accumulation in the presence of MitoVES, which was suppressed by the mitochondrially targeted UbQ (MitoQ) [18] or superoxide dismutase (SOD) (Figs. 3A and B). The two antioxidants also suppressed MitoVES-induced apoptosis (Fig. 3B), implicating a role for ROS in the process. To assess the kinetics of ROS generation, we utilized the Tet21N neuroblastoma cells transiently transfected with pHyPer-dMito. The level of mitochondrial hydrogen peroxide was monitored using a confocal microscope that allows real-time visualization of ROS generation. Exposure of the cells to MitoVES resulted in the appearance of ROS within 5 min after addition of the

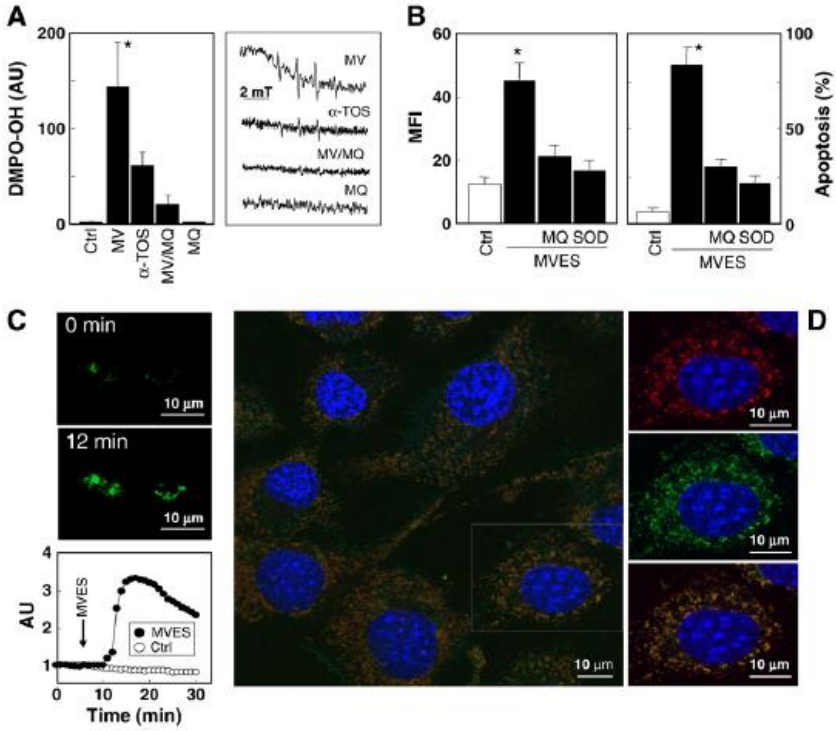

Fig. 3. MitoVES triggers rapid generation of ROS and localizes to mitochondria. (A, B) Jurkat cells were exposed to 50 μM α-TOS or 5 μM MitoVES (MV) for 2 h (A, B, left) or 12 h (B, right), in the presence of MitoQ (MQ; 2 μM, 1 h pretreatment) or SOD (PEG-SOD, 750 units/mg, cotreatment) and assessed for ROS generation by (A) EPR spectroscopy and DMPO (AU, arbitrary units) or (B) flow cytometry (mean fluorescence intensity, MFI) and DHE (left) and for (B) apoptosis induction (right). (C) Tet21N cells grown on coverslips were transiently transfected with pHyPer-dMito and placed on the stage of a live-confocal microscope. After 16 h, 10 μM MitoVES was added to the cells. Images were taken each 1 min and the level of green fluorescence was evaluated. The arrow indicates addition of MitoVES. The images show green fluorescence in two cells before and 12 min after addition of MitoVES. (D) NeuTL cells were labeled with MitoTracker red, supplemented with 20 μM MitoVES-F, and observed by confocal microscopy. The image on the left shows a cluster of cells labeled with Hoechst 33342 to visualize nuclei (blue), MitoTracker red to show mitochondria (red), and MitoVES-F to indicate the localization of the agent (green). The boxed cell is shown in detail on the right with blue/red, blue/green, and an overlay of the three colors. The data shown are mean values ± SD ($n = 3$); the images are representative of three independent experiments. The data in (C) are derived from one experiment representative of three independent experiments. *$p < 0.05$, significant difference between cells treated with MitoVES only and the other treatments as well as control cells.

stressor, indicating a very rapid response (Fig. 3C). The structure of MitoVES, i.e., its TPP^+ group, determines the accumulation of the agent in mitochondria because of the high negative potential at the matrix face of the MIM. To unequivocally document mitochondrial localization of the agent, we prepared its green fluorescent analog, MitoVES-F, by attachment of fluorescein to the free carboxylic group of MitoVES. The murine breast cancer NeuTL cells pretreated with MitoTracker red were then supplemented with MitoVES-F and inspected by confocal microscopy. Fig. 3D documents that MitoVES accumulated predominantly in mitochondria, validating our strategy of targeting anti-cancer compounds to mitochondria by tagging them with the cationic TPP^+ group.

We next tested whether apoptosis induced by MitoVES is dependent on mitochondria. Exposure of Jurkat cells and their Bax^- counterparts to 50 μM α-TOS or 5 μM MitoVES resulted in efficient apoptosis in the two sublines. In contrast, when the Bax^-/Bak^- cells were exposed to α-TOS, cell death was delayed by ~24 h, and MitoVES was ineffective (Fig. 4A). TEM revealed delayed morphological changes characteristic of cell death in Bax^-/Bak^- Jurkat cells exposed to α-TOS but no morphological alterations were evident in the presence of MitoVES (Fig. 4B), demonstrating Bax/Bak dependence of the process. The apoptosis-resistant Bax^-/Bak^- Jurkat cells responded to MitoVES with ROS accumulation (Fig. 4C), indicating that ROS generation precedes apoptosis. In the wild-type Jurkat cells, the MitoVES-induced apoptosis was suppressed by a caspase-9 but not a caspase-8 inhibitor (Fig. 4D), further pointing to mitochondria as critical mediators of MitoVES-triggered apoptosis.

Given the role of Bax/Bak in MitoVES-induced apoptosis, we next studied the mechanism of mitochondrial outer membrane (MOM) channel formation. First, we observed cytosolic translocation of cytochrome c (Cyt *c*) and Smac/Diablo, and mitochondrial translocation of Bax, in Jurkat cells exposed to MitoVES, but not in their Bax^-/Bak^- counterparts. No mobilization of the AIF protein was observed in either cell line (Fig. 5A). Gel filtration of mitochondrial lysates of MitoVES-treated cells followed by Western blotting indicated formation of oligomers of Bak and Bax (Fig. 5B). However, only the Bak protein revealed a significant conformational change, as shown by conformation-specific antibodies using flow cytometry. Moreover, the substantial conformational change in the Bak protein was seen already at 4 h, at which stage no change was observed for the Bax protein (Fig. 5C). Because this suggests a major role for Bak in the mitochondrial channel formation, we prepared Bak-deficient Jurkat cells by stable transfection of the parental cells with BAK shRNA. Of the four shRNAs used, three efficiently suppressed the Bak protein, with BAK shRNA3 showing no expression of Bak, and BAK shRNA1 and shRNA4 showing low levels of the protein (Fig. 5D, inset). The sublines with low or no expression of Bak were relatively resistant to MitoVES, in particular at its lower concentrations (Fig. 5D), indicating the dominant role of Bak in apoptosis induced by MitoVES.

We next tested the level of Bcl-2 family proteins critical for modulation of mitochondrial homeostasis in cells exposed to MitoVES, of which the BH3-only proteins Noxa and Puma showed increased mRNA levels, but only Noxa was increased at the protein level (Figs. 6A and B). In addition, levels of the Mcl-1 protein decreased in MitoVES-treated cells (Fig. 6B). The model for Bak channel formation involves upregulation of Noxa, which displaces the antiapoptotic protein Mcl-1 or Bcl-x_L from its association with Bak [36]. Because MitoVES induces Noxa expression, we studied its transcriptional regulation and found that it was controlled by the FoxO1 protein, as evidenced by the ChIP analysis (Fig. 6C). This assay, coupled with qPCR analysis, revealed 2.3-fold higher binding of the FoxO1 protein to the *NOXA* promoter in MitoVES-exposed cells. We also found that MitoVES activated the Mst1 kinase, which is known to phosphorylate FoxO1 (Fig. 6D) [37,38]. To further document a role for Mst1 in apoptosis induced by MitoVES, we knocked down the protein in MCF7 cells and exposed them to the agent. Fig. 6E reveals that lowering the level of the kinase Mst1 caused higher resistance of the

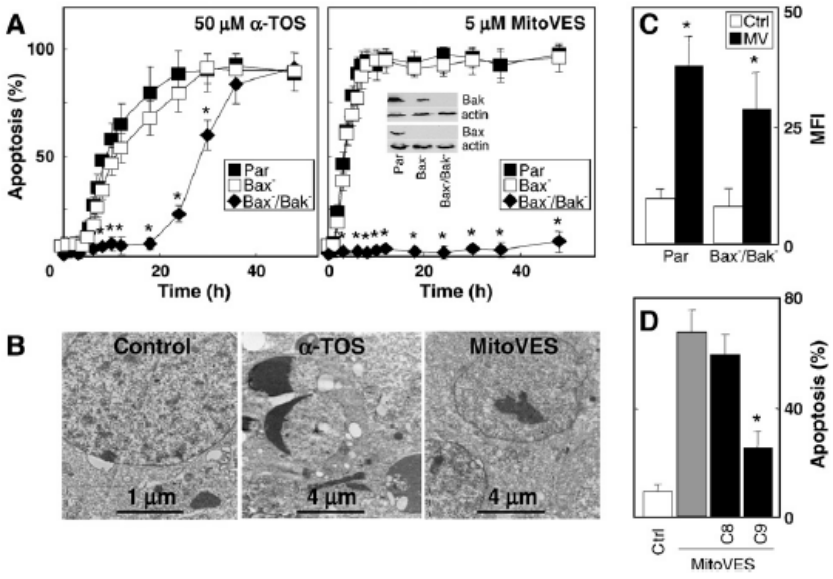

Fig. 4. MitoVES-induced apoptosis is dependent on mitochondria. Parental (Par), Bax^-, and Bax^-/Bak^- Jurkat cells were exposed to 50 μM α-TOS or 5 μM MitoVES for (A) the times shown, (B) 36 h, or (C) 2 h and assessed for (A) apoptosis induction, (B) morphological alterations using TEM, and (C) ROS accumulation using flow cytometry. The inset in (A) shows the status of the expression of the Bax and/or Bak proteins in parental, Bax^-, and Bax^-/Bak^- cells. (D) Jurkat cells were exposed to 5 μM MitoVES in the presence of 25 μM caspase-8 inhibitor (IETD-FMK) or caspase-9 inhibitor (LEHD-FMK) for 5 h and assessed for apoptosis level. The data shown are mean values ± SD ($n = 3$); the images are representative of three independent experiments. *$p < 0.05$, significant difference between Bax^-/Bak^- cells and parental or Bax^- cells (A), cells treated with MitoVES and control cells (C), and cells treated with MitoVES in the presence or absence of a caspase-9 inhibitor (D).

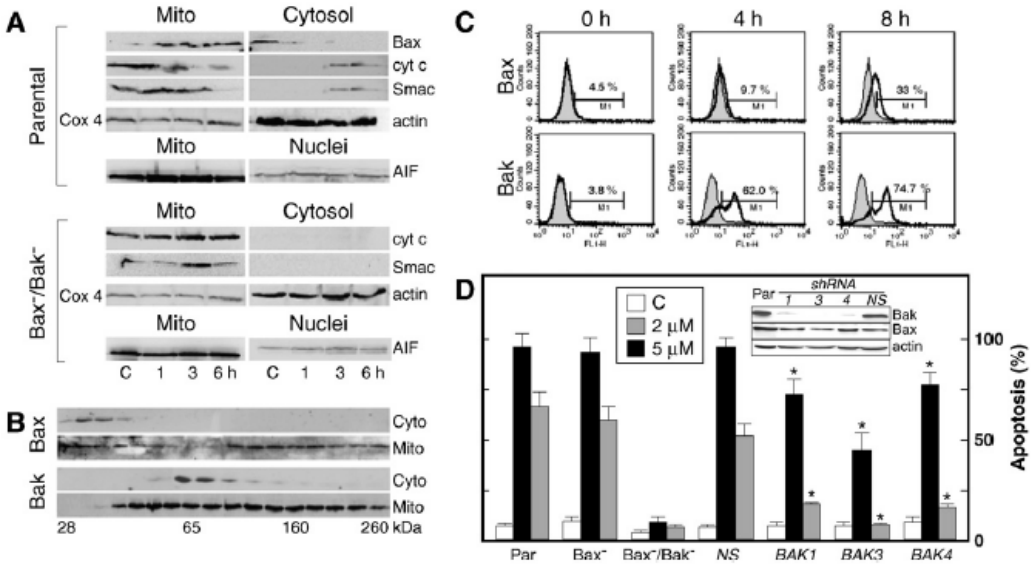

Fig. 5. MitoVES-dependent apoptosis is mediated preferentially by Bak. (A) Parental and Bax^{-}/Bak^{-} Jurkat cells were exposed to 5 µM MitoVES; fractionated into the mitochondrial, cytosolic, and nuclear compartments; and assessed by Western blotting for the levels of Bax, Cyt *c*, Smac/Diablo, and AIF. (B) Jurkat cells were exposed to 5 µM MitoVES for 12 h, the mitochondrial fraction was lysed and subjected to fractionation by size-exclusion chromatography, and the individual fractions were probed by Western blotting for the presence of the Bax or Bak proteins. (C) Jurkat cells were treated with 5 µM MitoVES and assessed for conformational change of the Bax or Bak protein using specific antibodies and flow cytometry. (D) Parental, Bax^{-}, and Bax^{-}/Bak^{-} Jurkat cells and Jurkat cells stably transfected with NS or BAK shRNAs with different expression of the Bak protein (inset) were exposed to 2 or 5 µM MitoVES for 9 h and assessed for apoptosis. The data shown are mean values ± SD ($n = 3$); the images are representative of three independent experiments. *$p < 0.05$, significant difference between the level of apoptosis in cells stably transfected with BAK shRNA and with NS shRNA exposed to the same level of MitoVES.

cells to killing by MitoVES. These results suggest a role for the Mst1/FoxO1/Noxa axis in the formation of a Bak channel in cancer cells exposed to MitoVES.

To assess the effect of MitoVES on tumors, two preclinical models were used, including the FVB/N *c-neu* transgenic mice with spontaneous ductal breast carcinomas driven by high expression of the oncogene *erbB2* in mammary epithelial cell [26] and nude mice with xenografts derived from HCT116 cells. After tumors reached ~40 mm^3, the mice were treated by ip administration of either MitoVES at 1–2 µmol or α-TOS at 15 µmol per animal per dose. Fig. 7 shows that MitoVES very efficiently suppressed carcinoma growth (>90% in both models), in some cases causing tumors to diminish in size. This effect of MitoVES was much stronger than when α-TOS was used at 10-fold higher concentration, indicating the superior effect of the mitochondrially targeted analog.

Discussion

In industrialized countries, the number of deaths from neoplastic disease has surpassed the number of deaths from cardiovascular pathologies [39], and the future trend is grim [40]. While there has been some success in treating certain types of cancer, many recur and/or remain highly resilient to therapy and some, such as malignant mesothelioma, offer virtually no therapeutic modality [41]. Frequent mutations make the cancer landscape highly heterogeneous, allowing escape from immune tumor surveillance or therapeutic interventions, as well as making the design of targeted anti-cancer drugs challenging [42–44]. The widely used conventional anti-cancer therapies utilize mechanisms such as DNA intercalation, microtubule disruption, or folate inhibition and can offer great benefits, especially in combination. However, the same therapies show relatively little specificity for cancer cells and often result in severe side effects. On the other hand, the specific and successful agents such as Trastuzumab or Imatinib are targeted at certain subsets of cancers and are therefore suitable only for selected groups of patients.

This study investigated the possibility of delivering drug candidates specifically to mitochondria because these organelles are emerging as new and intriguing targets for cancer treatment [1–5,45]. It is becoming increasingly clear that cancer cell mitochondria differ from those in normal cells [4,46]. Our previous work has shown that the mitocan α-TOS, targeting the mitochondrial respiratory chain to induce apoptosis [16], selectively eliminates cancer cells while leaving noncancerous cells relatively unaffected [6]. α-TOS, however, is a partially hydrophobic molecule with the potential to be distributed not only to mitochondria but also to other (sub)cellular membranes. We therefore hypothesized that specific mitochondrial delivery could increase both its efficacy and its specificity. Recent pioneering work by Murphy and Smith [47] revealed a strategy for achieving efficient delivery of hydrophobic redox-active compounds to mitochondria, more specifically to the MIM, by joining the cationic TPP$^+$ group onto the aliphatic chain of agents such as UbQ or VE, considerably enhancing their bioactivity. Incorporation of cationic lipophilic compounds such as MitoVES inside tumor mitochondria is favored by the development of a higher electrical gradient (by 20–60 mV vs normal cell mitochondria), which in turn promotes increased lipophilic cation accumulation [48].

Modification of mitocans from the VE group by conjugation with TPP$^+$, exemplified by the mitochondrially targeted VES MitoVES, enhanced the apoptogenic efficacy of the parental compound by a factor of 1–2 logs. Preferential mitochondrial localization of MitoVES was documented by inspecting cells preloaded with MitoTracker red and incubated with a fluorescent variant of the agent, using confocal microscopy. We documented that mitochondria were crucial for apoptosis induced by MitoVES, in particular by showing that Bax^{-}/Bak^{-} Jurkat cells were resistant to MitoVES, while they were still induced into cell death, albeit delayed, when exposed to α-TOS.

Of particular importance is the rapid action with which MitoVES induces the cascade of reactions ultimately resulting in apoptosis. This is evidenced by time-lapse imaging of the generation of ROS in cancer cells transiently transfected with pHyPer-dMito, whose product, the

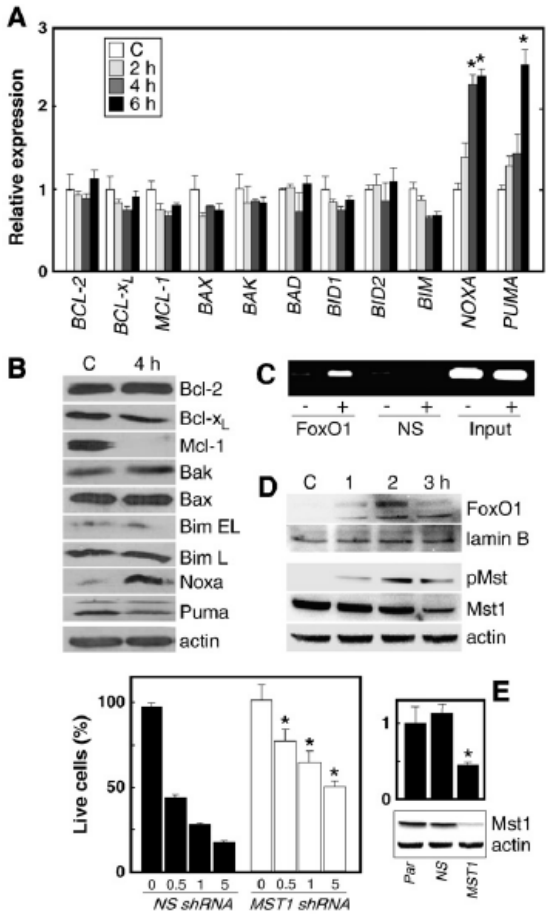

Fig. 6. MitoVES-induced apoptosis involves transcriptional upregulation of the Noxa protein. Jurkat cells were exposed to 5 μM MitoVES and assessed for the level of Bcl-2 family members by (A) qPCR and (B) Western blotting. (C) Jurkat cells were exposed to 5 μM MitoVES for 2 h and the nuclear fraction was analyzed for binding of FoxO1 protein to the *NOXA* promoter using the ChIP assay. (D) Jurkat cells were exposed to MitoVES at 5 μM for the times indicated, and Western blotting was used to probe the nuclear fraction for the level of the FoxO1 protein and the whole cell lysate for the levels of total Mst1 and pMst. (E) MCF7 cells stably transfected with NS or MST1 shRNA were exposed to MitoVES for 24 h at the concentrations shown (μM) and assessed for cell death using the crystal violet method. The graph on the right shows the level of expression of MST1 transcript assessed by qPCR in parental (Par) cells and in cells transfected with NS or MST1 shRNA. The Western blot indicates substantial lowering of the Mst1 protein in the transfected cells (upper row) with actin used as a loading control (lower row). The data shown in (A) are mean values ± SD ($n = 3$), the data in (E) mean values ± SEM ($n = 3$); the images are representative of three independent experiments. *$p < 0.05$, significant difference between gene expression in control and MitoVES-treated cells in (A), between the percentage of live cells in corresponding samples of cells transfected with NS and MST1 shRNA in (E) (left) and between the level of mRNA in parental cells or cells transfected with NS shRNA and in cells transfected with MST1 shRNA in (E) (right).

redox-sensitive OxyR, increases fluorescence in the presence of hydrogen peroxide [28], and exposed to MitoVES. We observed an increase in the green fluorescence of the cells 5 min after addition of the drug, which was followed by its plateau some 5–10 min later (Fig. 3C). Our experiments also clearly show that the oxidative burst induced in cancer cells by MitoVES is due to the fact that this drug targets CII [49], as we similarly found earlier for α-TOS. Importantly, too, we observed that an uncoupler considerably lowered apoptosis induced by MitoVES but not α-TOS in cancer cells [49], documenting the importance of mitochondrial potential for the targeting of MitoVES into the MIM.

Our results also help explain the molecular mechanism of the drug-induced MOM pore formation and indicate that in response to MitoVES, the Bak protein has a major role in forming channels in the MOM. This is supported by results revealing that Bax-deficient cancer cells are susceptible to MitoVES, whereas Bak-deficient cells are rather resistant to the agent. Formation of the Bak channel in cells exposed to MitoVES is probably regulated by the BH3-only protein Noxa. This process involves the transcriptional factor FoxO1, which itself is activated by the Mst1 kinase, in agreement with the published literature [37,38]. We propose that Noxa liberates Bak from its association with the antiapoptotic proteins such as Mcl-1, allowing efficient formation of the Bak channel [36]. This mechanism is further supported by the observed reduction in levels of the Mcl-1 protein detected in cells treated with MitoVES, which is compatible with reports showing proteasomal degradation of Mcl-1 occurring after the levels of Noxa become elevated [50] and is compatible with our recent findings for α-TOS [51].

To document the superior anti-cancer effects of MitoVES, we utilized two models of cancer, i.e., the FVB/N *c-neu* transgenic mice with spontaneous formation of HER2-high breast carcinomas [26] and nude mice with HCT116 cell-derived xenografts. Using the very precise USI-based evaluation of the tumor kinetics, MitoVES was >10-fold more efficient than the nontargeted α-TOS in both models [2,12,16]. This indicates a high anti-cancer efficacy of MitoVES that can be ascribed to its preferential association with mitochondria.

We conclude that MitoVES is an epitome of a new type of mitocans with a high level of apoptogenic activity. Hence, in principle, direct targeting of cancer cell mitochondria by MitoVES is expected to overcome many of the problems found with other drug targets for which genetic analyses have revealed a large degree of complexity and heterogeneity among individual types of cancer [52,53], with the implied difficulty in finding relatively universal treatments without serious side effects. The safety and eligibility of MitoVES as a payload with lipophilic TPP^+ as a pharmacophor for delivery are accentuated by phase I/II trials in which MitoQ-containing TPP^+ was used to treat patients with neurological disorders or hepatitis with no adverse effects even after more than 1 year of supplementation [54,55]. Thus, we propose that MitoVES, and the mitochondrially targeted mitocans in general, shows the potential to fulfill the promise of broadly applicable, selective anti-cancer drugs. Clinical trials using MitoVES are, therefore, imminent.

Acknowledgments

We thank Dr. I. Scheffler for the B1 and B9 cells, Dr. H. Rabinowich for the Bak$^-$ and Bax$^-$/Bak$^-$ Jurkat cells, Dr. E. Gottlieb for the $HCT116_{ODD\text{-}GFP}$ cells, Dr. W. Claycomb for the HL1 cells, Dr. B. Vojtesek for the H1299 and $MCF7_{DD9}$ cells, Dr. D. Spitz and Dr. F. Domann for pCR3.1-SDHC, Dr. J. Hancock for pEGFP-C3-H-Ras, and Dr. K. Lukyanov for pHyPer-dMito. This work was supported by grants from the Australian Research Council, the Cancer Council Queensland, the National Breast Cancer Foundation, the Grant Agency of the Czech Republic (204/08/0811, P301/10/1937), the Grant Agency of the Academy of Sciences of the Czech Republic (IAA500520702, KJB500970904, KAN200520703) to J.N., the Griffith Institute of Health Grant to L.F.D., the Otago University Research Grants Committee to R. A.J.S., the Swedish Research Council, the Swedish and the Stockholm Cancer Societies, the Swedish Childhood Cancer Foundation, the EC FP-6 (Chemores) and the FP-7 (Apo-Sys) programs to B.Z., the Grant Agency of the Czech Republic (GP204/09/P632) to L.P., the Grant Agency of the Academy of Sciences of the Czech Republic (200100801) to M.L., the Grant Agency of the Academy of Sciences of the Czech Republic (KJB500970904) to K.V., Grant MZE 0002716202 to J.T., and Grant P20RR016456 from the National Center

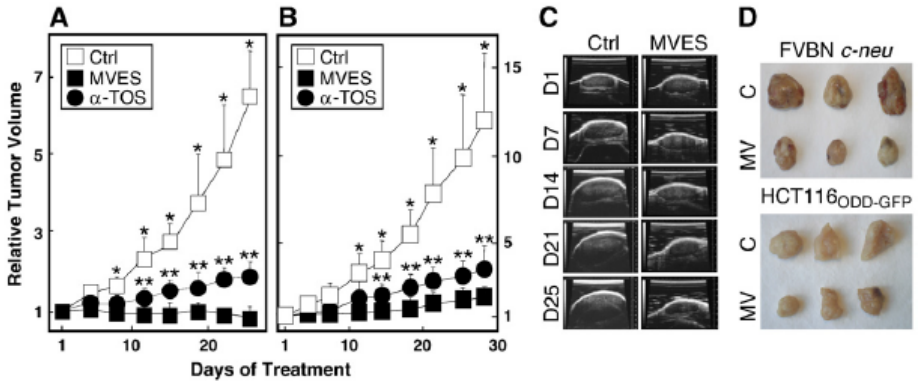

Fig. 7. MitoVES suppresses tumor progression. (A) FVB/N *c-neu* mice with breast carcinomas and (B) Balb c *nu/nu* mice with xenografts derived from HCT116 cells were treated by ip injection of 1–2 μmol MitoVES or 15 μmol α-TOS per mouse every 3–4 days, and tumors were visualized and their volume was quantified using USI. (C) Representative ultrasound images of tumors of control and MitoVES-treated *c-neu* mice acquired at the days shown. (D) Images of tumors excised at the end of the experiment. Data from USI quantification of tumor volume are mean values ± SD ($n = 5–7$). Typical photographic images are shown from each sample. *$p < 0.05$, significant difference between control and MitoVES-treated animals, **$p < 0.05$, significant difference in the tumor volumes of animals treated with MitoVES and α-TOS.

for Research Resources to E.M. and B.A.S. This work forms parts of the Ph.D. theses of R.F., R.Z., K.K., V.J.A.J., and M.S. L.P. was supported in part by funds from the Apoptosis Research Group, Griffith University (Southport, QLD, Australia).

References

[1] Fantin, V. R.; Leder, P. Mitochondriotoxic compounds for cancer therapy. *Oncogene* **25:**4787–9477; 2006.
[2] Fulda, S.; Galluzzi, L.; Kroemer, G. Targeting mitochondria for cancer therapy. *Nat. Rev. Drug Discov.* **9:**447–464; 2010.
[3] Gogvadze, V.; Orrenius, S.; Zhivotovsky, B. Mitochondria in cancer cells: what is so special about them? *Trends Cell Biol.* **18:**165–173; 2008.
[4] Moreno-Sánchez, R.; Rodríguez-Enríquez, S.; Marín-Hernández, A.; Saavedra, E. Energy metabolism in tumor cells. *FEBS J.* **274:**1393–1418; 2007.
[5] Trachootham, D.; Alexandre, J.; Huang, P. Targeting cancer cells by ROS-mediated mechanisms: a radical therapeutic approach? *Nat. Rev. Drug Discov.* **8:**579–591; 2009.
[6] Neuzil, J.; Dong, L. F.; Ramanathapuram, L.; Hahn, T.; Chladova, M.; Wang, X. F.; Zobalova, R.; Prochazka, L.; Gold, M.; Freeman, R. E., et al. Vitamin E analogues: a novel group of mitocans, anti-cancer agents that act by targeting mitochondria. *Mol. Aspects Med.* **28:**607–645; 2007.
[7] Neuzil, J.; Weber, T.; Gellert, N.; Weber, C. Selective cancer cell killing by α-tocopheryl succinate. *Br. J. Cancer* **84:**87–89; 2001.
[8] Yu, W.; Sanders, B. G.; Kline, K. RRR-α-Tocopheryl succinate-induced apoptosis of human breast cancer cells involves Bax translocation to mitochondria. *Cancer Res.* **63:**2483–2491; 2003.
[9] Zhang, Y.; Ni, J.; Messing, E. M.; Chang, E.; Yang, C. R.; Yeh, S. Vitamin E succinate inhibits the function of androgen receptor and the expression of prostate-specific antigen in prostate cancer cells. *Proc. Natl. Acad. Sci. USA* **99:**7408–7413; 2002.
[10] Hahn, T.; Szabo, L.; Gold, M.; Ramanathapuram, L.; Hurley, L. H.; Akporiaye, E. T. Dietary administration of the pro-apoptotic vitamin E analogue α-tocopherylox-yacetic acid inhibits metastatic murine breast cancer. *Cancer Res.* **66:**9374–9378; 2006.
[11] Malafa, M. P.; Fokum, F. D.; Mowlavi, A.; Abusief, M.; King, M. Vitamin E inhibits melanoma growth in mice. *Surgery* **131:**85–91; 2002.
[12] Neuzil, J.; Weber, T.; Schröder, A.; Lu, M.; Ostermann, G.; Gellert, N.; Mayne, G. C.; Olejnicka, B.; Nègre-Salvayre, A.; Sticha, M., et al. Induction of apoptosis in cancer cells by α-tocopheryl succinate: molecular pathways and structural require-ments. *FASEB J.* **15:**403–415; 2001.
[13] Stapelberg, M.; Gellert, N.; Swettenham, E.; Tomasetti, M.; Witting, P. K.; Procopio, A.; Neuzil, J. α-Tocopheryl succinate inhibits malignant mesothelioma by disrupting the FGF autocrine loop: the role of oxidative stress. *J. Biol. Chem.* **280:**25369–25376; 2005.
[14] Weber, T.; Lu, M.; Andera, L.; Lahm, H.; Gellert, N.; Fariss, M. W.; Korinek, V.; Sattler, W.; Ucker, D. S.; Terman, A., et al. Vitamin E succinate is a potent novel anti-neoplastic agent with high tumor selectivity and cooperativity with tumor necrosis factor-related apoptosis-inducing ligand (TRAIL, Apo2L) in vivo. *Clin. Cancer Res.* **8:**863–869; 2002.
[15] Shiau, C. W.; Huang, J. W.; Wang, D. S.; Weng, J. R.; Yang, C. C.; Lin, C. H.; Li, C.; Chen, C. S. Tocopheryl succinate induces apoptosis in prostate cancer cells in part through inhibition of Bcl-x_L/Bcl-2 function. *J. Biol. Chem.* **281:**11819–11825; 2006.
[16] Dong, L. F.; Low, P.; Dyason, J.; Wang, X. F.; Prochazka, L.; Witting, P. K.; Freeman, R.; Swettenham, E.; Valis, K.; Liu, J., et al. α-Tocopheryl succinate induces apoptosis by targeting ubiquinone-binding sites in mitochondrial respiratory complex II. *Oncogene* **27:**4324–4333; 2008.
[17] Sun, F.; Huo, X.; Zhai, Y.; Wang, A.; Xu, J.; Su, D.; Bartlam, M.; Rao, Z. Crystal structure of mitochondrial respiratory membrane protein complex II. *Cell* **121:**1043–1057; 2005.
[18] Kelso, G. F.; Porteous, C. M.; Coulter, C. V.; Hughes, G.; Porteous, W. K.; Ledgerwood, E. C.; Smith, R. A.; Murphy, M. P. Selective targeting of a redox-active ubiquinone to mitochondria within cells: antioxidant and antiapoptotic properties. *J. Biol. Chem.* **276:**4588–4596; 2001.
[19] Smith, R. A.; Porteous, C. M.; Gane, A. M.; Murphy, M. P. Delivery of bioactive molecules to mitochondria in vivo. *Proc. Natl. Acad. Sci. USA* **100:**5407–5412; 2003.
[20] Wang, G. Q.; Wieckowski, E.; Goldstein, L. A.; Wang, G. Q.; Wieckowski, E.; Goldstein, L. A.; Gastman, B. R.; Rabinovitz, A.; Gambotto, A.; Li, S.; Fang, B.; Yin, X. M.; Rabinowich, H. Resistance to granzyme B-mediated cytochrome c release in Bak-deficient cells. *J. Exp. Med.* **194:**1325–1337; 2001.
[21] Pass, H. I.; Stevens, E. J.; Oie, H.; Tsokos, M. G.; Abati, A. D.; Fetsch, P. A.; Mew, D. J.; Pogrebniak, H. W.; Matthews, W. J. Characteristics of nine newly derived mesothelioma cell lines. *Ann. Thorac. Surg.* **59:**835–844; 1995.
[22] Kotala, V.; Uldrijan, S.; Horky, M.; Trbusek, M.; Strnad, M.; Vojtesek, B. Potent induction of wild-type p53-dependent transcription in tumour cells by a synthetic inhibitor of cyclin-dependent kinases. *Cell. Mol. Life Sci.* **58:**1333–1339; 2001.
[23] Gogvadze, V.; Norberg, E.; Orrenius, D.; Zhivotovsky, B. Involvement of Ca^{2+} and ROS in α-tocopheryl succinate-induced mitochondrial permeabilization. *Int. J. Cancer* **127:**1823–1832; 2010.
[24] Jackaman, C.; Bundell, C. S.; Kinnear, B. F.; Smith, A. M.; Filion, P.; van Hagen, D.; Robinson, B. W.; Nelson, D. J. IL-2 intratumoral immunotherapy enhances $CD8^+$ T cells that mediate destruction of tumor cells and tumor-associated vasculature: a novel mechanism for IL-2. *J. Immunol.* **171:**5051–5063; 2003.
[25] Claycomb, W. C.; Lanson, N. A.; Stallworth, B. S.; Egeland, D. B.; Delcarpio, J. B.; Bahinski, A.; Izzo, N. J. HL-1 cells: a cardiac muscle cell line that contracts and retains phenotypic characteristics of the adult cardiomyocyte. *Proc. Natl. Acad. Sci. USA* **95:**2979–2984; 1998.
[26] Guy, C. T.; Webster, M. A.; Schaller, M.; Parsons, T. J.; Cardiff, R. D.; Muller, W. J. Expression of the neu protooncogene in the mammary epithelium of transgenic mice induces metastatic disease. *Proc. Natl. Acad. Sci. USA* **89:**10578–10582; 1992.
[27] Weber, T.; Dalen, H.; Andera, L.; Nègre-Salvayre, A.; Augé, N.; Sticha, M.; Loret, A.; Terman, A.; Witting, P. K.; Higuchi, M., et al. Mitochondria play a central role in apoptosis induced by α-tocopheryl succinate, an agent with anticancer activity. *Biochemistry* **42:**4277–4291; 2003.
[28] Belousov, V. V.; Fradkov, A. F.; Lukyanov, K. A.; Staroverov, D. B.; Shakhbazov, K. S.; Terskikh, A. V.; Lukyanov, S. Genetically encoded fluorescent indicator for intracellular hydrogen peroxide. *Nat. Methods* **3:**281–286; 2006.
[29] Griffiths, G. J.; Dubrez, L.; Morgan, C. P.; Jones, N. A.; Whitehouse, J.; Corfe, B. M.; Dive, C.; Hickman, J. A. Cell damage-induced conformational changes of the pro-apoptotic protein Bak in vivo precede the onset of apoptosis. *J. Cell Biol.* **144:**903–914; 1999.
[30] Hsu, Y. T.; Youle, R. J. Nonionic detergents induce dimerization among members of the Bcl-2 family. *J. Biol. Chem.* **272:**13829–13834; 1997.
[31] Dong, L. F.; Freeman, R.; Liu, J.; Zobalova, R.; Marin-Hernandez, A.; Stantic, M.; Rohlena, J.; Rodriguez-Enriquez, S.; Valis, K., et al. Suppression of tumor growth in vivo by the mitocan α-tocopheryl succinate requires respiratory complex II. *Clin. Cancer Res.* **15:**1593–1600; 2009.
[32] Dong, L. F.; Swettenham, E.; Eliasson, J.; Wang, X. F.; Gold, M.; Medunic, Y.; Stantic, M.; Low, P.; Prochazka, L.; Witting, P. K., et al. Vitamin E analogs inhibit angiogenesis by selective apoptosis induction in proliferating endothelial cells: the role of oxidative stress. *Cancer Res.* **67:**11906–11913; 2007.

[33] Wang, X. F.; Birringer, M.; Dong, L. F.; Veprek, P.; Low, P.; Swettenham, E.; Stantic, M.; Yuan, L. H.; Zobalova, R.; Wu, K., et al. A peptide adduct of vitamin E succinate targets breast cancer cells with high erbB2 expression. *Cancer Res.* **67:**3337–3344; 2007.
[34] Birringer, M.; EyTina, J. H.; Salvatore, B. A.; Neuzil, J. Vitamin E analogues as inducers of apoptosis: structure–function relationship. *Br. J. Cancer* **88:** 1948–1955; 2003.
[35] Ralph, S. J.; Rodríguez-Enríquez, S.; Neuzil, J.; Moreno-Sanchez, R. Bioenergetic pathways in tumor mitochondria as targets for cancer therapy and the importance of the ROS-induced apoptotic trigger. *Mol. Aspects Med.* **31:**29–59; 2010.
[36] Willis, S. N.; Chen, L.; Dewson, G.; Wei, A.; Naik, E.; Fletcher, J. I.; Adams, J. M.; Huang, D. C. Pro-apoptotic Bak is sequestered by Mcl-1 and Bcl-x_L, but not Bcl-2, until displaced by BH3-only proteins. *Genes Dev.* **19:**1294–1305; 2005.
[37] Lehtinen, M. K.; Yuan, Z.; Boaq, P. R.; Yang, Y.; Villén, J.; Becker, E. B.; DiBacco, S.; de la Iglesia, N.; Gygi, S.; Blackwell, T. K.; Bonni, A. A conserved MST–FOXO signalling pathway mediates oxidative-stress responses and extends life span. *Cell* **125:**987–1001; 2006.
[38] Obexer, P.; Geiger, K.; Ambros, P. F.; Meister, B.; Ausserlechner, M. J. FKHRL1-mediated expression of Noxa and Bim induces apoptosis via the mitochondria in neuroblastoma cells. *Cell Death Differ.* **14:**534–547; 2007.
[39] Twombly, R. Cancer surpasses heart disease as leading cause of death of all but the very elderly. *J. Natl. Cancer Inst.* **97:**330–331; 2005.
[40] Jemal, A.; Siegel, R.; Xu, J.; Ward, E. Cancer statistics, 2010. *CA Cancer J. Clin.* **60:** 277–300; 2010.
[41] Fennell, D. A.; Gaudino, G.; O'Byrne, K. J.; Mutti, L.; van Meerbeeck, J. Advances in the systemic therapy of malignant pleural mesothelioma. *Nat. Clin. Pract. Oncol.* **5:** 136–147; 2008.
[42] Chan, C. W.; Housseau, F. The 'kiss of death' by dendritic cells to cancer cells. *Cell Death Differ.* **15:**58–69; 2008.
[43] Dunn, G. P.; Bruce, A. T.; Ikeda, H.; Old, L. J.; Schreiber, R. D. Cancer immunoediting: from immunosurveillance to tumor escape. *Nat. Immunol.* **3:**991–998; 2002.
[44] Rodriguez-Nieto, S.; Zhivotovsky, B. Role of alterations in the apoptotic machinery in sensitivity of cancer cells to treatment. *Curr. Pharm. Des.* **12:**4411–4425; 2006.
[45] Neuzil, J.; Wang, X. F.; Dong, L. F.; Low, P.; Ralph, S. J. Molecular mechanism of 'mitocan'-induced apoptosis in cancer cells epitomizes the multiple roles of reactive oxygen species and Bcl-2 family proteins. *FEBS Lett.* **580:**5125–5129; 2006.
[46] Galluzzi, L.; Morselli, E.; Kepp, O.; Vitale, I.; Rigoni, A.; Vacchelli, E.; Michaud, M.; Zischka, H.; Castedo, M.; Kroemer, G. Mitochondrial gateways to cancer. *Mol. Aspects Med.* **31:**1–20; 2010.
[47] Murphy, M. P.; Smith, R. Targeting antioxidants to mitochondria by conjugation to lipophilic cations. *Annu. Rev. Pharmacol. Toxicol.* **47:**629–656; 2007.
[48] Rodríguez-Enríquez, S.; Marín-Hernández, A.; Gallardo-Pérez, J. C.; Carreño-Fuentes, L.; Moreno-Sánchez, R. Targeting of tumor energy metabolism. *Mol. Nutr. Food Res.* **53:**29–48; 2009.
[49] Dong, L. F.; Jameson, V. J. A.; Tilly, D.; Cerny, J.; Mahdavian, E.; Marín-Hernández, A.; Hernández-Esquivel, L.; Rodríguez-Enríquez, S.; Witting, P. K.; Stantic, B., et al. Mitochondrial targeting of vitamin E succinate enhances its pro-apoptotic and anti-cancer activity via mitochondrial complex II. *J. Biol. Chem.* **286:**3717–3728; 2011.
[50] Willis, S. N.; Fletcher, J. I.; Kaufmann, T.; van Delft, M. F.; Chen, L.; Czabotar, P. E.; Ierino, H.; Lee, E. F.; Fairlie, W. D.; Bouillet, P., et al. Apoptosis initiated when BH3 ligands engage multiple Bcl-2 homologs, not Bax or Bak. *Science* **315:**776–777; 2007.
[51] Prochazka, L.; Dong, L. F.; Valis, K.; Freeman, R.; Ralph, S. J.; Turanek, J.; Neuzil, J. α-Tocopheryl succinate causes mitochondrial permeabilization by preferential formation of Bak channel. *Apoptosis* **15:**782–794; 2010.
[52] Jones, S.; Zhang, X.; Parsons, D. W.; Lin, J. C.; Leary, R. J.; Angenendt, P.; Mankoo, P.; Carter, H.; Kamiyama, H.; Jimeno, A., et al. Core signaling pathways in human pancreatic cancers revealed by global genomic analyses. *Science* **321:**1801–1806; 2008.
[53] Parsons, D. W.; Jones, S.; Zhang, X.; Lin, J. C.; Leary, R. J.; Angenendt, P.; Mankoo, P.; Carter, H.; Siu, I. M.; Gallia, G. L., et al. An integrated genomic analysis of human glioblastoma multiforme. *Science* **321:**1807–1812; 2008.
[54] Gane, E. J.; Orr, D. W.; Keogh, G. F.; Gibson, M.; Lockhart, M. M.; Frampton, C. M.; Taylor, K. M.; Smith, R. A.; Murphy, M. P. The mitochondria-targeted anti-oxidant mitoquinone decreases liver damage in a phase II study of hepatitis C patients. *Liver Int.* **30:**1019–1026; 2010.
[55] Snow, B. J.; Rolfe, F. L.; Lockhart, M. M.; Frampton, C. M.; O'Sullivan, J. D.; Fung, V.; Smith, R. A.; Murphy, M. P.; Taylor, K. M. A double-blind, placebo-controlled study to assess the mitochondria-targeted antioxidant MitoQ as a disease-modifying therapy in Parkinson's disease. *Mov. Disord.* **25:**1670–1674; 2010.

ANTIOXIDANTS & REDOX SIGNALING
Volume 15, Number 12, 2011

DOI: 10.1089/ars.2011.4192

Mitochondrially Targeted α-Tocopheryl Succinate Is Antiangiogenic: Potential Benefit Against Tumor Angiogenesis but Caution Against Wound Healing

Jakub Rohlena,[1,*] Lan-Feng Dong,[2,*] Katarina Kluckova,[1] Renata Zobalova,[1,2] Jacob Goodwin,[2] David Tilly,[3] Jan Stursa,[3,4] Alena Pecinova,[5] Anatoly Philimonenko,[6] Pavel Hozak,[6] Jaideep Banerjee,[7] Miroslav Ledvina,[4] Chandan K. Sen,[7] Josef Houstek,[5] Mark J. Coster,[3] and Jiri Neuzil[1,2]

Abstract

Aims: A plausible strategy to reduce tumor progress is the inhibition of angiogenesis. Therefore, agents that efficiently suppress angiogenesis can be used for tumor suppression. We tested the antiangiogenic potential of a mitochondrially targeted analog of α-tocopheryl succinate (MitoVES), a compound with high propensity to induce apoptosis. ***Results:*** MitoVES was found to efficiently kill proliferating endothelial cells (ECs) but not contact-arrested ECs or ECs deficient in mitochondrial DNA, and suppressed angiogenesis *in vitro* by inducing accumulation of reactive oxygen species and induction of apoptosis in proliferating/angiogenic ECs. Resistance of arrested ECs was ascribed, at least in part, to the lower mitochondrial inner transmembrane potential compared with the proliferating ECs, thus resulting in the lower level of mitochondrial uptake of MitoVES. Shorter-chain homologs of MitoVES were less efficient in angiogenesis inhibition, thus suggesting a molecular mechanism of its activity. Finally, MitoVES was found to suppress HER2-positive breast carcinomas in a transgenic mouse as well as inhibit tumor angiogenesis. The antiangiogenic efficacy of MitoVES was corroborated by its inhibitory activity on wound healing *in vivo*. ***Innovation and Conclusion:*** We conclude that MitoVES, a mitochondrially targeted analog of α-tocopheryl succinate, is an efficient antiangiogenic agent of potential clinical relevance, exerting considerably higher activity than its untargeted counterpart. MitoVES may be helpful against cancer but may compromise wound healing. *Antioxid. Redox Signal.* 15, 2923–2935.

Introduction

CANCER IS A PATHOLOGY with a rather grim prognosis (20). This warrants the design and application of efficient new anticancer drugs acting *via* invariant targets that would allow broad applicability in different types of cancer. Mitochondria, an indispensable source of energy for most living cells, are increasingly recognized as such targets (12, 18, 24, 43). In this context, agents with anticancer activity acting on mitochondria, termed mitocans, present an intriguing group of compounds with relatively good selectivity for cancer cells (16, 27, 31). Mitocans are classified into eight groups, according to their mode of action (26). Vitamin E (VE) analogs belonging to group 5 mitocans act on the mitochondrial electron redox chain. These compounds are epitomized by the redox-silent α-tocopheryl succinate (α-TOS), an agent with high apoptogenic activity and selectivity for cancer cells (26, 30, 32). α-TOS has been shown to suppress a variety of tumors in mouse models, such as colorectal, breast (including HER2-positive tumors),

Innovation

The findings of this report show the very strong antiangiogenic activity of an analog of VE, α-TOS, tagged by addition of a TPP^+ group to localize to mitochondria. This endows the agent, MitoVES, with a particularly strong proapoptotic activity toward proliferating but not quiescent ECs, a paradigm that is helpful against tumor angiogenesis but may complicate wound angiogenesis and wound healing.

[1]Molecular Therapy Group, Institute of Biotechnology, Academy of Sciences of the Czech Republic, Prague, Czech Republic.
[2]School of Medical Science, Griffith University, Southport, Queensland, Australia.
[3]Eskitis Institute for Cell and Molecular Therapies, Griffith University, Nathan, Queensland, Australia.
Institutes of [4]Organic Chemistry and Biochemistry, [5]Physiology, and [6]Molecular Genetics, Academy of Sciences of the Czech Republic, Prague, Czech Republic.
[7]Davis Heart and Lung Research Institute, Ohio State University, Columbus, Ohio.
*These two authors contributed equally to this work.

mesothelioma, prostate, and pancreatic cancer as well as melanomas (22, 23, 40, 42, 45, 47).

Anticancer drugs can exert their activity *via* several modes of action. Most agents act by direct killing of malignant cells. However, an intriguing option to promote suppression of tumors is to starve them of energy and oxygen, that is, suppress the process of neovascularization of tumors by inhibiting angiogenesis (14). The process of neovascularization is based either on sprouting of new blood vessels from preexisting vessels (15) or on recruitment and differentiation of endothelial progenitor cells (35). It has been reported that angiogenesis can be suppressed by interfering with processes essential for its promotion and maintenance, in particular, disrupting paracrine signaling between tumor cells and endothelial cells (ECs) (3). This has been shown also for α-TOS, interfering with the generation and secretion of mitogenic cytokines such as the fibroblast growth factor-2 by malignant cells (29, 40).

Another possibility to suppress angiogenesis is the induction of apoptosis selectively in proliferating ECs. Several agents have been reported to possess such activity, including an analog of arsenite oxide (5) and α-TOS (10), consistent with the notion that targeting mitochondria of proliferating ECs is also an efficient way to suppress angiogenesis. Moreover, these results suggest that agents such as arsenites or α-TOS will efficiently kill angiogenic ECs of tumorigenic blood vessels while being nontoxic to the arrested ECs of normal blood vessels (33).

We have recently synthesized novel analogs of α-TOS that are targeted to mitochondria, more specifically to the interface of the matrix and the mitochondrial inner membrane (MIM). This mitochondrially targeted analog of α-TOS, MitoVES, is superior to its untargeted counterpart α-TOS in apoptosis induction and cancer suppression (7, 8). In this communication, we investigated whether MitoVES efficiently and selectively kills angiogenic ECs. The results indicate that MitoVES is much more efficient in angiogenic EC killing than the parental untargeted compound α-TOS, owing to the greater mitochondrial inner transmembrane potential ($\Delta\Psi_{m,i}$) of the proliferating EC, which translates to suppression of tumor progression and angiogenesis in an *in vivo* model of breast cancer.

Results

We first studied whether exposure of ECs to MitoVES (for its structure, see Fig. 1, where MitoVES is termed Mito$VE_{11}S$) results in apoptosis induction in the cells based on their proliferative status. For this, cells were seeded at two different confluencies, ~50%, with high proliferative status, and 100%, at which majority of the cells is growth arrested in G0. The proliferative status is documented by cell-cycle analysis, revealing majority of the proliferating ECs in the S phase, whereas confluent ECs were found mostly arrested in G0 (Fig. 2A, inset). Proliferating cells were susceptible to MitoVES, with almost all cells in apoptosis after 24-h exposure to 5 μM MitoVES. On the other hand, confluent ECs were highly resistant to the agent with substantial apoptosis (reaching ~40%) only at the highest concentration of MitoVES and at the longest exposures tested (Fig. 2A). Similarly, we observed accumulation of reactive oxygen species (ROS) in proliferating ECs exposed to MitoVES, whereas there was hardly any detectable increase in the level of ROS in confluent cells exposed to the agent (Fig. 2B). To see whether ROS generation and apoptosis induction in proliferating ECs exposed to MitoVES are causally linked, we treated the cells with the agent in the presence of a mitochondrially targeted analog of coenzyme Q (MitoQ) (21, 25). Data in Figure 2C and D document that the presence of the mitochondrially targeted antioxidant MitoQ suppressed both apoptosis induction and ROS accumulation in proliferating ECs, thus strongly indicating that ROS are important for the induction of apoptosis. We also exposed proliferating ECs to VES4TPP, an analog of MitoVES in which the triphenyl phosphonium (TPP^+) group was attached to the free succinyl group of the agent *via* a 4-C spacer (Fig. 1), which caused only minimal apoptosis (not shown). This indicates the importance of the free carboxylate for the apoptosis-inducing effects of the drug and shows that the correct placing of the TPP^+ targeting group is essential. In addition, it also demonstrates that the TPP^+ group without the active compound does not have any perceptible pro-apoptotic activity.

To get a better proof for the resistance of growth-arrested ECs to MitoVES, we tested whether the agent disrupts the contacts between individual cells. To do this, we plated the cells so that they reached 100% confluency, following which the cells were left untreated or exposed to 5 μM MitoVES for 20 h. At this point, the cells were either photographed in a light microscope or, after staining with anticadherin VE IgG plus secondary FITC-conjugated antibody and DAPI, observed in a confocal microscope. As shown in Figure 2E, the MitoVES-exposed cells maintained their normal morphology and their cell-to-cell contacts, indistinguishable from the control cells, thus further documenting the resistance of arrested ECs to MitoVES.

We tested the effect of MitoVES on angiogenesis *in vitro* by using two assays. First, we applied the wound-healing assay. ECs were allowed to form a fully confluent monolayer, after which a strip of cells was removed, and the wound was allowed to heal. Images in Figure 3A document that although at 20 h the denuded region completely filled with cells that either proliferated or migrated, 5 μM MitoVES prevented the process. The effect of MitoVES was concentration dependent, as documented in Figure 3B, showing the healing curves at different MitoVES levels. We calculated the healing rates from these curves and plotted them against different concentrations of MitoVES. Data in Figure 3C show that the healing rate of ~35 μm/h for untreated cells was suppressed to almost 5 μm/h in the presence of 5 μM MitoVES. This is reflected by the level of apoptosis in the healing assays, which was lowest in control cells and highest at 5 μM MitoVES (Fig. 3D).

The second angiogenesis assay *in vitro* is based on the tube-forming capacity of EAhy926 cells in a three-dimensional setting. Figure 3E documents the number of capillaries formed when the cells were seeded on Matrigel in the absence and presence of 5 μM MitoVES. Evaluation of the number of tubes revealed a dose-dependent inhibitory effect of MitoVES, with some 20 tubes per field for control cells and less than 3 tubes for cells exposed to 5 μM MitoVES (Fig. 3F). After retrieval of the treated cells from Matrigel, we estimated the level of apoptosis and found that the inhibitory activity of MitoVES on the tube-forming activity of the EAhy926 is directly proportional to the apoptosis-inducing efficacy of the agent (Fig. 3G).

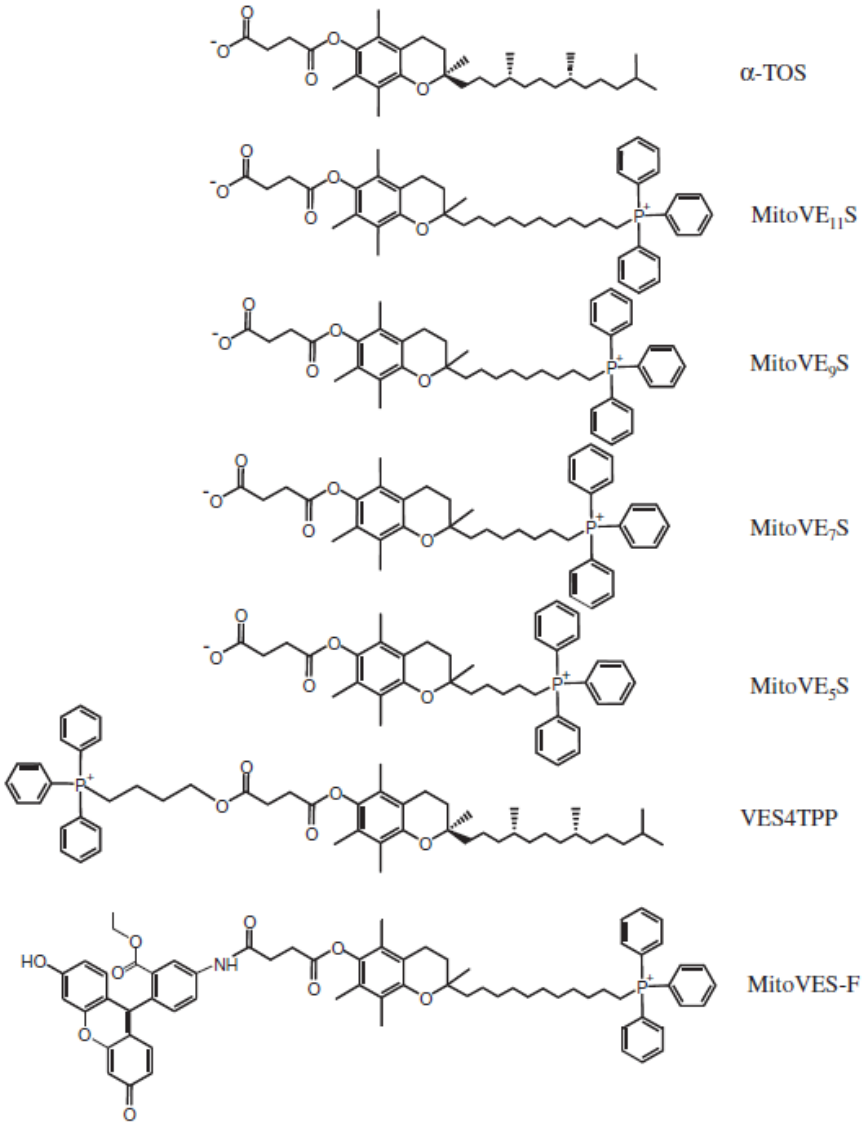

FIG. 1. Structures of the compounds used in the study. The structures shown are those of mitochondrially targeted analog of the vitamin E (VE) analog α-tocopheryl succinate (MitoVES) homologs that were used in the study and the mitochondrially untargeted analog, α-tocopheryl succinate (α-TOS).

We next tested the effect of MitoVES on angiogenesis *in vivo*, using the model of chronic ischemic wound employing the Laser Doppler blood flow imager (2, 36). In this model, proliferation of ECs is necessary to re-establish blood flow in the wounded area. Figure 4A documents that the agent at 20 μM inhibited the blood flow by $\sim$40%. Figure 4B shows representative images of control mice and mice treated with MitoVES. These results extend the previous *in vitro* anti-angiogenesis effect to an *in vivo* model.

Previous data indicate that mitochondria are important for the effect of MitoVES on proliferating ECs as indicated, in particular, by the protective effect of MitoQ. This can be expected due to the analogy of the mode of activity of MitoVES to that of α-TOS (46) and due to the mitochondrial targeting of the agent. To get stronger evidence, we tested mtDNA-depleted (ρ^0) EAhy926 cells for the effects of MitoVES on angiogenesis *in vitro* by using the wound-healing assays. We found that the ρ^0 EAhy926 cells are endowed with lower wound-healing activity compared with their parental counterparts. On the other hand, the wound-healing activity was strongly inhibited in the parental cells by MitoVES, whereas there was hardly any effect of the agent on the ρ^0 ECs (Fig. 5A, B). This resistance of the mtDNA-depleted ECs is likely due to their resistance to apoptosis induced in the assays by MitoVES (Fig. 5C). These results strongly point to the role of mitochondria in the effects of MitoVES on ECs just mentioned.

Mitochondrial localization of MitoVES is deduced from its chemistry, that is, tagging the VE analog with the cationic TPP^+ group and from its analogous structure to that of MitoQ (21, 25). To prove this supposition, we prepared a fluorescent analog of MitoVES by the addition of 5-aminofluorescein to the free carboxylate of MitoVES. Eahy926 cells, both proliferating and confluent, were then treated with fluorescently tagged MitoVES (MitoVES-F) after pretreatment of the cells with MitoTracker Red. Figure 6 shows that for proliferating ECs, MitoVES-F colocalized with MitoTracker Red, as

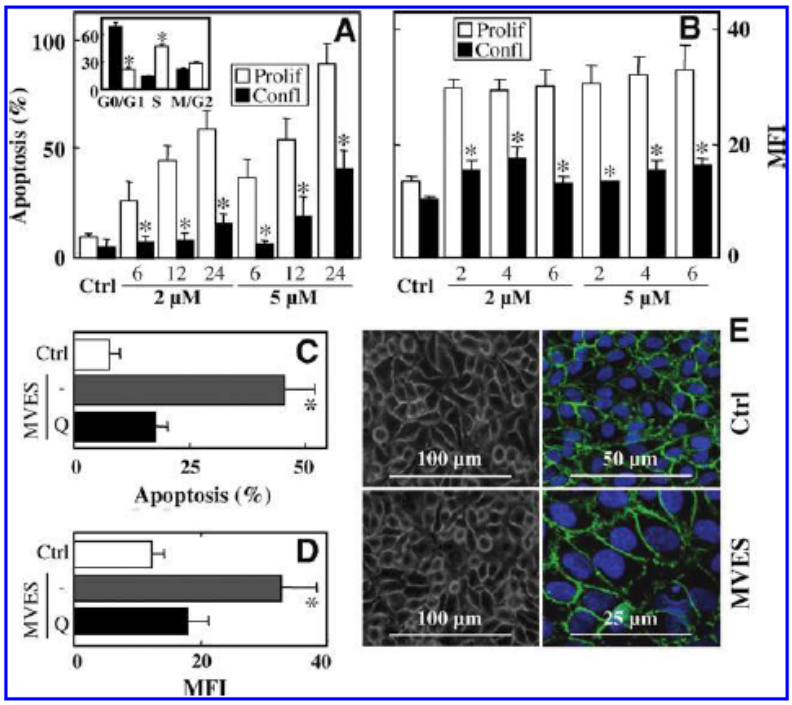

FIG. 2. MitoVES-dependent apoptosis is linked to the proliferative status of endothelial cells (ECs). EAhy926 cells plated to reach ~50% confluency (proliferating cells) and 100% confluency (confluent cells) were exposed to MitoVES at the concentrations and for the times shown. The cells were harvested and assessed for apoptosis by using annexin V-FITC/propidium iodide **(A)** and for the level of reactive oxygen species (ROS) using 2′,7′-dihydrodichlorofluorescein diacetate (DCFA) **(B)**. The *inset* in *panel* **(A)** documents the proliferative status of the cells at 50% and 100% confluency. *Panels* **(C)** and **(D)** show levels of apoptosis and ROS, respectively, in proliferating ECs preincubated with 2 μM mitochondrially targeted analog of coenzyme Q (MitoQ) and exposed to 5 μM MitoVES for 12 h **(C)** or 6 h **(D)**. **(E)** EAhy926 cells were seeded on cover slips and allowed to reach 100% confluence. After this, the cells were either left untreated (*upper panels*) or exposed for 20 h to 5 μM MitoVES (*lower panels*). The cells were then either photographed in a light microscope (*left panels*) or fixed, incubated with anticadherin VE IgG followed by secondary FITC-conjugated IgG, mounted in DAPI-containing Vectashield, and inspected in a confocal microscope. The data shown are mean values ± SD ($n = 3$), the symbol "*" indicated data from proliferating cells significantly different ($p < 0.05$) from those from arrested cells **(A, B)**, and significant differences ($p < 0.05$) in data from cells treated with MitoVES in the absence and presence of MitoQ **(C, D)**. The images in *panel* **(E)** are representative of three independent experiments. MFI, mean fluorescence intensity.

evidenced by the orange color of the organelles, documenting mitochondrial localization of the VE analog. However, we observed a rather diffuse pattern of green fluorescence in the confluent ECs which did not colocalize with the MitoTracker Red-positive structures, thus indicating that MitoVES associated much more with nonmitochondrial subcellular structures in the arrested compared with the proliferating ECs.

In the next experiments, we evaluated $\Delta\Psi_{m,i}$ in the proliferating and confluent ECs by using tetramethylrhodamine methyl ester (TMRM). We first estimated the levels of $\Delta\Psi_{m,i}$ by using confocal microscopy. Images in Figure 7A are suggestive of a higher intensity of TMRM fluorescence in the proliferating cells compared with their arrested counterparts. Further, the images indicate mitochondria in the arrested cells that appeared more round, consistent with the images in Figure 6 and those acquired by using transmission electron microscopy (TEM) (Fig. 7B). Flow cytometric analysis documented in Figure 7C reveals that $\Delta\Psi_{m,i}$ in the angiogenic cells was approximately twice the level in the arrested cells. Treatment with the uncoupler carbonyl cyanide 4-(trifluoromethoxy)phenylhydrazone (FCCP) at the concentration that completely dissipates $\Delta\Psi_{m,i}$ lowered the TMRM signal of the proliferating cells about three-fold, which is in sharp contrast to the confluent cells (Fig. 7C), where the drop in TMRM signal on FCCP addition was much more modest. To find out whether greater $\Delta\Psi_{m,i}$ is the reason for the susceptibility of angiogenic proliferating ECs to MitoVES, we tested apoptosis in the cells in the presence or absence of FCCP. Figure 7D indicates that FCCP significantly suppressed apoptosis in proliferating ECs exposed to MitoVES, whereas it had no effect on apoptosis induced by α-TOS that lacks the mitochondria-targeting cation. Inspection of lysates from confluent and arrested ECs by Native Blue electrophoresis showed virtually no difference in the assembly of the mitochondrial complexes (Fig. 7E). We next tested whether the lower $\Delta\Psi_{m,i}$ in confluent ECs, a reason for their greater resistance to MitoVES, is not potentially a result of lower number of mitochondria in confluent ECs. To do this, western blotting was performed on total cellular protein from confluent and proliferating ECs by using antibodies against subunits of complex I (CI), CII, CIII, and CV, all constituents of the MIM, as well as the mitochondrial outer membrane porin. Figure 7F reveals that the ratio of the level of the individual proteins, normalized to actin, in confluent and proliferating ECs is close to 1, thus indicating that similar or even smaller number of mitochondria are present in proliferating compared with arrested ECs. This is further supported by the activity of citrate synthase, which was 103 ± 3 and 76 ± 5 nmol/min/mg protein for confluent and proliferating ECs, respectively. We next assessed the total level of protein in proliferating and in confluent cells and found some 20% less total protein in the former. This means that per cell, proliferating cells do have considerably higher $\Delta\Psi_{m,i}$, that is, at least partially responsible for their susceptibility to MitoVES.

We earlier documented that α-TOS induces apoptosis by targeting the mitochondrial CII, which was recently crystallized (41). More specifically, we found that it interferes with the proximal (Q_P) and, most likely, too, distal ubiquinone-

binding site(s) of the protein (6, 9). We recently performed molecular modeling of the interaction of MitoVES with CII, taking into consideration the assumption that due to the positively charged TPP^+ group, the agent will be positioned so that the TPP^+ moiety will be adjacent to the matrix face of the MIM and the tocopheryl succinyl group will reach the Q_P site (7) only when the aliphatic chain of MitoVES is of sufficient length. Indeed, when we tested MitoVES homologs with 9-, 7-, or 5-C aliphatic chain (Fig. 1) in proliferating EC cells, we found that the full-length MitoVES was the most efficient one in induction of apoptosis and in suppressing angiogenesis *in vitro* using the wound-healing assay, whereas $MitoVE_5S$ exerted almost no activity (Fig. 8). These findings indicate that MitoVES relays its toxic effects on proliferating ECs by interacting with the Q_P site of CII.

Finally, we tested the effect of MitoVES on tumor progression in a transgenic mouse with HER2-positive breast carcinomas and on angiogenesis in the carcinomas employing the ultrasound imaging (USI) technique, which allows for noninvasive and precise evaluation of the progression of tumors and their vascularization (angiogenesis). Figure 9 documents a strong inhibitory effect of the agent on the tumors including angiogenesis. Thus, in the control tumors, the relative vascularization increased some 2.5-fold over the period of the treatment, whereas it basically did not change in the treated animals. This indicates suppression of blood vessel proliferation in tumors in mice treated with MitoVES and suggests that the results on angiogenesis *in vitro* (see above) are also reflected in experimental tumors.

Discussion

The Holy Grail in the development of anticancer agents would be a compound that would interfere with the tumor cells at multiple levels and, at the same time, would leave the noncancerous somatic cells unaffected. In addition, such a compound should be effective against as wide a range of various cancer types as possible, while retaining the aforementioned specificity for cancer cells. One desired exception to this specificity is the proliferating EC. Normally, ECs remain quiescent, forming the inner lining of the blood vessels. At a tumor site, this steady state is disturbed, and the quiescent ECs are induced to proliferate to participate in the formation of new blood vessels that provide the growing tumor

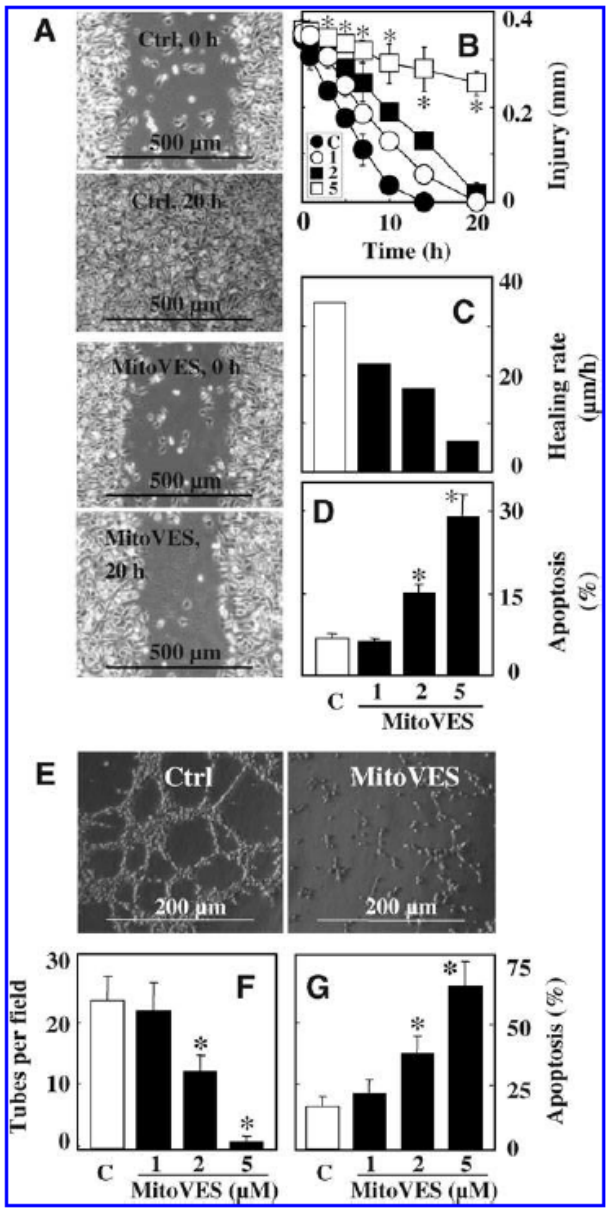

FIG. 3. MitoVES inhibits angiogenesis *in vitro*. For wound-healing activity assay, EAhy926 cells were seeded in culture dishes and allowed to reach complete confluency. The central part of the endothelial monolayer was wounded by removing a lane of cells ~0.5 mm across. Gap narrowing by proliferating and migrating cells was then followed in control cultures and in the presence of MitoVES. *Panel* **(A)** shows representative images of the dishes with ECs at time zero and 20 h in the absence or presence of 5 μM MitoVES. At different times, the gap width was assessed in the microscope and plotted as a function of time **(B)**. The "healing rate" was estimated from the slopes in *panel* **(B)** and expressed in μm/h **(C)**. The level of apoptosis in the "wounded" EAhy926 cultures was assessed at 42 h **(D)**. For the tube-forming activity assay, EAhy926 cells were seeded in 24-well plates with 300 μl of Matrigel per well so that the suspension of 200 μl of a complete medium with 5×10^5 cells were added to each well, and incubated in the absence or presence of MitoVES. *Panel* **(E)** shows micrographs of tubes formed in 12 h in the absence or presence of 5 μM MitoVES. The number of tubes in control cultures as well as those supplemented with MitoVES at concentrations shown (μM) was evaluated by counting the number of complete tubes connecting the points of individual polygons of the capillary network at 24 h as detailed in Materials and Methods section **(F)**. Cells were retrieved after 24 h from Matrigel and assessed for the level of apoptosis **(G)**. The micrographs in *panels* **(A)** and **(E)** are representative images of three independent experiments. The data in *panels* **(B)**, **(D)**, **(F)** and **(G)** are mean values ± SD ($n=3$). The symbol "*" in *panel* **(B)** denotes statistically significant difference of samples treated with the different concentrations of MitoVES form the controls, whereas in *panels* **(D)**, **(F)**, and **(G)**, it denotes statistically significant differences from the controls ($p<0.05$).

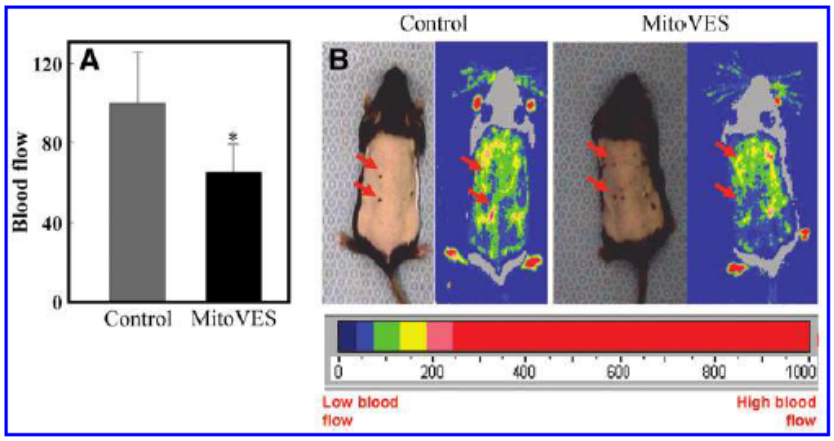

FIG. 4. MitoVES inhibits angiogenesis *in vivo*. Mice were wounded (*red arrows* indicate the wound positions) and treated with daily doses of 20 μM MitoVES in EtOH or identical volume of the excipient (control) for up to 7 days. On day 7, blood flow was visualized and quantified by a Lazer Doppler blood perfusion imager. **(A)** The data (blood flow), **(B)** representative images of the animals. The data shown are mean values ± SD ($n = 3$), the images are representative of three independent experiments. The symbol "*" denotes statistically significant differences from the controls ($p < 0.05$).

with nutrition and oxygen (13). This process, known as angiogenesis, is universal for all solid tumors, and its attenuation is considered beneficial and widely applicable to cancer treatment (14).

Potentially useful compounds in this regard are VE analogs, such as α-TOS and its mitochondrially-targeted derivative MitoVES that we recently developed. With regard to α-TOS, we already documented that it not only eliminates cancer cells but also proliferating ECs and inhibits angiogenesis (10, 33). We now show that the mitochondrial targeting of MitoVES by the TPP^+ group greatly enhances the effectivity of the parental, nontargeted compound and results in efficient killing of proliferating ECs already at concentrations as low as 2 μM, while discriminating between proliferating and arrested ECs. This would allow much lower therapeutic doses to be effectively used, which is preferential with regard to potential off-target effects. Selectivity for killing of angiogenic ECs was shown also for 4-(N-(S-glutathionylacetyl)amino) phenylarsenoxide, an arsenite analog, that was reported to induce apoptosis in proliferating ECs by interfering with the mitochondrial adenine nucleotide translocator (5).

It is apparent that MitoVES induces cell death in proliferating ECs by a mechanism similar to or identical with the parental, nontargeting α-TOS, which involves the increase of ROS before apoptosis induction as well as inhibition of angiogenesis in our models (10). This process is inhibited by the mitochondrially targeted antioxidant MitoQ and does not take place in the ECs with nonfunctional mitochondria, as shown using the ρ^0 EAhy926 cells. The shortening of the aliphatic linker between the succinate and the TTP^+ group also results in decreased activity of MitoVES, consistent with the requirement for the succinyl group to reach the ubiquinone-binding sites of mitochondrial CII, which has been shown to be the target through which α-TOS induces apoptosis in cancer cells (6, 9). This evidence shows that mitochondrial targeting using a linker of the right length between the targeting and the effector group is a plausible approach to increase effectivity of VE analogs while preserving the same or similar molecular mechanism, whereas the short-linker compounds lose effectivity, as their bioactive group cannot reach the target. Further downstream events, although not studied here, are likely to be mechanistically similar to those induced by α-TOS and MitoVES in cancer cells, where oxidative stress induced by the agents causes activation of the Hippo/Mst1 kinase, activation of the transcription factor FoxO1, and the subsequent increase in the expression of the Noxa protein, ultimately resulting in the generation of Bak-dependent channels in the mitochondrial outer membrane (8, 34, 44). Thus, since mitochondrial targeting also makes MitoVES an efficient and selective cancer cell killer (7), this modification produces an anticancer compound that promises to target tumors at multiple levels (direct tumor cell elimination and

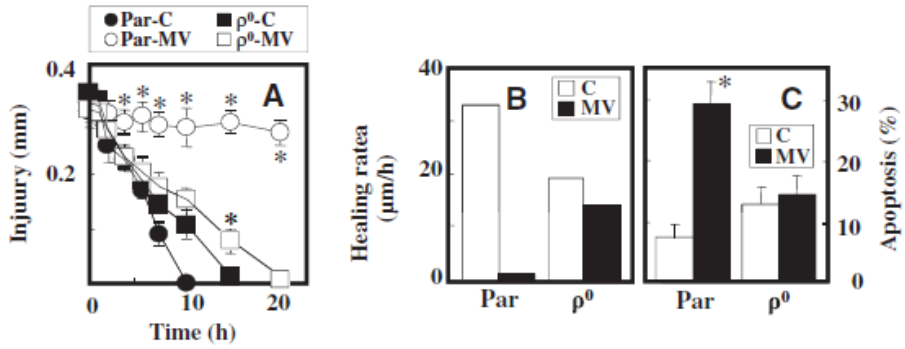

FIG. 5. ECs depleted of mtDNA are resistant to MitoVES. Proliferating parental and ρ^0 ECs were seeded in Petri dishes, allowed to reach confluency, and the endothelium was wounded. Regrowth was followed in the absence or presence of 5 μM MitoVES for up to 20 h, and the wound-healing activity expressed as the width of the wound as the function of time **(A)** and in $\mu m/h$ **(B)** as detailed in Materials and Methods section. At the end of the experiment (20 h), the individual cultures were assessed for the level of apoptosis. The data in *panels* **(A)** and **(C)** are mean values ± SD. ($n = 3$). The symbol "*" denotes statistically significant differences between control and treated cells.

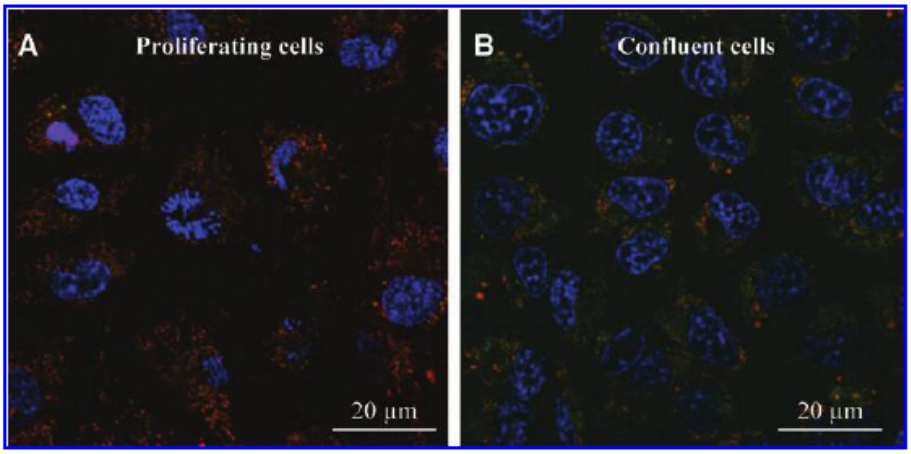

FIG. 6. MitoVES localizes to mitochondria. Proliferating **(A)** and confluent **(B)** EAhy926 cells were exposed to fluorescently tagged MitoVES (MitoVES-F) (green) at 10 μM for 30 min, after addition of MitoTracker Red and the Hoechst 33342 nuclear dye (blue), and live cells were inspected for green (MitoVES-F), red (MitoTracker Red), and blue fluorescence (Hoechst). The images are representative of 3 independent experiments.

angiogenesis inhibition) and with high efficiency and specificity, fulfilling the criteria for effective and broadly applicable anticancer agents.

Mitochondrial targeting of MitoVES is important for the observed high efficiency in killing proliferating ECs. This is exemplified by the propensity of fluorescently labeled MitoVES to accumulate in the mitochondria of proliferating ECs. In contrast, this accumulation was much less evident in confluent ECs, which are resistant to MitoVES-induced apoptosis. This suggests that mitochondrial uptake of MitoVES may be different in proliferating and confluent ECs. With regard to this, ECs represent a very interesting model that allows us to study the factors which determine MitoVES effectiveness and selectivity. Although MitoVES also displays preference for killing cancer cells as opposed to normal nontransformed cells, these represent different cell types harboring great differences in various cellular components. In contrast, it can be assumed that proliferating and confluent ECs are essentially identical in basic characteristics, and the factors associated with differences in susceptibility to MitoVES can be uncovered by using the cells at these two distinct proliferation states.

This article identifies that (at least) one major contributor to the difference in susceptibility of proliferating and arrested ECs to MitoVES is the considerable alteration in the mitochondrial potential ($\Delta\Psi_{m,i}$) of the two states of the cells. We show here, for the first time, that ($\Delta\Psi_{m,i}$) is higher in the proliferating ECs compared with confluent counterparts. That cells with greater $\Delta\Psi_{m,i}$ are susceptible to the killing activity of MitoVES is logical, given the notion that mitochondrial targeting of compounds tagged with the TPP^+ group is dependent on $\Delta\Psi_{m,i}$. Without relatively high $\Delta\Psi_{m,i}$, it is not possible for MitoVES to accumulate inside mitochondria. This is supported by the observation that the uncoupler FCCP, which dissipates $\Delta\Psi_{m,i}$, interferes with the induction of apoptosis by MitoVES, but not by the untargeted parental compound α-TOS. We have observed a similar paradigm also for cancer cells, which failed to undergo apoptosis when exposed to MitoVES in the presence of FCCP (7).

It should be noted that the difference in $\Delta\Psi_{m,i}$ is unlikely to be the sole factor that makes proliferating ECs susceptible to apoptosis induction by MitoVES. The nontargeted α-TOS also displays preference for eliminating proliferating ECs, albeit with much lower efficacy requiring the use of substantially higher concentrations for the desired effect to become apparent (10). Further research that is beyond the scope of this study will be necessary to elucidate these additional factors. For now, suffice to say that, given the safety of mitochondrial delivery by lipophilic TPP^+ accentuated by phase I/II trials with MitoQ-containing TPP^+ used for treatment of neurological disorders and hepatitis with no adverse effects even after more than 1 year of supplementation (17, 39), with MitoVES, we have an agent available that, besides specifically killing cancer cells (7), efficiently eliminates proliferating ECs while leaving the arrested confluent ECs unaffected. As such, MitoVES possesses a set of interesting biological properties that allow it to attack cancer simultaneously at several fronts and, in the future, turn the odds of cancer treatment in the patient's favor. This notion is epitomized by the profound effect of MitoVES on the tumor progression and inhibition of angiogenesis. We propose that given the anticancer effect of MitoVES due to selective killing of tumor cells (7, 8) and inhibiting tumorigenic angiogenesis (this report), clinical tests are warranted, taking into consideration the inhibitory effect of MitoVES on wound healing. To this end, MitoVES is one of very few compounds that have been reported to selectively kill proliferating but not arrested ECs, which endows it with a substantial clinical spin.

Materials and Methods

Cell culture and reagents

The endothelial-like EAhy926 cells (11) were maintained in DMEM supplemented with 10% fetal calf serum and antibiotics, plus HAT (100 μM hypoxanthine, 0.4 μM aminopterin, and 16 μM thymidine). These cells retain properties of ECs, including expression of factor VIII (11), tube-forming activity, and the propensity to persist in confluent cultures (1). EAhy926 cells deficient in mtDNA (ρ^0 phenotype) were prepared as detailed elsewhere (46). Acquisition of the ρ^0 phenotype was confirmed by the lack of expression of the mtDNA-coded cytochrome c oxidase subunit II but not its nDNA-coded subunit IV (data not shown). The proliferating and confluent ECs were used in the various experiments such that a similar number of cells was assessed.

The cells were treated under conditions of proliferation (40%–50% confluency) or arrest (100% confluency), in most cases with MitoVES, a compound with an 11-carbon linker joining the tocopheryl succinyl head group and the

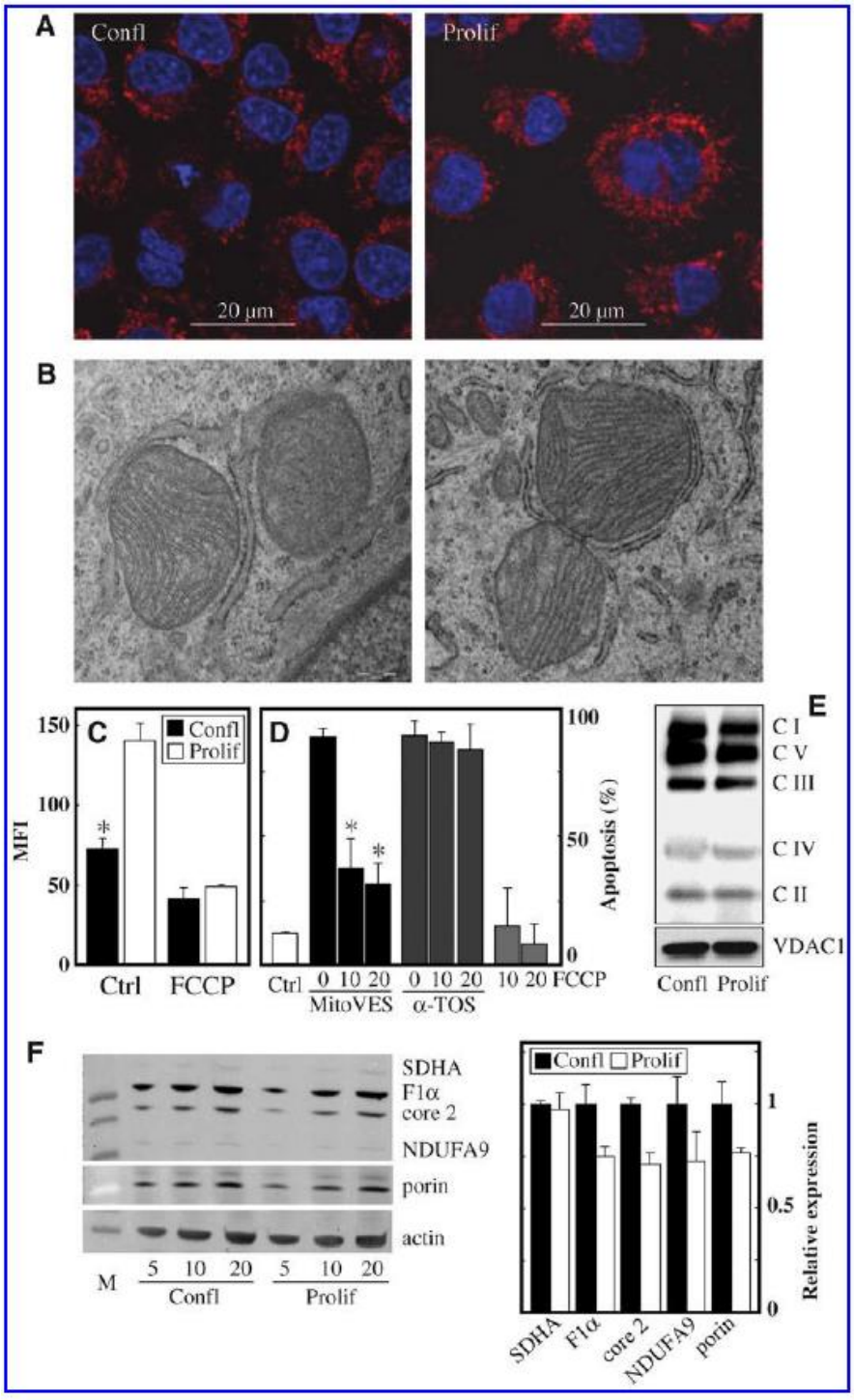

FIG. 7. Susceptibility of proliferating ECs to MitoVES is based on their higher mitochondrial potential. (A) Confluent (*left*) and proliferating (*right*) EAhy926 cells were supplemented with tetramethylrhodamine methyl ester (TMRM), the nuclei were stained with the Hoechst 33342 dye, and live cells were inspected by confocal microscopy. **(B)** Proliferating and confluent EAhy926 cells were fixed, sectioned, and inspected for mitochondrial morphology by transmission electron microscopy. **(C)** Proliferating and confluent EAhy926 cells were incubated with TMRM in the absence or presence of carbonyl cyanide 4-(trifluoromethoxy)-phenylhydrazone (FCCP), and the relative mitochondrial potential assessed by flow cytometry. **(D)** Proliferating EAhy926 cells were exposed to 5 μM MitoVES for 9 h in the presence or absence of FCCP at the concentrations shown (μM) and the level of apoptosis assessed. **(E)** Proliferating and confluent EAhy926 cells were subjected to Native Blue electrophoresis to visualize the individual mitochondrial complexes. VDAC1 was used as the loading control. **(F)** Cellular extract from confluent and proliferating ECs was subjected to SDS-PAGE followed by western blotting (*left panel*) using antibodies to subunits of complex II (CII) (SDHA), CV (F1α), CIII (core 2 subunit), and CI (NDUFA9), and to the outer membrane constituent porin. Actin was used as a loading control. The *right panel* shows the ratios of the relative level of individual proteins detected by western blotting related to actin after their densitometric evaluation. Images in panel **(A, B, E,** and **F,** *left*) are representative of three independent experiments, data in *panels* **(C)** and **(D)** are mean values ± SD ($n = 3$), and data in *panel* **(F)** (*right*) are average values ± SD derived from the densitograpic evaluation of the level of the different proteins obtained with three different amounts of total protein loaded (c.f. *panel* **F**, *left*). The symbol "*" denotes statistically significant differences between the control and treated cells ($p < 0.05$).

mitochondria-targeting TPP^+ group (Fig. 1). We also exposed ECs to VES4TPP, a compound derived from α-TOS, in which the TPP^+ group is attached to the free carboxyl group of the succinyl moiety *via* a 4-carbon linker, as well as to shorter-chain homologs of MitoVES (Fig. 1). To show mitochondrial localization, a fluorescent analog of MitoVES (MitoVES-F; for structure see Fig. 1) was prepared by addition of 5-aminofluorescein to the free carboxylate of MitoVES. The detailed description of the synthesis of the mitochondrially targeted compounds shown in Figure 1 will be published separately.

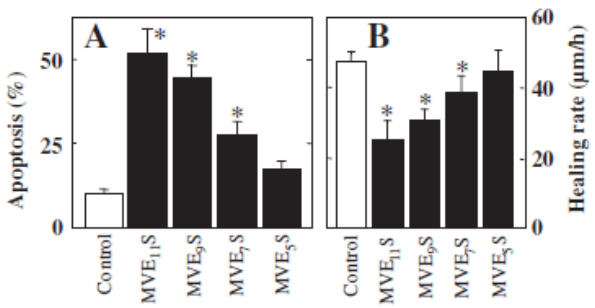

FIG. 8. Susceptibility of ECs to MitoVES is dependent on its structure. (A) EAhy926 cells at 50%–60% confluency were exposed to MitoVES homologs with different length of the aliphatic chain at 5 μM for 12 h, after which the cells were assessed for the level of apoptosis. **(B)** Fully confluent EAhy926 cells were "injured," and their re-growth followed in the presence of different MitoVES homologs at 5 μM. The "healing rate" was evaluated as detailed in Materials and Methods section. The data are mean values ± SD ($n = 3$), and the symbol "*" denotes statistically significant differences between the control and treated cells ($p < 0.05$).

Assessment of generation of intracellular ROS

Intracellular ROS levels were assessed by using the fluorescent dye 2′7′-dichlorofluorescein diacetate (DCFA). ECs were seeded in 24-well flat-bottom plates, treated, re-suspended in PBS, and supplemented with 5 μM DCFA, a cell-permeable, ROS-sensitive dye. After a 30-min incubation in the dark, the cells were collected, washed, and analyzed by flow cytometry (FACS Calibur; Becton Dickinson). The level of ROS was detected as fluorescence intensity and expressed as fold change with regard to the control.

Assessment of apoptosis and cell cycle

Apoptosis was quantified by using the annexin V-FITC method, which detects phosphatidyl serine externalized in the early phases of apoptosis (28, 46). After exposure to various compounds, floating and attached cells were collected, washed with PBS, re-suspended in 100 μl binding buffer, incubated for 20 min at room temperature with 2 μl annexin V-FITC plus 10 μl propidium iodide (PI) (10 μg/ml), and analyzed by flow cytometry by using channel 1 for annexin V-FITC binding and channel 2 for PI staining. Cell cycle was assessed as reported elsewhere (28).

Assessment of $\Delta\Psi_{m,i}$

To assess the mitochondrial membrane potential ($\Delta\Psi_{m,i}$), we used the $\Delta\Psi_{m,i}$-sensitive fluorescent probe TMRM (Sigma) at 50 nM, followed by flow cytometry assessment of red fluorescence of the mitochondria-accumulated probe. The mitochondrial uncoupler carbonyl cyanide 4-(trifluoromethoxy)-phenylhydrazone (FCCP; Sigma) was used as a control to determine nonspecific TMRM loading. The amounts of cells for various conditions were kept similar.

Native Blue electrophoresis

Confluent and proliferating EAhy926 cells were harvested by tripsinization, and the cells were resuspended in the Tris/EGTA buffer containing 200 mM sucrose and homogenized on ice with glass homogenizer at 1600 rpm. Mitochondria were isolated by differential centrifugation as follows. Lyzed cells were first centrifuged at 900 g for 10 min, and the mitochondria-containing supernatant was spun down by centrifugation at 7000 g for 15 min. Mitochondria were solubilized in the extraction buffer (1.5 M aminocaproic acid, 50 mM Bis-Tris, 0.5 M EDTA, and pH 7) containing 1.3% lauryl maltoside. Samples comprising 30–60 μg of protein were then mixed with the sample buffer (0.75 M aminocaproic acid, 50 mM Bis-Tris, 0.5 M EDTA, pH 7, 5% Serva-Blue G-250, and 12% glycerol) and loaded on the precasted NativePAGE Novex 4%–6% Bis-Tris gels run overnight at a constant voltage of 25 V. Separated protein complexes were then transferred to the PVDF membrane using the Transblot Invitrogen system. CI, CV, and CIII were detected with the Mitoprofile total OXPHOS blue native antibody coctail (MitoSciences MS 603), CIV was detected with the MTCO1 (ID6) antibody (Abcam AB14705-100), and CII was detected with the SDHA (2E3) antibody (Abcam AB14715-200).

Western blotting and citrate synthase assay

The relative number of mitochondria in the proliferating and confluent ECs was estimated by using SDS-PAGE (37) followed by western blotting using a cocktail of monoclonal antibodies against the following mitochondrial subunits: NDUFA9 subunit of CI, SDHA subunit of CII, UQCRC2 (core 2) subunit of CIII and ATP5A1 (F1α) subunit of CV (Mitosciences), and polyclonal antibody against porin/VDAC1 (4). Monoclonal antibody against actin (Calbiochem) was used as a loading control. The membranes were incubated with secondary antibodies labeled with Alexa Fluor 680 or 780 (Invitrogen; 1:3000), and the fluorescence was detected by using the Odyssey Imager (LI-COR) and quantified using the Aida 3.21 Image Analyzer software (Raytest).

The activity of the mitochondrial matrix enzyme citrate synthase was spectrophotometrically determined as described elsewhere (38).

Cadherin VE expression

For immunofluorescence microscopy, EAhy926 cells at 100% confluence were incubated with anticadherin VE IgG followed by secondary FITC-conjugated IgG and mounted with DAPI-containing Vectashield. The cells were inspected by using a confocal microscope.

Assay of mitochondrial localization of MitoVES

For the acquisition of the localization of MitoVES, the fluorescently tagged compound (MitoVE$_{11}$S-F, green) was synthesized as will be published elsewhere. EAhy926 cells were grown on cover slips (at either 50%–60% or 100% confluency), stained with the nuclear dye Hoechst 33342 (blue), MitoTracker Red (Molecular Probes), and incubated with 10 μM MitoVES-F for 30 min, after which they were inspected by using a confocal microscope.

Wound healing and tube-forming activity assessment

ECs were seeded and cultured to complete confluence. The central region of a monolayer of cells was "wounded" by scraping away cells, generating a denuded 0.5-mm wide stripe. Re-growth of cells was assessed by following the kinetics of filling the gap, visualized under a microscope

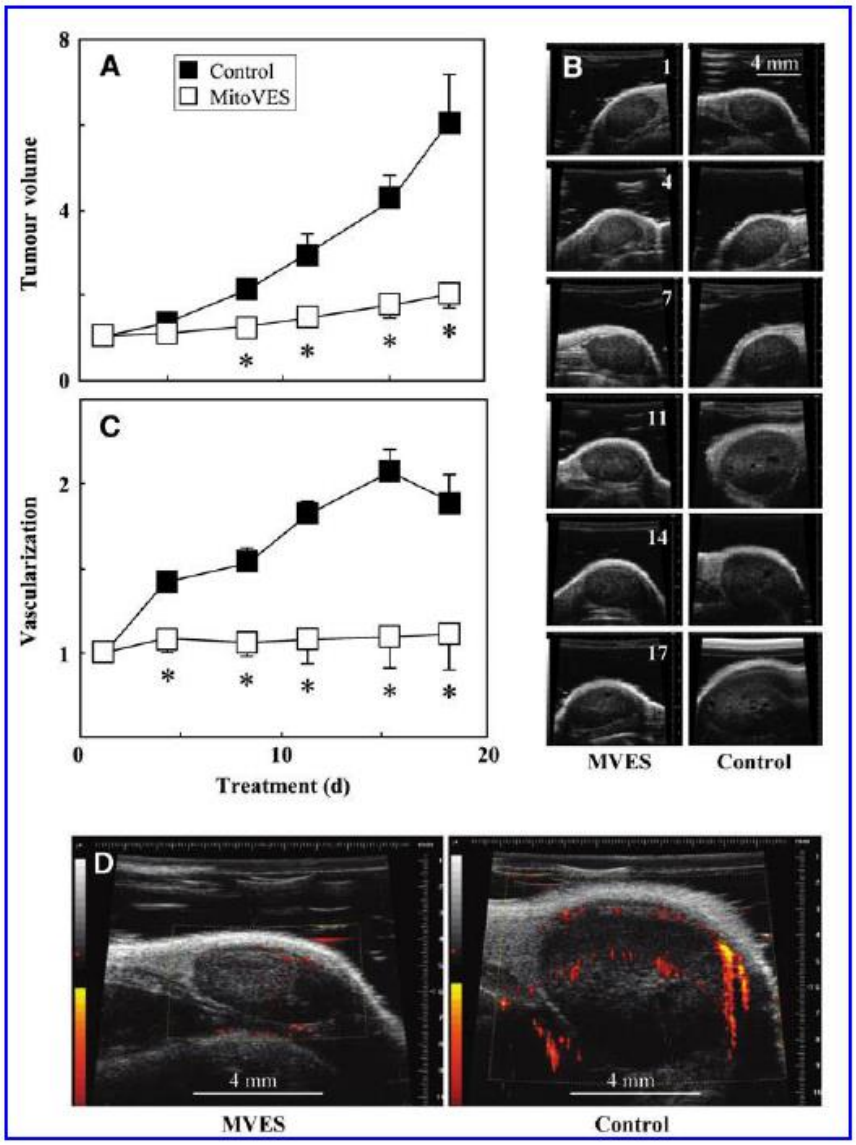

FIG. 9. MitoVES suppresses tumor progression and angiogenesis in a mouse model. Female FVB/N *c-neu* mice with small tumors ($\sim$40 mm^3) were treated by intraperitoneal injection twice a week with 100 μl 6 m*M* MitoVES in corn oil with 4% EtOH. Ultrasound imaging was used to noninvasively monitor and quantify tumor progression (relative volume, **A**) and tumor vascularization **(C)**. *Panel* **(B)** shows a representative tumor of treated and control mice on the individual days of the experiment, *panel* **(D)** vascularization (2D ultrasonograph) of a representative tumor of the treated and control mouse on day 17. The data in *panels* **(A)** and **(C)** are mean values $\pm$ SD ($n=6$), and the symbol "*" denotes statistically significant differences between the control and treated animals ($p<0.05$).

equipped with a grid in the eyepiece. The healing rate was expressed in μm/h.

For the tube-forming activity of ECs, formation of capillary-like structures in a 3-D setting was assessed, essentially as described elsewhere (11). Briefly, 300 μl of cold Matrigel (BD Biosciences) per well was transferred with a cold tip by using a 24-well plate. Matrigel was overlaid with a suspension of EAhy926 cells so that a total of 200 μl of complete media with 5×10^5 cells was added to each well. After 6 h in the incubator, the polygonal structures, made by a network of EAhy926 capillaries, were established. The cells were treated, and the tube-forming activity was estimated by counting the number of complete capillaries connecting individual points of the polygonal structures in a light microscope 24 h after transferring the cells onto Matrigel. Three fields in the central area were randomly chosen in every well. The number of capillaries in control cultures was considered 100%.

Assessment of wound healing in vivo

The mouse *in vivo* model of wound healing was essentially used as described (36), employing the MoorLDI-Mark 2 lazer Doppler blood perfusion imager (Moore Instruments Ltd.) (2). C57BL/6 mice between the ages of 8 and 10 weeks were used. The back of the mouse was shaved with standard animal hair clippers (No. 40 blade) and disinfected with betadine. Using microdissecting forceps, the skin of the animal was lifted along the line as shown, and a 4-mm dermal biopsy punch was driven through the two folds of skin. MitoVES was dissolved in EtOH and applied at the final concentration of 20 μ*M*. Control mice received an identical volume of EtOH. On day 1, 10 μl of the drug or the excipient were applied at 4 points surrounding the wound *via* an inward injection. On day 2 and onward, the drug was topically applied through the tegaderm dressing. The images were acquired on day 7.

Transmission electron microscopy

Cells were subjected to TEM after being processed as described (46).

Animal tumor studies

Transgenic FVB/N202 *c-neu* mice carrying the rat HER2/neu proto-oncogene driven by the MMTV promoter on the H-2^q FVB/N background (19) were established at the Griffith University Animal Facility and maintained under strict inbreeding conditions. About 70% of the female mice develop spontaneous mammary carcinomas with a mean latency time of 10 months (6–12 months). Female FVB/N202 rat *c-neu* mice with small tumors (about 40 mm^3) were treated with either 100 μl 6 m*M* MitoVES in 4% ethanol/corn oil or the same volume of the excipient by intraperitoneal injection once every 3 or 4 days. Tumor volume and relative vascularization were quantified by using the Power Doppler Mode of the USI instrument (the Vevo770 device fitted with the RMV704 scanhead from VisualSonics) twice a week after each treatment. Both the treated and the control group contained at least 6 mice. Mouse body temperature and the setting of the Power Doppler mode were kept the same throughout the experiment.

All animal experiments were performed according to the guidelines of the Australian and New Zealand Council for the Care and Use of Animals in Research and Teaching and were approved by the Griffith University Animal Ethics Committee.

Statistical analysis

All data shown are mean values of three independent experiments (unless stated otherwise) ±SD. Statistical significance was assessed by using Student's *t*-test, and differences were considered significant at $p < 0.05$. For animal experiments, the difference in the mean relative tumor size ± SEM was examined by using analyses of covariance (ANCOVA) with days as the covariate. Statistical analyses were performed by using SPSS® 10.0 analytical software (SPSS). Differences were considered statistically significant when the value of $p < 0.05$.

Acknowledgments

This project was supported in part by grants from the Australian Research Council, the National Health and Medical Research Council of Australia, the Cancer Council Queensland, the Grant Agency of the Czech Republic (204/08/0811, 305/07/1008, P301/10/1937) and the Grant Agency of the Academy of Sciences of the Czech Republic (KAN200520703) to J.N., the National Institutes of Health (NS42617, GM77185, and GM69589) to C.K.S, and the Ministry of Education, Youth and Sports of the Czech Republic (1M6837805002) to J.H. The authors thank Ivana Novakova for technical assistance.

Author Disclosure Statement

The authors disclose no conflict of interest.

References

1. Albini A, Marchisone C, Del Grosso F, Benelli R, Masiello L, Tacchetti C, Bono M, Ferrantini M, Rozera C, Truini M, Belardelli F, Santi L, and Noonan DM. Inhibition of angiogenesis and vascular tumor growth by interferon-producing cells: a gene therapy approach. *Am J Pathol* 156: 1381–1393, 2000.
2. Biswas S, Roy S, Banerjee J, Hussain SR, Khanna S, Meenakshisundaram G, Kuppusamy P, Friedman A, and Sen CK. Hypoxia inducible microRNA 210 attenuates keratinocyte proliferation and impairs closure in a murine model of ischemic wounds. *Proc Natl Acad Sci U S A* 107: 6976–6981, 2010.
3. Cross MJ and Claesson-Walsh L. FGF and VEGF function in angiogenesis: signalling pathways, biological responses and therapeutic inhibition. *Trends Pharmacol Sci* 22: 201–207, 2001.
4. De Pinto V, Prezioso G, Thinnes F, Link TA, and Palmieri F. Peptide-specific antibodies and proteases as probes of the transmembrane topology of the bovine heart mitochondrial porin. *Biochemistry* 30: 10191–10200, 1991.
5. Don AS, Kisker O, Dilda P, Donoghue N, Zhao X, Decollogne S, Creighton B, Flynn E, Folkman J, and Hogg PJ. A peptide trivalent arsenical inhibits tumor angiogenesis by perturbing mitochondrial function in angiogenic endothelial cells. *Cancer Cell* 3: 497–509, 2003.
6. Dong LF, Freeman R, Liu J, Zobalova R, Marin-Hernandez A, Stantic M, Rohlena J, Rodriguez-Enriquez S, Valis K, Butcher B, Goodwin J, Brunk UT, Witting PK, Moreno-Sanchez R, Scheffler IE, Ralph SJ, and Neuzil J. Suppression of tumour growth *in vivo* by the mitocan α-tocopheryl succinate requires respiratory complex II. *Clin Cancer Res* 15: 1593–1600, 2009.
7. Dong LF, Jameson VJA, Tilly D, Cerny J, Mahdavian E, Marín-Hernández A, Hernández-Esquivel L, Rodríguez-Enríquez S, Witting PK, Stantic B, Rohlena J, Truksa J, Kluckova K, Dyason JC, Salvatore BA, Moreno-Sánchez R, Coster MJ, Ralph SJ, Smith RAJ, and Neuzil J. Mitochondrial targeting of vitamin E succinate enhances its pro-apoptotic and anti-cancer activity via mitochondrial complex II. *J Biol Chem* 286: 3717–3728, 2011.
8. Dong LF, Jameson VJA, Tilly D, Prochazka L, Rohlena J, Valis K, Truksa J, Zobalova R, Mahdavian E, Kluckova K, Stantic M, Stursa J, Wang XF, Freeman R, Witting PK, Norberg E, Goodwin J, Salvatore BA, Novotna J, Turanek J, Ledvina M, Hozak P, Zhivotovsky B, Coster MJ, Ralph SJ, Smith RAJ, and Neuzil J. Mitochondrial targeting of α-tocopheryl succinate enhances its pro-apoptotic efficacy: A new paradigm of efficient anti-cancer therapy. *Free Radic Biol Med* 50: 1546–1555, 2011.
9. Dong LF, Low P, Dyason J, Wang XF, Prochazka L, Witting PK, Freeman R, Swettenham E, Valis K, Liu J, Zobalova R, Turanek J, Spitz DR, Domann FE, Scheffler IE, Ralph SJ, and Neuzil J. α-Tocopheryl succinate induces apoptosis by targeting ubiquinone-binding sites in mitochondrial respiratory complex II. *Oncogene* 27: 4324–4335, 2008.
10. Dong LF, Swettenham E, Eliasson J, Wang XF, Gold M, Medunic Y, Stantic M, Low P, Prochazka L, Witting PK, Turanek J, Akporiaye ET, Ralph SJ, and Neuzil J. Vitamin E analogs inhibit angiogenesis by selective apoptosis induction in proliferating endothelial cells: The role of oxidative stress. *Cancer Res* 67: 11906–11913, 2007.
11. Edgell CJ, McDonald CC, and Graham JB. Permanent cell line expressing human factor VIII-related antigen established by hybridization. *Proc Natl Acad Sci U S A* 80: 3734–3737, 1983.
12. Fantin VR and Leder P. Mitochondriotoxic compounds for cancer therapy. *Oncogene* 5: 4787–4797, 2006.
13. Folkman J. Angiogenesis. *Annu Rev Med* 57: 1–18, 2006.

14. Folkman J. Angiogenesis: an organizing principle for drug discovery? *Nat Rev Drug Discov* 6: 273–286, 2007.
15. Folkman J and Shing Y. Angiogenesis. *J Biol Chem* 267: 10931–10934, 1992.
16. Fulda S, Galluzzi L, and Kroemer G. Targeting mitochondria for cancer therapy. *Nat Rev Drug Discov* 9: 447–464, 2010.
17. Gane EJ, Orr DW, Keogh GF, Gibson M, Lockhart MM, Frampton CM, Taylor KM, Smith RA, and Murphy MP. The mitochondria-targeted anti-oxidant mitoquinone decreases liver damage in a phase II study of hepatitis C patients. *Liver Int* 30: 1019–1026, 2010.
18. Gogvadze V, Orrenius S, and Zhivotovsky B. Mitochondria in cancer cells: what is so special about them? *Trends Cell Biol* 18: 165–173, 2008.
19. Guy CT, Webster MA, Schaller M, Parsons TJ, Cardiff RD, and Muller WJ. Expression of the neu protooncogene in the mammary epithelium of transgenic mice induces metastatic disease. *Proc Natl Acad Sci U S A* 89: 1078–1082, 1992.
20. Jemal A, Siegel R, Ward E, Hao Y, Xu J, and Thun MJ. Cancer statistics, 2010. *CA Cancer J Clin* 60: 277–300, 2010.
21. Kelso GF, Porteous CM, Coulter CV, Hughes G, Porteous WK, Ledgerwood EC, Smith RA, and Murphy MP. Selective targeting of a redox-active ubiquinone to mitochondria within cells: antioxidant and antiapoptotic properties. *J Biol Chem* 276: 4588–4596, 2001.
22. Malafa MP, Fokum FD, Andoh J, Neitzel LT, Bandyopadhyay S, Zhan R, Iiizumi M, Furuta E, Horvath E, and Watabe K. Vitamin E succinate suppresses prostate tumor growth by inducing apoptosis. *Int J Cancer* 118: 2441–2447, 2006.
23. Malafa MP, Fokum FD, Mowlavi A, Abusief M, and King M. Vitamin E inhibits melanoma growth in mice. *Surgery* 131: 85–91, 2002.
24. Moreno-Sánchez R, Rodríguez-Enríquez S, Marín-Hernández A, and Saavedra E. Energy metabolism in tumor cells. *FEBS J* 274: 1393–1418, 2007.
25. Murphy MP and Smith R. Targeting antioxidants to mitochondria by conjugation to lipophilic cations. *Annu Rev Pharmacol Toxicol* 47: 629–656, 2007.
26. Neuzil J. Vitamin E succinate and cancer treatment: a vitamin E prototype for selective anti-tumour activity. *Br J Cancer* 89: 1822–1826, 2003.
27. Neuzil J, Dong LF, Ramanathapuram L, Hahn T, Chladova M, Wang XF, Zobalova R, Prochazka L, Gold M, Freeman RE, Turanek J, Akporiaye ET, Dyason J, and Ralph SJ. Vitamin E analogues: a novel group of mitocans, anti-cancer agents that act by targeting mitochondria. *Mol Aspects Med* 28: 607–645, 2007.
28. Neuzil J, Schröder A, von Hundelshausen P, Zernecke A, Weber T, Gellert N, and Weber C. Inhibition of inflammatory endothelial responses by a pathway involving caspase activation and p65 cleavage. *Biochemistry* 40: 4686–4692, 2001.
29. Neuzil J, Swettenham E, Wang XF, Dong LF, and Stapelberg M. α-Tocopheryl succinate inhibits angiogenesis by disrupting paracrine FGF2 signalling. *FEBS Lett* 581: 5611–5615, 2007.
30. Neuzil J, Tomasetti M, Zhao Y, Dong LF, Birringer M, Wang XF, Low P, Wu K, Salvatore BA, and Ralph SJ. Vitamin E analogs, a novel group of 'mitocans', as anti-cancer agents: The importance of being redox-silent. *Mol Pharmacol* 71: 1185–1199, 2007.
31. Neuzil J, Wang XF, Dong LF, Low P, and Ralph SJ. Molecular mechanism of 'mitocan'-induced apoptosis in cancer cells epitomizes the multiple roles of reactive oxygen species and Bcl-2 family proteins. *FEBS Lett* 580: 5125–5129, 2006.
32. Neuzil J, Weber T, Gellert N, and Weber C. Selective cancer cell killing by α-tocopheryl succinate. *Br J Cancer* 84: 87–89, 2001.
33. Park D and Dilda P. Mitochondria as targets in angiogenesis inhibition. *Mol Asp Med* 31: 113–131, 2010.
34. Prochazka L, Dong LF, Valis K, Freeman R, Ralph SJ, Turanek J, and Neuzil J. α-Tocopheryl succinate causes mitochondrial permeabilization by preferential formation of Bak channel. *Apoptosis* 15: 782–794, 2010.
35. Rafii S, Lyden D, Benezra R, Hattori K, and Heissig B. Vascular and haematopoietic stem cells: novel targets for anti-angiogenesis therapy? *Nat Rev Cancer* 2: 826–835, 2002.
36. Roy S, Biswas S, Khanna S, Gordillo G, Bergdall V, Green J, Marsh CB, Gould LJ, and Sen CK. Characterization of a preclinical model of chronic ischemic wound. *Physiol Genomics* 37: 211–224, 2009.
37. Schägger H and von Jagow G. Tricine-sodium dodecyl sulfate-polyacrylamide gel electrophoresis for the separation of proteins in the range from 1 to 100 kDa. *Anal Biochem* 166: 368–379, 1987.
38. Singh M, Brooks GC, and Srere PA. Subunit structure and chemical characteristics of pig heart citrate synthase. *J Biol Chem* 245: 4636–4640, 1970.
39. Snow BJ, Rolfe FL, Lockhart MM, Frampton CM, O'Sullivan JD, Fung V, Smith RA, Murphy MP, and Taylor KM. A double-blind, placebo-controlled study to assess the mitochondria-targeted antioxidant MitoQ as a disease-modifying therapy in Parkinson's disease. *Mov Disord* 25: 1670–1674, 2010.
40. Stapelberg M, Gellert N, Swettenham E, Tomasetti M, Witting PK, Procopio A, and Neuzil J. α-Tocopheryl succinate inhibits malignant mesothelioma by disrupting the FGF autocrine loop: the role of oxidative stress. *J Biol Chem* 280: 25369–25376, 2005.
41. Sun F, Huo X, Zhai Y, Wang A, Xu J, Su D, Bartlam M, and Rao Z. Crystal structure of mitochondrial respiratory membrane protein complex II. *Cell* 121: 1043–1057, 2005.
42. Tomasetti M, Gellert N, Procopio A, and Neuzil J. A vitamin E analogue suppresses malignant mesothelioma in a preclinical model: a prototype of a future drug against a fatal neoplastic disease? *Int J Cancer* 109: 641–642, 2004.
43. Trachootham D, Alexandre J, and Huang P. Targeting cancer cells by ROS-mediated mechanisms: a radical therapeutic approach? *Nat Rev Drug Discov* 8: 579–591, 2009.
44. Valis K, Prochazka L, Boura E, Chladova M, Obsil T, Rohlena J, Truksa J, Dong LF, Ralph SJ, and Neuzil J. Hippo/Mst1 stimulates transcription of *NOXA* in a FoxO1-dependent manner. *Cancer Res* 71: 946–954, 2011.
45. Wang XF, Birringer M, Dong LF, Veprek P, Low P, Swettenham E, Stantic M, Yuan LH, Zobalova R, Wu K, Ralph SJ, Ledvina M, and Neuzil J. A peptide adduct of vitamin E succinate targets breast cancer cells with high erbB2 expression. *Cancer Res* 67: 3337–3344, 2007.
46. Weber T, Dalen H, Andera L, Nègre-Salvayre A, Augé N, Sticha M, Loret A, Terman A, Witting PK, Higuchi M, Plasilova M, Zivny J, Gellert N, Weber C, and Neuzil J. Mitochondria play a central role in apoptosis induced by α-tocopheryl succinate, an agent with anticancer activity. Comparison with receptor-mediated pro-apoptotic signaling. *Biochemistry* 42: 4277–4291, 2003.

47. Weber T, Lu M, Andera L, Lahm H, Gellert N, Fariss MW, Korinek V, Sattler W, Ucker DS, Terman A, Schröder A, Erl W, Brunk U, Coffey RJ, Weber C, and Neuzil J. Vitamin E succinate is a potent novel anti-neoplastic agent with high tumor selectivity and cooperativity with tumor necrosis factor-related apoptosis-inducing ligand (TRAIL, Apo2L) *in vivo*. *Clin Cancer Res* 8: 863–869, 2002.

Address correspondence to:
Prof. Jiri Neuzil
School of Medical Science
Griffith University
Southport QLD 4222
Australia

E-mail: j.neuzil@griffith.edu.au

Dr. Lan-Fang Dong
School of Medical Science
Griffith University
Southport QLD 4222
Australia

E-mail: l.dong@griffith.edu.au

Dr. Jakub Rohlena
Institute of Biotechnology
Academy of Sciences of the Czech Republic
Prague 142 20
Czech Republic

E-mail: jakub.rohlena@img.cas.cz

Date of first submission to ARS Central, July 26, 2011; date of final revised submission, August 29, 2011; date of acceptance, August 30, 2011.

Abbreviations Used

α-TOS = α-tocopheryl succinate
$\Delta\Psi_{m,i}$ = mitochondrial inner trans-membrane potential
CI = complex I
DCFA = 2′,7′-dihydrodichlorofluorescein diacetate
ECs = endothelial cells
FCCP = carbonyl cyanide 4-(trifluoromethoxy) phenylhydrazone
MIM = mitochondrial inner membrane
MitoQ = mitochondrially targeted analog of coenzyme Q
MitoVES = mitochondrially targeted analog of α-tocopheryl succinate
MitoVES-F = fluorescently tagged MitoVES
PI = propidium iodide
Q_P = proximal ubiquinone-binding site
ROS = reactive oxygen species
TEM = transmission electron microscopy
TMRM = tetramethylrhodamine methyl ester
TPP^+ = triphenyl phosphonium
USI = ultrasound imaging
VE = vitamin E

Apoptosis (2013) 18:286–299
DOI 10.1007/s10495-012-0795-1

ORIGINAL PAPER

Mitochondrial targeting overcomes ABCA1-dependent resistance of lung carcinoma to α-tocopheryl succinate

Lubomir Prochazka · Stepan Koudelka · Lan-Feng Dong · Jan Stursa · Jacob Goodwin · Jiri Neca · Josef Slavik · Miroslav Ciganek · Josef Masek · Katarina Kluckova · Maria Nguyen · Jaroslav Turanek · Jiri Neuzil

Published online: 9 January 2013

Abstract α-Tocopheryl succinate (α-TOS) is a promising anti-cancer agent due to its selectivity for cancer cells. It is important to understand whether long-term exposure of tumour cells to the agent will render them resistant to the treatment. Exposure of the non-small cell lung carcinoma H1299 cells to escalating doses of α-TOS made them resistant to the agent due to the upregulation of the ABCA1 protein, which caused its efflux. Full susceptibility of the cells to α-TOS was restored by knocking down the ABCA1 protein. Similar resistance including *ABCA1* gene upregulation was observed in the A549 lung cancer cells exposed to α-TOS. The resistance of the cells to α-TOS was overcome by its mitochondrially targeted analogue, MitoVES, that is taken up on the basis of the membrane potential, bypassing the enhanced expression of the ABCA1 protein. The in vitro results were replicated in mouse models of tumours derived from parental and resistant H1299 cells. We conclude that long-term exposure of cancer cells to α-TOS causes their resistance to the drug, which can be overcome by its mitochondrially targeted counterpart. This finding should be taken into consideration when planning clinical trials with vitamin E analogues.

Keywords Vitamin E analogues · Apoptosis · Mitochondrial targeting · ABCA1 · Acquired resistance

L. Prochazka (✉) · S. Koudelka · J. Neca · J. Slavik · M. Ciganek · J. Masek · J. Turanek
Veterinary Research Institute, Brno, Czech Republic
e-mail: lubomir.pr@gmail.com

L. Prochazka · J. Neuzil (✉)
Apoptosis Research Group, School of Medical Science and Griffith Health Institute, Griffith University, Gold Coast Campus, Southport, QLD 4222, Australia
e-mail: j.neuzil@griffith.edu.au

L.-F. Dong · J. Stursa · J. Goodwin · M. Nguyen · J. Neuzil
School of Medical Science, Griffith University, Southport, QLD 4222, Australia

J. Stursa
Institute of Organic Chemistry and Biochemistry, Academy of Sciences of the Czech Republic, Prague, Czech Republic

K. Kluckova · J. Neuzil
Institute of Biotechnology, Academy of Sciences of the Czech Republic, Prague, Czech Republic

Introduction

In spite of the recent progress in molecular medicine, cancer is an unrelenting problem World-wide [1–3]. A reason for the very grim prognosis in neoplastic pathologies is the constant tendency of malignant cells to mutate. It has been documented that even the same types of cancer differ considerably in their number of mutations [4, 5]. It is therefore unlikely that neoplastic diseases in a wider scope could be treated with agents that target one gene or a single pathway [6]. What is needed is a therapeutic approach that would hit the 'Achilles heel' of cancer, i.e. an invariant feature that is essential for the propagation of tumours [7].

Such a target is presented by mitochondria, a recent focus of cancer research due to their major role in the physiology of cancer cell and due to being an emerging target for anti-cancer therapies [8–10]. A group of compounds targeting mitochondria to induce apoptosis and suppress cancer, mitocans, has been defined [11]. These agents are classified into groups based on their molecular target in and around mitochondria [12]. Many mitocans are selective anti-cancer agents, as shown for example for

α-tocopheryl succinate (α-TOS), targeting the mitochondrial electron transport chain [13, 14].

We have been studying the intriguing α-TOS for its potential anti-cancer activity. The agent targets mitochondria to produce reactive oxygen species (ROS) that then trigger apoptosis [15–17]. More specifically, ROS promote phosphorylation of the Mst1 kinase, resulting in phosphorylation of the transcription factor FoxO1 that translocates into the nucleus. This is followed by increased expression of Noxa that diverts Mcl-1 from Bak, causing formation of pores in the mitochondrial outer membrane, whereby promoting the apoptotic cascade downstream of mitochondria [18–20].

The target of α-TOS is the ubiquinone (UbQ)-binding site of the mitochondrial complex II (CII) [21, 22]. The agent does not substantially inhibit the succinate dehydrogenase activity of CII, therefore the electrons formed via conversion of succinate to fumarate are channelled to the UbQ site [23]. Since α-TOS displaces UbQ, the electrons interact with oxygen to form ROS. We designed a mitochondrially targeted vitamin E (VE) succinate (MitoVES) by tagging the parental compound with the triphenylphosphonium (TPP^+) group. It was much more efficient than α-TOS in both apoptosis induction and tumour suppression while maintaining selectivity for malignant cells [24, 25].

Analogues of VE have been tested for their anti-cancer activity in a number of cancer models (reviewed in [26]). We therefore studied the efficacy of α-TOS against lung cancer that ranks second in the number of new cases and first in the number of deaths. Moreover, the 5-year survival of lung cancer patients is as low as 16 % [1–3, 27]. Here we studied the effect of α-TOS on lung cancer cells and found that the cells became resistant upon long-term exposure to the agent due to increased expression of the ABCA1 protein. We report that this resistance can be overcome by MitoVES.

Materials and methods

Cell culture and treatment

The p53-deficient H1299 cells [28] were grown in the RPMI-1640 medium supplemented with antibiotics and 10 % FBS. A549 lung carcinoma cells were grown in the DMEM medium supplemented with antibiotics and 10 % FBS. The cells were treated at 80–90 % confluency. α-TOS (Sigma), α-tocopheryloxyacetic acid (α-TEA) [29] and α-tocopheryl maleyl amide (α-TAM) [30] were freshly dissolved in EtOH. MitoVES [24, 25] was dissolved in the DMSO and EtOH mixture (1:1) and stored at −20 °C. In some cases, the cells were pre-incubated with 5 μM carbonyl cyanide 3-chlorophenyl-hydrazone (CCCP; Sigma) for 20 min The H1299- and A549-resistant ($H1299^{res}$, $A549^{res}$) sub-lines were derived from parental ($H1299^{par}$, $A549^{par}$) cells by their long-term incubation with increasing levels of α-TOS. The authentication of the cell lines using analysis of short tandem repeat DNA profiles and the ATCC database confirmed that both resistant and parental cell lines were *bone fide* cells.

Isolation of secondary tumour cell lines from tumour tissue was performed using the cold trypsin method. The clonal selection of the 'secondary' $H1299^{par}$ and $H1299^{res}$ cells was achieved by their repeated passaging for 3 weeks. The cells derived from tumours were not contaminated by mouse fibroblasts, as documented by lack of the p53 protein (data not shown).

MTT cytotoxicity test

The MTT colorimetric assay was performed as described [31]. The IC_{50} values were calculated using non-linear regression fitting dose–response inhibitory curves.

Confocal and fluorescence microscopy

Cells were washed with ice-cold PBS and fixed with 0.25 % paraformaldehyde, and incubated with the anti-ABCA1 IgG diluted 1:50 in digitonin-PBS (100 μg/ml) and with FITC-labelled anti-mouse secondary IgG diluted 1:75 in digitonin-PBS. For evaluation of mitochondrial potential, cells were incubated with 250 nM tetramethylrhodamine (TMRM; Life Technologies) for 30 min. Nuclei were counterstained using Hoechst 33258 for 1 h before treatment. In some cases, nuclei were stained using 4′,6-diamidino-2-phenylindole dihydrochloride (DAPI; Sigma). The setting of the microscope for red fluorescence (TMRM staining) was adjusted to $H1299^{res}$ cells, therefore the level of red staining of $H1299^{par}$ cells is low.

Real-time RT-PCR

Total RNA was isolated with the QIAzol Lysis reagent (Qiagen) and RNeasy columns (Qiagen) and reverse-transcribed to cDNA using oligo dT primers (Invitrogen) and the M-MLV reverse transcriptase (Invitrogen). Quantitative real-time PCR (qPCR) was performed using the LightCycler 480 instrument (Roche). 200 ng of cDNA and primers at 0.1 μM were used for the PCR reaction. Relative quantification of target genes expression was performed using the formula described elsewhere [32]; *β*-actin was used as a house-keeping gene. PCR primers were as follows; *β-actin*: forward 5′-AAT CTG GCA CCA CAC CTT CT-3′, reverse 5′-AG CAC AGC CTG GATAGC AAC-3′; *ABCA1*: forward 5′-TCT CCA GAG CCA ACC TGG CAG CA-3′, reverse 5′-CCA CAG GAG ACA GCA GGC TAG

CGA-3′; *TAP* (SEC14-like 2): forward 5′-AGT TTC GGG AGA ATG TCC AGG ATG-3′, reverse 5′-CAC TCA GGA AGG GTT TGA TGA GGT-3′; *SCARB1*: forward 5′-GGT GCG GCG GTG ATG ATG-3′, reverse 5′-CCC AGA GTC GGA GTT GTT GAG-3′.

Western blot analysis

To obtain whole cell lysates, the cell pellet was resuspended in the whole cell lysis (WCL) buffer (10 mM Tris at pH 7.4, 1 mM NaF, 1 mM Na_3VO_4, 1 mM PMSF, 0.1 % SDS, 1 % Triton X-100 and the protease inhibitor cocktail), after which it was lysed by freezing-thawing followed by sonication. The protein level was estimated using the BCA method (Pierce). The lysate was diluted in 2× Laemmli loading buffer and boiled for 4 min. To obtain tumour lysates, the tumour tissue was cut into pieces and lysed in the WCL buffer supplemented with 0.5 % SDS, homogenised using the dounce homogeniser and sonication on ice. The lysate was then spun down at 16,000×*g* for 3 min, and the resulting supernatant used for sample preparation by mixing with 2× Laemmli buffer. Proteins were resolved by SDS-PAGE and transferred to PVDF membranes (GE Healthcare). After probing with a specific primary antibody and the horse radish peroxidise (HRP)-conjugated secondary antibody, the protein bands were detected by the ECL kit using X-ray film (Kodak). The antibodies used were: anti-ABCA1 IgG (AB.H10; Millipore), anti-MnSOD IgG (MnS-1; Alexis), anti-Cu,ZnSOD (71G8; Cell Signalling), anti-catalase IgG (S-20; SCBT), anti-actin IgG (AC-15), anti-p53 IgG (1C12), anti-actin IgG (20-33), goat anti-mouse IgG-HRP, rabbit anti-goat IgG-HRP and goat anti-mouse IgG-FITC (all from Sigma).

HPLC analysis of VE analogues

α-TOS-treated cells grown in 60 cm^2 Petri dishes were collected and washed with PBS. The cellular pellet was lysed in 300 µl of 0.1 M SDS and sonicated on ice. Aliquots of the lysate (60 µl) were used for protein level evaluation and western blotting. The remaining 240 µl of the lysate were mixed with 60 µl of 5 % ascorbic acid in SDS and vortexed. EtOH (450 µl) was added and the lysate was vigorously shaken. Finally, 800 µl of hexane were added to the mixture, which was shaken for 30 s followed by centrifugation at 12,000×*g* for 3 min. The top hexane layer (750 µl) containing lipophilic molecules was transferred into a glass vial and evaporated to dryness under nitrogen. The remainder was dissolved in 400 µl of 2.5 % ascorbic acid in methanol and injected into the HPLC system. The chromatographic analysis was performed as described [33] using the Beckman Gold Noveau system equipped with a diode array detector and the Agilent Eclipse XDB-C18 column (150 × 4.6 mm, 4 µm). The acidified mobile phase (0.03 % acetic acid) of MetOH and water (97:3, v/v) was run isocratically at the flow rate of 1.3 ml/min.

For MitoVES evaluation, the treated cells were washed with PBS and resuspended in 1 ml of PBS, of which 100 µl was used for protein assay and 900 µl spun down, and the cellular pellet resuspended in ethylacetate containing 0.5 % trifluoroacetic acid. The suspension was sonicated on ice and the aggregated proteins spun down at 16,000×*g* for 3 min. The clear supernatant (800 µl) was transferred to a glass vial and evaporated to dryness under nitrogen. The remainder was dissolved in 200 µl of DMSO/EtOH (1:1, v/v) and injected into the Waters HPLC system equipped with a diode array detector and the Zorbax Eclipse XDB C18 column (150 × 4.6 mm, 5-mm). The mobile phase of acetonitrile and water (80:20 v/v) plus 0.1 % trifluoroacetic acid was run isocratically at 1.2 ml/min.

LC/MS of GSH

Cells were collected, washed twice with PBS and resuspended in 1 ml of PBS. 100 µl of the suspension was used for protein evaluation, 900 µl of the suspension was spun down and the pellet resuspended in MetOH and sonicated on ice. The aggregated proteins were spun down at 16,000×*g* for 3 min and the supernatant used for HPLC/tandem MS analysis uaing the following conditions: the Kinetex C18 column (15 cm × 4.6 mm, 2.6 µm); acetonitril/water gradient mobile phase; MRM mode for determination of individual species in the positive mode (e.g. GSH transition m/z 308 → 162, 308 → 233; GSSG transition m/z 613 → 355). The analysis of GSH and GSSG was performed using the Agilent 1200 binary pump system in connection with a triple-quadrupole mass spectrometer TripleQuad 6410 (Agilent) equipped with an electrospray ion source.

GC/MS analysis of cholesterol

Cells were extracted with EtOH and an aliquot used for protein assay. The rest was evaporated to dryness under nitrogen and treated with TriSil TBT (a 3:2 mixture of trimethylsilylimidazole and trimethylchlorosilane) at 70 °C for 30 min to convert hydroxyls to trimethylsilyl derivatives (TMS). TMS derivatives of cholesterol were extracted twice with 1 ml of hexane. Pooled extracts were evaporated to dryness and dissolved in 200 µl of 2,2,4-trimethylpentane, of which 1 µl was analysed by GC/tandem MS.

Cell death assay

Apoptosis was evaluated by flow cytometry (FACS Calibur, BD Bioscience) using the annexin V FITC and propidium iodide method as described [34].

RNA interference

Cells were grown to 30 % confluence in the absence of antibiotics and incubated with 100 nM *ABCA1* siRNA or non-silencing (NS) siRNA (Ambion) pre-incubated with lipofectamine RNAiMax and supplemented with Opti-MEM medium (both Invitrogen). After 7 h, the OptiMEM medium was replaced with the same volume of complete RPMI medium without antibiotics. After additional 48 h, the cells were assessed for the levels of individual proteins, accumulation of α-TOS or for apoptosis induced by the VE analogue.

Mouse tumour experiments

Balb c *nu/nu* mice were inoculated subcutaneously (s.c.) with 10^6 H1299^{par} or H1299^{res} cells in 100 µl of 50 % Matrigel, with four mice in each group. Animals were checked by ultrasound imaging (USI) using the Vevo770 USI apparatus equipped with the 30-µm resolution RMV708 scan head (VisualSonics) as detailed [35, 36]. After tumours reached ~30 mm^3, the mice were injected i.p. with 0.5 µmol α-TOS/g body weight or 40 nmol MitoVES/g body weight every 3 or 4 days. α-TOS and MitoVES were prepared in corn oil containing 4 % EtOH. Progression of tumour growth was assessed every 3 or 4 days using USI, which enables precise quantification of tumour volume. All animal experiments were performed according to the guidelines of the Australian and New Zealand Council for the Care and Use of Animals in Research and Teaching and were approved by the Griffith University Animal Ethics committee.

Statistics

Unless stated otherwise, data were analysed using the GraphPad PRISM 5.00 software, and represent mean ± SD or SEM of three independent experiments. Images are representative of at least three independent experiments.

Results

Long-term treatment of H1299 cells with α-TOS causes their resistance to the agent

Since α-TOS is considered a promising anti-cancer compound, it is important to find out whether long-term administration of the agent causes resistance. We exposed in parallel three separate batches of H1299 cells to 25 µM α-TOS for 1 week, after which the live cells were expanded and cultured for another week with 30 µM α-TOS, then 35 µM α-TOS and finally 40 µM α-TOS, which was the highest dose the selected cells could survive for >4 months. The IC_{50} value almost doubled for the H1299-resistant (H1299^{res}) cells when compared to their parental, susceptible counterparts (H1299^{par}) (Fig. 1a). The resistant phenotype developed in all groups and remained unchanged even after culturing of the H1299^{res} cells for one month without α-TOS (not shown). The resistant cells proliferated normally in 40 µM α-TOS while parental cells exhibited typical signs of programmed cell death within 48 h of exposure to 40 µM α-TOS (Fig. 1b). H1299^{res} cells were also more resistant to two other VE analogues, α-TEA and α-TAM (Fig. 1a).

Resistance of H1299 cells is independent of esterase activity and ROS generation

One possible reason for the resistance of H1299^{res} cells to α-TOS is increased activity of non-specific esterases that cleave the agent to the non-toxic α-tocopherol (α-TOH) in non-cancerous cells. Their role is unlikely, one reason being that the cells are resistant also to α-TEA and α-TAM, which do not contain an ester bond, the other reason being that exposure of H1299^{res} cells to α-TOS for 24 h did not result in increased levels of α-TOH (Fig. 1c). The possibility that the H1299^{res} cells are more resistant to ROS, which mediate apoptosis triggered by α-TOS, was tested by exposing the two sub-lines to hydrogen peroxide. Figure 1d reveals similar susceptibility of H1299^{par} and H2199^{res} cells to this source of ROS. Further, the cells featured very similar expression of the anti-oxidant enzymes CuZnSOD, MnSOD and catalase (Fig. 1e) as well as the level of reduced glutathione (Fig. 1f).

Resistant cells accumulate less α-TOS due to high level of expression of the ABCA1 protein

We next tested the intracellular levels of α-TOS in H1299^{par} and H1299^{res} cells, first exposing H2199^{par} and H2199^{res} cells to 50 µM α-TOS for 5 h and assessing them for its intracellular levels. HPLC analysis revealed ~40-45 % lower α-TOS in H1299^{res} cells, below the IC_{50} value for α-TOS in H1299^{par} cells (Fig. 2a, left). We next prepared cellular extracts after additional incubation of the cells in α-TOS-free medium for 2 h and observed its even more profound decrease, probably due to its efflux (Fig. 2a, right). Evaluation of the level of cholesterol revealed it to be about 2-times lower in H1299^{res} than in H1299^{par} cells (Fig. 2b).

The above data suggest a possible role for one of the ABC proteins in the lower level of α-TOS in H1299^{res} cells. Further, the low concentration of cholesterol in these cells indicates the possible function of the ABCA1 protein.

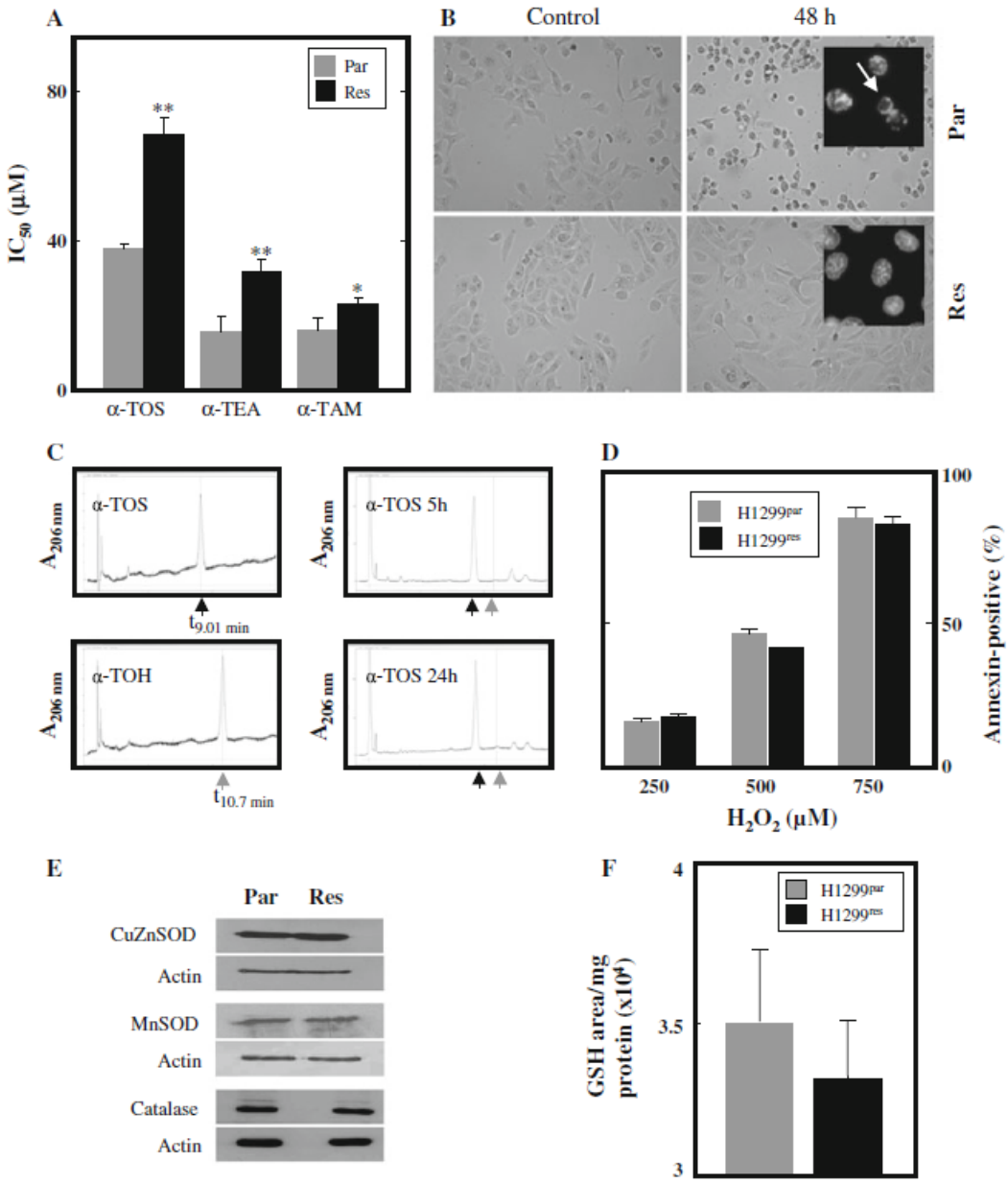

Fig. 1 Sensitivity of H1299 cells to VE analogues. **a** MTT cytotoxicity tests (48 h) of the mitocans α-TOS, α-TEA and α-TAM for parental ($H1299^{par}$) and resistant ($H1299^{res}$) cells were evaluated and the IC_{50} values plotted. The results represent mean ± SD ($n = 3$). The symbols '*' and '**' denote significant differences between parental and resistant cells with $p < 0.05$ and $p < 0.01$, respectively. Sigmoidal dose–response curves were used to calculate the IC_{50} values. **b** Phase-contrast and fluorescence microscopy (DAPI) was used to document morphological changes in $H1299^{par}$ and $H1299^{res}$ cells treated with 40 μM α-TOS for 48 h. The images are representative of at least three independent experiments. **c** H1299 cells were treated with 50 μM α-TOS for 5 h (*left chromatogram*) or 24 h (*right chromatogram*) and analysed by HPLC for α-TOS and α-TOH. The *arrows* show the position of α-TOS and α-TOH as found using standards of the compounds. **d** $H1299^{par}$ and $H1299^{res}$ cells were exposed to H_2O_2 for 10 min followed by 12 h of incubation in normal medium, after which apoptosis was evaluated by the annexin V method and flow cytometry. The results represent mean ± SD ($n = 3$). **e** $H1299^{par}$ and $H1299^{res}$ cells were evaluated for CuZnSOD, MnSOD and catalase by western blotting using actin as a loading control. **f** $H1299^{par}$ and $H1299^{res}$ cells were evaluated for the GSH levels using LC/MS. The results represent mean ± SD ($n = 3$)

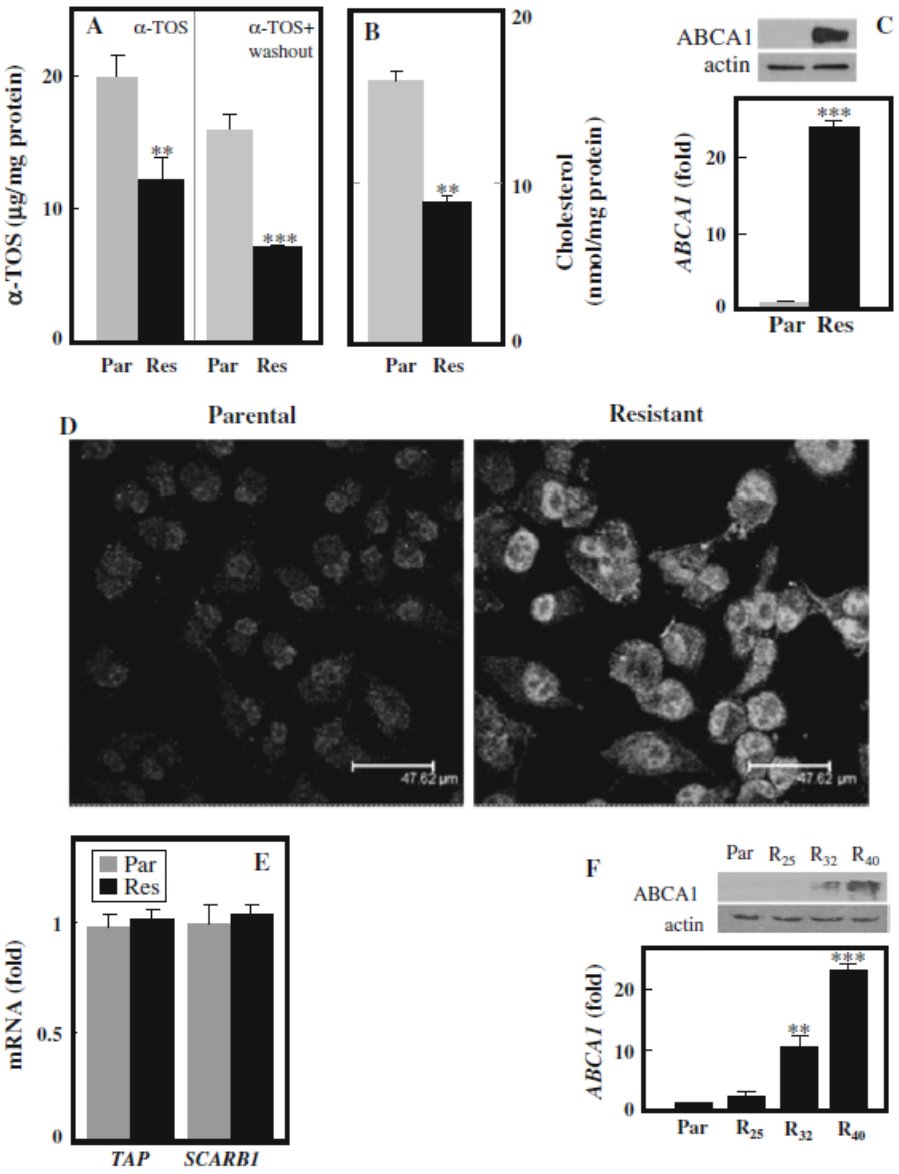

Fig. 2 Resistant H1299 cells express high levels of the ABCA1 transporter. **a** $H1299^{par}$ and $H1299^{res}$ cells were exposed to 50 μM α-TOS for 5 h and the lipophilic compounds extracted before (*left bars*) or after a 2-h incubation in the absence of α-TOS (*right bars*). The extracts were used for the analysis of α-TOS by HPLC. The results represent mean ± SD ($n = 3$), the symbol '**' indicates significant differences with $p = 0.0011$, the symbol '***' $p = 0.0001$. **b** $H1299^{par}$ and $H1299^{res}$ cells were extracted and the level of cholesterol assessed by GC/MS. The results represent mean ± SD ($n = 3$); the symbol '**' indicates significant differences with $p < 0.01$. **c** $H1299^{par}$ and $H1299^{res}$ cells were analysed for the level of the ABCA1 protein expression by western blotting with actin as a loading control and *ABCA1* mRNA by qPCR; the ABCA1 protein levels were also assessed by immunocytocheemistry **d**. The results represents mean ± SD ($n = 3$), the symbol '***' indicates significant difference with $p < 0.001$, the images are representative of at least three independent experiments. **e** $H1299^{par}$ and $H1299^{res}$ cells were evaluated for the mRNA level of the *TAP* (*Sec14-like2*) and *SCARB1* transporters by qPCR. The results represent mean ± SD ($n = 3$). **f** H1299 cells exposed to various doses of α-TOS for prolonged time were analysed for the level of ABCA1 protein expression by western blotting with actin as a loading control and *ABCA1* mRNA by qPCR. R_{25}, R_{32} and R_{40} cells represent H1299 cells growing in 25, 32 and 40 μM α-TOS, respectively. The cells labeled R_{40} equal $H1299^{res}$ cells. The western blot images represent three independent experiments. The qPCR results represent mean ± SD ($n = 3$), with the symbol '**' indicating significant differences with $p < 0.01$ and '***' with $p < 0.001$

Indeed, we found that the ABCA1 protein was highly upregulated in H1299^{res} cells as shown in Fig. 2c using qPCR and western blotting and in Fig. 2d using immunofluorescence and confocal microscopy. We next tested the H1299^{par} and H1299^{res} cells for the level of the TAP and SCARB1 genes, and found no difference (Fig. 2e). This points to the ABCA1 protein as the major reason for the resistance to α-TOS.

To get a better insight into the increase in the ABCA1 during the exposure of H1299 cells to α-TOS, we analysed the levels of the ABCA1 protein and mRNA in the cells persistently growing at the presence of α-TOS of different levels. Fig. 2f documents that the higher the concentration of the agent, the higher the expression of the *ABCA1* gene. These data reveal a directly proportional relationship between the level of resistance of H1299 cells and the expression of the ABCA1 protein.

Cellular uptake of α-TOS is regulated by ABCA1 and its knock-down restores susceptibility to the agent

To find out whether the ABCA1 protein is responsible for the resistance of H1299^{res} cells, we knocked it down using RNA interference (RNAi). This resulted in considerably lower level of the protein (Fig. 3a) associated with increased intracellular concentrations of α-TOS (Fig. 3b), reaching its levels in H1299^{par} cells (c.f. Fig. 2a). Exposure of H1299^{res} cells pre-treated with NS siRNA to α-TOS had no effect on the level of the ABCA1 protein (Fig. 3b, insert).

Knocking down the ABCA1 protein made H1299^{res} cells susceptible to α-TOS. This is depicted in Fig. 3c showing the morphology of NS siRNA- and ABCA1 siRNA-pre-treated cells, and in Fig. 3d, e documenting high level of apoptosis in the ABCA1 siRNA-pre-treated H1299^{res} cells

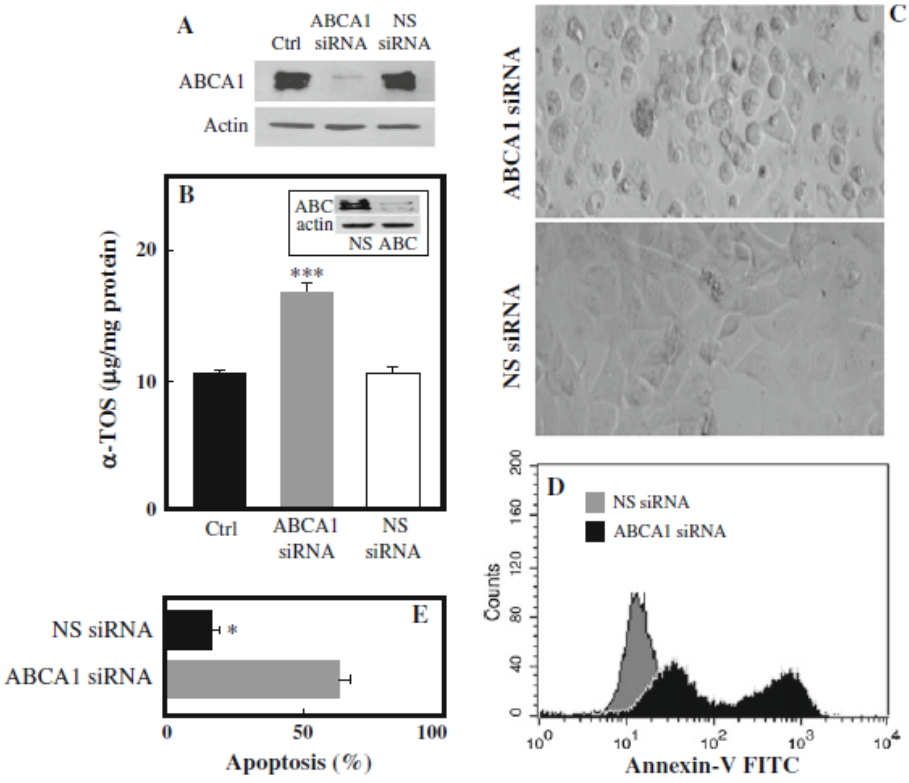

Fig. 3 Downregulation of ABCA1 in H1299^{res} cells restores the sensitivity to α-TOS. **a** The level of ABCA1 was analysed by western blotting in control H1299^{par} cells and in cells transfected with *ABCA1* siRNA and NS siRNA, using actin as a loading control. **b** Control and *ABCA1* siRNA- and NS siRNA-transfected H1299^{res} cells were incubated with 50 μM α-TOS for 5 h, and analysed for the levels of the VE analogue and ABCA1 protein (*insert*). The results show mean values ± S.D., the symbol '***' indicates significant differences with $p = 0.0009$. H1299^{res} cells transfected with *ABCA1* siRNA or NS siRNA were exposed to 50 μM α-TOS for 48 h and evaluated for cellular morphology by phase-contrast microscopy (**c**) and for apoptosis using the annexin V assay and flow cytometry (**d** representative histogram, **e** evaluation of apoptosis). The results show mean values ± S.D., the symbol '*' indicates significant differences with $p < 0.01$. The images are representative of at least three independent experiments

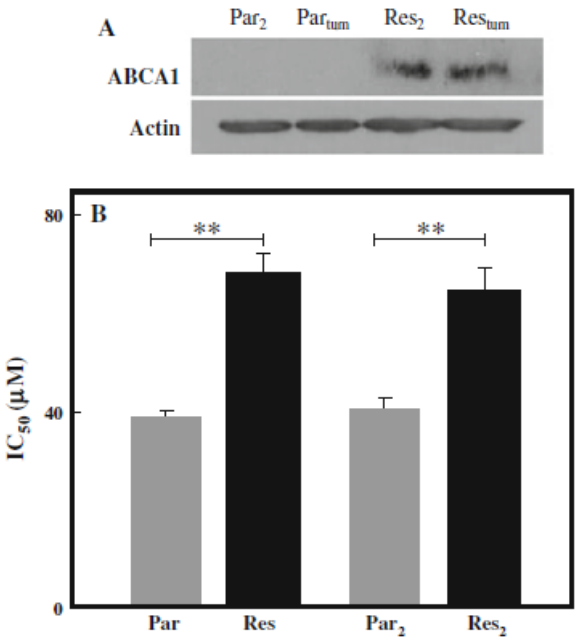

Fig. 4 α-TOS-induced resistance of H1299 cells is stable. **a** Tumours derived from H1299^{par} and H1299^{res} cells (Par_{tum}, Res_{tum}) as well as the explanted cells (Par_2, Res_2) were assessed for the expression of the ABCA1 protein by western blotting with actin as a loading control. **b** Original cell lines (Par, Res) and cell lines explanted from tumours (Par_2, Res_2) were used to evaluate the IC_{50} values for 48 h treatment with 50 μM α-TOS. The results represent mean ± SD. ($n = 3$), the symbol '**' indicates significant differences with $p = 0.0023$

when exposed to α-TOS. Further, the IC_{50} value for killing by α-TOS was slightly over 40 μM in these cells (data not shown), which is similar to that of H1299^{par} cells (c.f. Fig. 1a).

Resistance of H1299 cells to α-TOS is stable

We studied whether the resistance to α-TOS mediated by the ABCA1 protein is a transient event or whether it persists. The latter possibility appeared more likely, since we observed that culturing H1299^{res} cells in the absence of α-TOS did not cause their reversal to the H1299^{par} phenotype. We prepared tumours in nude mice from H1299^{par} and H1299^{res} cells, which were used for protein extraction and cell preparation. Fig. 4 documents that while the H1299^{par} tumours as well as the tumour-derived cells contained low level of the ABCA1 protein, they also exerted low IC_{50} values towards α-TOS. On the contrary, H1299^{res} tumours and the derived cell line expressed high levels of the ABCA1 protein and high IC_{50} towards the VE analogue.

Fig. 5 Targeting of vitamin E succinate to mitochondria overcomes resistance of H1299 cells. **a** H1299^{par} and H1299^{res} cells were treated with 5 μM MitoVES for 4 h, without or with 20-min pre-treatment with 5 μM CCCP, and assessed for apoptosis using annexin V and flow cytometry. The *upper insert* shows $\Delta\Psi_{m,i}$ of H1299^{par} and H1299^{res} cells with the value for the latter set as 1, using TMRM and flow cytometry, evaluated as mean fluorescence intensity. The *lower insert* shows the level of MitoVES (μmol/mg protein) in H1299^{par} and H1299^{res} cells following their incubation with 10 μM MitoVES for 1 h. The results represent mean ± SD ($n = 3$), the symbol '*' indicates differences with $p < 0.05$, the symbol '***' $p < 0.001$. **b** H1299^{par} and H1299^{res} cells were pre-incubated with 5 μM CCCP for 20 min and incubated with 5 μM MitoVES for 24 h, after which the cells were observed by phase-contrast microscopy. **c** H1299^{par} and H1299^{res} cells were incubated with 250 nM TMRM and DAPI. Confocal microscopy was used to observe the level of $\Delta\Psi_{m,i}$ indicated by *red fluorescence*. **d** H1299^{par} cells were incubated with 20 μM FITC-labelled α-TOS for 1 h or 2.5 μM MitoVES for 1 h as well as with DAPI and MitoTracker Red. The cells were then observed in a confocal microscope. The *right panels* show the overlay of the images. The images are representative of at least three independent experiments (Color figure online)

Mitochondrial targeting of VE analogues bypasses ABCA1-induced resistance

We recently documented that cellular uptake of the highly efficient MitoVES is driven by the mitochondrial potential ($\Delta\psi_{m,i}$) [24, 25], and observed that H1299^{res} cells exert higher $\Delta\psi_{m,i}$ than H1299^{par} cells, as documented by using the probe TMRM and flow cytometry (Fig. 5a, insert) or confocal microscopy (Fig. 5c). Accordingly, we found that H1299^{res} cells were more susceptible to MitoVES than H1299^{par} cells, as shown using annexin V and flow cytometry (Fig. 5a) as well as by optical microscopy (Fig. 5b). Further, pre-treatment of both sub-lines with the uncoupler CCCP increased their resistance to MitoVES (Fig. 5a). Finally, using fluorescently tagged α-TOS and MitoVES and MitoTracker Red, we found exclusively mitochondrial localisation of MitoVES, while α-TOS showed diffused staining (Fig. 5d, e). This is consistent with the notion that TPP^+ tagging localises hydrophobic compounds to these organelles [24, 25, 37].

Resistance to α-TOS is not unique to H1299 cells

To see whether other than H1299 cells develop resistance to α-TOS, we studied this paradigm in A549 cells, another lung cell line. Similarly as for H1299 cells, the A549 cells developed resistance to the agent upon long-term exposure of the cells to escalating doses of α-TOS, using the protocol we applied to H1299 cells. Figure 6a shows that the resistant cells increased their IC_{50} value to α-TOS from the original ~65 to ~105 μM, documenting their lower susceptibility to the agent. Figure 6b indicates that hardly any morphological alterations were observed when A549^{res} cells were exposed to 60 μM α-TOS for 48 h, while all

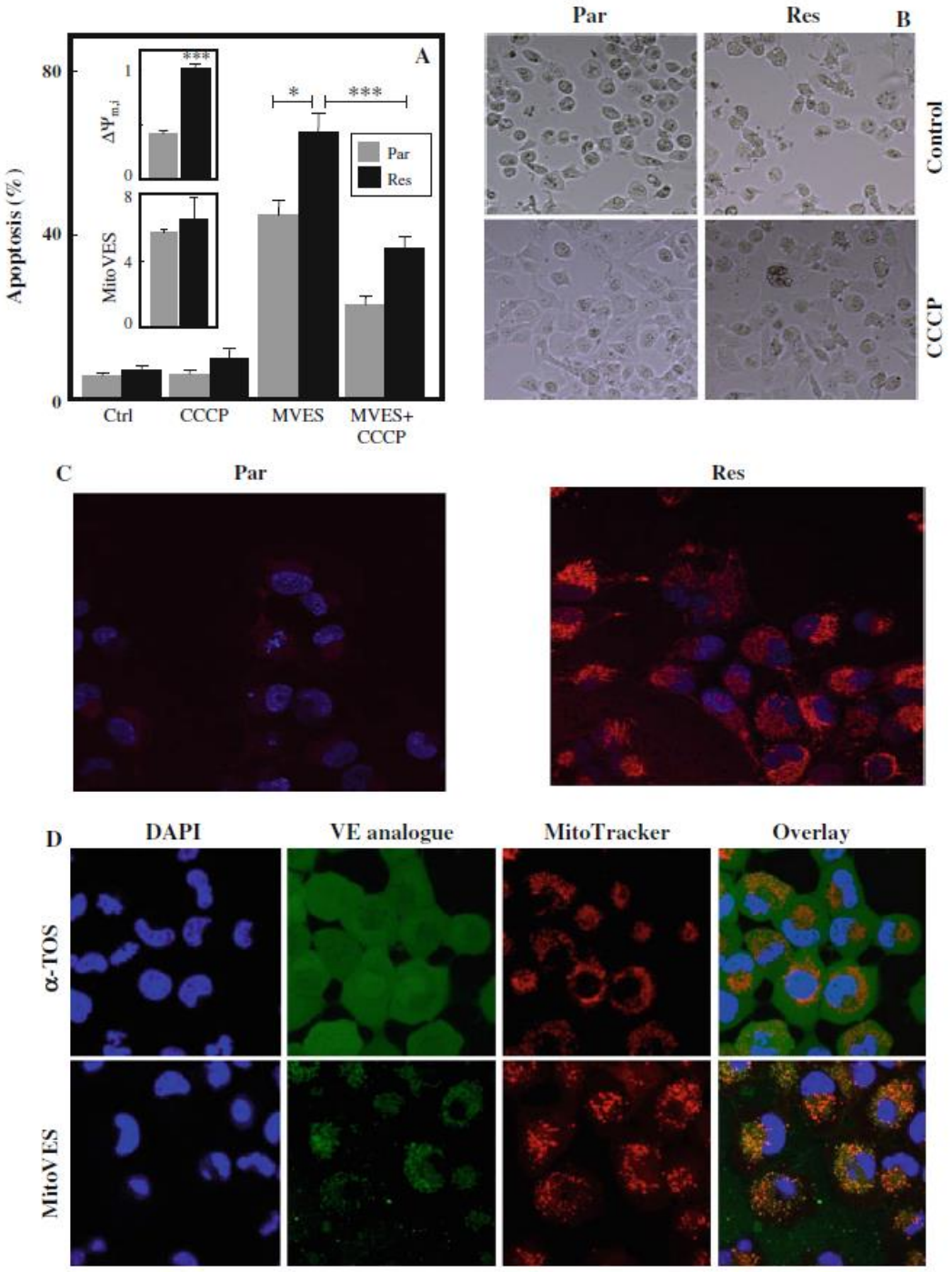

A549^{par} cells died. Importantly, we found that the A549^{res} cells express much higher level of the ABCA1 mRNA and protein (Fig. 6c), similarly as found for H1299 cells (c.f. Fig. 2c).

α-TOS-resistant tumours are susceptible to MitoVES

We next tested the effect of α-TOS and MitoVES on the progression of tumours derived in nude mice from

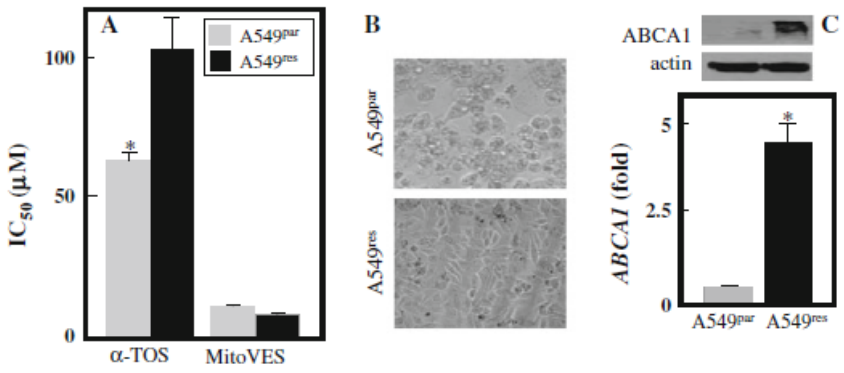

Fig. 6 Lung cancer A549 cells develop resistance to α-TOS. A549 cells were exposed to escalating doses of α-TOS, as described earlier for H1299 cells. **a** The IC_{50} values were calculated for the $A549^{par}$ and $A549^{res}$ cells. **b** $A549^{par}$ and $A549^{res}$ cells were exposed to 60 μM α-TOS for 48 h and assessed for morphological change using phase-contrast microscopy. **c** $A549^{par}$ and $A549^{res}$ cells were assessed for the level of expression of the *ABCA1* gene using western blotting with actin as the loading control as well as qPCR. The data shown are mean ± S.D. ($n = 3$), the symbol '*' indicates significantly different values with $p < 0.05$, the images are representative of at least three independent experiments

$H1299^{par}$ and $H1299^{res}$ cells The mice were given 0.5 μmol α-TOS and 40 nmol MitoVES per 1 g body weight. Figure 7 documents that while α-TOS suppressed tumours derived from $H1299^{par}$ cells by ~30 % and MitoVES by close to 80 % (albeit the latter was given at doses >10-times lower than the former), tumours derived from $H1299^{res}$ cells were completely resistant to α-TOS and highly susceptible to MitoVES.

Discussion

The redox-silent VE analogue α-TOS is a promising drug against a variety of tumour types in pre-clinical models [26]. Here we studied its effect on the refractory lung cancer cells [27] represented by the H1299 cell line. Figure 1 documents that H1299 cells are susceptible to the VE analogue with the IC_{50} values close to 40 μM. The cells are even more susceptible to two other VE analogues that have been shown to be apoptogenic [29, 30], of which α-TAM is toxic to mice unless administered in a liposomal formulation [38]. Long-term exposure to escalating doses of α-TOS rendered the cells resistant to the agent with the IC_{50} value about twice the level found for parental cells. This indicates that the cells adapt to the conditions of stress, which can potentially cause a problem for the use of α-TOS as an anti-cancer agent. Interestingly, the $H1299^{res}$ cells were also more resistant to α-TEA and α-TAM, indicating a common denominator of the resistance.

Since it has been documented that VE analogues cause apoptosis via early ROS generation [34] and since adaptation to stress can result in the upregulation of anti-oxidant enzymes [39], we tested whether long-term exposure to escalating doses of α-TOS causes an increase in the anti-oxidant enzymes CuZnSOD, MnSOD and catalase. Figure 1e documents that there was no change in the expression of the proteins. Further, we found that the change in the GSH level in $H1299^{res}$ cells compared to $H1299^{par}$ cells was not significant, and the susceptibility of $H1299^{par}$ and $H1299^{res}$ cells to hydrogen peroxide was almost identical. These findings rule out a better protection of H1299 cells to oxidative stress as a mechanism for their resistance to α-TOS.

Another possible explanation for the resistance of H1299 cells is lower accumulation of α-TOS. This was, indeed, the case: $H1299^{res}$ cells contained less α-TOS compared to $H1299^{res}$ cells (Fig. 2), indicative of either impaired uptake of α-TOS or active expulsion of the agent. Since we observed lowering of the intracellular level of α-TOS in $H1299^{res}$ cells in the 'washout' experiments, the latter option appears more likely, possibly involving the activity of a 'pump' from the ABC family of proteins. Several proteins may be involved in the active transport of α-TOS and α-TOH as well as in cancer cell susceptibility to VE analogues. The α-TOH transfer protein cannot efflux α-TOS, unlike α-TOH, as reported [40], while the ABCA1 protein is a possible candidate for the active efflux of α-TOS [40]. On the other hand, active uptake of α-TOS could be performed by the transporters TAP (Sec14-like-2) and SCARB1 [41, 42]. Neither of these, however, was found to show different level of expression in $H1299^{par}$ and $H1299^{res}$ cells (Fig. 2e).

ABCA1 is a member of the family of ABC transporters that play an important role in cellular and body metabolism; they are frequently 'utilised' by cancer cells for their protection from chemotherapeutic agents [43]. The role of 13 ABC transporters associated with drug or multidrug resistance (MDR) has been rather well characterised [44]. To support a role of the ABCA1 transporter in the

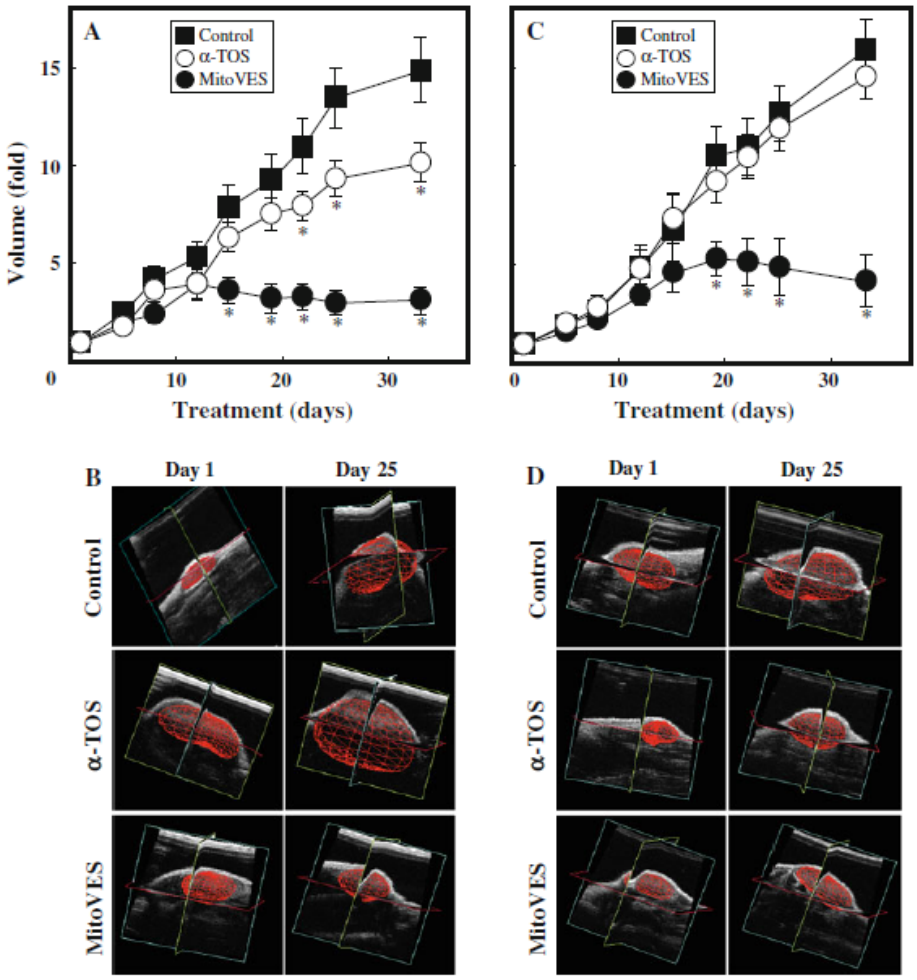

Fig. 7 MitoVES suppresses the growth of α-TOS-resistant tumours. Balb c *nu/nu* mice were injected with H1299^{par} cells (**a**, **b**) and H1299^{res} cells (**c**, **d**) at 10^6 cells/mouse. When tumours reached ~30 mm^3, the animals were treated with 0.5 μmol α-TOS or 40 nmol MitoVES per 1 g of body weight every 3 or 4 days by *ip* injection. Tumours were visualised and volumes quantified by USI (**a**, **c**). Panels **b** and **d** show representative 3D images of tumours from days 1 and 25 of control and treated mice. Each group contained 4 mice. The data in panels **a** and **c** are mean values ± SEM ($n = 4$), the symbol '*' indicates differences with $p < 0.05$

acquired resistance of H1299 cells to α-TOS, we tested the level of cholesterol in H1299^{par} and H1299^{res} cells, and found it to be twice lower in the latter, similarly as observed for the VE analogue. This indicates that the ABCA1 protein may be involved, since it is known to remove cholesterol from cells in the process of reverse cholesterol transport [45]. The role of the ABCA1 transporter in cancer is not well understood. It has been shown that in malignant mesothelioma cells the level of the *ABCA1* transcript is 100-fold lower than in their non-malignant counterparts, similarly as in breast cancer tissue or hepatocellular carcinoma compared to the corresponding normal tissue [46–48], and microarray analysis of human breast tumours indicated a link between higher level of the *ABCA1* transcript and poorer response to neoadjuvant chemotherapy [49].

A role for the ABCA1 protein in transporting chemotherapeutics from cancer cells has not been established [50], although the COMPARE computational analysis correlating IC_{50} values and mRNA expression of *ABC* transporters provided several possible substrates for the ABCA1 protein [51, 52]. Moreover, curcumin was observed to have lower effect on human melanoma M14 cells than on breast cancer curcumin-sensitive MDA-MB-231, probably linked to increased ABCA1 levels in the former [53]. Thus far, experiments in which the ABCA1 protein was suppressed in drug-resistant cells failed to render them more susceptible to the agent [51], making the idea that the ABCA1 transporter could confer resistance of cancer cells apoptosis-inducing drugs obscure.

We observed that H1299^{res} cells express high levels of the ABCA1 protein as well as mRNA, barely detectable in

H1299^{par} cells (Fig. 2). Importantly, we found that knocking down the ABCA1 protein using the RNAi approach restored the susceptibility of the cells to α-TOS. This was accompanied by levels of α-TOS that were similar in the ABCA1 siRNA-treated H1299^{res} cells to those in H1299^{par} cells, directly documenting the role of the ABCA1 transporter in the resistance of H1299 cells to the VE analogue. To the best of our knowledge, this is the first time when ABCA1's role in acquired resistance to an anti-cancer agent has been unequivocally documented. Further, we found that this increase is preserved: long-term culturing of H1299^{res} cells in the absence of α-TOS did not make them susceptible to the agent (Fig. 3), nor were susceptible the cells explanted from a tumour prepared in nude mice from H1299^{res} cells (Fig. 4). To see, whether this phenomenon is unique to H1299 cells, we studied another lung cancer cell line. A549 cells developed resistance to α-TOS similarly as H1299 cells upon long-term exposure to the agent. Also, the A549^{res} cells featured increased expression of the ABCA1 protein (Fig. 6). This indicates that resistance of α-TOS is not limited to a single type of lung cancer cell line but appears to be a more general phenomenon.

The above data clearly document the role of the ABCA1 protein in resistance of lung cancer cells to α-TOS and indicate that this is not a transient process, making it a potential problem when designing a clinical trial. It has recently been suggested that acquired resistance mediated by MDR proteins during chemotherapy may be bypassed by targeting anti-cancer drugs to mitochondria [54]. We therefore hypothesised that the mitochondrially targeted derivative of α-TOS, MitoVES, may kill the resistant cells. This idea was fuelled by our finding that $\Delta\Psi_{m,i}$ of H1299^{res} cells is more than twice higher than that of H1299^{par} cells (Fig. 5). Treatment of H1299^{par} and H1299^{res} cells with MitoVES caused more death of the latter, which correlated with slightly increased level of intracellular MitoVES. Further, our preliminary data indicate that while respiration in both sub-lines is comparable, the resistant cells utilise more CII unlike the parental cells that respire largely via CI. Notably, CII is a target for MitoVES [24, 25]. These data point to a potential reason further underlying the high susceptibility of H1299^{res} cells to MitoVES. The precise molecular mechanism of the higher susceptibility of H1299^{res} cells compared to H1299^{par} cells is a subject of our separate ongoing studies.

We also tested the mitochondrial localisation of MitoVES in H1299 cells and found virtually all of the agent co-localised with the MitoTracker. While also co-localising with MitoTracker, the staining for α-TOS was largely diffuse within the cell (Fig. 5d). Thus, MitoVES bypasses the resistance of H1299 cells to α-TOS that is given by the increased expression of the ABCA1 protein. The plausible reason for the activity of the agent is that it targets cells and their mitochondria on the basis of $\Delta\Psi_{m,i}$ due to the TPP$^+$ tag [24, 25, 37]. Indeed, pre-treatment of H1299^{res} cells with the uncoupler CCCP that efficiently dissipates $\Delta\Psi_{m,i}$ made them more resistant to MitoVES (Fig. 5).

The susceptibility of H1299^{res} cells to MitoVES is a finding that may have clinical implications. To get a better insight into this aspect of our work, we prepared tumours from H1299^{par} and H1299^{res} cells in nude mice and treated them with α-TOS and MitoVES. In support of the in vitro results, α-TOS caused suppression of the H1299^{par} cell-derived carcinomas, while their counterparts derived from H1299^{res} cells were completely resistant. On the other hand, the H1299^{res} cell-derived tumours were susceptible to MitoVES, rather similarly to H1299^{par} cell-derived carcinomas (Fig. 7). This result confirms that the tumours resistant to α-TOS due to the upregulation of the ABCA1 protein are susceptible to MitoVES, whose cellular uptake and high anti-cancer activity are governed by $\Delta\Psi_{m,i}$, whereby circumventing the high level of expression of the transporter.

Our results show an intriguing phenomenon: long-term exposure of lung cancer cells to α-TOS renders them resistant to the VE analogue, which can be overcome by tagging the agent with a mitochondria-targeting TPP$^+$ group, a finding that ought to be taken into consideration when planning clinical trials. Further, we believe that this is the first report showing the role of the ABCA1 transporter in acquired resistance of cancer cells to an apoptosis inducer.

Acknowledgments The authors wish to thank Dr. Vojtesek for providing the H1299 cells and Prof. Akporiaye for α-TEA. This study was supported in part by Grants from the Australian Research Council, the National Health and Medical Research Council of Australia, the Clem Jones Foundation and the Czech Science Foundation (P301/10/1937) to J.N, and by the Grant from the Czech Science Foundation 204/09/P632 to L.P and by the Grant CZ.1.07/2.3.00/20.0164 and P304/10/1951 (Czech Scientific Foundation) to J.T.

References

1. Siegel R, Naishadham D, Jemal A (2012) Cancer statistics, 2012. CA-Cancer J Clin 62:10–29
2. Jemal A, Bray F, Center MM, Ferlay J, Ward E, Forman D (2011) Global cancer statistics. CA-Cancer J Clin 61:69–90
3. Simard EP, Ward EM, Siegel R, Jemal A (2012) Cancers with increasing incidence trends in the United States: 1999 through 2008. CA-Cancer J Clin 62:118–128
4. Jones S, Zhang XS, Parsons DW, Lin JCH, Leary RJ, Angenendt P, Mankoo P, Carter H, Kamiyama H, Jimeno A, Hong SM, Fu BJ, Lin MT, Calhoun ES, Kamiyama M, Walter K, Nikolskaya T, Nikolsky Y, Hartigan J, Smith DR, Hidalgo M, Leach SD, Klein AP, Jaffee EM, Goggins M, Maitra A, Iacobuzio-Donahue C, Eshleman JR, Kern SE, Hruban RH, Karchin R, Papadopoulos N,

Parmigiani G, Vogelstein B, Velculescu VE, Kinzler KW (2008) Core signaling pathways in human pancreatic cancers revealed by global genomic analyses. Science 321:1801–1806
5. Parsons DW, Jones S, Zhang XS, Lin JCH, Leary RJ, Angenendt P, Mankoo P, Carter H, Siu IM, Gallia GL, Olivi A, McLendon R, Rasheed BA, Keir S, Nikolskaya T, Nikolsky Y, Busam DA, Tekleab H, Diaz LA, Hartigan J, Smith DR, Strausberg RL, Marie SKN, Shinjo SMO, Yan H, Riggins GJ, Bigner DD, Karchin R, Papadopoulos N, Parmigiani G, Vogelstein B, Velculescu VE, Kinzler KW (2008) An integrated genomic analysis of human glioblastoma multiforme. Science 321:1807–1812
6. Hayden EC (2008) Cancer complexity slows quest for cure. Nature 455(7210):148
7. Kroemer G, Pouyssegur J (2008) Tumor cell metabolism: cancer's Achilles' heel. Cancer Cell 13:472–482
8. Gogvadze V, Orrenius S, Zhivotovsky B (2008) Mitochondria in cancer cells: what is so special about them? Trends Cell Biol 18:165–173
9. Jones RG, Thompson CB (2009) Tumor suppressors and cell metabolism: a recipe for cancer growth. Genes Dev 23:537–548
10. Fulda S, Galluzzi L, Kroemer G (2010) Targeting mitochondria for cancer therapy. Nat Rev Drug Discov 9:447–464
11. Neuzil J, Dyason JC, Freeman R, Dong LF, Prochazka L, Wang XF, Scheffler I, Ralph SJ (2007) Mitocans as anti-cancer agents targeting mitochondria: lessons from studies with vitamin E analogues, inhibitors of complex II. J Bioenerg Biomembr 39:65–72
12. Rohlena J, Dong LF, Ralph SJ, Neuzil J (2011) Anticancer drugs targeting the mitochondrial electron transport chain. Antioxid Redox Signal 15:2951–2974
13. Fariss MW, Fortuna MB, Everett CK, Smith JD, Trent DF, Djuric Z (1994) The selective antiproliferative effects of α-tocopheryl hemisuccinate and cholesteryl hemisuccinate on murine leukemia-cells result from the action of the intact compounds. Cancer Res 54:3346–3351
14. Neuzil J, Weber T, Gellert N, Weber C (2001) Selective cancer cell killing by α-tocopheryl succinate. Br J Cancer 84:87–89
15. Neuzil J (2003) Vitamin E succinate and cancer treatment: a vitamin E prototype for selective antitumour activity. Br J Cancer 89:1822–1826
16. Yu WP, Sanders BG, Kline K (2003) RRR-α-tocopheryl succinate-induced apoptosis of human breast cancer cells involves Bax translocation to mitochondria. Cancer Res 63:2483–2491
17. Gogvadze V, Norberg E, Orrenius S, Zhivotovsky B (2010) Involvement of Ca^{2+} and ROS in α-tocopheryl succinate-induced mitochondrial permeabilization. Int J Cancer 127:1823–1832
18. Prochazka L, Dong LF, Valis K, Freeman R, Ralph SJ, Turanek J, Neuzil J (2010) α-Tocopheryl succinate causes mitochondrial permeabilization by preferential formation of Bak channels. Apoptosis 15:782–794
19. Valis K, Prochazka L, Boura E, Chladova J, Obsil T, Rohlena J, Truksa J, Dong LF, Ralph SJ, Neuzil J (2011) Hippo/Mst1 stimulates transcription of the proapoptotic mediator NOXA in a FoxO1-dependent manner. Cancer Res 71:946–954
20. Kruspig B, Nilchian A, Bejarano I, Orrenius S, Zhivotovsky B, Gogvadze V (2012) Targeting mitochondria by α-tocopheryl succinate kills neuroblastoma cells irrespective of MycN oncogene expression. Cell Mol Life Sci 69:2091–2099
21. Dong LF, Low P, Dyason JC, Wang XF, Prochazka L, Witting PK, Freeman R, Swettenham E, Valis K, Liu J, Zobalova R, Turanek J, Spitz DR, Domann FE, Scheffler IE, Ralph SJ, Neuzil J (2008) α-Tocopheryl succinate induces apoptosis by targeting ubiquinone-binding sites in mitochondrial respiratory complex II. Oncogene 27:4324–4335
22. Dong LF, Freeman R, Liu J, Zobalova R, Marin-Hernandez A, Stantic M, Rohlena J, Valis K, Rodriguez-Enriquez S, Butcher B, Goodwin J, Brunk UT, Witting PK, Moreno-Sanchez R, Scheffler IE, Ralph SJ, Neuzil J (2009) Suppression of tumor growth in vivo by the mitocan α-tocopheryl succinate requires respiratory complex II. Clin Cancer Res 15:1593–1600
23. Sun F, Huo X, Zhai YJ, Wang AJ, Xu JX, Su D, Bartlam M, Rao ZH (2005) Crystal structure of mitochondrial respiratory membrane protein complex II. Cell 121:1043–1057
24. Dong LF, Jameson VJA, Tilly D, Prochazka L, Rohlena J, Valis K, Truksa J, Zobalova R, Mandavian E, Kluckova K, Stantic M, Sturs a J, Freeman R, Witting PK, Norberg E, Goodwin J, Salvatore BA, Novotna J, Turanek J, Ledvina M, Hozak P, Zhivotovsky B, Coster MJ, Ralph SJ, Smith RAJ, Neuzil J (2011) Mitochondrial targeting of α-tocopheryl succinate enhances its pro-apoptotic efficacy: a new paradigm for effective cancer therapy. Free Radic Biol Med 50:1546–1555
25. Dong LF, Jameson VJA, Tilly D, Cerny J, Mahdavian E, Marin-Hernandez A, Hernandez-Esquivel L, Rodriguez-Enriquez S, Sturs a J, Witting PK, Stantic B, Rohlena J, Truksa J, Kluckova K, Dyason JC, Ledvina M, Salvatore BA, Moreno-Sanchez R, Coster MJ, Ralph SJ, Smith RAJ, Neuzil J (2011) Mitochondrial targeting of vitamin E succinate enhances its pro-apoptotic and anti-cancer activity via mitochondrial complex II. J Biol Chem 286:3717–3728
26. Zhao Y, Neuzil J, Wu K (2009) Vitamin E analogues as mitochondria-targeting compounds: from the bench to the bedside? Mol Nutr Food Res 53:129–139
27. Goldstraw P, Ball D, Jett JR, Le Chevalier T, Lim E, Nicholson AG, Shepherd FA (2011) Non-small-cell lung cancer. Lancet 378:1727–1740
28. Giaccone G, Battey J, Gazdar AF, Oie H, Draoui M, Moody TW (1992) Neuromedin-b is present in lung-cancer cell-lines. Cancer Res 52:S2732–S2736
29. Hahn T, Szabo L, Gold M, Ramanathapuram L, Hurley LH, Akporiaye ET (2006) Dietary administration of the proapoptotic vitamin E analogue α-tocopheryloxyacetic acid inhibits metastatic murine breast cancer. Cancer Res 66:9374–9378
30. Tomic-Vatic A, EyTina J, Chapman J, Mahdavian E, Neuzil J, Salvatore BA (2005) Vitamin E amides, a new class of vitamin E analogues with enhanced proapoptotic activity. Int J Cancer 117:188–193
31. Mosmann T (1983) Rapid colorimetric assay for cellular growth and survival - application to proliferation and cyto-toxicity assays. J Immunol Methods 65:55–63
32. Pfaffl MW (2001) A new mathematical model for relative quantification in real-time RT-PCR. Nucleic Acids Res 29:6
33. Koudelka S, Masek J, Neuzil J, Turanek J (2010) Lyophilised liposome-based formulations of α-tocopheryl succinate: preparation and physico-chemical characterisation. J Pharm Sci 99:2434–2443
34. Weber T, Dalen H, Andera L, Negre-Salvayre A, Auge N, Sticha M, Lloret A, Terman A, Witting PK, Higuchi M, Plasilova M, Zivny J, Gellert N, Weber C, Neuzil J (2003) Mitochondria play a central role in apoptosis induced by α-tocopheryl succinate, an agent with antineoplastic activity: comparison with receptor-mediated pro-apoptotic signaling. Biochemistry 42:4277–4291
35. Dong LF, Swettenham E, Eliasson J, Wang XF, Gold M, Medunic Y, Stantic M, Low P, Prochazka L, Witting PK, Turanek J, Akporiaye ET, Ralph SJ, Neuzil J (2007) Vitamin E analogues inhibit angiogenesis by selective induction of apoptosis in proliferating endothelial cells: the role of oxidative stress. Cancer Res 67:11906–11913
36. Wang XF, Birringer M, Dong LF, Veprek P, Low P, Swettenham E, Stantic M, Yuan LH, Zobalova R, Vu K, Ledvina M, Ralph SJ, Neuzil J (2007) A peptide conjugate of vitamin E succinate targets breast cancer cells with high ErbB2 expression. Cancer Res 67:3337–3344

37. Murphy MP, Smith RAJ (2007) Targeting antioxidants to mitochondria by conjugation to lipophilic cations. Annu Rev Pharmacol Toxicol 47:629–656
38. Turanek J, Wang XF, Knotigova P, Koudelka S, Dong LF, Vrublova E, Mahdavian E, Prochazka L, Sangsura S, Vacek A, Salvatore BA, Neuzil J (2009) Liposomal formulation of α-tocopheryl maleamide: in vitro and in vivo toxicological profile and anticancer effect against spontaneous breast carcinomas in mice. Toxicol Appl Pharmacol 237:249–257
39. Park SY, Chang I, Kim JY, Kang SW, Park SH, Singh K, Lee MS (2004) Resistance of mitochondrial DNA-depleted cells against cell death - Role of mitochondrial superoxide dismutase. J Biol Chem 279:7512–7520
40. Ni J, Pang ST, Yeh S (2007) Differential retention of α-vitamin E is correlated with its transporter gene expression and growth inhibition efficacy in prostate cancer cells. Prostate 67:463–471
41. Ni J, Wen XQ, Yao J, Chang HC, Yin Y, Zhang M, Xie SZ, Chen M, Simons B, Chang P, di Sant'Agnese A, Messing EM, Yeh SY (2005) Tocopherol-associated protein suppresses prostate cancer cell growth by inhibition of the phosphoinositide 3-kinase pathway. Cancer Res 65:9807–9816
42. Hrzenjak A, Reicher H, Wintersperger A, Steinecker-Frohnwieser B, Sedlmayr P, Schmidt H, Nakamura T, Malle E, Sattler W (2004) Inhibition of lung carcinoma cell growth by high density lipoprotein-associated α-tocopheryl-succinate. Cell Mol Life Sci 61:1520–1531
43. Gillet JP, Efferth T, Remacle J (2007) Chemotherapy-induced resistance by ATP-binding cassette transporter genes. Biochim Biophys Acta-Rev Cancer 1775:237–262
44. Gillet JP, Gottesman MM (2011) Advances in the molecular detection of ABC transporters involved in multidrug resistance in cancer. Curr Pharm Biotechnol 12:686–692
45. Chinetti G, Lestavel S, Bocher V, Remaley AT, Neve B, Torra IP, Teissier E, Minnich A, Jaye M, Duverger N, Brewer HB, Fruchart JC, Clavey V, Staels B (2001) PPAR-α and PPAR-γ activators induce cholesterol removal from human macrophage foam cells through stimulation of the ABCA1 pathway. Nat Med 7:53–58
46. Shukla A, Hillegass JM, MacPherson MB, Beuschel SL, Vacek PM, Pass HI, Carbone M, Testa JR, Mossman BT (2010) Blocking of ERK1 and ERK2 sensitizes human mesothelioma cells to doxorubicin. Mol Cancer 9:13
47. Schimanski S, Wild PJ, Treeck O, Horn F, Sigruener A, Rudolph C, Blaszyk H, Klinkhammer-Schalke M, Ortmann O, Hartmann A, Schmitz G (2010) Expression of the lipid transporters ABCA3 and ABCA1 is diminished in human breast cancer tissue. Horm Metab Res 42:102–109
48. Moustafa MA, Ogino D, Nishimura M, Ueda N, Naito S, Furukawa M, Uchida T, Ikai L, Sawada H, Fukumoto M (2004) Comparative analysis of ATP-binding cassette (ABC) transporter gene expression levels in peripheral blood leukocytes and in liver with hepatocellular carcinoma. Cancer Sci 95:530–536
49. Park S, Shimizu C, Shimoyama T, Takeda M, Ando M, Kohno T, Katsumata N, Kang YK, Nishio K, Fujiwara Y (2006) Gene expression profiling of ATP-binding cassette (ABC) transporters as a predictor of the pathologic response to neoadjuvant chemotherapy in breast cancer patients. Breast Cancer Res Treat 99:9–17
50. Fletcher JI, Haber M, Henderson MJ, Norris MD (2010) ABC transporters in cancer: more than just drug efflux pumps. Nat Rev Cancer 10:147–156
51. Gillet JP, Efferth T, Steinbach D, Hamels J, de Longueville F, Bertholet V, Remacle J (2004) Microarray-based detection of multidrug resistance in human tumor cells by expression profiling of ATP-binding cassette transporter genes. Cancer Res 64:8987–8993
52. Szakacs G, Annereau JP, Lababidi S, Shankavaram U, Arciello A, Bussey KJ, Reinhold W, Guo YP, Kruh GD, Reimers M, Weinstein JN, Gottesman MM (2004) Predicting drug sensitivity and resistance: profiling ABC transporter genes in cancer cells. Cancer Cell 6:129–137
53. Bachmeier BE, Iancu CM, Killian PH, Kronski E, Mirisola V, Angelini G, Jochum M, Nerlich AG, Pfeffer U (2009) Overexpression of the ATP binding cassette gene ABCA1 determines resistance to Curcumin in M14 melanoma cells. Mol Cancer 8:12
54. Fulda S, Kroemer G (2011) Mitochondria as therapeutic targets for the treatment of malignant disease. Antioxid Redox Signal 15:2937–2949

Biochimica et Biophysica Acta 1827 (2013) 552–564

Contents lists available at SciVerse ScienceDirect

Biochimica et Biophysica Acta

journal homepage: www.elsevier.com/locate/bbabio

Review

Mitochondrial complex II, a novel target for anti-cancer agents☆

Katarina Kluckova [a], Ayanachew Bezawork-Geleta [b], Jakub Rohlena [a], Lanfeng Dong [c], Jiri Neuzil [a,c,*]

[a] Institute of Biotechnology, Czech Academy of Sciences, Prague, Czech Republic
[b] La Trobe University, Melbourne, Vic, Australia
[c] School of Medical Science, Griffith University, Southport, Qld, Australia

ARTICLE INFO

Article history:
Received 14 September 2012
Received in revised form 28 October 2012
Accepted 29 October 2012
Available online 6 November 2012

Keywords:
Mitochondrion
Complex II
Anti-cancer agent
Cancer therapy
Mitocan

ABSTRACT

With the arrival of the third millennium, in spite of unprecedented progress in molecular medicine, cancer remains as untamed as ever. The complexity of tumours, dictating the potential response of cancer cells to anti-cancer agents, has been recently highlighted in a landmark paper by Weinberg and Hanahan on hallmarks of cancer [1]. Together with the recently published papers on the complexity of tumours in patients and even within the same tumour (see below), the cure for this pathology seems to be an elusive goal. Indisputably, the strategy ought to be changed, searching for targets that are generally invariant across the landscape of neoplastic diseases. One such target appears to be the mitochondrial complex II (CII) of the electron transfer chain, a recent focus of research. We document and highlight this particularly intriguing target in this review paper and give examples of drugs that use CII as their molecular target. This article is part of a Special Issue entitled: Respiratory complex II: Role in cellular physiology and disease.

1. Introduction

The improvement in sequencing and bioinformatic technology lead to a realisation that tumours are heterogeneous, as exemplified by recent reports revealing the extraordinary variability of mutations in tumours of the same type in different patients [2–4]. This grim notion has been further accentuated by a publication documenting the differences in mutational signatures in different regions of a single tumour and the derived metastases, as shown for renal carcinoma patients [5]. These findings underscore the improbable task of finding a good cancer cure that would target only a single gene or a single signalling pathway. This is most likely also a major reason why cancer incidence is either stagnating or on the rise, depending on the particular type of tumour [6–8]. Therefore, mitochondria came into the focus of contemporary research of cancer biologists.

The importance of mitochondria as potential targets in cancer cells stems from the fact that they are a reservoir of proteins that promote the apoptotic death when mobilised into the cytosol [9,10]. This notion and the fact that mitochondria are functional, at least to some extent, in most if not all cancer cells, has fuelled considerable interest in these organelles [10–16]. Due to the intriguing nature of mitochondria and accumulating evidence for these organelles comprising a variety of targets for anti-tumour agents, we decided to group these agents under the collective name of 'mitocans', an acronym epitomising the terms 'mitochondria' and 'cancer' [17,18]. The classification of mitocans has been proposed: we defined 8 classes, according to the individual molecular targets at and inside mitochondria (Fig. 1) [19]. Some of these agents have been trialled pre-clinically and are undergoing clinical trials, showing promise to be developed into clinically relevant drugs [20].

Our major interest has been focused on class 5 mitocans, *i.e.* agents acting on the mitochondrial electron transport chain (ETC.) [20]. The reason for this has been that in our aspiration to understand the molecular mechanism of the induction of apoptosis by the redox-silent vitamin E (VE) analogue α-tocopheryl succinate (α-TOS), which is also a selective anti-cancer drug as shown in pre-clinical experiments [21–25], we discovered that the molecular target for the agent is the mitochondrial

Abbreviations: BH3, Bcl-2 homology-3; 3BP, 3-bromopyruvate; CI, complex I; DCA, dichloroacetate; ETC., electron transport chain; HIF, hypoxia-inducible factor; MIM, mitochondrial inner membrane; MitoVES, mitochondrially targeted vitamin E succinate; MOM, mitochondrial outer membrane; mtDNA, mitochondrial DNA; nDNA, nuclear DNA; 3NP, 3-nitropropionic acid; ODD, oxygen-dependent destruction; OXPHOS, oxidative phosphorylation; Q_p, proximal UbQ-binding site in CII; Q_d, distal UbQ-binding site in CII; PDK, pyruvate dehydrogenase kinase; PGL, paraganglioma; PHD, prolyl hydroxylase; PHEO, pheochromocytoma; ROS, reactive oxygen species; SDH, succinate dehydrogenase; SDHA, succinate dehydrogenase subunit A; SDHAF1, succinate dehydrogenase assembly factor 1; SQR, succinate quinone reductase; TCA cycle, tricarboxylic acid cycle; α-TOS, α-tocopheryl succinate; α-TEA, α-tocopheryloxyacetic acid; TPP^+, triphenylphosphonium; TTFA, thenoyltrifluoroacetate; UbQ, ubiquinone; $UbQH_2$, ubiquinol; VDAC, voltage-dependent anion channel; VE, vitamin E

☆ This article is part of a Special Issue entitled: Respiratory complex II: Role in cellular physiology and disease.

* Corresponding author at: School of Medical Science and the Griffith Institute of Health and Medical Research, Griffith University, Southport, 4222 Qld, Australia. Tel.: +61 2 55529109; fax: +61 2 555 28444.
E-mail address: j.neuzil@griffith.edu.au (J. Neuzil).

0005-2728/$ – see front matter © 2012 Elsevier B.V. All rights reserved.
http://dx.doi.org/10.1016/j.bbabio.2012.10.015

complex II (CII) [26,27]. Since CII is invariant in most types of cancer and since VE analogues are likely to enter clinical trials, we believe that it is of importance to document the role of CII as a site of the action of anti-cancer drugs, which is the thrust of this review paper.

2. Biology of complex II

Mitochondrial complex II (CII), also known as succinate dehydrogenase (SDH) or succinate:ubiquinone oxidoreductase (SQR), contains four nuclear encoded subunits: SDHA, SDHB, SDHC and SDHD (called Sdh1–4 in yeast and SdhA–SdhD in bacteria) and, unlike other mitochondrial complexes, lacks subunits encoded by the mitochondrial genome. CII has a dual role, *i.e.* in the ETC. and the tricarboxylic acid (TCA) cycle, linking the two essential energy-producing processes of the cell [28–30]. In TCA cycle, SDH oxidises the metabolite succinate to fumarate, and this reaction is inherent to the SDH activity of CII [30]. As a component of the respiratory complex, it transfers electrons from succinate to ubiquinone (UbQ), referred to as the SQR activity. Bacterial fumarate reductase (also known as succinate:quinone oxidoreductase), which has functional and structural homology to CII [31,32], catalyses the reverse reaction of reducing fumarate to succinate during anaerobic respiration [31,33]. The structure of CII purified from porcine heart resolved at 2.4 Å resolution [34] revealed the head-tail arrangement of the hydrophobic subunits (SDHC and SDHD) embedded within the mitochondrial inner membrane (MIM) with a short segment extended into the intermembrane space, while the catalytic subunit SDHA and the SDHB subunit are projected into the matrix (see Fig. 2 for CII structure and function).

In contrast to the semi-sequential assembly manner of CI [35], the presence of all subunits of hydrophilic and hydrophobic cores is essential for the stability of functional CII as demonstrated in yeast. Thus, yeast lacking one of the subunits shows a low abundance of the other subunits [36]. However, the catalytic subunits of *Escherichia coli* fumarate reductase are stable and partially active even in the absence of hydrophilic subunits [37]. These findings led to the question how mammalian mitochondrial SDH evolved and whether it features unique assembly and regulatory mechanisms.

To carry out its dual activity of electron transfer to UbQ and of oxidising succinate to fumarate, prosthetic groups are required. Accordingly, CII comprises five prosthetic groups including FAD in the SDHA subunit, three iron–sulfur clusters ([2Fe–2S], [4Fe–4S] and [3Fe–4S]) bound in SDHB, and heme inserted within the hydrophobic pocket between SDHC and SDHD. Attachment of these prosthetic groups to the individual subunits, although considered to be autocatalytic, has been documented to require specific proteins collectively termed 'assembly factors' that assist the insertion of prosthetic groups into the holo-form of subunits. Studies on the biogenesis of CI indicated that it requires more than 9 assembly factors [35,38]. Similarly, numerous factors are also required for the assembly of CIII, CIV and CV. On the other hand, the assembly of mammalian CII is not known in much detail and thus far only two assembly factor proteins have been identified. SDH assembly factor-1 (SDHAF1) is required for the insertion of iron–sulfur clusters in SDHB [39] and SDHAF2, also known as SDH5, for the flavination of SDHA [36].

SDHAF1 belongs to the LYR family of proteins that contain the conserved LYR (LYK) tripeptide motif in the N-terminal region, which is a typical signature of proteins involved in iron–sulfur cluster metabolism. Analogously, other LYR protein family members localise to mitochondria, such as NDUFA6 and NDUFB9 of CI. This implicates a role for the iron–sulfur cluster formation in CI, while the yeast Mzm1 protein assists the assembly of the Rieske iron–sulfur protein Rip1 in CIII [40]. Molecular details of the role of SDHAF1 in the insertion of iron–sulfur clusters in the SDHC subunit, which is associated with CII assembly, however, remain to be determined.

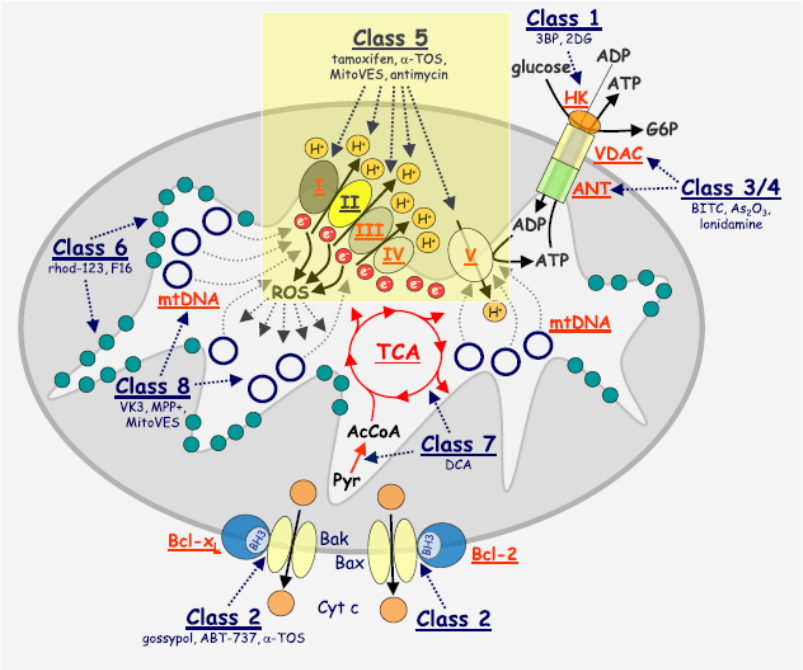

Fig. 1. The classification of mitocans. Mitocans, small molecules with anti-cancer activity that act upon mitochondria, are classified into several classes. Class 1 mitocans comprises agents targeting HK, Class 2 compounds acting on Bcl-2 family proteins (BH3 mimetics and similar compounds), Class 3 and 4 compouds with redox-inhibitory function and acting on the VDAC and ANT channel proteins, Class 5 agents targeting the ETC., Class 7 lipophilic compounds targeting the inner membrane, Class 7 agents targeting the TCA cycle, and Class 8 compounds acting on mtDNA. Highlighted are the Class 5 mitocans and CII, which as a target for anti-cancer drugs is the subject of this paper. Adapted from [19].

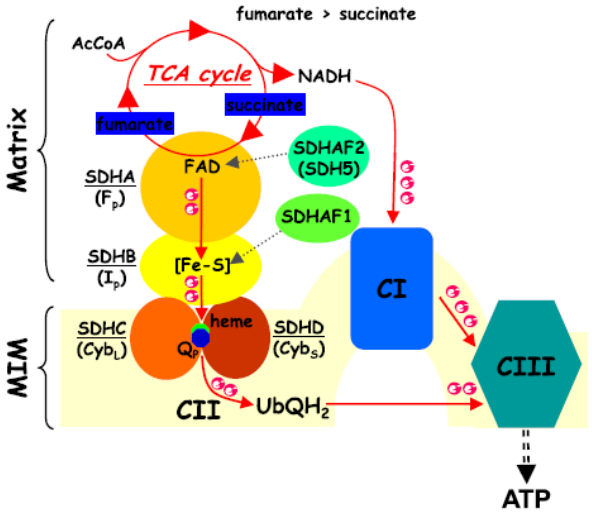

Fig. 2. The structure of complex II. Complex II consists of four subunits, the 70 kDa SDHA (F_p), the 30 kDa SDHB (I_p), the 15 kDa SDHC (Cyb_L) and the 13 kDa SDHD (Cyb_S) subunit. The SDHA subunit contains the prosthetic group FAD, which participates in the TCA cycle, converting succinate to fumarate (SDH activity of CII), resulting in the generation of $FADH_2$ that feeds electrons to CII. The two electrons generated from conversion of succinate to fumarate are mobilised to the SDHB subunit that comprises three [Fe–S] clusters arranged to force the movement of electrons to the membrane 'portion' of CII composed of the SDHC and SDHD subunits with the heme and UbQ prosthetic groups. Heme helps stabilise electrons adjacent to UbQ to help with the two-electron reduction of UbQ to $UbQH_2$ (SQR activity of CII). $UbQH_2$ then leaves its site in CII to transverse to CIII, where it is re-oxidised, returning to CII. Shown are also two assembly factors, SDHAF2 (SDH5) helping insert FAD into SDHA, and SDHAF1 with a role in the insertion of the [Fe–S] clusters into the SDHB subunit. Adapted from [19].

SDH5 has been discovered in an effort to characterise previously unannotated mitochondria proteins [36,41]. Subsequent sequence analyses have suggested that SDH5 is not a *bona fide* member of any superfamily and is not homologous with any known domain or motif; it is now assigned its own specific group called 'SDH5 superfamily'. It has been shown that SDH5 physically associates with SDHA and that it is essential for incorporation of FAD to form the active SDHA flavoprotein. The molecular mechanism of SDH5-assisted insertion of FAD to SDHA is still to be completely resolved in eukaryotes, while recent studies using a homologous bacterial protein SdhE revealed that SdhE itself directly binds FAD via a covalent chemical interaction [42]. It is likely that SdhE acquires FAD from the aqueous environment and hands it over to SdhA. Similarly as for eukaryotes, the mechanism of FAD mobilisation from SdhE to SdhA is not precisely known, and neither is it known whether other macromolecules are involved in the flavination of SdhA. In yeast mitochondria, the flavin transporter Flx1 [43] and the 'chaperone-like' Tcm62 protein [44] have also been reported as assembly factors of CII, although it is not clear yet whether they play a broader role in mitochondria or are dedicated solely to the assembly process [45–47].

Additional modification of CII was proposed on the post-translational level that could modulate its activity. Proteome-wide screen showed that SDHA features 13 acetylated lysine residues [48], which lead to the proposition that deacetylation of these residues by SIRT3 might modulate the SDH activity of CII in a tissue-dependent manner [48,49]. Also, *in vitro* experiments revealed that the Fgr tyrosine kinase phosphorylates two Tyr residues (Y535 and Y596) of SDHA [50], although the physiological significance of this post translational modification remains unclear. Additional experiments are needed to better understand the precise molecular mechanism of the assembly and modifications of the subunits of CII in order to comprehend the importance of the role of CII at the 'crossroads' of the TCA cycle and the ETC. The importance of the assembly factors in the function of CII is accentuated by their recently discovered role as tumour suppressors [36,39].

3. The role of complex II in mitochondrial bioenergetics and mutagenesis

With respect to CII as a target for anti-cancer drugs, it is useful to note that CII subunits function as tumour suppressors. Genes coding for complex II (CII) subunits have received considerable attention in the context of cancer susceptibility genes since 2000, when first germline mutations in SDHD and SDHC were reported in families with hereditary paraganglioma (PGL) [51,52]. Very soon familial pheochromocytoma (PHEO) revealed SDHD germline mutations [53], and in the same year these authors found germline SDHB mutations in both familial diseases [54]. Finally, very recently a mutation in the SDHA subunit was identified in a PGL patient [55]. The role of CII in PGL was further strengthened by the finding that the CII assembly factor SDH5 was also marked as a tumour susceptibility gene [36]. In addition, mutations in several other genes have been found to be associated with this syndrome [56]. More on SDH mutations and associated cancers can be found in a recent review by Bardella, Pollard and Tomlinson [57] and elsewhere in this issue.

It is not yet entirely clear why CII deficiency gives rise to cancer. It has been reported that the activity of CII in tumours bearing SDHA-D mutations is compromised [58–61]. As CII converts succinate to fumarate in the TCA cycle, this results in succinate accumulation and substrate inhibition of prolyl hydroxylase enzymes (PHDs), which also form succinate as an end product. PHDs play an important regulatory role, as they hydroxylate hypoxia-inducible factors (HIF1 and HIF2) and in this way mark them for proteasomal degradation [62]. When HIFs are present, they activate transcription of various genes implicated in cancer like glucose transporters, enzymes promoting glycolysis and the pro-angiogenic vascular endothelial growth factor. Indeed, HIF protein stabilisation has now been demonstrated in a number of CII deficient tumours [59,60,63]. In addition, it has been shown in a yeast model of SDHB deficiency that increased succinate levels may inhibit histone demethylases [64]. Similarly to isocitrate dehydrogenase mutations [65], it was subsequently demonstrated that CII mutations may result in altered epigenetics in mammalian cells [66], but this has as yet not been shown for human cancers.

The accumulation of succinate is undoubtedly an important feature of CII-deficient cancers, but the 'succinate theory' cannot explain all of the clinical observations. For example, the deficiency in the SDHA subunit should result in massive succinate accumulation as SDHA contains the catalytic site responsible for the succinate to fumarate conversion, yet SDH-deficient tumours are extremely rare, while mutations in SDHB-D are much more common. SDHA was in fact not considered a tumour suppressor until 2010 when heterozygous mutation was identified in a catecholamine-secreting abdominal paraganglioma [55]. An alternative theory has been proposed, suggesting reactive oxygen species (ROS) as culprits of increased tumourigenesis. CII has been shown to be a site of ROS generation (references [67,68] and Moreno-Sanchez et al., submitted for publication), and in SDHA-deficiency there could be no ROS produced from CII due to the absence of electron flow from the non-existent active site, which is consistent with the limited occurrence of SDHA tumours. Increased ROS may result in HIF1 accumulation, but also in increased DNA mutational rate and tumourigenesis [69–71]. However, various groups using various models have reported either increased or normal levels of ROS in CII deficient cells, and this issue remains to be resolved [69,70,72,73]. Increased ROS have not been detected in SDHB-deficient tumours, but the tumour tissue featured elevated superoxide dismutase expression, suggesting that the cells could have adapted to an increase in ROS production over time [61]. It is possible that the individual factors (such as succinate accumulation and ROS production) may be of varying importance based on

the tissue from which the tumour originates and the individual CII subunit that is absent or harbours the tumour-associated mutation(s).

Clinical manifestation of cancer differs, depending on which one of the CII subunits is defective. In PGL/PHEO, the most aggressive tumours are those deficient or malfunctional in SDHB due to their high metastatic potential; they are generally diagnosed at younger age [74,75]. In contrast, SDHD-deficient tumours give rise to metastasis only very infrequently, and SDHC-deficient tumours even less so, while SDHA-derived tumours are extremely rare. SDHB tumours are relatively frequent in sporadic cases, while SDHC and SDHD tumours are mostly hereditary [75]. This appears an enigma, as 'SDHC/SDHD cases' often involve a complete loss of the subunit, which then results in the absence of SDHB as well (probably due to the failure to properly assemble CII), and one would therefore expect that the manifestation will be the same or not too dissimilar. It was even suggested that the absence of SDHB in PGL/PHEO biopsies could be a surrogate marker for the presence of mutations in SDHB, SDHC or SDHD [76]. To our knowledge, these differences remain unexplained, and no rigorous biochemical examination has been performed to compare SDHB and SDHC/SDHD tumours or *in vitro* models. However, a possibility exists that these differences derive from the chromosomal location of individual SDH genes. For the development of PGL/PHEO, the second allele of the particular SDH gene harbouring the germline mutation is usually inactivated, and this may result in the concomitant elimination of additional tumour suppressor genes in the vicinity of the loci during somatic loss of the second allele [75].

Based on the two mechanisms proposed to be responsible for tumour formation, α-ketoglutarate derivatives and antioxidants were proffered as a therapy, or as a prevention in individuals with familial history of CII mutations. Cell permeable α-ketoglutarate derivatives, substrates for PHD enzymes, were shown to restore the PHD activity in CII-deficient cells, relieve pseudohypoxia [77] and reverse the hypoxia-mediated HIF1α stabilisation with decrease in glycolysis and ensuing cell death in a xenograft tumour model [78]. A lipid soluble antioxidant, vitamin E, protected cells with CII mutations from oxidative damage represented by lipid peroxidation and reversed their phenotype characterised by apoptosis resistance [79].

Since CII may serve as a target for anti-cancer agents, it is necessary to realise that CII deficiency is present only in the minority of cancers, and even though CII-deficient cells display lower response to CII-targeted agents such as α-TOS/MitoVES [27,80], this should not present a substantial problem overall. In addition, despite the typical pro-glycolytic changes in many cancer cells, the oxidative phosphorylation (OXPHOS) in large majority of cancer cells is present, albeit often attenuated. This may stem from the fact that in most cancers the glycolytic pathway may be required to supply necessary building blocks for biosynthetic pathways, and not from the necessity to supply the cell with ATP, and cancer cells still mostly have functional OXPHOS [81–84]. Therefore, in most cancers, components of OXPHOS are a suitable target not only for CII-directed agents, but also for other compounds that kill cancer cells by targeting the other respiratory complexes [20]. In addition, it could be perhaps possible to pharmacologically manipulate a cancer cell in such a way that it would be 'primed' for CII-targeted therapy. For example, Pistollato and colleagues reported that the glucose analogue 2-deoxyglucose, which inhibits hexokinase, the first enzyme of the glycolytic pathway, caused an increase in the SDH activity of CII and decreased succinate levels in glioblastoma multiforme cells [85]. It is important to bear in mind, though, that acute inhibition of glycolysis would reduce OXPHOS as well, because the end product of glycolysis, pyruvate, would be less abundant and hence there would be less 'fuel' for the TCA cycle to produce the NADH and $FADH_2$ for respiration. A plausible approach is to re-direct the metabolite flow of cancer cells to mitochondria using dichloroacetate (DCA), which inhibits the key enzyme regulating the fate of pyruvate, pyruvate dehydrogenase kinase (PDK) and is already used in the clinic to treat lactic acidosis [86]. PDK is overexpressed in cancer cells and phosphorylates and inhibits pyruvate dehydrogenase, so that the end product of glycolysis, pyruvate, cannot enter the mitochondrial TCA cycle and is instead converted to lactate in the cytoplasm. Using DCA, glycolysis could still supply pyruvate to maintain the electron flow through OXPHOS, and further with the inhibition of lactate production by lactate dehydrogenase [87] the redox balance would be impaired and the cell would be more vulnerable to the oxidative stress induced by CII targeting.

4. Complex II as a target for anti-cancer agents

4.1. General aspects

CII, the smallest of the respiratory complexes [34,88], has recently attracted considerable attention, one reason being since it is at the branching point connecting the TCA cycle and the ETC. While other complexes of the respiratory chain contribute to the maintenance of the proton gradient across the MIM, CII lacks this activity. It can be postulated that the major role of CII is to drive the TCA cycle in the 'clockwise' direction by the conversion of succinate to fumarate, *i.e.* in the direction whereby generating NADH, feeding into CI. The electrons released from the conversion succinate to fumarate are then mobilised to the UbQ molecule bound in the membrane 'portion' of CII, causing its reduction to $UbQH_2$. Further, UbQ in its reduced form relaxes its association with CII and donates the two electrons to CIII, where it causes reduction of CIII's UbQ, itself being re-oxidised. Due to its increased affinity for its CII site, it re-associates with its natural binding domain. Thus, the diversion of electrons from the CII's FAD keeps the SDH activity at the optimum rate.

The crystal structure of CII of both prokaryotes (*E. coli*) and eukaryotes (porcine complex) has been resolved, which gave us a detailed and reasonably precise understanding of its structure and its potential functional consequences [31,34]. This also made it more feasible to design strategies of targeting CII for apoptosis induction in cancer cells. Apart from papers studying agents that bind to various sites of CII and are considered excellent molecular tools rather than potential anti-cancer agents, the first report, to the best of our knowledge, indicating that CII plays a role in apoptosis, was published by Albayrak and colleagues [89]. In this paper the authors reported on efficient apoptosis in parental cells and its suppression upon mutation in one of the CII subunits (SDHC). The triggers used were both small pharmacological agents as well as ligands activating the death receptors, as exemplified by the Fas ligand. This breadth of inducers suggested that CII is not an actual target for all these agents but, rather, a mediator of, probably, the earlier stages of the apoptotic process. This is in particular true for apoptosis induced via activation of the death receptors.

4.2. Vitamin E analogues

We have been studying for some time the molecular mechanism and the anti-oxidant properties of a redox-silent VE analogue α-TOS (Table 1). This agent is of considerable interest, since it is derived from the nutritionally essential α-tocopherol but, unlike its redox-active counterpart, lacks the anti-oxidant activity and suppresses cancer in animal models [21,90]. A particularly intriguing feature of α-TOS is its selectivity for cancer cells [91]. The potential importance of α-TOS stems from findings that it is efficient, without secondary toxicity, against a number of experimental cancers, including colon, breast, prostate and lung cancer, as well as mesotheliomas and melanomas, to name only a few [21,22,24,92–97]. A variant of α-TOS, α-tocopheryloxyacetic acid (α-TEA), was shown to suppress ovarian and breast cancer in experimental animals [98,99]. We found that the ether α-TEA is more efficient in suppressing spontaneous breast carcinomas in the transgenic FVB/N *c-neu* mice due to its longer half-life *in vivo* compared to the ester α-TOS [100].

α-TOS induces apoptosis in cancer cells by causing a rapid generation of ROS, with ensuing formation of a Bax or Bak pore in the mitochondrial outer membrane (MOM) [17,21,23,101]. We found that addition of radical scavengers, such as α-tocopherol, suppressed ROS generation and apoptosis induction [21]. The radical species formed is most likely superoxide that then promotes apoptosis. It has been proposed that this can occur either in a transcription-independent manner via Bax dimerisation and its insertion into the MOM or transcriptionally via Noxa upregulation and formation of a Bak channel in the MOM [17] (see below).

More detailed analysis identified that, at least in some types of cancer cells (as shown for Jurkat T lymphoma and non-small cell lung carcinoma cells), following the initial ROS generation in response of α-TOS stimulation, the Mst1 kinase is activated, phosphorylating and activating the transcription factor FoxO1. This results in transcriptional upregulation of the Bcl-2 homology-3 (BH3)-only protein Noxa [25]. Noxa then diverts the anti-apoptotic protein Mcl-1 from Bak, which is free to form a channel in the MOM [102]. ROS dependent mobilisation of Bax to the MOM has also been proposed [17,23,101].

Shiau et al. [103] reported that α-TOS and its analogues have the propensity to interact with the BH3 domains of Bcl-2 and Bcl-x_L, whereby inhibiting their anti-apoptotic function. This may be a reason why α-TOS and its analogues have been shown to synergise with several anti-cancer agents, including TRAIL [27,104], paclitaxel [105], cisplatin [106], or tamoxifen [107]. The notion that α-TOS interacts with BH3 domains of Bcl-2 family of proteins places the agent and its analogues to Class 2 of mitocans [19] (Fig. 1). However, the fact that cancer cells respond to the agent by rapid ROS generation [23,108–111] indicates that α-TOS targets a particular site in mitochondria that results in ROS formation. Such a target has been proposed for α-TOS to be the mitochondrial CI, although the precise mechanism for the interaction with this multicomponent respiratory complex has not been documented [111].

Our attempt to find the molecular target for α-TOS resulted in the identification of CII as the species via which the VE analogue interacts to induce apoptosis in cancer cells [26]. This was shown initially using biochemical methods, which allowed us to suggest the UbQ site(s) in CII as the target for α-TOS, rather than the FAD site in its SDHA subunit. Molecular modelling indicated strong interaction of α-TOS with both the proximal (Q_p) and the distal UbQ site (Q_d) [34] of CII [26]. More specifically, α-TOS was found to have a strong hydrogen bond with the ubiquinone-binding Ser68 of Q_p in the SDHA subunit (Fig. 3A,B) and with SDHD's Lys128/135 [26] of the less well characterised Q_d [34]. The notion that CII is a target for α-TOS was corroborated by loss of apoptosis and ROS generation in cells with a mutation causing a loss of the SDHC subunit, which was overcome by reconstitution of the functional complex [26]. Importantly, too, tumours derived from CII-compromised H-Ras-transformed Chinese hamster lung fibroblasts were resistant, while the tumours derived from CII-competent (either parental or reconstituted) cells were susceptible to α-TOS treatment [27] (Fig. 3C–E). These findings clearly document CII as a novel target for compounds with a clinical potential, epitomised by the promising α-TOS. Consistent with this, we also reported that α-TOS and α-TEA selectively suppress angiogenesis by interacting with CII of the proliferating endothelial cells [112].

Identification of the target for α-TOS within the MIM prompted us to develop a novel group of anti-cancer agents by tagging VE analogues with a cationic triphenylphosphonium (TPP^+) group. This reasoning was based on the pioneering work of Murphy and Smith, who attached the TPP^+ group to a range of compounds, in particular the redox-active UbQ to form mitochondrially targeted ubiquinone (MitoQ) as well as to radical scavengers accumulating in mitochondria, such as MitoB and MitoP used to evaluate the production of hydrogen peroxide inside mitochondria of live cells [113–115]. The principle of targeting a hydrophobic agent into mitochondria by tagging it with TPP^+ is based on the fact that the delocalised charge on the quarternary phosphorus will cause up to 1000-fold accumulation of the modified compound in mitochondria, such that the TPP^+ group will be at the matrix face of the MIM and the bioactive, hydrophobic part (as in MitoQ) inside the MIM [114]. We applied this principle to vitamin E succinate (VES) to generate mitochondrially targeted VES (MitoVES) (Table 1) [80,116].

Based on the above assumptions, we can reason that due to its chemico-physical properties, MitoVES will span the interface of the MIM and the mitochondrial matrix with the bioactive tocopheryl succinyl group in the proximity of Ser68 of the Q_p site (Fig. 4A,B). For reasons of being anchored at the interface by the TPP^+ group, MitoVES will never reach the Q_d site. In other words, by tagging VES with TPP^+, we send the agent directly where it matters, *i.e.* to its site in the MIM, increasing its concentration within the mitochondria theoretically by the factor of 10^3 compared to that of the untagged parental compound. MitoVES was found to be very efficient in apoptosis induction in cancer cells, some 20–50 more than found for α-TOS [80,116]. It triggered apoptosis by interaction with the CII's Q_p, causing rapid generation of ROS followed by activation of Mst1, nuclear translocation of FoxO1, increased expression of the Noxa protein and generation of the Bak pore in the MOM [80,116], essentially as found earlier for α-TOS [25,102]. Interestingly, too, unlike α-TOS that could induce apoptosis, albeit delayed, MitoVES was completely inefficient in apoptosis induction in Jurkat cells lacking both Bak and Bax proteins, a prerequisite for the formation of an MOM pore [80,116]. This documents that while α-TOS can also destabilise other structures than mitochondria (such as lysosomes) [117,118], MitoVES is mitochondria-specific due to its localisation (Fig. 4A, B).

The molecular target of MitoVES in CII is particularly intriguing. We found that the length of the aliphatic chain linking the tocopheryl succinyl group and the TPP^+ group of 11 carbons is optimal for MitoVES, since its shortening by 2 carbons at a time causes gradual loss of the activity of the agent, such that MitoVE7S and MitoVE5S have a barely detectable ROS-and apoptosis-inducing activity [80,116]. Further, we found that MitoVES suppressed the two activities of CII with different efficacy: the SDH activity with IC_{50} ~ 70 μM and the SQR activity with IC_{50} ~ 1.7 μM. This is a very important finding, since it points to preferential inhibition by MitoVES of the SQR activity by way of interfering with UbQ binding in the Q_p site. At relatively low levels of MitoVES, the SDH activity will be relatively high, allowing for

Table 1
Compounds targeting complex II.

Compound	Structure
α-Tocopheryl succinate (α-TOS)	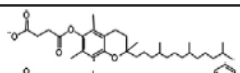
Mitochondrially targeted vitamin E succinate (MitoVES)	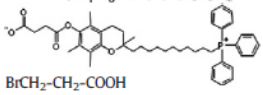
3-Bromopyruvate (3BP)	$BrCH_2$–CH_2–COOH
Malonate	
Nitropropionic acid (3NP)	O_2N-CH_2–COOH
Thenoyltrifluoroacetone (TTFA)	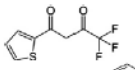
Troglitazone	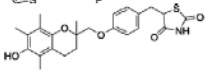
Atpenin A5	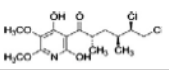

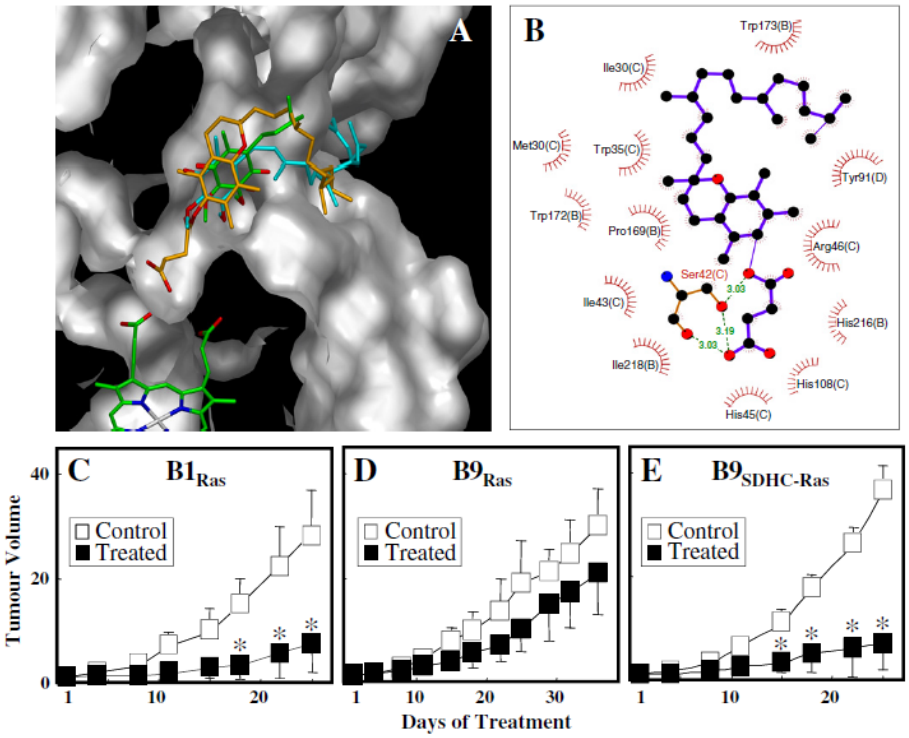

Fig. 3. Model of the interaction of α-TOS with CII and its effect on CII-functional and dysfunctional tumours. Molecular modelling indicates the position of α-TOS in relation to UbQ and heme between the SDHC and SDHD subunits of CII (A), and its interaction with the Ser68 (shown here as Ser42 as used in the study by Sun et al. [34], which binds UbQ in the Q_p site. Strong hydrogen bonds of the oxo groups of the succinyl moiety of α-TOS with the SDHC's Ser68 are indicated (B). Parental B1, SDHC-deficient B9 and SDHC-reconstituted $B9_{SDHC}$ cells were transformed with H-Ras and grafted into nude mice to form tumours. The carcinomas were treated with α-TOS, indicating a good response of the CII-functional and very little response of the CII-compromised tumours (C–E).
Adapted from [26] and [116].

conversion of succinate to fumarate, giving rise to electron generation and their mobilisation towards Q_p. Due to displacement of UbQ with MitoVES, however, electrons will not be intercepted by their natural acceptor and will react with molecular oxygen to form the apoptosis-inducing superoxide [80,116] (Fig. 4C).

The clinical relevance of MitoVES is documented by its highly efficient anti-cancer effect in two models of neoplastic disease: the transgenic FVB/N *c-neu* mice with spontaneous $HER2^{high}$ breast carcinomas and nude mice with colon cancer xenografts [80,116] (Fig. 5A,B). The agent was more than 20-fold more efficient than the untargeted α-TOS with only marginal if any secondary toxicity, which is of considerable importance for the translational potential of MitoVES. Interestingly, we observed that the molecular mode of action of the agent uncovered in tissue culture experiments is similar to that exerted by the agent *in vivo*, as documented in Fig. 5C. In these experiments, we used HCT116 (colorectal) cells stably transfected with the oxygen-dependent destruction (ODD) domain of HIF1α, that controls its stability, fused with GFP. Treatment of the cells with MitoVES for extended periods of time generated green fluorescence, presumably due to pseudohypoxia based on higher accumulation of succinate [62,78]. The same cells were used to form a tumour in nude mice (*c.f.* Fig. 5B), and the treatment of the mice with MitoVES induced development of green fluorescence, as detected in tumour sections (Fig. 5C).

We have found yet another intriguing effect of MitoVES. In Fig. 1, MitoVES is also placed in Class 8 of mitocans, *i.e.* compounds that affect mtDNA. The reason is that the agent at concentrations below those needed to induce apoptosis, considerably suppresses the level of mtDNA transcripts, in particular the *D-LOOP* transcript, affecting mitochondrial homeostasis and cancer cell proliferation (Truksa et al., submitted for publication). This was not observed for the untargeted α-TOS. The fact that the effect on the *D-LOOP* transcript was gradually lost with shortening the aliphatic chain of MitoVES indicates that in this case, the effect of MitoVES on mtDNA may be, after all, mediated by its initial interaction with CII, although this has to be resolved. In any case, this is an interesting bioactivity of MitoVES that makes the agent suppress cancer cell proliferation in an apoptosis-independent manner. Collectively, the above data endow mitochondrially targeted VE analogues, epitomised by MitoVES, with a great translational potential.

4.3. 3-Bromopyruvate

3-Bromopyruvate (3BP) is an interesting compound acting via several modes (Table 1, Fig. 1). It is a Class 1 mitocan, interfering with hexokinase (HK) activity [119–121]. Its major effect on HK stems from its being an alkylating agent, binding to HK2 and causing its dissociation from the voltage-dependent anion channel (VDAC) [122]. It is apparent that 3BP causes the death of cancer cells by means of fast depletion of ATP, which translated into anti-tumour activity in animal models [119,123]. 3BP is also an inhibitor of CII, interfering with the SDH activity [124], and we used 3BP to document that α-TOS does not inhibit CII by preferential interaction with the SDHA subunit [26]. Notwithstanding the effect of 3BP on CII, its main target is considered to be HK2. The clinical relevance of this compound is documented by

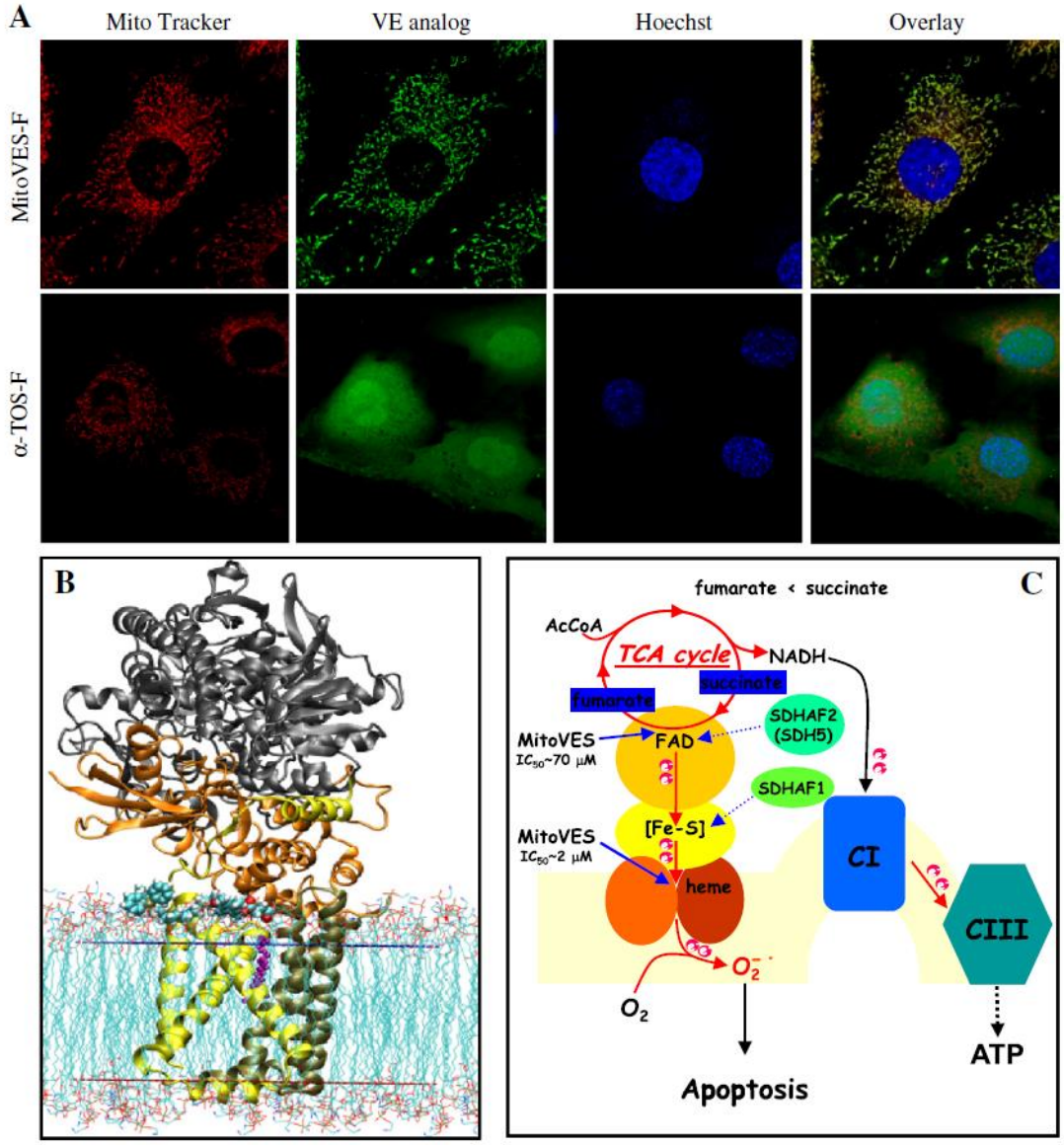

Fig. 4. Mitochondrial localisation of MitoVES, its interaction with CII and the molecular mechanism of its effect on CII. A. Mouse breast cancer NeuTL cells were incubated with MitoTracker Red and fluorescently labelled MitoVES or α-TOS and inspected by confocal microscopy. Hoechst 33342 was used to visualise the nuclei. B. Molecular modelling indicated the position of MitoVES at the interface of the MIM and matrix components of CII. C. MitoVES inhibits both SDH and SQR activity of CII, the former with IC_{50}~70 μM, the latter with IC_{50}~2 μM. Due to this scenario, the conversion of succinate to fumarate occurs in the presence of MitoVES, albeit at a lower rate, generating electrons that are forced to transverse to the membrane components of CII. In the situation when UbQ is displaced from the Q_p site in CII, electrons lack their natural acceptor and recombine with molecular oxygen to give rise to superoxide. This then triggers a series of reactions that result in the induction of the apoptotic cascade, resulting in the demise of the cell.
Adapted from [19,80,116].

a recent issue of *J. Bioenerg. Biomembr.* dedicated to 3BP [125]. In this issue, a case study was published in which 3BP was successful to extend the life of a fibrolamellar hepatocellular carcinoma patient, indicating a possible clinical application of the agent [126].

4.4. Malonate and 3-nitropropionic acid

Malonate and 3-nitropropionic acid (3NP) are compounds specifically inhibiting the SDH activity of CII; this results in the generation of ROS and induction of apoptosis [127,128]. Malonate is an important tool when studying the contribution of individual complexes to respiration of cells and tissues. 3NP has also been used in the elucidation of the precise architecture of CII [34]. As anti-cancer agents, the two compounds are of limited value due to their secondary toxicity, in particular being neurotoxic as documented in experimental animals, where they cause severe neurological disorders [129,130].

Hence, with regard to future anti-cancer drug development, the UbQ-binding sites in the SDHC and SDHD subunits may prove to be better suited targets than sites in the SDHA catalytic domain given the associated problem of neurotoxicity. Inhibiting SDH activity also

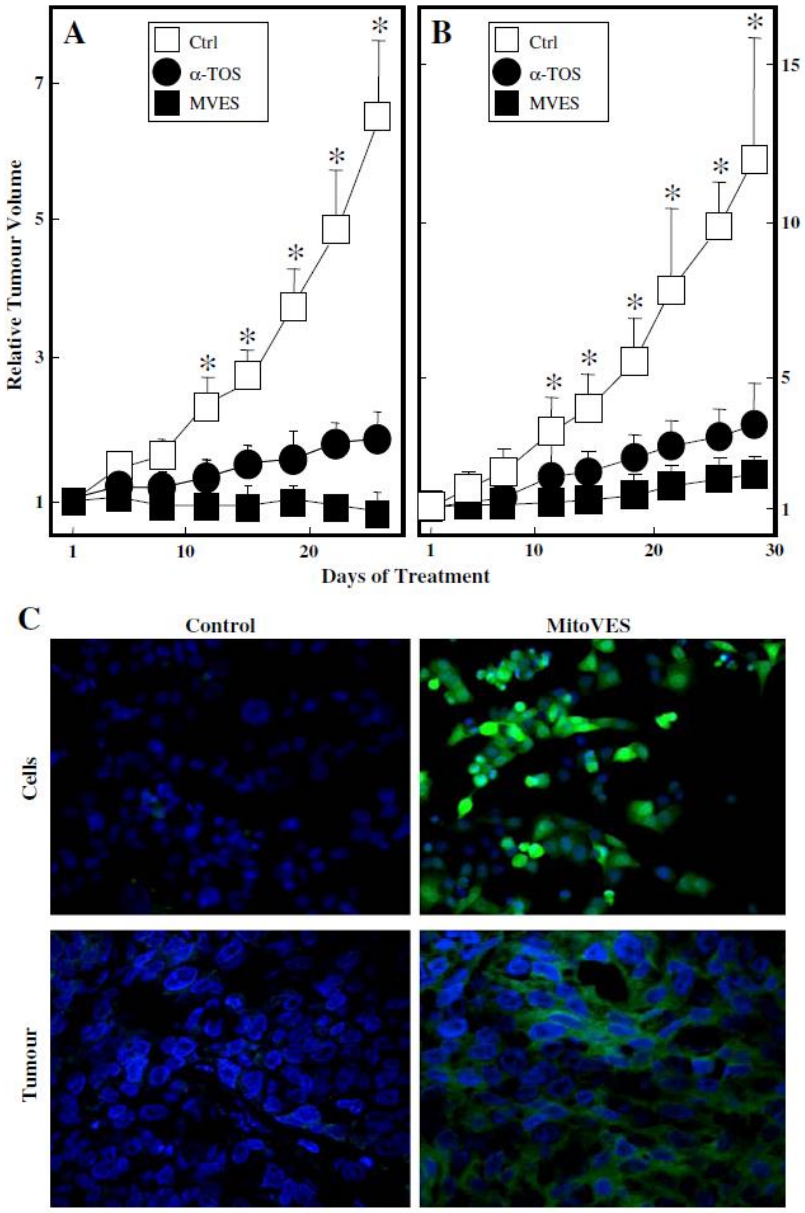

Fig. 5. MitoVES efficiently suppresses tumours and induces pseudohypoxia in cancer cells and in tumours. FVB/N *c-neu* transgenic mice with spontaneous breast carcinomas (A) and nude mice with xenografts derived from colorectal HCT116 cells (B) were treated with α-TOS and with MitoVES at 10-fold lower doses than that of the former. Ultrasound imaging documents a superior activity of MitoVES over its untargeted counterpart. C. HCT116 colon cancer cells were stably transfected with the *ODD-GFP* gene-containing plasmid. The cells were exposed to 5 μM MitoVES for 12 h and green colour, indicative of the accumulation of the chimeric ODD-GFP protein observed using confocal microscopy (upper images). Sections from $HCT116_{ODD\text{-}GFP}$-derived tumours treated with MitoVES were inspected by confocal microscopy, revealing green fluorescence. The *in vitro* and *in vivo* experiments document that the mechanism by which MitoVES induces apoptosis is similar in both settings.
Adapted from [80] and [116].

blocks the TCA cycle as well as the transfer of electrons to the UbQ pool and hence, the metabolic TCA cycle arrest could have much more serious consequences for the cell than the selective inhibition of electron transfer involving the UbQ sites. In the latter case, the TCA cycle would not become fully inhibited, but the disruption of the electron flow at the UbQ sites would still allow for efficient superoxide formation.

4.5. Thenoyltrifluoroacetone

While malonate and 3NP act at the level of the SDHA subunit of CII, thenoyltrifluoroacetone (TTFA) interferes with the UbQ-binding site between the SDHC and SDHD subunits. It was discovered in the 1960s as a compound that interferes with the oxidation of succinate [131]. It was further found that TTFA affects the UbQ site in CII and SQR

activity that causes reduction of UbQ to $UbQH_2$ [132,133]. TTFA was shown to induce apoptosis, cause generation of superoxide/hydrogen peroxide and increase the Ca^{2+} levels [134]. The problem with clinical use of TTFA is that it is highly toxic to non-cancerous cells such as hepatocytes [135], in stark contrast to VE analogues [91]. Thus, TTFA is used as a molecular tool to study the structure and function of CII, and was useful in precise defining the Q_p site in the porcine CII that was recently crystallised [34].

4.6. Troglitazone

Similarly as the anti-diabetic agent metformin that was found to also act on CI to induce ROS generation and apoptosis [136], the anti-diabetic drugs from the group of thiazolidinedione compounds [137] represented by troglitazone were found to interfere with the activity of CII [138]. However, since troglitazone and several other thialidinediones have been found to be highly toxic, including hepatotoxicity and cardiotoxicity, they have been withdrawn [139,140], which limits their use as potential anti-cancer agents.

4.7. Atpenins

An interesting group of agents acting via targeting CII are atpenins. They were discovered some 25 years ago as fungal metabolites [141]. Soon after, one of the members of the group, atpenin B, was found to considerably suppress ATP levels in the Raji B lymphoma cells [142]. Some 10 years later, it was found that atpenins, epitomised by atpenin A5, act by interfering with the UbQ site in CII and prevent reduction of UbQ [143,144]. While a lot has been done in terms of understanding the molecular target for atpenins, not much is known about their anti-cancer activity. Thus far there is only one paper reporting on the inhibitory effect of synthetic atpenins on prostate cancer cells [145]. A recent report describes that natural compounds, including atpenins, can suppress the growth of prostate cancer cells by targeting the prostate stromal cells via reducing the expression of the insulin-like growth factor-I [146]. Of considerable interest are findings that by targeting CII, atpenins protect non-malignant tissues, such as the heart muscle, from the pathological effect of events like ischemic insult [147–149]. Very recently, atpenin A5 was used to better understand the mechanism of ROS generation from CII [67]. This is an important report, since it clearly documents that CII can contribute to the formation of superoxide, which has biological and pathological implications. Since more analogues of atpenins are being synthesised, it is only a question of time when their effects on cancer cells and tumours will be tested and reported in the literature [150–152].

5. Conclusions, further perspectives and clinical relevance

CII is a pharmacologically interesting target, given the possibility to relatively independently interfere with its two enzymatic activities, the 'main' SDH activity which maintains the TCA cycle, and the SQR activity, which supports the SDH activity by electron transfer to UbQ. The inhibition of the former may be clinically problematic, due to high level of side effects such as neurotoxicity, possible related to high dependence of neurons on oxidative phosphorylation and TCA. From our experience and from the literature, it appears that the SQR activity may be a preferred target within CII that may be of clinical relevance. Differences in affinity (full blockade versus partial blockade of SQR activity at intracellular concentrations) between indiscriminately cytotoxic TTFA and cancer-specific VE analogues may perhaps explain the different effects in non-cancerous cells. TTFA may inhibit SQR too efficiently and thus compromise the SDH activity too much in all cells, leading to the loss of specificity. In addition, unknown side effects and indiscriminate uptake by various types of cells may also contribute to TTFA toxicity. The specificity of VE analogues for cancer cells may be also co-determined by the following issues. First, the succinyl moiety of the ester analogues is hydrolysed by esterases abundant in non-cancerous cells. Second, they are increased levels of anti-oxidant defense systems in normal cells. Finally, being weak acids, agents like α-TOS will be more readily taken up by cancer cells due to the acidic nature of the tumour interstitium. MitoVES then appears to derive its selectivity for cancer cells largely from the fact that it crosses the plasma membrane on the basis of the potential, which is higher in cancer cells than in normal cells. It then specifically associates with mitochondria (spanning the MIM/matrix interface) due to high MIM potential of cancer cells. MitoVES has the optimum length of the aliphatic chain to span the interface and reach and interfere with the Q_p site of CII, yet allowing SDH activity to proceed to some degree. The electrons, however, cannot be all intercepted by UbQ and form the apoptosis-inducing superoxide [80,116].

The eligibility of CII as a target for anti-cancer drugs is not compromised by the occurrence of mutations in its subunits in cancers. These mutations are associated with relatively infrequent and non-aggressive familiar neoplasias such as paragangliomas and pheochromocytomas, certain percentage of gastrointestinal stromal tumours and pre-cancerous hamartomas in the Cowden syndrome [58,153–155]. Therefore, CII represents an invariant target in most cancers.

We have started with low scale clinical trials of α-TOS focusing on the currently fatal mesotheliomas. To this end, a single mesothelioma patient was receiving trans-dermal α-TOS, which increased her survival by several years. While we still not completely understand the reasons for possible development of resistance to α-TOS, we found that in cancer cells, their long-term exposure to the agent causes upregulation of a member of the ABC family protein that renders the cells resistant to the drug. We also found that this resistance is overcome by MitoVES (Prochazka et al., submitted for publication). These findings provide us with knowledge how to proceed in the planned clinical trials. If successful, this will place CII at the pedestal of clinically relevant targets, whose exploitation is at its very beginning but is already showing considerable promise.

Acknowledgements

J.N. was supported in part by the Australian Research Council, National Health and Medical Research Council of Australia, Cancer Council Queensland, the Clem Jones Foundation and the Czech Science Foundation (P301/10/1937), L.F.D. by the Australian Research Council, K.K. and J.R. by the Czech Science Foundation (P301/12/1851).

References

[1] D. Hanahan, R.A. Weinberg, Hallmarks of cancer: the next generation, Cell 144 (2011) 646–674.

[2] S. Jones, X. Zhang, D.W. Parsons, J.C. Lin, R.J. Leary, P. Angenendt, P. Mankoo, H. Carter, H. Kamiyama, A. Jimeno, S.M. Hong, B. Fu, M.T. Lin, E.S. Calhoun, M. Kamiyama, K. Walter, T. Nikolskaya, Y. Nikolsky, J. Hartigan, D.R. Smith, M. Hidalgo, S.D. Leach, A.P. Klein, E.M. Jaffee, M. Goggins, A. Maitra, C. Iacobuzio-Donahue, J.R. Eshleman, S.E. Kern, R.H. Hruban, R. Karchin, N. Papadopoulos, G. Parmigiani, B. Vogelstein, V.E. Velculescu, K.W. Kinzler, Core signaling pathways in human pancreatic cancers revealed by global genomic analyses, Science 321 (2008) 1801–1806.

[3] D.W. Parsons, S. Jones, X. Zhang, J.C. Lin, R.J. Leary, P. Angenendt, P. Mankoo, H. Carter, I.M. Siu, G.L. Gallia, A. Olivi, R. McLendon, B.A. Rasheed, S. Keir, T. Nikolskaya, Y. Nikolsky, D.A. Busam, H. Tekleab, L.A. Diaz Jr., J. Hartigan, D.R. Smith, R.L. Strausberg, S.K. Marie, S.M. Shinjo, H. Yan, G.J. Riggins, D.D. Bigner, R. Karchin, N. Papadopoulos, G. Parmigiani, B. Vogelstein, V.E. Velculescu, K.W. Kinzler, An integrated genomic analysis of human glioblastoma multiforme, Science 321 (2008) 1807–1812.

[4] E. Check Hayden, Cancer complexity slows quest for cure, Nature 455 (2008) 148.

[5] M. Gerlinger, A.J. Rowan, S. Horswell, J. Larkin, D. Endesfelder, E. Gronroos, P. Martinez, N. Matthews, A. Stewart, P. Tarpey, I. Varela, B. Phillimore, S. Begum, N.Q. McDonald, A. Butler, D. Jones, K. Raine, C. Latimer, C.R. Santos, M. Nohadani, A.C. Eklund, B. Spencer-Dene, G. Clark, L. Pickering, G. Stamp, M. Gore, Z. Szallasi, J. Downward, P.A. Futreal, C. Swanton, Intratumor heterogeneity and branched evolution revealed by multiregion sequencing, N. Engl. J. Med. 366 (2012) 883–892.

[6] R. Siegel, D. Naishadham, A. Jemal, Cancer statistics, 2012, CA Cancer J. Clin. 62 (2012) 10–29.
[7] R. Siegel, C. DeSantis, K. Virgo, K. Stein, A. Mariotto, T. Smith, D. Cooper, T. Gansler, C. Lerro, S. Fedewa, C. Lin, C. Leach, R.S. Cannady, H. Cho, S. Scoppa, M. Hachey, R. Kirch, A. Jemal, E. Ward, Cancer treatment and survivorship statistics, 2012, CA Cancer J. Clin. 62 (2012) 220–241.
[8] E.P. Simard, E.M. Ward, R. Siegel, A. Jemal, Cancers with increasing incidence trends in the United States: 1999 through 2008, CA Cancer J. Clin. (in press).
[9] D.R. Green, G. Kroemer, The pathophysiology of mitochondrial cell death, Science 305 (2004) 626–629.
[10] S.J. Ralph, S. Rodriguez-Enriquez, J. Neuzil, E. Saavedra, R. Moreno-Sanchez, The causes of cancer revisited: "mitochondrial malignancy" and ROS-induced oncogenic transformation – why mitochondria are targets for cancer therapy, Mol. Aspects Med. 31 (2010) 145–170.
[11] V. Gogvadze, S. Orrenius, B. Zhivotovsky, Mitochondria in cancer cells: what is so special about them? Trends Cell Biol. 18 (2008) 165–173.
[12] S. Fulda, L. Galluzzi, G. Kroemer, Targeting mitochondria for cancer therapy, Nat. Rev. Drug Discov. 9 (2010) 447–464.
[13] D.C. Wallace, W. Fan, V. Procaccio, Mitochondrial energetics and therapeutics, Annu. Rev. Pathol. 5 (2010) 297–348.
[14] F. Wang, M.A. Ogasawara, P. Huang, Small mitochondria-targeting molecules as anti-cancer agents, Mol. Aspects Med. 31 (2010) 75–92.
[15] S. Fulda, G. Kroemer, Mitochondria as therapeutic targets for the treatment of malignant disease, Antioxid. Redox Signal. 15 (2011) 2937–2949.
[16] O. Kepp, L. Galluzzi, M. Lipinski, J. Yuan, G. Kroemer, Cell death assays for drug discovery, Nat. Rev. Drug Discov. 10 (2011) 221–237.
[17] J. Neuzil, X.F. Wang, L.F. Dong, P. Low, S.J. Ralph, Molecular mechanism of 'mitocan'-induced apoptosis in cancer cells epitomizes the multiple roles of reactive oxygen species and Bcl-2 family proteins, FEBS Lett. 580 (2006) 5125–5129.
[18] J. Neuzil, J.C. Dyason, R. Freeman, L.F. Dong, L. Prochazka, X.F. Wang, I. Scheffler, S.J. Ralph, Mitocans as anti-cancer agents targeting mitochondria: lessons from studies with vitamin E analogues, inhibitors of complex II, J. Bioenerg. Biomembr. 39 (2007) 65–72.
[19] J. Neuzil, L.F. Dong, J. Rohlena, J. Truksa, S.J. Ralph, Classification of mitocans, anti-cancer drugs acting on mitochondria, Mitochondrion (in press).
[20] J. Rohlena, L.F. Dong, S.J. Ralph, J. Neuzil, Anticancer drugs targeting the mitochondrial electron transport chain, Antioxid. Redox Signal. 15 (2011) 2951–2974.
[21] J. Neuzil, T. Weber, A. Schroder, M. Lu, G. Ostermann, N. Gellert, G.C. Mayne, B. Olejnicka, A. Negre-Salvayre, M. Sticha, R.J. Coffey, C. Weber, Induction of cancer cell apoptosis by α-tocopheryl succinate: molecular pathways and structural requirements, FASEB J. 15 (2001) 403–415.
[22] T. Weber, M. Lu, L. Andera, H. Lahm, N. Gellert, M.W. Fariss, V. Korinek, W. Sattler, D.S. Ucker, A. Terman, A. Schroder, W. Erl, U.T. Brunk, R.J. Coffey, C. Weber, J. Neuzil, Vitamin E succinate is a potent novel antineoplastic agent with high selectivity and cooperativity with tumor necrosis factor-related apoptosis-inducing ligand (Apo2 ligand) *in vivo*, Clin. Cancer Res. 8 (2002) 863–869.
[23] T. Weber, H. Dalen, L. Andera, A. Negre-Salvayre, N. Auge, M. Sticha, A. Lloret, A. Terman, P.K. Witting, M. Higuchi, M. Plasilova, J. Zivny, N. Gellert, C. Weber, J. Neuzil, Mitochondria play a central role in apoptosis induced by α-tocopheryl succinate, an agent with antineoplastic activity: comparison with receptor-mediated pro-apoptotic signaling, Biochemistry 42 (2003) 4277–4291.
[24] M. Stapelberg, N. Gellert, E. Swettenham, M. Tomasetti, P.K. Witting, A. Procopio, J. Neuzil, α-Tocopheryl succinate inhibits malignant mesothelioma by disrupting the fibroblast growth factor autocrine loop: mechanism and the role of oxidative stress, J. Biol. Chem. 280 (2005) 25369–25376.
[25] K. Valis, L. Prochazka, E. Boura, J. Chladova, T. Obsil, J. Rohlena, J. Truksa, L.F. Dong, S.J. Ralph, J. Neuzil, Hippo/Mst1 stimulates transcription of the proapoptotic mediator NOXA in a FoxO1-dependent manner, Cancer Res. 71 (2011) 946–954.
[26] L.F. Dong, P. Low, J.C. Dyason, X.F. Wang, L. Prochazka, P.K. Witting, R. Freeman, E. Swettenham, K. Valis, J. Liu, R. Zobalova, J. Turanek, D.R. Spitz, F.E. Domann, I.E. Scheffler, S.J. Ralph, J. Neuzil, α-Tocopheryl succinate induces apoptosis by targeting ubiquinone-binding sites in mitochondrial respiratory complex II, Oncogene 27 (2008) 4324–4335.
[27] L.F. Dong, R. Freeman, J. Liu, R. Zobalova, A. Marin-Hernandez, M. Stantic, J. Rohlena, K. Valis, S. Rodriguez-Enriquez, B. Butcher, J. Goodwin, U.T. Brunk, P.K. Witting, R. Moreno-Sanchez, I.E. Scheffler, S.J. Ralph, J. Neuzil, Suppression of tumor growth *in vivo* by the mitocan α-tocopheryl succinate requires respiratory complex II, Clin. Cancer Res. 15 (2009) 1593–1600.
[28] B.A. Ackrell, Progress in understanding structure–function relationships in respiratory chain complex II, FEBS Lett. 466 (2000) 1–5.
[29] M. Saraste, Oxidative phosphorylation at the fin de siecle, Science 283 (1999) 1488–1493.
[30] G. Cecchini, Function and structure of complex II of the respiratory chain, Annu. Rev. Biochem. 72 (2003) 77–109.
[31] V. Yankovskaya, R. Horsefield, S. Tornroth, C. Luna-Chavez, H. Miyoshi, C. Leger, B. Byrne, G. Cecchini, S. Iwata, Architecture of succinate dehydrogenase and reactive oxygen species generation, Science 299 (2003) 700–704.
[32] E. Maklashina, D.A. Berthold, G. Cecchini, Anaerobic expression of *Escherichia coli* succinate dehydrogenase: functional replacement of fumarate reductase in the respiratory chain during anaerobic growth, J. Bacteriol. 180 (1998) 5989–5996.
[33] C. Hagerhall, Succinate: quinone oxidoreductases. Variations on a conserved theme, Biochim. Biophys. Acta 1320 (1997) 107–141.
[34] F. Sun, X. Huo, Y. Zhai, A. Wang, J. Xu, D. Su, M. Bartlam, Z. Rao, Crystal structure of mitochondrial respiratory membrane protein complex II, Cell 121 (2005) 1043–1057.
[35] M. McKenzie, M.T. Ryan, Assembly factors of human mitochondrial complex I and their defects in disease, IUBMB Life 62 (2010) 497–502.
[36] H.X. Hao, O. Khalimonchuk, M. Schraders, N. Dephoure, J.P. Bayley, H. Kunst, P. Devilee, C.W. Cremers, J.D. Schiffman, B.G. Bentz, S.P. Gygi, D.R. Winge, H. Kremer, J. Rutter, SDH5, a gene required for flavination of succinate dehydrogenase, is mutated in paraganglioma, Science 325 (2009) 1139–1142.
[37] K. Nakamura, M. Yamaki, M. Sarada, S. Nakayama, C.R. Vibat, R.B. Gennis, T. Nakayashiki, H. Inokuchi, S. Kojima, K. Kita, Two hydrophobic subunits are essential for the heme b ligation and functional assembly of complex II (succinate–ubiquinone oxidoreductase) from *Escherichia coli*, J. Biol. Chem. 271 (1996) 521–527.
[38] J. Nouws, L.G. Nijtmans, J.A. Smeitink, R.O. Vogel, Assembly factors as a new class of disease genes for mitochondrial complex I deficiency: cause, pathology and treatment options, Brain 135 (2012) 12–22.
[39] D. Ghezzi, P. Goffrini, G. Uziel, R. Horvath, T. Klopstock, H. Lochmuller, P. D'Adamo, P. Gasparini, T.M. Strom, H. Prokisch, F. Invernizzi, I. Ferrero, M. Zeviani, SDHAF1, encoding a LYR complex-II specific assembly factor, is mutated in SDH-defective infantile leukoencephalopathy, Nat. Genet. 41 (2009) 654–656.
[40] A. Atkinson, O. Khalimonchuk, P. Smith, H. Sabic, D. Eide, D.R. Winge, Mzm1 influences a labile pool of mitochondrial zinc important for respiratory function, J. Biol. Chem. 285 (2010) 19450–19459.
[41] H.X. Hao, J. Rutter, Revealing human disease genes through analysis of the yeast mitochondrial proteome, Cell Cycle 8 (2009) 4007–4008.
[42] M.B. McNeil, J.S. Clulow, N.M. Wilf, G.P. Salmond, P.C. Fineran, SdhE is a conserved protein required for flavinylation of succinate dehydrogenase in bacteria, J. Biol. Chem. 287 (2012) 18418–18428.
[43] T.A. Giancaspero, R. Wait, E. Boles, M. Barile, Succinate dehydrogenase flavoprotein subunit expression in *Saccharomyces cerevisiae*-involvement of the mitochondrial FAD transporter, Flx1p, FEBS J. 275 (2008) 1103–1117.
[44] E. Dibrov, S. Fu, B.D. Lemire, The *Saccharomyces cerevisiae* TCM62 gene encodes a chaperone necessary for the assembly of the mitochondrial succinate dehydrogenase (complex II), J. Biol. Chem. 273 (1998) 32042–32048.
[45] J. Rutter, D.R. Winge, J.D. Schiffman, Succinate dehydrogenase – assembly, regulation and role in human disease, Mitochondrion 10 (2010) 393–401.
[46] A. Tzagoloff, J. Jang, D.M. Glerum, M. Wu, FLX1 codes for a carrier protein involved in maintaining a proper balance of flavin nucleotides in yeast mitochondria, J. Biol. Chem. 271 (1996) 7392–7397.
[47] C. Klanner, W. Neupert, T. Langer, The chaperonin-related protein Tcm62p ensures mitochondrial gene expression under heat stress, FEBS Lett. 470 (2000) 365–369.
[48] L.W. Finley, W. Haas, V. Desquiret-Dumas, D.C. Wallace, V. Procaccio, S.P. Gygi, M.C. Haigis, Succinate dehydrogenase is a direct target of sirtuin 3 deacetylase activity, PLoS One 6 (2011) e23295.
[49] H. Cimen, M.J. Han, Y. Yang, Q. Tong, H. Koc, E.C. Koc, Regulation of succinate dehydrogenase activity by SIRT3 in mammalian mitochondria, Biochemistry 49 (2010) 304–311.
[50] M. Salvi, N.A. Morrice, A.M. Brunati, A. Toninello, Identification of the flavoprotein of succinate dehydrogenase and aconitase as *in vitro* mitochondrial substrates of Fgr tyrosine kinase, FEBS Lett. 581 (2007) 5579–5585.
[51] B.E. Baysal, R.E. Ferrell, J.E. Willett-Brozick, E.C. Lawrence, D. Myssiorek, A. Bosch, A. van der Mey, P.E. Taschner, W.S. Rubinstein, E.N. Myers, C.W. Richard III, C.J. Cornelisse, P. Devilee, B. Devlin, Mutations in SDHD, a mitochondrial complex II gene, in hereditary paraganglioma, Science 287 (2000) 848–851.
[52] S. Niemann, U. Muller, Mutations in SDHC cause autosomal dominant paraganglioma, type 3, Nat. Genet. 26 (2000) 268–270.
[53] D. Astuti, F. Douglas, T.W. Lennard, I.A. Aligianis, E.R. Woodward, D.G. Evans, C. Eng, F. Latif, E.R. Maher, Germline SDHD mutation in familial phaeochromocytoma, Lancet 357 (2001) 1181–1182.
[54] D. Astuti, F. Latif, A. Dallol, P.L. Dahia, F. Douglas, E. George, F. Skoldberg, E.S. Husebye, C. Eng, E.R. Maher, Gene mutations in the succinate dehydrogenase subunit SDHB cause susceptibility to familial pheochromocytoma and to familial paraganglioma, Am. J. Hum. Genet. 69 (2001) 49–54.
[55] N. Burnichon, J.J. Briere, R. Libe, L. Vescovo, J. Riviere, F. Tissier, E. Jouanno, X. Jeunemaitre, P. Benit, A. Tzagoloff, P. Rustin, J. Bertherat, J. Favier, A.P. Gimenez-Roqueplo, SDHA is a tumor suppressor gene causing paraganglioma, Hum. Mol. Genet. 19 (2010) 3011–3020.
[56] L. Fishbein, K.L. Nathanson, Pheochromocytoma and paraganglioma: understanding the complexities of the genetic background, Cancer Genet. 205 (2012) 1–11.
[57] C. Bardella, P.J. Pollard, I. Tomlinson, SDH mutations in cancer, Biochim. Biophys. Acta 1807 (2011) 1432–1443.
[58] K.A. Janeway, S.Y. Kim, M. Lodish, V. Nose, P. Rustin, J. Gaal, P.L. Dahia, B. Liegl, E.R. Ball, M. Raygada, A.H. Lai, L. Kelly, J.L. Hornick, M. O'Sullivan, R.R. de Krijger, W.N. Dinjens, G.D. Demetri, C.R. Antonescu, J.A. Fletcher, L. Helman, C.A. Stratakis, Defects in succinate dehydrogenase in gastrointestinal stromal tumors lacking KIT and PDGFRA mutations, Proc. Natl. Acad. Sci. U. S. A. 108 (2011) 314–318.
[59] P.J. Pollard, J.J. Briere, N.A. Alam, J. Barwell, E. Barclay, N.C. Wortham, T. Hunt, M. Mitchell, S. Olpin, S.J. Moat, I.P. Hargreaves, S.J. Heales, Y.L. Chung, J.R. Griffiths, A. Dalgleish, J.A. McGrath, M.J. Gleeson, S.V. Hodgson, R. Poulsom, P. Rustin, I.P. Tomlinson, Accumulation of Krebs cycle intermediates and over-expression of HIF1α in tumours which result from germline FH and SDH mutations, Hum. Mol. Genet. 14 (2005) 2231–2239.

[60] J. Favier, J.J. Briere, N. Burnichon, J. Riviere, L. Vescovo, P. Benit, I. Giscos-Douriez, A. De Reynies, J. Bertherat, C. Badoual, F. Tissier, L. Amar, R. Libe, P.F. Plouin, X. Jeunemaitre, P. Rustin, A.P. Gimenez-Roqueplo, The Warburg effect is genetically determined in inherited pheochromocytomas, PLoS One 4 (2009) e7094.
[61] S.M. Fliedner, N. Kaludercic, X.S. Jiang, H. Hansikova, Z. Hajkova, J. Sladkova, A. Limpuangthip, P.S. Backlund, R. Wesley, L. Martiniova, I. Jochmanova, N.K. Lendvai, J. Breza, A.L. Yergey, N. Paolocci, A.S. Tischler, J. Zeman, F.D. Porter, H. Lehnert, K. Pacak, Warburg effect's manifestation in aggressive pheochromocytomas and paragangliomas: insights from a mouse cell model applied to human tumor tissue, PLoS One 7 (2012) e40949.
[62] M.A. Selak, S.M. Armour, E.D. MacKenzie, H. Boulahbel, D.G. Watson, K.D. Mansfield, Y. Pan, M.C. Simon, C.B. Thompson, E. Gottlieb, Succinate links TCA cycle dysfunction to oncogenesis by inhibiting HIF-α prolyl hydroxylase, Cancer Cell 7 (2005) 77–85.
[63] Y. Ni, X. He, J. Chen, J. Moline, J. Mester, M.S. Orloff, M.D. Ringel, C. Eng, Germline SDHx variants modify breast and thyroid cancer risks in Cowden and Cowden-like syndrome via FAD/NAD-dependant destabilization of p53, Hum. Mol. Genet. 21 (2012) 300–310.
[64] E.H. Smith, R. Janknecht, L.J. Maher III, Succinate inhibition of α-ketoglutarate-dependent enzymes in a yeast model of paraganglioma, Hum. Mol. Genet. 16 (2007) 3136–3148.
[65] C. Lu, P.S. Ward, G.S. Kapoor, D. Rohle, S. Turcan, O. Abdel-Wahab, C.R. Edwards, R. Khanin, M.E. Figueroa, A. Melnick, K.E. Wellen, D.M. O'Rourke, S.L. Berger, T.A. Chan, R.L. Levine, I.K. Mellinghoff, C.B. Thompson, IDH mutation impairs histone demethylation and results in a block to cell differentiation, Nature 483 (2012) 474–478.
[66] M. Xiao, H. Yang, W. Xu, S. Ma, H. Lin, H. Zhu, L. Liu, Y. Liu, C. Yang, Y. Xu, S. Zhao, D. Ye, Y. Xiong, K.L. Guan, Inhibition of α-KG-dependent histone and DNA demethylases by fumarate and succinate that are accumulated in mutations of FH and SDH tumor suppressors, Genes Dev. 26 (2012) 1326–1338.
[67] C.L. Quinlan, A.L. Orr, I.V. Perevoshchikova, J.R. Treberg, B.A. Ackrell, M.D. Brand, Mitochondrial complex II can generate reactive oxygen species at high rates in both the forward and reverse reactions, J. Biol. Chem. 287 (2012) 27255–27264.
[68] C. Gleason, S. Huang, L.F. Thatcher, R.C. Foley, C.R. Anderson, A.J. Carroll, A.H. Millar, K.B. Singh, Mitochondrial complex II has a key role in mitochondrial-derived reactive oxygen species influence on plant stress gene regulation and defense, Proc. Natl. Acad. Sci. U. S. A. 108 (2011) 10768–10773.
[69] R.D. Guzy, B. Sharma, E. Bell, N.S. Chandel, P.T. Schumacker, Loss of the SdhB, but Not the SdhA, subunit of complex II triggers reactive oxygen species-dependent hypoxia-inducible factor activation and tumorigenesis, Mol. Cell. Biol. 28 (2008) 718–731.
[70] K.M. Owens, N. Aykin-Burns, D. Dayal, M.C. Coleman, F.E. Domann, D.R. Spitz, Genomic instability induced by mutant succinate dehydrogenase subunit D (SDHD) is mediated by $O_2(-^{\bullet})$ and H_2O_2, Free Radic. Biol. Med. 52 (2012) 160–166.
[71] T. Ishii, K. Yasuda, A. Akatsuka, O. Hino, P.S. Hartman, N. Ishii, A mutation in the SDHC gene of complex II increases oxidative stress, resulting in apoptosis and tumorigenesis, Cancer Res. 65 (2005) 203–209.
[72] A.M. Cervera, N. Apostolova, F.L. Crespo, M. Mata, K.J. McCreath, Cells silenced for SDHB expression display characteristic features of the tumor phenotype, Cancer Res. 68 (2008) 4058–4067.
[73] M.A. Selak, R.V. Duran, E. Gottlieb, Redox stress is not essential for the pseudo-hypoxic phenotype of succinate dehydrogenase deficient cells, Biochim. Biophys. Acta 1757 (2006) 567–572.
[74] V. Kantorovich, K. Pacak, Pheochromocytoma and paraganglioma, Prog. Brain Res. 182 (2010) 343–373.
[75] B. Pasini, C.A. Stratakis, SDH mutations in tumorigenesis and inherited endocrine tumours: lesson from the phaeochromocytoma–paraganglioma syndromes, J. Intern. Med. 266 (2009) 19–42.
[76] F.H. van Nederveen, J. Gaal, J. Favier, E. Korpershoek, R.A. Oldenburg, E.M. de Bruyn, H.F. Sleddens, P. Derkx, J. Riviere, H. Dannenberg, B.J. Petri, P. Komminoth, K. Pacak, W.C. Hop, P.J. Pollard, M. Mannelli, J.P. Bayley, A. Perren, S. Niemann, A.A. Verhofstad, A.P. de Bruine, E.R. Maher, F. Tissier, T. Meatchi, C. Badoual, J. Bertherat, L. Amar, D. Alataki, E. Van Marck, F. Ferrau, J. Francois, W.W. de Herder, M.P. Peeters, A. van Linge, J.W. Lenders, A.P. Gimenez-Roqueplo, R.R. de Krijger, W.N. Dinjens, An immunohistochemical procedure to detect patients with paraganglioma and phaeochromocytoma with germline SDHB, SDHC, or SDHD gene mutations: a retrospective and prospective analysis, Lancet Oncol. 10 (2009) 764–771.
[77] E.D. MacKenzie, M.A. Selak, D.A. Tennant, L.J. Payne, S. Crosby, C.M. Frederiksen, D.G. Watson, E. Gottlieb, Cell-permeating α-ketoglutarate derivatives alleviate pseudohypoxia in succinate dehydrogenase-deficient cells, Mol. Cell. Biol. 27 (2007) 3282–3289.
[78] D.A. Tennant, C. Frezza, E.D. MacKenzie, Q.D. Nguyen, L. Zheng, M.A. Selak, D.L. Roberts, C. Dive, D.G. Watson, E.O. Aboagye, E. Gottlieb, Reactivating HIF prolyl hydroxylases under hypoxia results in metabolic catastrophe and cell death, Oncogene 28 (2009) 4009–4021.
[79] Y. Ni, C. Eng, Vitamin E protects against lipid peroxidation and rescues tumorigenic phenotypes in Cowden/Cowden-like patient-derived lymphoblast cells with germline SDHx variants, Clin. Cancer Res. 18 (2012) 4954–4961.
[80] L.F. Dong, V.J. Jameson, D. Tilly, J. Cerny, E. Mahdavian, A. Marin-Hernandez, L. Hernandez-Esquivel, S. Rodriguez-Enriquez, J. Stursa, P.K. Witting, B. Stantic, J. Rohlena, J. Truksa, K. Kluckova, J.C. Dyason, M. Ledvina, B.A. Salvatore, R. Moreno-Sanchez, M.J. Coster, S.J. Ralph, R.A. Smith, J. Neuzil, Mitochondrial targeting of vitamin E succinate enhances its pro-apoptotic and anti-cancer activity via mitochondrial complex II, J. Biol. Chem. 286 (2011) 3717–3728.
[81] M.G. Vander Heiden, L.C. Cantley, C.B. Thompson, Understanding the Warburg effect: the metabolic requirements of cell proliferation, Science 324 (2009) 1029–1033.
[82] X.L. Zu, M. Guppy, Cancer metabolism: facts, fantasy, and fiction, Biochem. Biophys. Res. Commun. 313 (2004) 459–465.
[83] R. Moreno-Sanchez, S. Rodriguez-Enriquez, A. Marin-Hernandez, E. Saavedra, Energy metabolism in tumor cells, FEBS J. 274 (2007) 1393–1418.
[84] M. Busk, M.R. Horsman, P.E. Kristjansen, A.J. van der Kogel, J. Bussink, J. Overgaard, Aerobic glycolysis in cancers: implications for the usability of oxygen-responsive genes and fluorodeoxyglucose-PET as markers of tissue hypoxia, Int. J. Cancer 122 (2008) 2726–2734.
[85] F. Pistollato, S. Abbadi, E. Rampazzo, G. Viola, A. Della Puppa, L. Cavallini, C. Frasson, L. Persano, D.M. Panchision, G. Basso, Hypoxia and succinate antagonize 2-deoxyglucose effects on glioblastoma, Biochem. Pharmacol. 80 (2010) 1517–1527.
[86] S. Bonnet, S.L. Archer, J. Allalunis-Turner, A. Haromy, C. Beaulieu, R. Thompson, C.T. Lee, G.D. Lopaschuk, L. Puttagunta, G. Harry, K. Hashimoto, C.J. Porter, M.A. Andrade, B. Thebaud, E.D. Michelakis, A mitochondria-K^+ channel axis is suppressed in cancer and its normalization promotes apoptosis and inhibits cancer growth, Cancer Cell 11 (2007) 37–51.
[87] A. Le, C.R. Cooper, A.M. Gouw, R. Dinavahi, A. Maitra, L.M. Deck, R.E. Royer, D.L. Vander Jagt, G.L. Semenza, C.V. Dang, Inhibition of lactate dehydrogenase A induces oxidative stress and inhibits tumor progression, Proc. Natl. Acad. Sci. U. S. A. 107 (2010) 2037–2042.
[88] I.E. Scheffler, Mitochondria, Second edition John Wiley & Sons, Inc., Hoboken, New Jersey, USA, 2008.
[89] T. Albayrak, V. Scherhammer, N. Schoenfeld, E. Braziulis, T. Mund, M.K. Bauer, I.E. Scheffler, S. Grimm, The tumor suppressor cybL, a component of the respiratory chain, mediates apoptosis induction, Mol. Biol. Cell 14 (2003) 3082–3096.
[90] J. Neuzil, T. Weber, A. Terman, C. Weber, U.T. Brunk, Vitamin E analogues as inducers of apoptosis: implications for their potential antineoplastic role, Redox Rep. 6 (2001) 143–151.
[91] J. Neuzil, T. Weber, N. Gellert, C. Weber, Selective cancer cell killing by α-tocopheryl succinate, Br. J. Cancer 84 (2001) 87–89.
[92] X.F. Wang, M. Birringer, L.F. Dong, P. Veprek, P. Low, E. Swettenham, M. Stantic, L.H. Yuan, R. Zobalova, K. Wu, M. Ledvina, S.J. Ralph, J. Neuzil, A peptide conjugate of vitamin E succinate targets breast cancer cells with high ErbB2 expression, Cancer Res. 67 (2007) 3337–3344.
[93] K. Kline, W. Yu, B.G. Sanders, Vitamin E and breast cancer, J. Nutr. 134 (2004) 3458S–3462S.
[94] M.P. Malafa, F.D. Fokum, J. Andoh, L.T. Neitzel, S. Bandyopadhyay, R. Zhan, M. Iiizumi, E. Furuta, E. Horvath, K. Watabe, Vitamin E succinate suppresses prostate tumor growth by inducing apoptosis, Int. J. Cancer 118 (2006) 2441–2447.
[95] J. Quin, D. Engle, A. Litwiller, E. Peralta, A. Grasch, T. Boley, S. Hazelrigg, Vitamin E succinate decreases lung cancer tumor growth in mice, J. Surg. Res. 127 (2005) 139–143.
[96] M. Tomasetti, N. Gellert, A. Procopio, J. Neuzil, A vitamin E analogue suppresses malignant mesothelioma in a preclinical model: a future drug against a fatal neoplastic disease? Int. J. Cancer 109 (2004) 641–642.
[97] M.P. Malafa, F.D. Fokum, A. Mowlavi, M. Abusief, M. King, Vitamin E inhibits melanoma growth in mice, Surgery 131 (2002) 85–91.
[98] K. Anderson, M. Simmons-Menchaca, K.A. Lawson, J. Atkinson, B.G. Sanders, K. Kline, Differential response of human ovarian cancer cells to induction of apoptosis by vitamin E succinate and vitamin E analogue, α-TEA, Cancer Res. 64 (2004) 4263–4269.
[99] T. Hahn, L. Szabo, M. Gold, L. Ramanathapuram, L.H. Hurley, E.T. Akporiaye, Dietary administration of the proapoptotic vitamin E analogue α-tocopheryloxyacetic acid inhibits metastatic murine breast cancer, Cancer Res. 66 (2006) 9374–9378.
[100] L.F. Dong, G. Grant, H. Massa, R. Zobalova, E. Akporiaye, J. Neuzil, α-Tocopheryloxyacetic acid is superior to alpha-tocopheryl succinate in suppressing HER2-high breast carcinomas due to its higher stability, Int. J. Cancer 131 (2012) 1052–1058.
[101] W. Yu, B.G. Sanders, K. Kline, RRR-α-tocopheryl succinate-induced apoptosis of human breast cancer cells involves Bax translocation to mitochondria, Cancer Res. 63 (2003) 2483–2491.
[102] L. Prochazka, L.F. Dong, K. Valis, R. Freeman, S.J. Ralph, J. Turanek, J. Neuzil, α-Tocopheryl succinate causes mitochondrial permeabilization by preferential formation of Bak channels, Apoptosis 15 (2010) 782–794.
[103] C.W. Shiau, J.W. Huang, D.S. Wang, J.R. Weng, C.C. Yang, C.H. Lin, C. Li, C.S. Chen, α-Tocopheryl succinate induces apoptosis in prostate cancer cells in part through inhibition of Bcl-xL/Bcl-2 function, J. Biol. Chem. 281 (2006) 11819–11825.
[104] M. Tomasetti, M.R. Rippo, R. Alleva, S. Moretti, L. Andera, J. Neuzil, A. Procopio, α-Tocopheryl succinate and TRAIL selectively synergise in induction of apoptosis in human malignant mesothelioma cells, Br. J. Cancer 90 (2004) 1644–1653.
[105] K. Kanai, E. Kikuchi, S. Mikami, E. Suzuki, Y. Uchida, K. Kodaira, A. Miyajima, T. Ohigashi, J. Nakashima, M. Oya, Vitamin E succinate induced apoptosis and enhanced chemosensitivity to paclitaxel in human bladder cancer cells *in vitro* and *in vivo*, Cancer Sci. 101 (2010) 216–223.

[106] K. Anderson, K.A. Lawson, M. Simmons-Menchaca, L. Sun, B.G. Sanders, K. Kline, α-TEA plus cisplatin reduces human cisplatin-resistant ovarian cancer cell tumor burden and metastasis, Exp. Biol. Med. (Maywood) 229 (2004) 1169–1176.
[107] R. Tiwary, W. Yu, L.A. deGraffenried, B.G. Sanders, K. Kline, Targeting cholesterol-rich microdomains to circumvent tamoxifen-resistant breast cancer, Breast Cancer Res. 13 (2011) R120.
[108] P. Ottino, J.R. Duncan, Effect of α-tocopherol succinate on free radical and lipid peroxidation levels in BL6 melanoma cells, Free Radic. Biol. Med. 22 (1997) 1145–1151.
[109] Y.H. Kang, E. Lee, M.K. Choi, J.L. Ku, S.H. Kim, Y.G. Park, S.J. Lim, Role of reactive oxygen species in the induction of apoptosis by alpha-tocopheryl succinate, Int. J. Cancer 112 (2004) 385–392.
[110] V. Gogvadze, E. Norberg, S. Orrenius, B. Zhivotovsky, Involvement of Ca^{2+} and ROS in α-tocopheryl succinate-induced mitochondrial permeabilization, Int. J. Cancer 127 (2010) 1823–1832.
[111] G.A. dos Santos, R.S. Abreu e Lima, C.R. Pestana, A.S. Lima, P.S. Scheucher, C.H. Thome, H.L. Gimenes-Teixeira, B.A. Santana-Lemos, A.R. Lucena-Araujo, F.P. Rodrigues, R. Nasr, S.A. Uyemura, R.P. Falcao, H. de The, P.P. Pandolfi, C. Curti, E.M. Rego, (+)α-Tocopheryl succinate inhibits the mitochondrial respiratory chain complex I and is as effective as arsenic trioxide or ATRA against acute promyelocytic leukemia *in vivo*, Leukemia 26 (2012) 451–460.
[112] L.F. Dong, E. Swettenham, J. Eliasson, X.F. Wang, M. Gold, Y. Medunic, M. Stantic, P. Low, L. Prochazka, P.K. Witting, J. Turanek, E.T. Akporiaye, S.J. Ralph, J. Neuzil, Vitamin E analogues inhibit angiogenesis by selective induction of apoptosis in proliferating endothelial cells: the role of oxidative stress, Cancer Res. 67 (2007) 11906–11913.
[113] G.F. Kelso, C.M. Porteous, C.V. Coulter, G. Hughes, W.K. Porteous, E.C. Ledgerwood, R.A. Smith, M.P. Murphy, Selective targeting of a redox-active ubiquinone to mitochondria within cells: antioxidant and antiapoptotic properties, J. Biol. Chem. 276 (2001) 4588–4596.
[114] M.P. Murphy, R.A. Smith, Targeting antioxidants to mitochondria by conjugation to lipophilic cations, Annu. Rev. Pharmacol. Toxicol. 47 (2007) 629–656.
[115] H.M. Cocheme, C. Quin, S.J. McQuaker, F. Cabreiro, A. Logan, T.A. Prime, I. Abakumova, J.V. Patel, I.M. Fearnley, A.M. James, C.M. Porteous, R.A. Smith, S. Saeed, J.E. Carre, M. Singer, D. Gems, R.C. Hartley, L. Partridge, M.P. Murphy, Measurement of H_2O_2 within living *Drosophila* during aging using a ratiometric mass spectrometry probe targeted to the mitochondrial matrix, Cell Metab. 13 (2011) 340–350.
[116] L.F. Dong, V.J. Jameson, D. Tilly, L. Prochazka, J. Rohlena, K. Valis, J. Truksa, R. Zobalova, E. Mahdavian, K. Kluckova, M. Stantic, J. Stursa, R. Freeman, P.K. Witting, E. Norberg, J. Goodwin, B.A. Salvatore, J. Novotna, J. Turanek, M. Ledvina, P. Hozak, B. Zhivotovsky, M.J. Coster, S.J. Ralph, R.A. Smith, J. Neuzil, Mitochondrial targeting of α-tocopheryl succinate enhances its pro-apoptotic efficacy: a new paradigm for effective cancer therapy, Free Radic. Biol. Med. 50 (2011) 1546–1555.
[117] J. Neuzil, I. Svensson, T. Weber, C. Weber, U.T. Brunk, α-Tocopheryl succinate-induced apoptosis in Jurkat T cells involves caspase-3 activation, and both lysosomal and mitochondrial destabilisation, FEBS Lett. 445 (1999) 295–300.
[118] J. Neuzil, M. Zhao, G. Ostermann, M. Sticha, N. Gellert, C. Weber, J.W. Eaton, U.T. Brunk, α-Tocopheryl succinate, an agent with *in vivo* anti-tumour activity, induces apoptosis by causing lysosomal instability, Biochem. J. 362 (2002) 709–715.
[119] S.P. Mathupala, Y.H. Ko, P.L. Pedersen, Hexokinase II: cancer's double-edged sword acting as both facilitator and gatekeeper of malignancy when bound to mitochondria, Oncogene 25 (2006) 4777–4786.
[120] A. Nakano, H. Miki, S. Nakamura, T. Harada, A. Oda, H. Amou, S. Fujii, K. Kagawa, K. Takeuchi, S. Ozaki, T. Matsumoto, M. Abe, Up-regulation of hexokinaseII in myeloma cells: targeting myeloma cells with 3-bromopyruvate, J. Bioenerg. Biomembr. 44 (2012) 31–38.
[121] C. Rodrigues-Ferreira, A.P. da Silva, A. Galina, Effect of the antitumoral alkylating agent 3-bromopyruvate on mitochondrial respiration: role of mitochondrially bound hexokinase, J. Bioenerg. Biomembr. 44 (2012) 39–49.
[122] Z. Chen, H. Zhang, W. Lu, P. Huang, Role of mitochondria-associated hexokinase II in cancer cell death induced by 3-bromopyruvate, Biochim. Biophys. Acta 1787 (2009) 553–560.
[123] Y.H. Ko, B.L. Smith, Y. Wang, M.G. Pomper, D.A. Rini, M.S. Torbenson, J. Hullihen, P.L. Pedersen, Advanced cancers: eradication in all cases using 3-bromopyruvate therapy to deplete ATP, Biochem. Biophys. Res. Commun. 324 (2004) 269–275.
[124] A.P. Pereira da Silva, T. El-Bacha, N. Kyaw, R.S. dos Santos, W.S. da-Silva, F.C. Almeida, A.T. Da Poian, A. Galina, Inhibition of energy-producing pathways of HepG2 cells by 3-bromopyruvate, Biochem. J. 417 (2009) 717–726.
[125] P.L. Pedersen, 3-Bromopyruvate (3BP) a fast acting, promising, powerful, specific, and effective "small molecule" anti-cancer agent taken from labside to bedside: introduction to a special issue, J. Bioenerg. Biomembr. 44 (2012) 1–6.
[126] Y.H. Ko, H.A. Verhoeven, M.J. Lee, D.J. Corbin, T.J. Vogl, P.L. Pedersen, A translational study "case report" on the small molecule "energy blocker" 3-bromopyruvate (3BP) as a potent anticancer agent: from bench side to bedside, J. Bioenerg. Biomembr. 44 (2012) 163–170.
[127] M. Gomez-Lazaro, M.F. Galindo, R.M. Melero-Fernandez de Mera, F.J. Fernandez-Gomez, C.G. Concannon, M.F. Segura, J.X. Comella, J.H. Prehn, J. Jordan, Reactive oxygen species and p38 mitogen-activated protein kinase activate Bax to induce mitochondrial cytochrome c release and apoptosis in response to malonate, Mol. Pharmacol. 71 (2007) 736–743.
[128] L.S. Huang, G. Sun, D. Cobessi, A.C. Wang, J.T. Shen, E.Y. Tung, V.E. Anderson, E.A. Berry, 3-Nitropropionic acid is a suicide inhibitor of mitochondrial respiration that, upon oxidation by complex II, forms a covalent adduct with a catalytic base arginine in the active site of the enzyme, J. Biol. Chem. 281 (2006) 5965–5972.
[129] P. Bonsi, D. Cuomo, G. Martella, G. Sciamanna, M. Tolu, P. Calabresi, G. Bernardi, A. Pisani, Mitochondrial toxins in basal ganglia disorders: from animal models to therapeutic strategies, Curr. Neuropharmacol. 4 (2006) 69–75.
[130] G. Liot, B. Bossy, S. Lubitz, Y. Kushnareva, N. Sejbuk, E. Bossy-Wetzel, Complex II inhibition by 3-NP causes mitochondrial fragmentation and neuronal cell death via an NMDA- and ROS-dependent pathway, Cell Death Differ. 16 (2009) 899–909.
[131] S. Takemori, T.E. King, Coenzyme Q: reversal of inhibition of succinate cytochrome c reductase by lipophilic compounds, Science 144 (1964) 852–853.
[132] R.R. Ramsay, B.A. Ackrell, C.J. Coles, T.P. Singer, G.A. White, G.D. Thorn, Reaction site of carboxanilides and of thenoyltrifluoroacetone in complex II, Proc. Natl. Acad. Sci. U. S. A. 78 (1981) 825–828.
[133] V.G. Grivennikova, A.D. Vinogradov, Kinetics of ubiquinone reduction by the resolved succinate: ubiquinone reductase, Biochim. Biophys. Acta 682 (1982) 491–495.
[134] A. Mehta, C. Shaha, Apoptotic death in *Leishmania donovani* promastigotes in response to respiratory chain inhibition: complex II inhibition results in increased pentamidine cytotoxicity, J. Biol. Chem. 279 (2004) 11798–11813.
[135] J.G. Zhang, M.A. Tirmenstein, F.A. Nicholls-Grzemski, M.W. Fariss, Mitochondrial electron transport inhibitors cause lipid peroxidation-dependent and -independent cell death: protective role of antioxidants, Arch. Biochem. Biophys. 393 (2001) 87–96.
[136] M.R. Owen, E. Doran, A.P. Halestrap, Evidence that metformin exerts its anti-diabetic effects through inhibition of complex 1 of the mitochondrial respiratory chain, Biochem. J. 348 (Pt 3) (2000) 607–614.
[137] S. Mudaliar, R.R. Henry, New oral therapies for type 2 diabetes mellitus: the glitazones or insulin sensitizers, Annu. Rev. Med. 52 (2001) 239–257.
[138] M. Soller, S. Drose, U. Brandt, B. Brune, A. von Knethen, Mechanism of thiazolidinedione-dependent cell death in Jurkat T cells, Mol. Pharmacol. 71 (2007) 1535–1544.
[139] J.C. Parker, Troglitazone: the discovery and development of a novel therapy for the treatment of Type 2 diabetes mellitus, Adv. Drug Deliv. Rev. 54 (2002) 1173–1197.
[140] D.J. Graham, L. Green, J.R. Senior, P. Nourjah, Troglitazone-induced liver failure: a case study, Am. J. Med. 114 (2003) 299–306.
[141] S. Omura, H. Tomoda, K. Kimura, D.Z. Zhen, H. Kumagai, K. Igarashi, N. Imamura, Y. Takahashi, Y. Tanaka, Y. Iwai, Atpenins, new antifungal antibiotics produced by *Penicillium* sp. Production, isolation, physico-chemical and biological properties, J. Antibiot. (Tokyo) 41 (1988) 1769–1773.
[142] K. Oshino, H. Kumagai, H. Tomoda, S. Omura, Mechanism of action of atpenin B on Raji cells, J. Antibiot. (Tokyo) 43 (1990) 1064–1068.
[143] H. Miyadera, K. Shiomi, H. Ui, Y. Yamaguchi, R. Masuma, H. Tomoda, H. Miyoshi, A. Osanai, K. Kita, S. Omura, Atpenins, potent and specific inhibitors of mitochondrial complex II (succinate–ubiquinone oxidoreductase), Proc. Natl. Acad. Sci. U. S. A. 100 (2003) 473–477.
[144] R. Horsefield, V. Yankovskaya, G. Sexton, W. Whittingham, K. Shiomi, S. Omura, B. Byrne, G. Cecchini, S. Iwata, Structural and computational analysis of the quinone-binding site of complex II (succinate–ubiquinone oxidoreductase): a mechanism of electron transfer and proton conduction during ubiquinone reduction, J. Biol. Chem. 281 (2006) 7309–7316.
[145] M. Kawada, I. Momose, T. Someno, G. Tsujiuchi, D. Ikeda, New atpenins, NBRI23477 A and B, inhibit the growth of human prostate cancer cells, J. Antibiot. (Tokyo) 62 (2009) 243–246.
[146] M. Kawada, H. Inoue, S. Ohba, T. Masuda, I. Momose, D. Ikeda, Leucinostatin A inhibits prostate cancer growth through reduction of insulin-like growth factor-I expression in prostate stromal cells, Int. J. Cancer 126 (2010) 810–818.
[147] A.P. Wojtovich, P.S. Brookes, The complex II inhibitor atpenin A5 protects against cardiac ischemia–reperfusion injury via activation of mitochondrial KATP channels, Basic Res. Cardiol. 104 (2009) 121–129.
[148] S. Drose, L. Bleier, U. Brandt, A common mechanism links differently acting complex II inhibitors to cardioprotection: modulation of mitochondrial reactive oxygen species production, Mol. Pharmacol. 79 (2011) 814–822.
[149] S.J. Ralph, R. Moreno-Sanchez, J. Neuzil, S. Rodriguez-Enriquez, Inhibitors of succinate: quinone reductase/complex II regulate production of mitochondrial reactive oxygen species and protect normal cells from ischemic damage but induce specific cancer cell death, Pharm. Res. 28 (2011) 2695–2730.
[150] T.P. Selby, K.A. Hughes, J.J. Rauh, W.S. Hanna, Synthetic atpenin analogs: potent mitochondrial inhibitors of mammalian and fungal succinate–ubiquinone oxidoreductase, Bioorg. Med. Chem. Lett. 20 (2010) 1665–1668.
[151] M. Ohtawa, K. Sugiyama, T. Hiura, S. Izawa, K. Shiomi, S. Omura, T. Nagamitsu, Stereoselective total synthesis of atpenins a4 and b, harzianopyridone, and NBRI23477 B, Chem. Pharm. Bull. (Tokyo) 60 (2012) 898–906.
[152] C. Sakai, E. Tomitsuka, H. Esumi, S. Harada, K. Kita, Mitochondrial fumarate reductase as a target of chemotherapy: from parasites to cancer cells, Biochim. Biophys. Acta 1820 (2012) 643–651.
[153] F. Schiavi, C.C. Boedeker, B. Bausch, M. Peczkowska, C.F. Gomez, T. Strassburg, C. Pawlu, M. Buchta, M. Salzmann, M.M. Hoffmann, A. Berlis, I. Brink, M. Cybulla, M. Muresan, M.A. Walter, F. Forrer, M. Valimaki, A. Kawecki, Z.

Szutkowski, J. Schipper, M.K. Walz, P. Pigny, C. Bauters, J.E. Willet-Brozick, B.E. Baysal, A. Januszewicz, C. Eng, G. Opocher, H.P. Neumann, Predictors and prevalence of paraganglioma syndrome associated with mutations of the SDHC gene, JAMA 294 (2005) 2057–2063.
[154] M. Peczkowska, A. Cascon, A. Prejbisz, A. Kubaszek, B.J. Cwikla, M. Furmanek, Z. Erlic, C. Eng, A. Januszewicz, H.P. Neumann, Extra-adrenal and adrenal pheochromocytomas associated with a germline SDHC mutation, Nat. Clin. Pract. Endocrinol. Metab. 4 (2008) 111–115.
[155] Y. Ni, K.M. Zbuk, T. Sadler, A. Patocs, G. Lobo, E. Edelman, P. Platzer, M.S. Orloff, K.A. Waite, C. Eng, Germline mutations and variants in the succinate dehydrogenase genes in Cowden and Cowden-like syndromes, Am. J. Hum. Genet. 83 (2008) 261–268.

ANTIOXIDANTS & REDOX SIGNALING
Volume 00, Number 00, 2015

DOI: 10.1089/ars.2013.5594

ORIGINAL RESEARCH COMMUNICATION

Mitochondrially Targeted Vitamin E Succinate Modulates Expression of Mitochondrial DNA Transcripts and Mitochondrial Biogenesis

Jaroslav Truksa,[1,*] Lan-Feng Dong,[2,*] Jakub Rohlena,[1,*] Jan Stursa,[2,3,*] Magdalena Vondrusova,[1] Jacob Goodwin,[2] Maria Nguyen,[2] Katarina Kluckova,[1] Zuzana Rychtarcikova,[1] Sandra Lettlova,[1] Jana Spacilova,[1,#] Michael Stapelberg,[2] Mario Zoratti,[4] and Jiri Neuzil[1,2]

Abstract

Aims: To assess the effect of mitochondrially targeted vitamin E (VE) analogs on mitochondrial function and biogenesis. ***Results:*** Mitochondrially targeted vitamin E succinate (MitoVES) is an efficient inducer of apoptosis in cancer cells. Here, we show that unlike its untargeted counterpart α-tocopheryl succinate, MitoVES suppresses proliferation of cancer cells at sub-apoptotic doses by way of affecting the mitochondrial DNA (mtDNA) transcripts. We found that MitoVES strongly suppresses the level of the displacement loop transcript followed by those of mtDNA genes coding for subunits of mitochondrial complexes. This process is coupled to the inhibition of mitochondrial respiration, dissipation of the mitochondrial membrane potential, and generation of reactive oxygen species. In addition, exposure of cancer cells to MitoVES led to decreased expression of TFAM and diminished mitochondrial biogenesis. The inhibition of mitochondrial transcription was replicated *in vivo* in a mouse model of $HER2^{high}$ breast cancer, where MitoVES lowered the level of mtDNA transcripts in cancer cells but not in normal tissue. ***Innovation:*** Our data show that mitochondrially targeted VE analogs represent a novel class of mitocans that not only induce apoptosis at higher concentrations but also block proliferation and suppress normal mitochondrial function and transcription at low, non-apoptogenic doses. ***Conclusions:*** Our data indicate a novel, selective anti-cancer activity of compounds that act by targeting mitochondria of cancer cells, inducing significant alterations in mitochondrial function associated with transcription of mtDNA-coded genes. These changes subsequently result in the arrest of cell proliferation. *Antioxid. Redox Signal.* 00, 000–000.

Introduction

MITOCHONDRIA ARE ORGANELLES essential for maintaining the life of a cell as well as instrumental for its death (58). Recent research indicates that mitochondria are intriguing targets for a variety of anti-cancer drugs (17, 20, 25, 33, 42, 50, 54, 63) that have been termed "mitocans" (42, 44, 54). A prime example is the redox-silent analog of vitamin E (VE), α-tocopheryl succinate (α-TOS) that acts by affecting the mitochondrial complex II (CII) (11, 15). Modification of the apoptogenic VE analogs by addition of the mitochondria-targeting triphenylphosphonium (TPP^+) cationic group (41) substantially enhances the apoptogenic activity of the parental compound that translates into higher anti-cancer efficacy (13, 14), corroborating the premise of mitochondria as central purveyors of anti-cancer activity of mitocans (20).

Besidess the nucleus, mitochondria are the only organelles with their own DNA in animal cells. Mitochondrial DNA

[1]Molecular Therapy Group, Institute of Biotechnology, Academy of Sciences of the Czech Republic, Prague, Czech Republic.
[2]Apoptosis Research Group, School of Medical Science and the Griffith Institute of Health, Griffith University, Southport, Australia.
[3]Department of Chemistry of Natural Compounds, Institute of Chemical Technology, Prague, Czech Republic.
[4]CNR Institute of Neuroscience and Department of Biomedical Sciences, University of Padova, Padova, Italy.
*These four authors contributed equally to the work.
#*Current affiliation:* Department of Pediatrics and Adolescent Medicine, Charles University, Prague, Czech Republic.

Innovation

This study presents novel findings revealing that mitochondrially targeted vitamin E analogs, besides inducing apoptosis, also inhibit mitochondrial transcription and biogenesis at sub-apoptotic concentrations, resulting in the inhibition of proliferation of cancer cells. This newly described activity lowers the effective concentration needed to arrest tumor growth and achieve a therapeutic effect, and it increases the promise of these compounds for further development as cancer therapeutics.

(mtDNA) consists of densely packed genes in two strands coding for 13 proteins that are subunits of complexes of the mitochondrial electron transport chain (ETC), 22 tRNAs, two rRNA, and the so-called displacement loop (*D-LOOP*) (3). Disruption of the mitochondrial replication/transcription machinery often results in mitochondrial malfunction with ensuing energetic insufficiency causing aging or apoptosis induction (66). Several agents have been shown to modulate the replication or transcription or mtDNA. For example, vitamin K3 (menadione) targets mtDNA by inhibiting the mtDNA-specific DNA polymerase γ (POLG), followed by apoptosis induction (56). Similar effects were reported for fialuridine, leading to mitochondrial structural defects (34). The Parkinsonian toxin 1-methyl-4-phenylpyridinium causes reduction of the copy number of mtDNA by destabilization of the structure of mitochondrial *D-LOOP* (39, 64).

Here, we studied the effect of mitochondrially targeted VE succinate (MitoVES) on the level of transcription of individual mtDNA-encoded genes and found that it substantially suppresses the level of the *D-LOOP* transcript followed by other mtDNA genes at sub-apoptotic levels, which results in the suppression of mitochondrial biogenesis and inhibition of proliferation of cancer cells both *in vitro* and *in vivo*, in a cancer-specific manner. Our data point to a novel, selective activity of MitoVES, and suggest that this agent can exert anti-cancer activity in an apoptosis-independent way, circumventing the complications associated with frequent mutations of apoptosis-related genes.

Results

MitoVES suppresses the level of mtDNA transcripts and proliferation in cancer cells

Exposure of Jurkat cells to MitoVES (compound **5**, referred to as MitoVE11S in Supplementary Fig. S1; Supplementary Data are available online at www.liebertpub.com/ars) at 5 μM for short periods resulted in profound suppression of the level of the *D-LOOP* transcript (Fig. 1A), while longer exposure (18 h) of MCF7 cells to MitoVE11S suppressed the level of transcripts of all mtDNA genes with the *D-LOOP* transcript affected the most (Fig. 1B). We observed a similar effect in mouse breast cancer NeuTL cells (26), human colorectal SW620 and RKO cells, and non-small cell lung cancer H1299 cells. Interestingly, no effect was detected either in breast tissue-derived MCF10A cells representing a non-malignant counterpart of MCF7 cells or in the foreskin fibroblasts BJ (Fig 1C and Supplementary Fig. S2). MitoVE11S suppressed mtDNA transcripts in proliferating endothelial cells (ECs) but not in their arrested counterparts (Table 1 and Supplementary Fig. S2), which is consistent with the previously described selective killing of proliferating ECs by MitoVE11S (53). The inhibitory effect on the *D-LOOP* transcript was independent of apoptosis induction, since it occurred at times before the onset of apoptosis and at MitoVE11S levels lower than those needed to promote cell death in cancer cells of breast, leukemic, and prostate origin (Fig. 1D–F and Supplementary Fig. S3C–F) or in proliferating ECs (Supplementary Fig. S3A). In addition, longer incubation of cancer cells (48 h) with low doses of MitoVE11S resulted in a strong inhibition of proliferation at concentrations as low as 0.25 μM, while we do see significant apoptosis (>10%) only at concentrations above 1 μM (Supplementary Fig. S3D, F).

Notably, we found that mitochondrial targeting *via* attaching the TPP^+ group is instrumental for the propensity of the agent to suppress mtDNA transcripts, since α-TOS was much less efficient even at apoptogenic doses (Fig. 1E). This can be reconciled with the cellular distribution of the agents, with virtually exclusive mitochondrial localization of MitoVE11S while α-TOS presents a highly diffuse staining due to its indiscriminate association with lipidic (sub-) cellular structures (Fig. 1G).

The ability of VE analogs to suppress mtDNA transcripts depends on their structure

We next tested whether different TPP^+-tagged agents affect the level of mtDNA transcripts. Figure 2 documents a very small effect of MitoVE7S (the 7-C homolog of MitoVE11S; **4**), and VES4TPP (a compound derived from α-TOS with the TPP^+ group attached to the succinyl moiety; **6**). No effect was observed for MitoVE5S (**3**). A strong effect was found for undecyl-TPP (mitochondrially targeted undecyl [MitoC11]; **8**), while heptyl-TPP (mitochondrially targeted heptyl [MitoC7]; **7**) was rather inefficient. The succinylated analogs MitoC7S (**9**) and MitoC11S (**10**) exerted virtually no effect. The polyphenolic compounds tagged with TPP^+ *via* a 4-C spacer, quercetin-7-butylTPP (mitochondrially targeted quercetin-7-butyl [MitoQ7B]; **11**) and resveratrol-3-BTPP (mitochondrially targeted resveratrol-7-butyl [MitoR3B]; **12**) (7, 38) increased the level of the *D-LOOP* transcript. These data show that the presence of TPP^+ alone does not suffice for the suppressive effect on mtDNA transcripts.

MitoVE11S alters mitochondrial morphology, mitochondrial membrane potential, and reactive oxygen species levels leading to the suppression of mtDNA transcripts

MCF7 cells stably transfected with mitochondria-targeted green fluorescent protein (GFP) were used for testing the effect of MitoVE11S on mitochondrial morphology and potential ($\Delta\Psi_m$). Exposure of the cells to 5 μM MitoVE11S caused mitochondrial rounding in < 15 min accompanied by the loss of red tetramethylrhodamine (TMRM) fluorescence, indicating early $\Delta\Psi_m$ dissipation (Fig. 3A). No morphological signs of apoptosis were discernible for at least 2.5 h of the treatment (shown are the first 90 min), indicating an apoptosis-independent process. A similar and earlier effect was observed for MitoC11 (Fig. 3B).

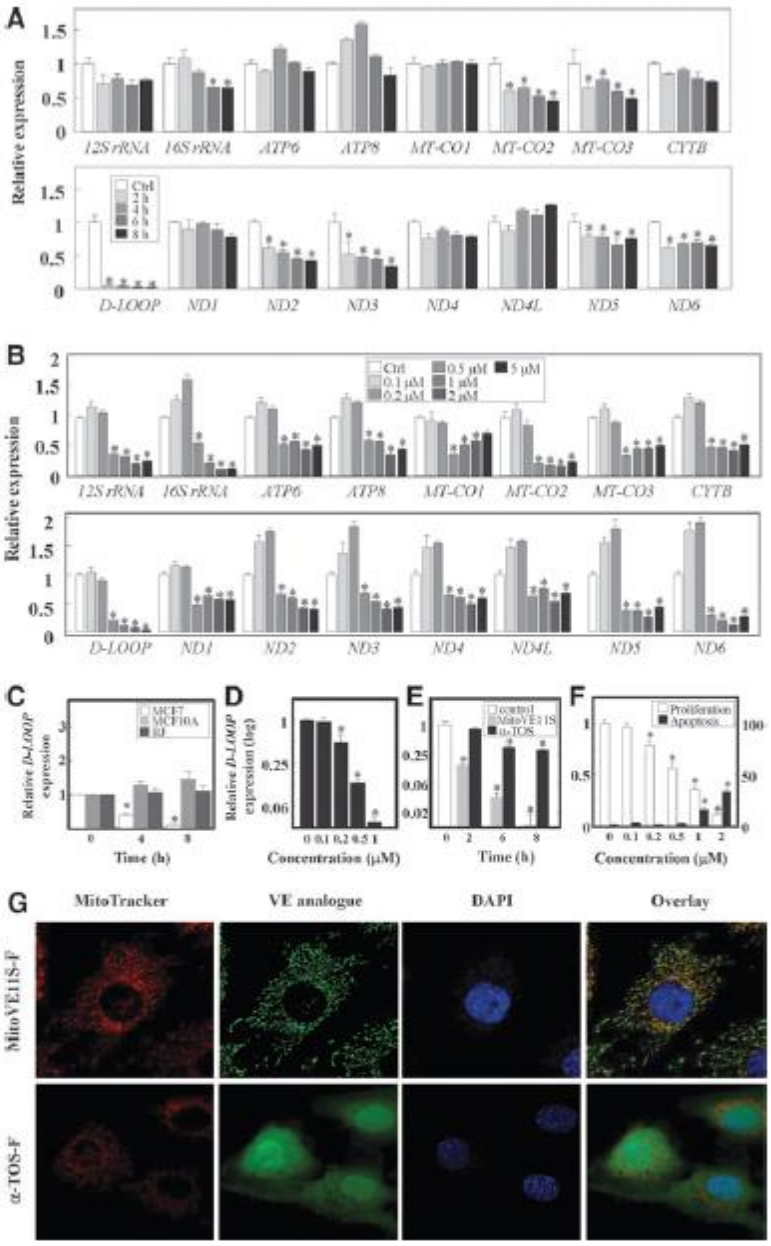

FIG. 1. MitoVE11S suppresses mitochondrial transcripts due to TPP^+ tagging at sub-apoptotic doses and localizes to mitochondria. **(A)** Jurkat cells were treated with 5 μM MitoVE11S for the times shown, and **(B)** MCF7 cells were treated with MitoVE11S at the concentrations shown for 18 h. Individual mitochondrial transcripts were analyzed by qPCR. **(C)** Indicated malignant and non-malignant cell lines were incubated with 1 μM MitoVE11S for 4 and 8 h, and the *D-LOOP* transcript levels were determined by qPCR. **(D)** Jurkat cells were exposed to MitoVE11S at the concentrations shown for 24 h and assessed for the level of the *D-LOOP* transcript using qPCR. **(E)** Documents the effect of 5 μM MitoVE11S and 50 μM α-TOS on the *D-LOOP* transcript at the times shown, and **(F)** shows Jurkat cells assayed for proliferation *via* the MTT assay and apoptosis using the annexin V method. **(G)** NeuTL cells were exposed to 5 μM MitoVE11S-F or α-TOS for 30 min (green fluorescence), incubated with MitoTracker Red and 4′,6-diamidino-2-phenylindole (blue fluorescence), and inspected by confocal microscopy. The data are mean values ± SD ($n = 3$), the symbol "*" indicates significantly different data compared with the controls with $p < 0.05$. The images are representative of three biological replicates. D-LOOP, displacement loop; MitoVES, mitochondrially targeted vitamin E succinate; qPCR, quantitative polymerase chain reaction; TPP^+, triphenylphosphonium; α-TOS, α-tocopheryl succinate. To see this illustration in color, the reader is referred to the web version of this article at www.liebertpub.com/ars

We compared the relative efficacy of α-TOS, mitochondrially targeted compounds, and mitochondrial respiration inhibitors antimycin A and rotenone to dissipate $\Delta\Psi_m$ and cause reactive oxygen species (ROS) generation. Figure 4 reveals that MitoVE11S caused a sharp loss of $\Delta\Psi_m$ and high ROS formation within 1 h. It further shows different kinetics of $\Delta\Psi_m$ dissipation in response to individual TPP^+-tagged agents, documenting that MitoC11 is very efficient in $\Delta\Psi_m$ dissipation, followed by MitoVE11S, MitoC7, and MitoVE7S. α-TOS was inefficient as were rotenone and antimycin A. Using fluorescently labeled MitoVE11S (structure **15** in Supplementary Fig. S1), accumulation of the compound in the mitochondria was documented to inversely correlate with $\Delta\Psi_m$ loss (Fig. 5). The ability of MitoVE11S and the other agents to disrupt $\Delta\Psi_m$ correlates with their ability to cause ROS generation. The most potent inducer of ROS was MitoVE11S, followed by MitoC11 and MitoVE7S. Rotenone and antimycin A generated some ROS while α-TOS, MitoC7, and MitoQ7B generated almost no ROS. Notably, rotenone and antimycin A suppressed the *D-LOOP* transcript (Supplementary Fig. S3B). Collectively, these data indicate an important role of $\Delta\Psi_{mi}$ and mitochondrial ROS generation

Table 1. Effect of Mitochondrially Targeted Vitamin E Succinate on Mitochondrial DNA Genes of Proliferating and Confluent Endothelial Cells

	Proliferating cells[a]			*Confluent cells*		
Transcript	*0 h*	*4 h*	*8 h*	*0 h*	*4 h*	*8 h*
D-LOOP	1±0.13	**0.42±0.08**	**0.43±0.09**	1±0.24	**1.6±0.03**	**3.8±0.43**
12S	1±0.19	**0.56±0.06**	**0.38±0.04**	1±0.23	0.97±0.12	0.99±0.38
ND1	1±0.21	**0.46±0.03**	**0.31±0.13**	1±0.07	0.96±0.11	1.08±0.12
MT-CO3	1±0.16	**0.41±0.04**	**0.43±0.06**	1±0.12	0.81±0.02	1.17±0.08
CYTB	1±0.28	**0.43±0.03**	**0.38±0.05**	1±0.37	1.19±0.32	0.89±0.14
ATP6	1±0.26	**0.38±0.05**	**0.36±0.03**	1±0.21	0.95±0.05	1.24±0.36

EAhy926 cells at 50%[a] or 100% confluency were exposed to 1 μM MitoVES for 4 or 8 h and assessed for the level of mitochondrial DNA transcripts using quantitative polymerase chain reaction. Data are shown as mean values ± standard deviation ($n=3$).
Bold face indicates significantly different results between transcript in control and treated endothelial cells ($p<0.05$).
MitoVES, mitochondrially targeted vitamin E succinate.

for the inhibitory effect of mitochondrially targeted compounds on the level of mtDNA transcripts.

To see whether the different effects of the various MitoVES-related compounds on the *D-LOOP* transcript are linked to their efficacy to associate with mitochondria, we inspected cells incubated with fluorescently labeled MitoVE11S, MitoVE7S, MitoC11S, and MitoC7S by confocal microscopy. Supplementary Figure S4A reveals similar mitochondrial localization, which was reduced on dissipation of $\Delta\Psi_m$.

Reduction in mitochondrial ROS levels alleviates the inhibition of the D-LOOP transcript elicited by MitoVE11S

We next evaluated the effect of hydrogen peroxide and the antioxidant *N*-acetyl cysteine (NAC) on the *D-LOOP* transcript. Hydrogen peroxide suppressed the transcript level, while NAC did not prevent the inhibitory effect of either MitoVE11S or exogenous hydrogen peroxide (Fig. 6A). This suggests that ROS within mitochondria may regulate the *D-LOOP* transcript level and NAC cannot penetrate into mitochondria, as it failed to prevent ROS generation induced by MitoVE11S (Fig. 6B). Pre-treatment of Jurkat cells with PEG-SOD/CAT diminished the production of ROS (preferably superoxide, as it was measured with dihydroethidium [DHE]) in response to MitoVE11S, and this led to the protection of the *D-LOOP* transcript (Fig. 6C–E). This finding was further corroborated by pre-treatment with MitoQ7B (2 μM), which led to a decrease in ROS production elicited by MitoVE11S and resulted in the prevention of the *D-LOOP* transcript (Fig. 6F, G). This reflects the double nature of the flavonoid, which can act as a pro-oxidant, an ROS-generating compound, or as a scavenger of radicals. Similarly, MitoR3B protected the *D-LOOP* transcript, but this compound alone caused an increase in the *D-LOOP* level (Fig. 6F, G). Mitochondrial ROS thus appear important for the *D-LOOP* transcript suppression, and untargeted antioxidants such as NAC are not protective.

Regulation of mtDNA transcripts by MitoVE11S is linked to its effect on respiration in an ATP-independent manner

The earlier data show that agents efficiently suppressing mtDNA transcripts (Fig. 2) cause fast dissipation of $\Delta\Psi_m$ and induce ROS generation (Fig. 4). We next tested the effect of the agents on mitochondrial respiration of MCF7 cells. Figure 7 documents that MitoVE11S caused a transient increase in respiration, probably due to initial uncoupling (51), while its inhibition occurred at doses >2.5 μM. MitoVE7S caused a profound inhibition of respiration but did not promote uncoupling. MitoC11, while not initially enhancing respiration, caused a very rapid inhibition of respiration at 0.5 μM, similar to rotenone and antimycin. MitoC7 exerted milder inhibition of respiration but was more potent than MitoVE7S. MitoQ7B did not affect respiration at all, while the effect of α-TOS was very mild. Together with the earlier results (Fig. 4), these findings indicate that agents that block mitochondrial respiration and generate ROS alone (antimycin A, rotenone) or together with the dissipation of $\Delta\Psi_m$ (MitoVE11S, MitoC11) are efficient in lowering mtDNA transcripts, in particular the *D-LOOP* transcript.

Since mitochondrial respiration is essential for ATP synthesis, we tested the possibility that MitoVE11S suppresses mtDNA transcripts by regulating ATP levels. Exposure of MCF7 cells to the agent in glucose-containing medium showed an initial mild ATP reduction, which reverted to normal levels. MitoVE11S caused a drop in ATP when the cells were grown in galactose-containing medium (Supplementary Fig. S3C). Suppression of the *D-LOOP* transcript was similar under both conditions (Supplementary Fig. S3D), ruling out a direct role for ATP in mtDNA transcript suppression.

MitoVE11S suppresses TFAM and inhibits mitochondrial biogenesis and replication

To elucidate the molecular mechanism leading to the inhibition of mtDNA transcripts, we evaluated the expression levels of components of the mitochondrial transcriptional/replication machinery. TFAM, a mitochondrial transcription factor (mTF) responsible for RNA polymerase as well as POLG binding to mtDNA, was significantly suppressed by MitoVE11S on the mRNA as well as protein level (Fig. 8A, G). No effect was observed on the POLG itself, and the mRNA levels of mTFs coded by *TFB1M* and *TFB2M* were also largely unaffected (Fig. 8G). On the other hand, mitochondrial topoisomerase *TOP1MT* was reduced (Fig. 8A). These data suggest that MitoVE11S lowers the amount of the functional mtDNA transcriptional/replication complex

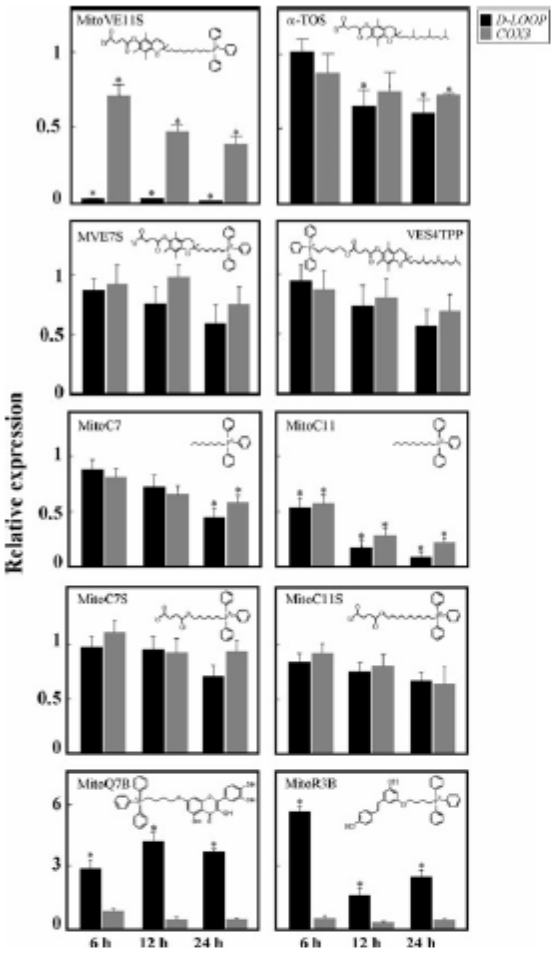

FIG. 2. The structure of VE analogs is important for their effect on mtDNA transcripts. MCF7 cells were exposed to mitochondrially targeted agents at 5 μM or α-TOS at 50 μM for the times shown and assessed for the level of the *D-LOOP* and *COX3* transcripts by qPCR. The name and structure of the individual compound are shown in each *panel*. The data are mean values ± SD ($n = 3$), and the symbol "*" indicates significantly different data compared with the controls with $p < 0.05$. mtDNA, mitochondrial DNA; VE, vitamin E.

through the reduction of TFAM, but does not affect total levels of mitochondrial POLG.

The important role of TFAM in D-LOOP suppression is supported by the observation that antimycin A, rotenone, and hydrogen peroxide, agents that reduced D-LOOP transcript similarly to MitoVES, also reduced TFAM protein levels to a similar extent. Furthermore, silencing of TFAM expression by siRNA compromised mitochondrial transcription and the D-LOOP transcript in particular, photocopying the effects of MitoVES (Fig. 8I). It thus appears that the downregulation of TFAM is the driving force behind the effects on mitochondrial transcription observed for MitoVES and the other agents.

In line with its effect on TFAM, MitoVES treatment lowered the mtDNA/nuclear DNA (nDNA) ratio by ~20% in MCF7 cells (Fig. 8B), and we also detected a decrease in the mitochondrially coded cytochrome *c* oxidase 1 protein (COX1, encoded by the *MT-CO1* gene) by in cell enzyme-linked immunosorbent assay. This was similar for the inhibitor of mitochondrial biogenesis chloramphenicol, and differed for α-TOS, which had no effect on COX1. MitoVES, in addition, also reduced the protein levels of SDHA, while α-TOS and chloramphenicol had no effect on this protein. (Fig. 8E, F). This suggests that the MitoVES agent also regulates the level of nuclear-encoded proteins imported into mitochondria. These data were confirmed by Western blot analysis (Fig. 8D).

Important regulators of mitochondrial biogenesis, nuclear gene transcription, and antioxidant response genes were further studied. PGC1α/β encoded by *PPARGA1A* and *PPARGA1B* were down-regulated by MitoVE11S, while the expression of *NRF1* or *PRC1* was not changed and an antioxidant response gene *NFE2L2*, also known as *NRF2*, was up-regulated (Fig. 8C). On the protein level, the PGC1-β protein was up-regulated by MitoVE11S, while protein levels of other important mitochondrial regulators such as C-myc were not changed (Fig. 8D). This suggests that MitoVE11S is able to suppress mitochondrial biogenesis and the SDHA and COX1 proteins despite activation of PGC1-α/β.

The effect of MitoVE11S on mtDNA transcripts requires functional CII

MitoVE11S induces apoptosis *via* the proximal ubiquinone (UbQ)-binding site (Q_P) of CII (13, 14). To resolve whether it is needed for the effect of MitoVE11S on mtDNA transcripts, we utilized the H-Ras-transformed CII-dysfunctional B9 cells and their counterparts with restored CII activity ($B9_{wt}$ cells), and B9 cells transfected with SDHC with the S69A mutation in the Q_p site ($B9_{S68A}$ cells) (13, 62). Exposure of $B9_{wt}$ cells to MitoVE11S resulted in the decrease in mtDNA transcripts, while B9 cells and $B9_{S8A}$ cells were not affected. All sub-lines were susceptible to MitoC11, indicating its indiscriminate effect, while MitoC11S was inefficient (Fig. 9A). Dysfunctional CII is documented by native blue electrophoresis (NBE), revealing no assembly of the full CII for B9 cells; while in $B9_{wt}$ and $B9_{S68A}$, CII is assembled, although only $B9_{wt}$ cells exert high succinate quinone reductase (SQR) activity of CII (Fig. 9B).

All three sub-lines showed similar $\Delta\Psi_m$ (Fig. 9C) as well as relatively comparable mitochondrial accumulation of MitoVE11S (Fig. 9D). We next tested whether MitoVE11S and MitoC11 cause generation of ROS and dissipation $\Delta\Psi_m$ in the B9 sub-lines. Figure 9E documents that MitoVE11S was efficient in ROS generation only in $B9_{wt}$ cells, while MitoC11 was indiscriminate. Similar results were found for the effect of the two agents on $\Delta\Psi_m$ (Supplementary Fig. S4B, C). Collectively, these results corroborate the premise that functional CII is important for the activity of MitoVE11S to suppress mtDNA transcripts.

MitoVE11S suppresses mtDNA transcripts in vivo in a selective manner

MitoVE11S suppresses mtDNA transcripts in tumors in the transgenic FVB/N c-*neu* mice with spontaneous $HER2^{high}$

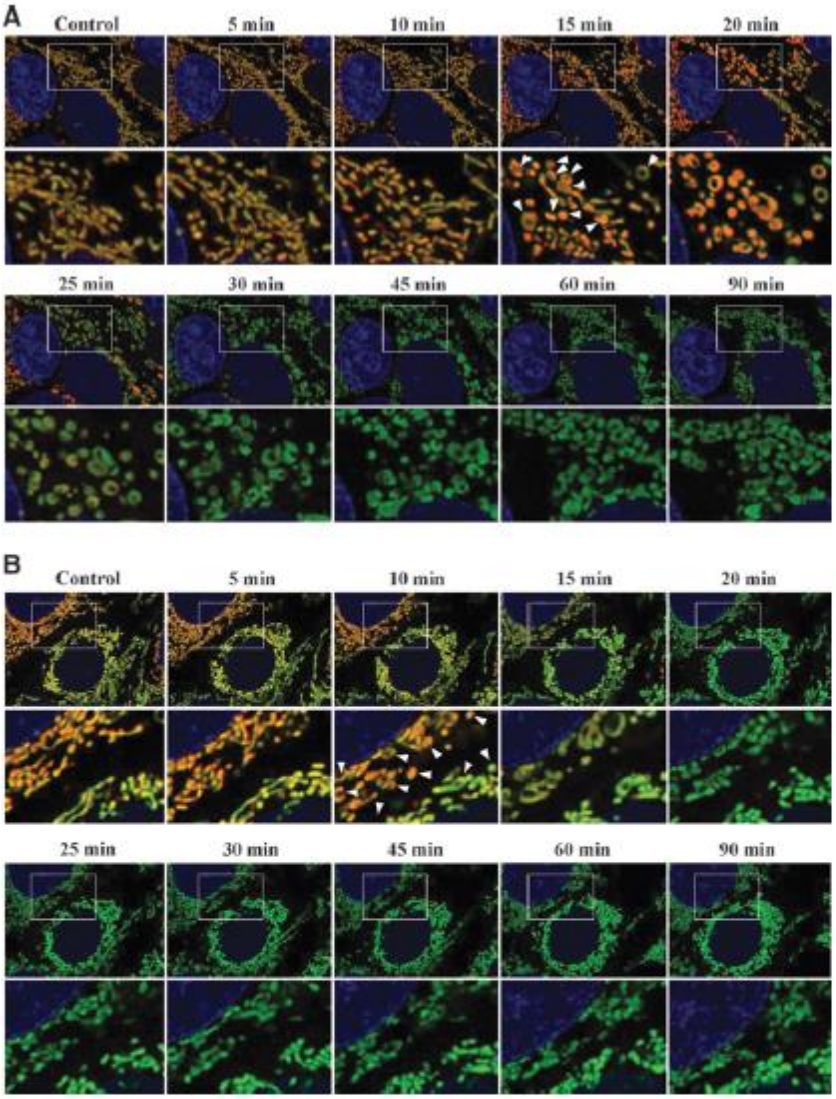

FIG. 3. MitoVE11S and MitoC11 alter mitochondrial morphology and suppress $\Delta\Psi_m$. (**A**) MCF7 cells stably transfected with mitochondrially targeted GFP and preloaded with TMRM were exposed to 5 μM MitoVES or (**B**) MitoC11 for the times indicated. The nuclei were counterstained with Hoechst33342. Time-lapse confocal microscopy was used to obtain detailed images of mitochondrial morphology. The *white arrow heads* indicate mitochondria with altered morphology. The images are representative of three biological replicates. GFP, green fluorescent protein; MitoC11, mitochondrially targeted undecyl; TMRM, tetramethylrhodamine. To see this illustration in color, the reader is referred to the web version of this article at www.liebertpub.com/ars

breast carcinomas (26). The effect of MitoVE11S on mtDNA transcripts was selective for tumor tissues, since we observed no discernible effect in the liver and kidney (Fig. 10A). We did not observe any change in the level of mtDNA transcripts when the mice were treated with α-TOS (**1**) or α-tocopheryl acetic acid ether (α-TEA; **2**) (Fig. 10B), even though these two non-targeted agents were applied at doses 10-fold higher than those of MitoVE11S that suppress tumors in *c-neu* mice (Fig. 10C). The effect of MitoVE11S on mtDNA genes of tumors was accompanied by suppression of tumor vascularization (Fig. 10D). Inspection of tumor sections by immunostaining documented a profound effect of MitoVE11S on proliferation of tumor cells in the transgenic animals. We also observed a lower level of expression of CD31 in the treated tumors. These effects were not observed in the liver tissue (Supplementary Fig. S5A). Fluorescently tagged MitoVE11S (MitoVE11S-F; **15**) was used to document the selectivity of the uptake of the VE analog by tumor cells, as revealed by confocal microscopy (Supplementary Fig. S5B). These data indicate that MitoVE11S selectively targets tumor tissue *in vivo*.

Discussion

In this communication, we present evidence that the mitochondrially targeted VE analog MitoVE11S, unlike its untargeted counterpart α-TOS that does not accumulate in mitochondria, possesses additional anti-cancer activity that is independent of its ability to induce apoptosis, the mechanism of which we have previously characterized (11, 13–16, 43, 45, 46). This novel activity decreases the level of mtDNA transcripts, in particular the *D-LOOP* transcript, *via* reduction

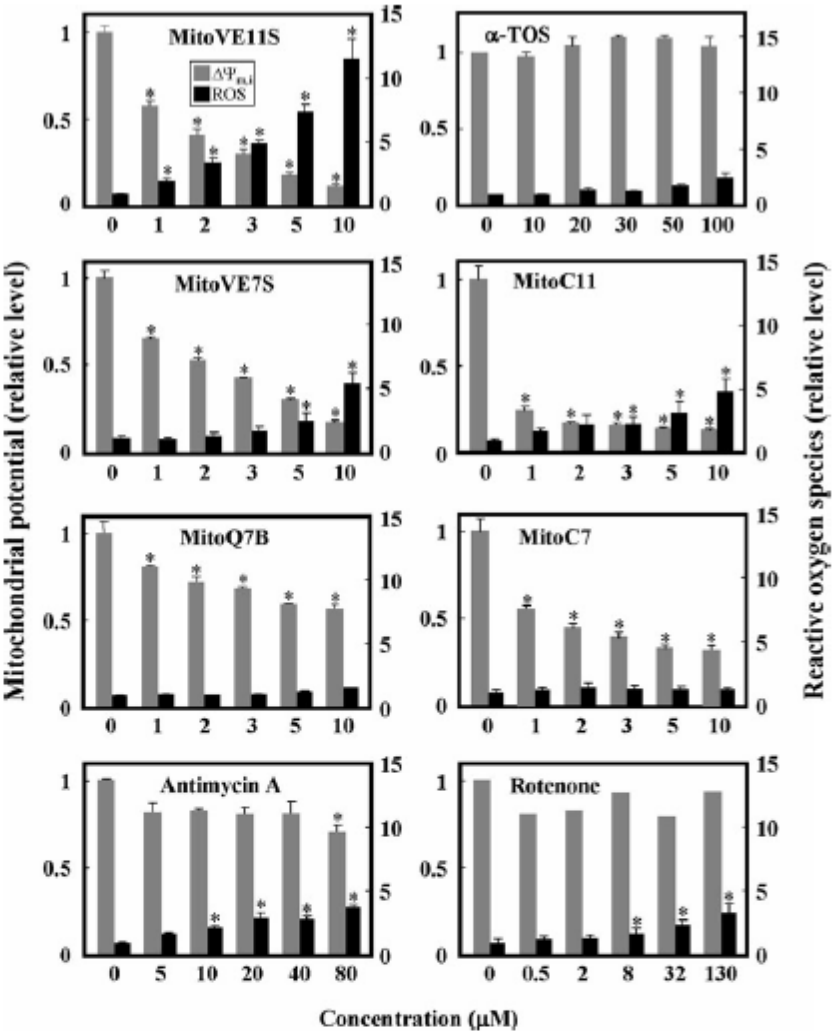

FIG. 4. VE analogs and mitochondrial poisons cause dissipation of $\Delta\Psi_m$ and generation of ROS. MCF7 cells were treated with the agents as stated in individual *panels* at the indicated concentrations for 1 h and assessed for the dissipation of $\Delta\Psi_m$ and generation of ROS using TMRM and DCF-DA, respectively, and flow cytometry. The data are mean values ± SD ($n = 3$), and the symbol "*" indicates significantly different data compared with the controls with $p < 0.05$. DCF, 2′,7′-dichlorodihydrofluorescein diacetate; ROS, reactive oxygen species.

of TFAM levels, leading to the arrest in cell proliferation. We observed this phenomenon in many malignant cells (Fig. 1C, D and Supplementary Fig. S3C–F) as well as proliferating ECs (Supplementary Fig. S3A), while there was no effect in non-malignant MCF10A and BJ cells (Fig. 1C and Supplementary Fig. S2). We also provide confirmation of this activity of MitoVES in an *in vivo* model of HER2^{high} breast carcinoma, the FVB/N202 *c-neu* mice (Fig. 10). This novel activity of MitoVE11S appears to be the dominant mode of action at concentrations that are sub-apoptotic and do not yet lead to cell death. It thus seems that depending on the available MitoVE11S concentration, the cell will either commit apoptosis if concentration is high enough or suppress proliferation if concentration does not exceed a certain threshold.

The effect of MitoVE11S on cell proliferation and mitochondrial transcription/biogenesis is an intrinsic component of its anti-cancer activity and appears to be governed by similar mechanistic principals as apoptosis induction. This is supported by the observation that cells resistant to apoptosis induction by MitoVE11S, such as B9 cells lacking CII (48) or possessing CII with mutations in the SDHC subunit (Fig. 9) as well as arrested ECs (Table 1), do not reduce mitochondrial transcription and the *D-LOOP* transcript level on MitoVE11S treatment either, irrespective of the underlying molecular reasons for insensitivity to MitoVE11S. These reasons differ in both situations. Whereas B9 cells do not possess a functional CII, the molecular target of MitoVE11S in mitochondria (11, 13–15) leading to a defect in ROS production in these cells on MitoVE11S treatment, mitochondria in arrested ECs may take up MitoVE11S less efficiently due to their lower $\Delta\Psi_m$ (16, 53). In addition, the shorter-chain MitoVE11S homologs MitoVE7S and MitoVE5S, as well as VES4TPP, that are less efficient apoptosis inducers owing to the shorter aliphatic chain, making them unlikely to reach the CII's UbQ binding site, also less efficiently reduced *D-LOOP* (Fig. 2). This underscores similarities in the regulation of mitochondrial transcription and

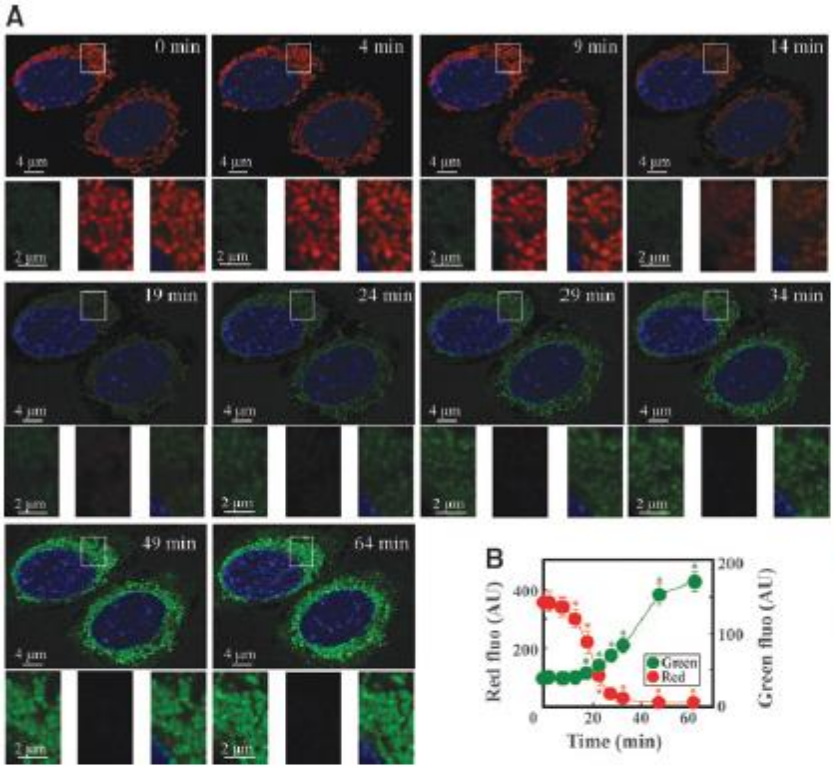

FIG. 5. Dissipation of $\Delta\Psi_m$ correlates with MitoVE11S uptake. (**A**) MCF7 cells were pre-loaded with TMRM and exposed to 4 μM MitoVE11S plus 1.4 μM MitoVES-F, and observed for the level of green fluorescence (MitoVES-F) and red fluorescence (TMRM) by time-lapse confocal microscopy. (**B**) Temporal changes in red and green fluorescence were derived by quantifying the green and red colour in 14 individual cells. The data are mean values ± SEM ($n = 14$), and the symbol "*" indicates significantly different data compared with the controls with $p < 0.05$. The images are representative of three biological replicates. To see this illustration in color, the reader is referred to the web version of this article at www.liebertpub.com/ars

apoptosis induction on MitoVE11S treatment. In this respect, it is interesting to note that the mitochondrially targeted analog MitoC11 lacking the chromanol ring suppressed the level of mtDNA transcripts even in CII-dysfunctional cells, suggesting that MitoVE11S, due to the charged succinyl group, needs its intracellular target, CII, to anchor in the mitochondrial inner membrane (MIM) to elicit changes on mtDNA transcripts. On the other hand, MitoC11, which lacks this group, is more hydrophobic and may anchor at the MIM more readily, not requiring functional CII to lower the *D-LOOP* transcript (Fig. 9).

Given that the untargeted MitoVE11S analog α-TOS only slightly affects mitochondrial transcription even at concentrations that induce apoptosis, it is possible that mitochondrial targeting, or the TPP^+ targeting group itself, is responsible for this effect. Most TPP^+-conjugated compounds reduced mtDNA transcription to some degree. However, MitoVE11S and MitoC11 showed a much stronger effect, and the TPP^+-conjugated antioxidants MitoQ7B and MitoR3B, (7, 38) had little effect on the *COX3* transcript and increased the level of the *D-LOOP* transcript by 4–5-fold (Fig. 2). While we cannot fully explain this observation, it is clear that the presence of the TPP^+ group by itself is not sufficient to elicit the reduction in mtDNA transcription.

Despite mitochondrial transcription being an energy-intensive process, cellular ATP did not seem to play a dominant role in *D-LOOP* reduction by MitoVE11S. While we observed a dramatic effect of MitoVE11S on intracellular ATP levels in cells grown in galactose-containing media, which forces the cells to generate ATP preferentially by oxidative phosphorylation, this reduction was very mild or absent in the glucose-containing medium where cells effectively produce ATP by glycolysis. In spite of these differences, we observed similar kinetics of *D-LOOP* suppression under both conditions (Supplementary Fig. S3), indicating that the mtDNA transcription is regulated by MitoVE11S independently of intracellular ATP.

The reduction in mtDNA transcripts is observed when mitochondria are challenged by increased ROS production, $\Delta\Psi_m$ dissipation, and inhibition of mitochondrial respiration. The compounds that meet at least two of these criteria seem to be effective inhibitors of mtDNA transcription, including MitoC11 and MitoVE11S, which efficiently dissipate $\Delta\Psi_m$ and affect mitochondrial morphology within minutes of treatment (Figs. 3 and 5), inhibit mitochondrial respiration, and cause effective production of ROS (Figs. 4 and 7). These effects were much less apparent for MitoC7 and MitoVE7S, which also reduced mtDNA transcription less efficiently. α-TOS and the mitochondrially targeted compounds MitoQ7B and MitoR3B, which do not acutely inhibit respiration, do not dissipate $\Delta\Psi_m$ and do not produce much ROS under our experimental conditions, and did not reduce the *D-LOOP* transcript either. In contrast, mitochondrial poisons antimycin A and rotenone, which do not dissipate $\Delta\Psi_m$ but strongly inhibit mitochondrial respiration and produce ROS in our experimental system (24, 31), reduced the *D-LOOP* transcript rather efficiently. In this respect, it is interesting to note the very high efficiency of ROS production by MitoVE11S (Fig. 7). It is

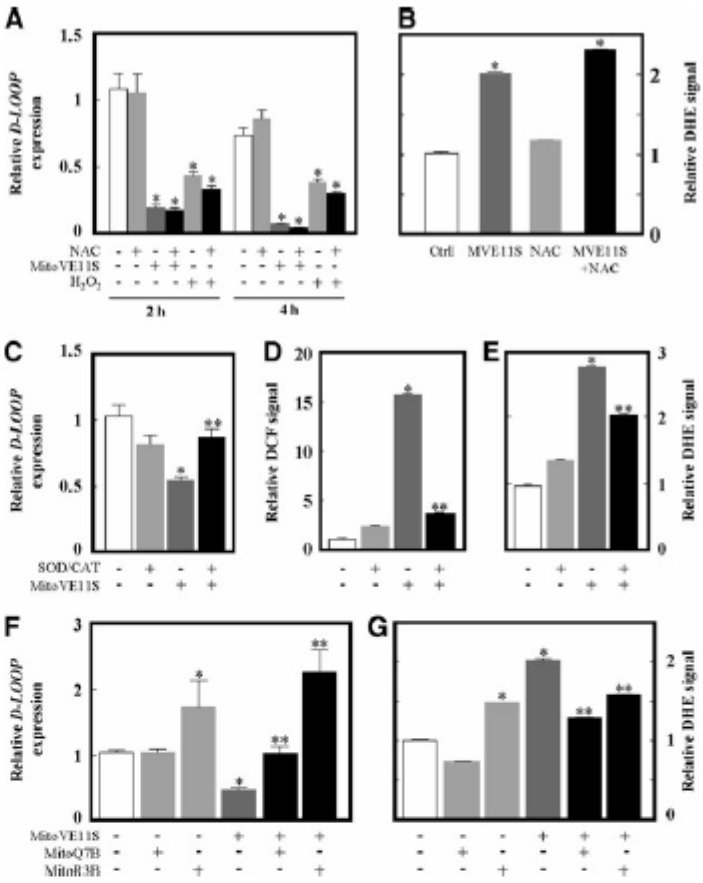

FIG. 6. Mitochondrially targeted antioxidants suppress the effect of MitoVE11S on the *D-LOOP* transcript. (A) Jurkat cells were pre-treated with 1 m*M* NAC and exposed to 1 μM MitoVE11S or 100 μM hydrogen peroxide and evaluated for the level of the *D-LOOP* transcript by qPCR after 2 or 4 h exposure and **(B)** for ROS generation using DHE after 2 h of treatment. **(C)** Jurkat cells were pre-treated for 6 h with PEG-SOD/PEG-CAT (750 U each), exposed to 1 μM MitoVE11S for 1 h, and assessed for the level of the *D-LOOP* transcript by qPCR as well as **(D)** for ROS level using DCF-DA or **(E)** DHE fluorophore. **(F)** Jurkat cells were pre-treated for 2 h with 2 μM MitoQ7B or MitoR3B, and the level of the *D-LOOP* transcript was evaluated by qPCR as well as **(G)** the level of ROS by DHE. The data are mean values ± SD ($n = 3$), the symbol "*" indicates significantly different data compared with the controls, and the symbol "**" indicates significantly differences between data for cells treated with MitoVE11S and MitoVE11S with antioxidants, with $p < 0.05$. DHE, dihydroethidium; NAC, *N*-acetyl cysteine.

perhaps counter-intuitive, as MitoVE11S dissipates $\Delta\Psi_m$, which is usually associated with decreased, not increased ROS production from the ETC, with electron carriers being in a more oxidized state that is less prone to electron leakage (40). In the case of MitoVE11S; however, the stimulation of electron flow through the ETC by initial uncoupling (see the rapid increase in respiration initially on MitoVE11S addition in Fig. 7), and simultaneous inhibition of CII UbQ-binding site (which leads to the diversion of electrons to superoxide) results in more electrons being available to form superoxide at the site of MitoVE11S binding. Hence, by increasing the amount of electrons available to form superoxide, MitoVE11S effectively enhances its own superoxide production.

To better understand the role of ROS in the process of inhibiting mtDNA transcription, we treated cells with exogenous hydrogen peroxide and tested the effect of several antioxidants on the capacity of MitoVE11S to suppress mtDNA transcripts. Hydrogen peroxide that is able to diffuse rapidly through membranes showed some, although much lower effect on the *D-LOOP* transcript compared with MitoVE11S (Fig. 6A). The antioxidant NAC did not exert any protective effect, likely due to its inability to efficiently penetrate into mitochondria since it did not suppress ROS generation (Fig. 6B). However, the mitochondria-permeable PEGylated SOD/CAT diminished the effect of MitoVE11S on the *D-LOOP* transcript and superoxide as measured with DHE (Fig. 6C–E), along with mitochondrially targeted antioxidants quercetin (MitoQ7B) and resveratrol (MitoR3B) (Fig. 6F, G). Therefore, the mitochondrial ROS appear necessary for effective reduction of mtDNA transcription. It also suggests an important role of ROS compartmentalization in the mitochondria, where superoxide formed at the interphase of the MIM and matrix is impermeable and may exert its effect on mitochondrial transcription and replication.

We observed significant inhibition of mitochondrial biogenesis (9, 19, 57) after MitoVE11S treatment, which is probably related to the observed decrease in *TFAM* and *TOP1MT* (Fig. 8A). This is consistent with the inhibition of the transcriptional/replicative machinery, since TFAM is a critical component that binds to the *D-LOOP* region and allows recruitment of other members of the machinery (4, 36). In addition, TFAM is required for the maintenance of nucleoid structures that contain mtDNA as well as the apparatus regulating replication and transcription of mtDNA, and to tether mtDNA to the MIM (8, 10, 28, 32, 36, 47, 59). However, the exact mechanism underlying the decrease of TFAM remains to be determined, but may be related to ROS, since the drop in TFAM levels takes as little as 15 min, and a similar decrease could also be seen with rotenone and antimycin A, which are able to induce mitochondrial ROS (Fig.

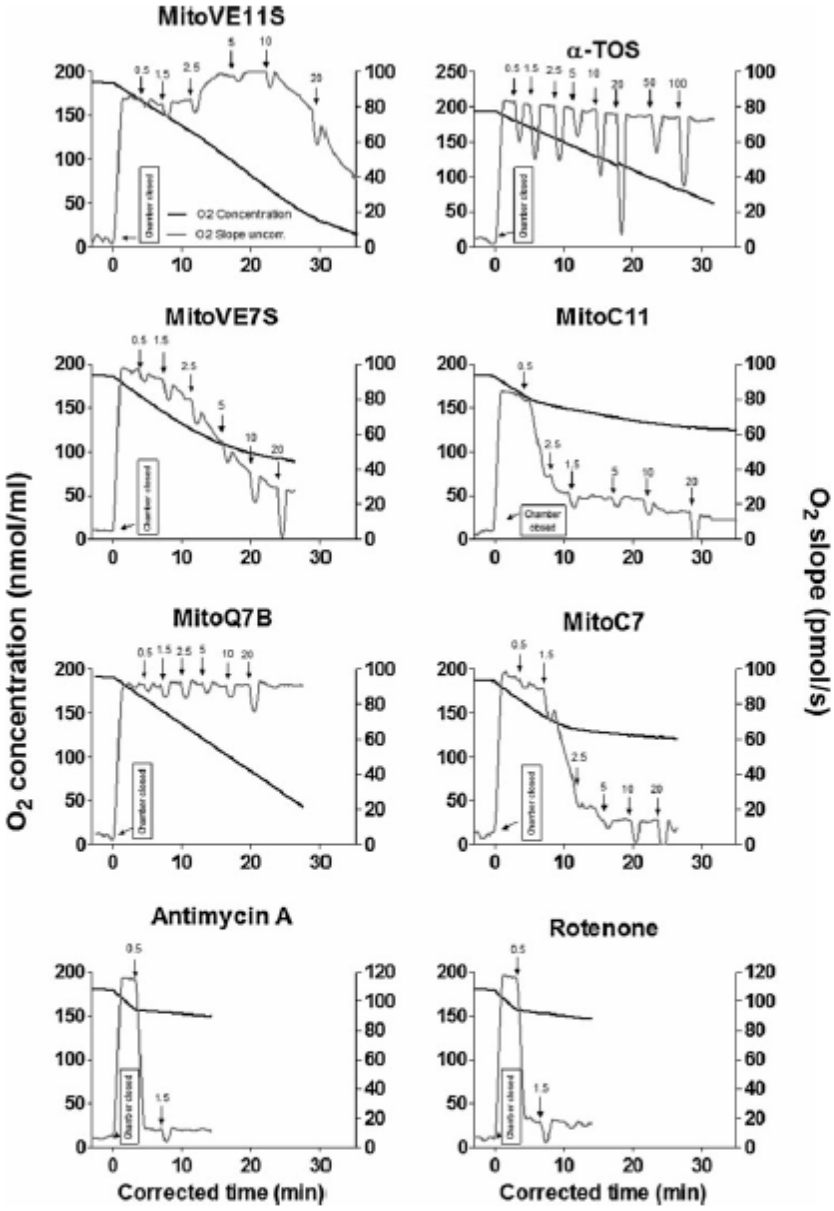

FIG. 7. Mitochondrial respiration is affected differently by individual agents. MCF7 cells were placed in the chamber of the Oxygraph at 2×10^6 per ml in DMEM and respiration was assessed after the addition of escalating doses (μM) of compounds as indicated in individual *panels*. The *left y* axis shows actual oxygen concentration (*black line*), while the *right y* axis shows derivation of the oxygen concentration and thus reflects the rate of respiration (*gray line*). The data are representative of three biological replicates.

8G, H). In contrast, protein levels of POLG were not changed in response to such stimuli, suggesting that TFAM, rather than the mitochondrial polymerase, is the main effector of the MitoVES effect. Further studies of mitochondrial biogenesis showed that MitoVE11S diminished the expression of proteins synthesized inside mitochondria (COX1) as well as nuclear-encoded proteins that are imported into mitochondria (SDHA), leading to the inhibition of mitochondrial biogenesis. Therefore, we assessed expression of several key mitochondrial regulators (57, 69) and found that whereas the mRNA levels of key regulators PGC1α/β coded for by *PPARGC1A/B* were reduced on MitoVE11S treatment, the protein level of PGC1β was increased, possibly in response to malfunctioning mitochondria, and this signaling axis is therefore unlikely to be the principal component of the MitoVE11S effect. At any rate, inhibition of mitochondrial biogenesis seems to be a delayed phenomenon that follows after the initial ROS production and mitochondrial membrane depolarization, and subsequent inhibition of the *D-LOOP* transcript further followed by delayed inhibition of other mitochondrial transcripts. The involvement of ROS is indicated by the activation of the redox sensor *NFE2L2*, known also as *NRF2* (21, 37), although the precise molecular mechanism is yet to be elucidated.

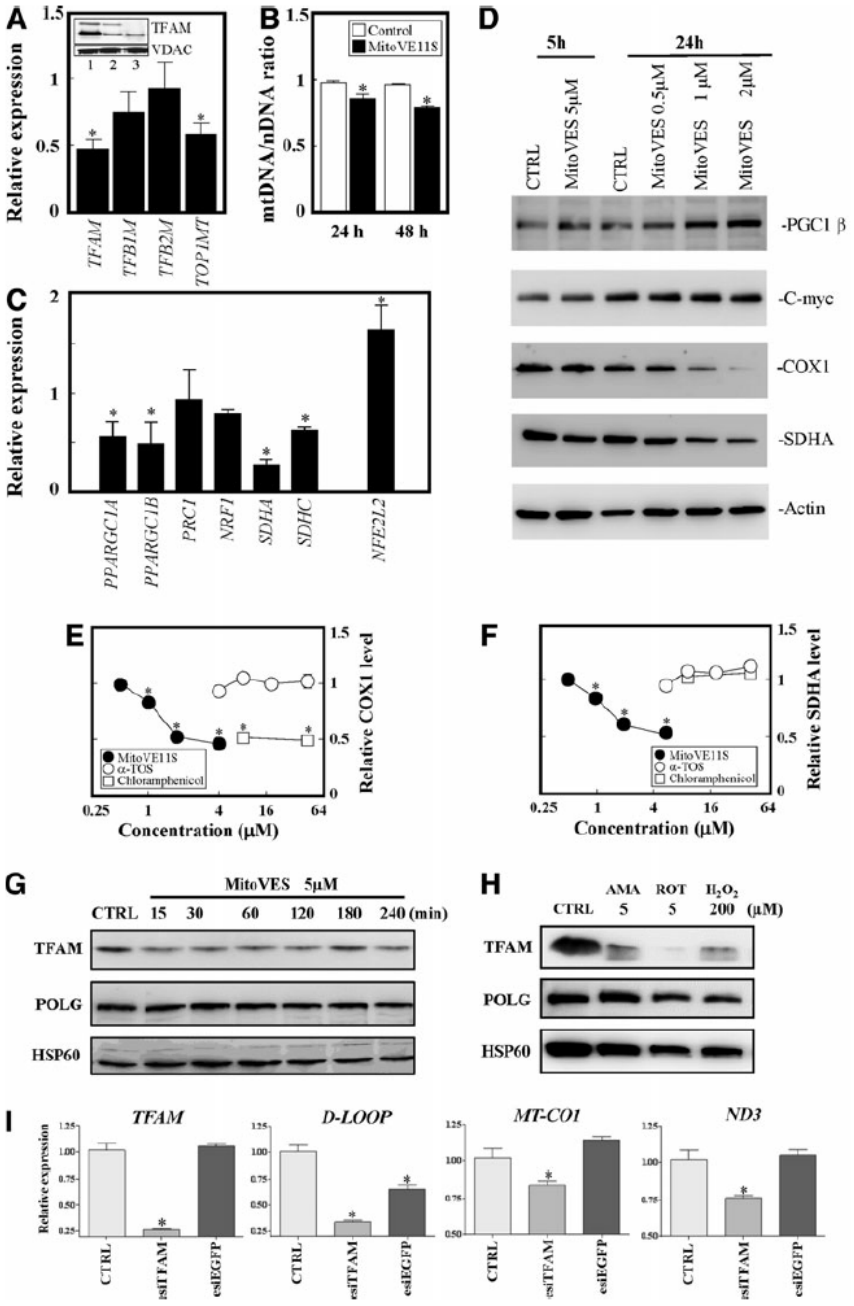

FIG. 8. MitoVE11S regulates mTFs and mitochondrial biogenesis. (**A**) MCF7 cells were exposed to 1 μM MitoVE11S for 24 h, and the level of mTFs and mitochondrial topoisomerase *TOP1MT* transcripts was evaluated by qPCR. The *insert* in (**A**) indicates the level of the TFAM protein in control MCF7 cells (1) and cells treated with MitoVE11S at 5 μM for 5 h (2) and at 1 μM for 24 h (3). (**B**) MCF7 cells were exposed to MitoVE11S at 1 μM for the times specified, and the mtDNA/nuclear DNA ratio was evaluated by qPCR as detailed in "Materials and Methods." (**C**) MCF7 cells were exposed to 1 μM MitoVE11S for 24 h and assessed for the transcripts of the mitochondrial biogenesis genes *PPAGC1A*, *PPARGC1B*, and *PRC*, the oxygen sensor gene *NRF1*, CII subunit genes *SDHA* and *SDHC*, and an antioxidant responsive transcription factor *NFE2L2* using qPCR. (**D**) MCF7 cells were treated with a range of MitoVES concentrations for an indicated time, and protein levels of mitochondrial regulators PGC1-β, C-myc and mitochondrial protein levels of COX1 and SDHA were assayed. Actin served as a loading control. MCF7 cells were exposed to MitoVE11S, α-TOS, and chloramphenicol for 48 h and at the concentrations shown, they were evaluated for (**E**) the COX1 and (**F**) SDHA protein by In Cell enzyme-linked immunosorbent assay. (**G**) MCF7 cells were treated with 5 μM MitoVES for the indicated times, and levels of TFAM and POLG in the mitochondrial fraction were assessed by Western blot analysis. (**H**) Similarly, the effects of antimycin A (AMA), rotenone (ROT), and hydrogen peroxide (H_2O_2) on intra-mitochondrial levels of TFAM and POLG in MCF7 cells after 4 h of incubation were assessed by Western blotting. (**I**) The effect of TFAM silencing on the levels of mitochondrial transcripts in MCF7 cells assessed by qPCR is also documented. The data are mean values ± SD ($n = 3$), and the symbol "*" indicates significantly different data compared with the controls with $p < 0.05$. CII, complex II; COX1, cytochrome *c* oxidase 1 protein; mTF, mitochondrial transcription factor; POLG, DNA polymerase γ.

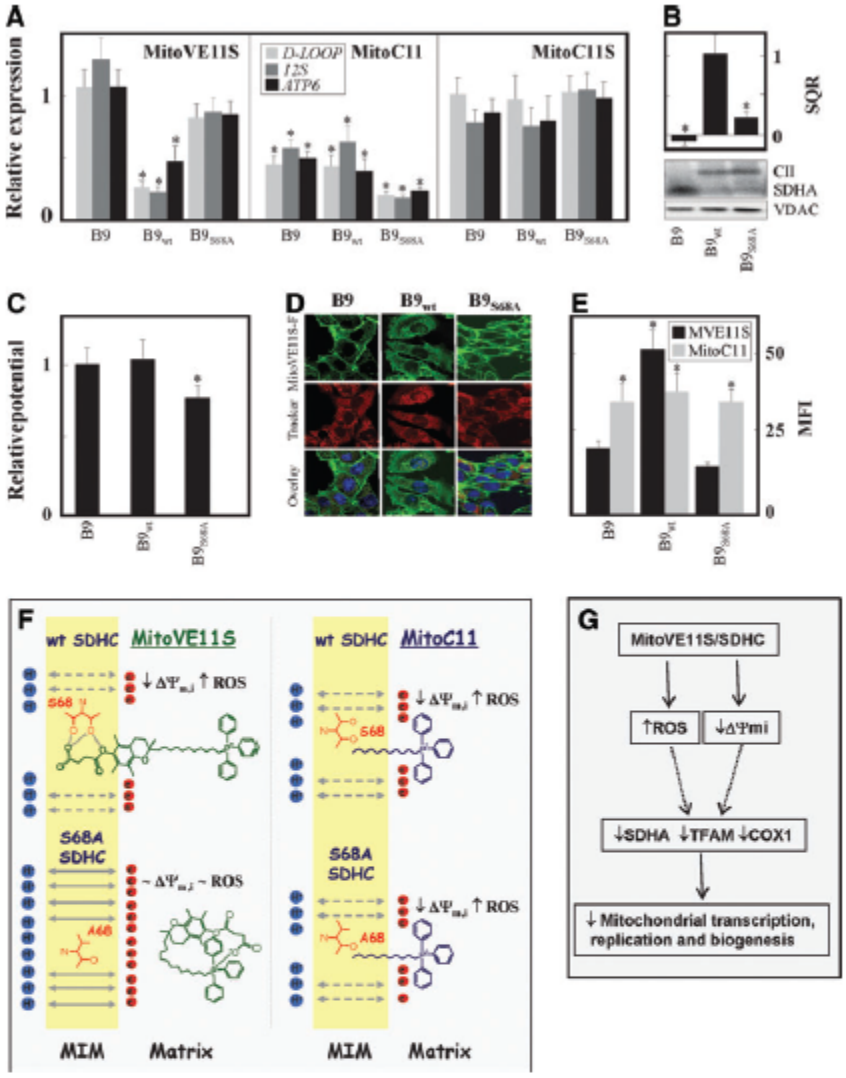

FIG. 9. Functional CII is important for the activity of MitoVE11S. **(A)** B9, $B9_{wt}$, and $B9_{S68S}$ cells were exposed to MitoVE11S, MitoC11, or MitoC11S at 5 μM for 8 h and assessed for the *D-LOOP*, *12S*, and *ATP6* transcripts by qPCR; the expression is related to the untreated controls of each cell line. **(B)** B9, $B9_{wt}$, and $B9_{S68S}$ cells were evaluated for the SQR activity using an enzymatic assay and for the assembly of CII using NBE. VDAC was used as a loading control. **(C)** B9, $B9_{wt}$, and $B9_{S68S}$ cells were assessed for the relative $\Delta\Psi_m$ also after 1-h pre-incubation with 5 μM CCCP using TMRM and flow cytometry. **(D)** B9, $B9_{wt}$, and $B9_{S68S}$ cells were incubated with MitoVE11S-F and MitoTracker Red and evaluated for green and red fluorescence by confocal microscopy. **(E)** B9, $B9_{wt}$, and $B9_{S68S}$ cells were exposed to 1 μM MitoVE11S or MitoC11 for 1 h, and the level of ROS expressed as mean fluorescence intensity was assessed using DHE and flow cytometry. **(F)** Schematic representation of MitoVES action. To suppress mtDNA transcripts, MitoVES needs to dissipate the $\Delta\Psi_{m,i}$, and, in particular, to generate ROS. These processes are promoted by stabilising the agent across the MIM/matrix interphase by means of the interaction of the carboxyl part of the succinyl moiety of the agent with S68 of the Q_p site of the CII SDHC subunit. Efficient ROS generation due to exposure of cells to MitoVES is lost on mutation of S68. Since MitoVE11S is not stabilized across the interphase, it likely forms a zwitterionic form (shown here) or a head-to-tail dimer in the matrix. MitoC11, due to its aliphatic chain, is located at the MIM/matrix interphase regardless of the nature of CII, and it causes both $\Delta\Psi_m$ dissipation and moderate generation of ROS. Due to the anchoring of MitoVE11S, it is more efficient in generating ROS than MitoC11, which is freely inserted across the interphase with a high level of dynamics. **(G)** Scheme depicting MitoVE11S effect on mitochondria. The data are mean values ± SD ($n = 3$), and the symbol "*" indicates significantly different data compared with the controls with $p < 0.05$. The images are representative of three biological replicates. MIM, mitochondrial inner membrane; NBE, native blue electrophoresis; SQR, succinate quinone reductase. To see this illustration in color, the reader is referred to the web version of this article at www.liebertpub.com/ars

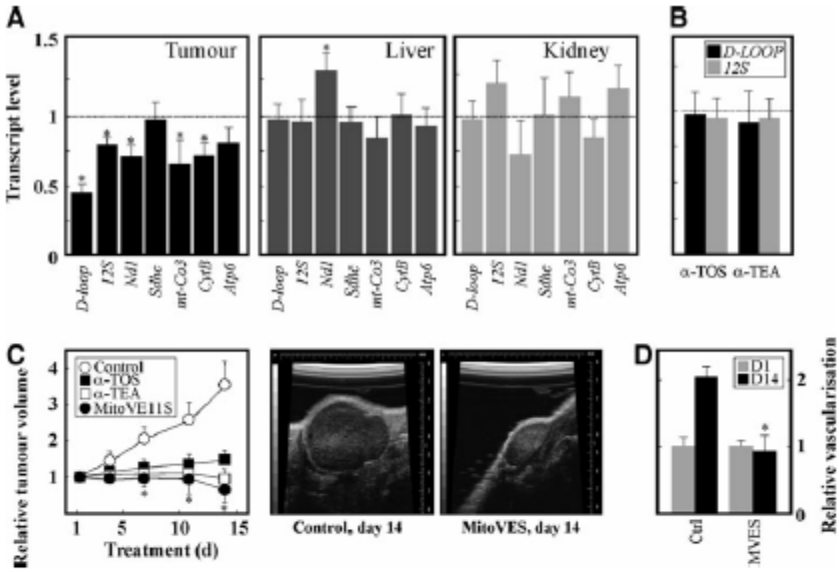

FIG. 10. MitoVE11S suppresses mtDNA in mice with breast cancer in a selective manner. (A) FBV/N *c-neu* mice with breast carcinomas were treated with MitoVES at 1.5 μmol per animal per dose every 3–4 days. At the end of the experiments, the control and treated mice were sacrificed and their breast carcinomas, liver, and kidney were assessed for the level of selected mtDNA transcripts in the treated animals related to that in the control mice using qPCR. **(B)** FVB/N *c-neu* mice were treated with α-TOS or α-TEA at 15 μmol per animal per dose as described earlier, and the tumor was assessed for the level of the *D-LOOP* and *12S* transcripts by qPCR. **(C)** Mice were treated as described earlier and assessed for the tumor kinetics and **(D)** vascularization (shown on days 1 and 14) as assessed non-invasively by ultrasound imaging (USI). The images in **(C)** are USI scans of representative tumors in control and treated animals on day 14. The data are mean values ± SD ($n = 3$), and the symbol "*" indicates significantly different data compared with controls with $p < 0.05$. The images are representative of three biological replicates. α-TEA, α-tocopheryl acetic acid ether.

Importantly, the inhibition of mtDNA transcription by MitoVE11S was verified *in vivo*, where the effect was observed specifically in tumors, and not in non-malignant tissue such as liver or kidney, providing an impetus for follow-up translational studies. The specificity of MitoVE11S for *D-LOOP* transcription in the tumor tissue is likely related to preferential uptake of the agent, since fluorescently tagged MitoVE11S localizes preferentially to tumor cells (Fig. 9 and Supplementary Fig. S5). This may be due to the greater (negative) plasma membrane potential in cancer cells compared with normal cells, a result of higher contribution of glycolysis to the generation of ATP in cancer cells (22, 27, 35, 52, 61, 65). Mitochondrially targeted compounds are taken up in response to membrane potential due to the delocalized charge on the TPP^+ group and accumulate in the MIM *in vitro* as well as *in vivo* (1, 5, 6, 30, 41, 50, 52, 55, 60).

Based on the findings described earlier, we propose a scheme explaining the initial steps in the activity of MitoVE11S toward mtDNA transcripts (Fig. 9F). MitoVE11S rapidly associates with mitochondria, where it is stabilized across the MIM/matrix interface *via* its interaction with the SDHC's S68. This results in initial uncoupling of respiration (Fig. 7) (51), promoting very efficient generation of ROS. Rapid dissipation of $\Delta\Psi_m$ at low concentrations of MitoVE11S is a result of the positioning of MitoVE11S across the matrix/MIM interphase. On the other hand, functional CII is disposable for ROS generation in response to MitoC11, which lacks the charged carboxyl group at the end of the alkyl chain, allowing it to penetrate membranes more easily and indiscriminately.

In summary, this study introduces a novel, previously unrecognized mechanism of anti-cancer activity of MitoVE11S, which forms an intrinsic component of its anti-cancer response. This component involves the reduction of mtDNA transcription and suppression of cell proliferation, and it is similarly regulated, yet functionally independent from the previously characterized apoptotic response. As such, it widens the appeal of ETC-directed mitochondria-targeted ROS-producing compounds such as VE analogs, as these agents are now shown to elicit effective responses in concentrations insufficient to induce apoptosis. This narrows the window of opportunity for cancer cells to escape treatment, and we can speculate that it may render VE analogs that are also effective in cancers insensitive to apoptosis induction due to defects in the apoptotic machinery. In addition, this mechanism might be relevant for the activity of other anti-cancer agents as well and accentuate the notion of mitochondria as attractive, relatively invariant cancer drug targets that might help circumvent the documented intra-tumor heterogeneity and different mutational profiles of individual tumors (23, 29, 49).

Materials and Methods

Cell culture and treatment

Except where shown, all cell lines were obtained from the ATCC. Human T lymphoma Jurkat cells were maintained in the RPMI-1640 medium with 10% fetal calf serum (FCS) and antibiotics, human MCF7 and mouse NeuTL breast cancer cells, human colorectal SW620 and RKO cells, and human non-small cell lung cancer H1299 cells were maintained in DMEM with 10% FCS and antibiotics. The immortalized EAhy926 ECs (2, 18) were maintained in DMEM with 10% FCS and antibiotics, plus 100 μM hypoxanthine, 0.4 μM aminopterin, and 16 μM thymidine. H-Ras-transformed Chinese hamster B9 cells lacking SDHC, $B9_{S68A}$ cells reconstituted with SDHC with an S68A mutation (both with dysfunctional CII), and $B9_{wt}$ cells with reconstituted CII (11, 15) were maintained in DMEM with 10% FCS, antibiotics, 10 mg/ml glucose, and 1% non-essential amino acids. MCF10A were cultivated in DMEM/F12 with 5% horse serum and antibiotics, supplemented with 0.1 ng/ml cholera toxin, 20 ng/ml epidermal growth factor, 0.5 μg/ml hydrocortisone, and 1 mg/ml insulin. BJ cells were were maintained in DMEM with low glucose (1 mg/ml) suplemented with 10% FCS and antibiotics. MCF7 cells with GFP-labeled mitochondria were prepared by transfection with *pTagGFP2-mito* (Evrogen) and selected for high GFP2.

Cells were treated with analogs of VE listed in Supplementary Figure S1, which include the MitoVES with an 11-C aliphatic chain spanning the tocopheryl succinyl and the TPP^+ group (MitoVE11S; **5**), the untargeted α-TOS (**1**), the ester α-TEA (**2**), a homolog of MitoVE11S with a 5-C chain (MitoVE5S; **3**) or with a 7-C chain (MitoVE7S; **4**), an analog of MitoVE11S with the TPP^+ group attached to the carboxyl of the tocopheryl succinyl group *via* a C-4 spacer (VES4TPP; **6**), analogs of MitoVE11S and MitoVE7S lacking the tocopheryl succinyl group (undecyl-TPP, MitoC11, **8**, and heptyl-TPP, MitoC7, **7**, respectively), analogs of MitoC7 and MitoC11 with a succinyl group at the end of the aliphatic chain, MitoC7S (**9**) and MitoC11S (**10**), respectively, and TPP^+-tagged quercetin (MitoQ7B; **11**) (38) and resveratrol (MitoR3B; **12**) (7). The preparation of MitoVES, MitoVE5, and MitoVE7S was recently published (13), and preparation of other VE analogs will be published elsewhere.

Apoptosis and proliferation assays

Apoptosis was assessed as detailed elsewhere (68) using the annexin V-fluorescein isothiocyanate/propidium iodide method. For B9, $B9_{wt}$, and $B9_{S68A}$ cells transformed with GFP-fused H-Ras, annexin V-PE was used. Proliferation was estimated using the MTT method according to a standard procedure.

Assessment of ATP level, mitochondrial potential, and ROS generation

Relative level of ATP was assessed by the Cell Titer-Glo Luminescent Cell Viability Assay (Promega) according to the manufacturer's instructions. To assess the mitochondrial membrane potential ($\Delta\Psi_{mi}$), we used the $\Delta\Psi_{mi}$-sensitive fluorescent probe TMRM (Sigma) in a non-quenching mode followed by flow cytometry (50 nM TMRM) or time-lapse confocal microscopy (10 nM TMRM). The mitochondrial uncoupler carbonyl cyanide 4-(trifluoromethoxy)phenylhydrazone (Sigma) was used as a control to determine non-specific TMRM loading. The levels or ROS were evaluated using the probes DHE or 2′,7′-dichlorodihydrofluorescein diacetate (both Sigma). The cells, control or treated, were incubated with either probe for 15 min under normal culture conditions, harvested and the fluorescence of the oxidized probes assessed by flow cytometry.

Assessment of respiration and SQR activity

Routine respiration of non-permeabilized cells was assessed in the DMEM medium in the Oxygraph instrument (Oroboros Instruments). This setup has the advantage that it closely resembles the *in vitro* conditions used in most experiments. Overall, 2×10^6 cells/ml were equilibrated in the DMEM medium and the experiment was started by closing the measurement chambers. Increasing concentrations of tested compounds were added as indicated, and total oxygen concentration and oxygen flux were recorded.

The SQR activity of the mitochondrial CII was assessed as detailed elsewhere (13).

Assessment of mtDNA and nDNA level

DNA was extracted and isolated from cells using the Wizard SV Genomic DNA purification system, and an equal load of DNA (10 ng) was added to the qPCR reaction. The amount of mtDNA and nDNA was evaluated by quantitative polymerase chain reaction (qPCR) using primers specified in the Supplementary Tables S1–S3 as MTRT1 and MTRT2 (mtDNA) plus MTAIB and MTBA (nDNA), and the mtDNA/nDNA ratio was calculated.

NBE and Western blotting

Cells were harvested, spun down, resuspended in the Tris/ethylene glycol tetraacetic acid buffer containing 200 mM sucrose, and homogenized on ice with a glass-Teflon homogenizer. Mitochondria were isolated by differential centrifugation. Lysed cells were first centrifuged at 900 g for 10 min, and mitochondria floating in the supernatant were pelleted by centrifugation at 7000 g for 15 min. Isolated mitochondria were solubilized in the extraction buffer (1.5 M aminocaproic acid, 50 mM Bis-Tris, 0.5 M ethylenediaminetetraaceticacid [EDTA], pH 7) with 1.3% lauryl maltoside. Samples containing 30–60 μg of protein were combined with the sample buffer (0.75 M aminocaproic acid, 50 mM Bis-Tris, 0.5 M EDTA, pH 7, 5% Serva-Blue G-250, 12% glycerol), loaded on pre-cast NativePAGE Novex 4–16% Bis-Tris gels, and run overnight at 25 V. Separated protein complexes were then transfered to the polyvinylidene fluoride membrane using the Transblot Invitrogen system. CII was detected using the anti-SDHA IgG (Abcam). For Western blotting after sodium dodecylsulfate-polyacrylamide gel electophoresis, the anti-VDAC IgG (Abcam), anti-TFAM IgG (Sigma), anti MT-CO1 IgG (Abcam), anti PGC1α/β IgG (Abcam), anti-c-Myc IgG (Cell Signaling), and anti-actin IgG (Santa Cruz) were used.

Real-time RT-PCR (qPCR)

All primers were designed using the NCBI Primer-Blast web application, and their sequences are listed in the

Supplementary Tables S1–S3. qPCR was accomplished basically as follows. RNA was purified from cells using the Aurum Total RNA purification kit (BioRad) according to the manufacturer's instructions. The purified RNA (2–5 μg) was used for reverse transcription employing the Revert Aid First-strand cDNA Synthesis Kit (Fermentas). One hundred nanograms of cDNA was used for the qPCR analysis, which was performed using the ssoFast Eva Green Master Mix (BioRad) under the following conditions: initial denaturation 98°C for 1 min followed by 38 cycles of 98°C for 5 s, 60°C for 15 s, and 72°C for 20 s. The Eco Illumina qPCR or the BioRadCFX96 instruments were used.

esi RNA experiments

Cells were seeded in a six-well plate at 1 day before the transfection at a concentration of 100,000 cells per well. The next day, cells were transfected with 100 ng of either esi TFAM RNA (EHU047401) or non-targeting EGFP esiRNA (EHUEGFP) as suggested by the manufacturer's instructions (Sigma). We used Dharmafect transfection reagent to deliver the siRNA into the cells at a concentration of 1 μl/100 ng siRNA. Cells were then transfected for 24 h with subsequent medium change and further incubation for 24 h. Cells were then collected, and RNA was extracted according to the protocol described earlier.

Cellular localization of VE analogs

To see the localization of MitoVES and α-TOS, cells were incubated with the VE analogs tagged with a fluorescent probe (MitoVES-F, α-TOS-F) (synthesized as described in the Supplementary Tables S1–S3) in the presence of MitoTracker Red, counterstained with Hoechst 33342 to visualize nuclei, and inspected in a confocal microscope.

Time-lapse confocal microscopy

Cells were seeded in glass bottom microscopy dishes (In Vitro Scientific) two days before the experiment. On the day of experiment, the cells were incubated in the complete medium with 100 ng/ml Hoechst 33342 nuclear dye for 30 min, washed with phosphate-buffered saline, and allowed to recover for 1 h. The medium was replaced with fresh medium containing 10 n*M* TMRM, and the plate was mounted on the stage of the SP5 confocal microscope (Leica Microsystems). Time lapse images of eight positions per plate were recorded using 63× oil immersion lens at 37°C and 5% CO_2, with the first image in the time series taken just before the addition of the tested compound. The images were recorded at regular intervals, with each image comprising a confocal stack of 2 μm thickness obtained using the minimal laser power to prevent bleaching. A minimum of three independent recordings were made for each condition. The images were deconvoluted using the Huygens Professional software (SVI) and presented as maximal intensity projections.

Immunohistochemistry

Tissue (tumors, kidney, liver) from control and MitoVES-treated mice was paraffin embedded, sectioned, and processed for the estimation of proliferation and vascularization using the anti-Ki67 and anti-CD31 IgG (both Cell Signaling), respectively. Morphology of the sections was documented using HandE staining performed according to a standard procedure.

Animal studies

Transgenic FVB/N202 *c-neu* mice carrying the rat human epidermal growth factor receptor 2 (HER2)/neu proto-oncogene driven by the MMTV promoter on the H-2^q FVB/N background were established at the Griffith University Animal Facility and maintained under strict inbreeding conditions. About 70% of the female mice develop spontaneous mammary carcinomas with a mean latency time of 8 months. Female *c-neu* mice with small tumors (~40 mm^3) were treated with either 100 μl 15 m*M* MitoVES or 150 m*M* α-TOS or α-TEA in 4% ethanol/corn oil or the same volume of the excipient by an intraperitoneal injection once in 3 or 4 days, essentially as reported (16, 12–14, 67). Tumor volume and relative vascularization were quantified using the Power Doppler Mode of the ultrasound imaginginstrument (the Vevo770 device fitted with the RMV704 scan-head; VisualSonics) twice a week after treatment. Both the treated and control group contained six mice. At the end of the experiment, the mice were euthanized and the tissue was removed and processed as detailed earlier (see "Immunohistochemistry"). All experiments were performed according to the guidelines of the Australian and New Zealand Council for the Care and Use of Animals in Research and Teaching and were approved by the Griffith University Animal Ethics Committee.

Acknowledgments

This work was supported in part by grants from the Australian Research Council, the National Health and Medical Research Council of Australia and Cancer Council Queensland, from the Czech Science Foundation (P301/10/1937) and the Grant Agency of the Academy of Sciences of the Czech Republic (KAN200520703) to J.N., the Czech Science Foundation (P305/12/1708) to J.T., and the Czech Science Foundation (P301/12/1851) to J.R. The study was further supported by the grant AV0Z50520701 to the Institute of Biotechnology ASCR and by BIOCEV CZ.1.05/1.1.00/02.0109 from the European Regional Development Fund. M.Z. was supported in part by the Excellence Grant from the CARIPARO Foundation and by MUIR PRIN grant 20107Z8XBW_004, and L.-F.D. was supported in part by the Australian Research Council and a Griffith University Research Fellowship.

Author Disclosure Statement

No competing financial interests exist.

Authors' Contributions

J.T., L.-F.D., J.R., and J.N. designed the study; J.T., L.-F.D., J.S., J.R., J.G., M.N., M.V., K.K., Z.R., J.S., and M.S. performed experiments; all authors analyzed data; and J.T., J.R., L.-F.D., J.S., M.Z., and J.N. wrote this article. J.T., L.-F.D., J.R., M.Z., and J.N. provided funding.

References

1. Adlam VJ, Harrison JC, Porteous CM, James AM, Smith RA, Murphy MP, and Sammut IA. Targeting an antioxidant

to mitochondria decreases cardiac ischemia-reperfusion injury. *FASEB J* 19: 1088–1095, 2005.
2. Albini A, Marchisone C, Del GF, Benelli R, Masiello L, Tacchetti C, Bono M, Ferrantini M, Rozera C, Truini M, Belardelli F, Santi L, and Noonan DM. Inhibition of angiogenesis and vascular tumor growth by interferon-producing cells: a gene therapy approach. *Am J Pathol* 156: 1381–1393, 2000.
3. Anderson S, Bankier AT, Barrell BG, de Bruijn MH, Coulson AR, Drouin J, Eperon IC, Nierlich DP, Roe BA, Sanger F, Schreier PH, Smith AJ, Staden R, and Young IG. Sequence and organization of the human mitochondrial genome. *Nature* 290: 457–465, 1981.
4. Asin-Cayuela J and Gustafsson CM. Mitochondrial transcription and its regulation in mammalian cells. *Trends Biochem Sci* 32: 111–117, 2007.
5. Asin-Cayuela J, Manas AR, James AM, Smith RA, and Murphy MP. Fine-tuning the hydrophobicity of a mitochondria-targeted antioxidant. *FEBS Lett* 571: 9–16, 2004.
6. Biasutto L, Dong LF, Zoratti M, and Neuzil J. Mitochondrially targeted anti-cancer agents. *Mitochondrion* 10: 670–681, 2010.
7. Biasutto L, Mattarei A, Marotta E, Bradaschia A, Sassi N, Garbisa S, Zoratti M, and Paradisi C. Development of mitochondria-targeted derivatives of resveratrol. *Bioorg Med Chem Lett* 18: 5594–5597, 2008.
8. Bogenhagen DF. Mitochondrial DNA nucleoid structure. *Biochim Biophys Acta* 1819: 914–920, 2012.
9. Bonawitz ND, Clayton DA, and Shadel GS. Initiation and beyond: multiple functions of the human mitochondrial transcription machinery. *Mol Cell* 24: 813–825, 2006.
10. Brown TA, Tkachuk AN, Shtengel G, Kopek BG, Bogenhagen DF, Hess HF, and Clayton DA. Superresolution fluorescence imaging of mitochondrial nucleoids reveals their spatial range, limits, and membrane interaction. *Mol Cell Biol* 31: 4994–5010, 2011.
11. Dong LF, Freeman R, Liu J, Zobalova R, Marin-Hernandez A, Stantic M, Rohlena J, Valis K, Rodriguez-Enriquez S, Butcher B, Goodwin J, Brunk UT, Witting PK, Moreno-Sanchez R, Scheffler IE, Ralph SJ, and Neuzil J. Suppression of tumor growth *in vivo* by the mitocan alpha-tocopheryl succinate requires respiratory complex II. *Clin Cancer Res* 15: 1593–1600, 2009.
12. Dong LF, Grant G, Massa H, Zobalova R, Akporiaye E, and Neuzil J. Alpha-tocopheryloxyacetic acid is superior to alpha-tocopheryl succinate in suppressing HER2-high breast carcinomas due to its higher stability. *Int J Cancer* 131: 1052–1058, 2012.
13. Dong LF, Jameson VJ, Tilly D, Cerny J, Mahdavian E, Marin-Hernandez A, Hernandez-Esquivel L, Rodriguez-Enriquez S, Stursa J, Witting PK, Stantic B, Rohlena J, Truksa J, Kluckova K, Dyason JC, Ledvina M, Salvatore BA, Moreno-Sanchez R, Coster MJ, Ralph SJ, Smith RA, and Neuzil J. Mitochondrial targeting of vitamin E succinate enhances its pro-apoptotic and anti-cancer activity via mitochondrial complex II. *J Biol Chem* 286: 3717–3728, 2011.
14. Dong LF, Jameson VJ, Tilly D, Prochazka L, Rohlena J, Valis K, Truksa J, Zobalova R, Mahdavian E, Kluckova K, Stantic M, Stursa J, Freeman R, Witting PK, Norberg E, Goodwin J, Salvatore BA, Novotna J, Turanek J, Ledvina M, Hozak P, Zhivotovsky B, Coster MJ, Ralph SJ, Smith RA, and Neuzil J. Mitochondrial targeting of alpha-tocopheryl succinate enhances its pro-apoptotic efficacy: a new paradigm for effective cancer therapy. *Free Radic Biol Med* 50: 1546–1555, 2011.
15. Dong LF, Low P, Dyason JC, Wang XF, Prochazka L, Witting PK, Freeman R, Swettenham E, Valis K, Liu J, Zobalova R, Turanek J, Spitz DR, Domann FE, Scheffler IE, Ralph SJ, and Neuzil J. Alpha-tocopheryl succinate induces apoptosis by targeting ubiquinone-binding sites in mitochondrial respiratory complex II. *Oncogene* 27: 4324–4335, 2008.
16. Dong LF, Swettenham E, Eliasson J, Wang XF, Gold M, Medunic Y, Stantic M, Low P, Prochazka L, Witting PK, Turanek J, Akporiaye ET, Ralph SJ, and Neuzil J. Vitamin E analogues inhibit angiogenesis by selective induction of apoptosis in proliferating endothelial cells: the role of oxidative stress. *Cancer Res* 67: 11906–11913, 2007.
17. Dos Santos GA, Abreu e Lima RS, Pestana CR, Lima AS, Scheucher PS, Thome CH, Gimenes-Teixeira HL, Santana-Lemos BA, Lucena-Araujo AR, Rodrigues FP, Nasr R, Uyemura SA, Falcao RP, De TH, Pandolfi PP, Curti C, and Rego EM. (+)Alpha-tocopheryl succinate inhibits the mitochondrial respiratory chain complex I and is as effective as arsenic trioxide or ATRA against acute promyelocytic leukemia *in vivo*. *Leukemia* 26: 451–460, 2012.
18. Edgell CJ, McDonald CC, and Graham JB. Permanent cell line expressing human factor VIII-related antigen established by hybridization. *Proc Natl Acad Sci U S A* 80: 3734–3737, 1983.
19. Falkenberg M, Larsson NG, and Gustafsson CM. DNA replication and transcription in mammalian mitochondria. *Annu Rev Biochem* 76: 679–699, 2007.
20. Fulda S, Galluzzi L, and Kroemer G. Targeting mitochondria for cancer therapy. *Nat Rev Drug Discov* 9: 447–464, 2010.
21. Gao M, Wang J, Wang W, Liu J, and Wong CW. Phosphatidylinositol 3-kinase affects mitochondrial function in part through inducing peroxisome proliferator-activated receptor gamma coactivator-1beta expression. *Br J Pharmacol* 162: 1000–1008, 2011.
22. Gatenby RA and Gillies RJ. Why do cancers have high aerobic glycolysis? *Nat Rev Cancer* 4: 891–899, 2004.
23. Gerlinger M, Rowan AJ, Horswell S, Larkin J, Endesfelder D, Gronroos E, Martinez P, Matthews N, Stewart A, Tarpey P, Varela I, Phillimore B, Begum S, McDonald NQ, Butler A, Jones D, Raine K, Latimer C, Santos CR, Nohadani M, Eklund AC, Spencer-Dene B, Clark G, Pickering L, Stamp G, Gore M, Szallasi Z, Downward J, Futreal PA, and Swanton C. Intratumor heterogeneity and branched evolution revealed by multiregion sequencing. *N Engl J Med* 366: 883–892, 2012.
24. Giulivi C, Boveris A, and Cadenas E. Hydroxyl radical generation during mitochondrial electron transfer and the formation of 8-hydroxydesoxyguanosine in mitochondrial DNA. *Arch Biochem Biophys* 316: 909–916, 1995.
25. Gogvadze V, Orrenius S, and Zhivotovsky B. Mitochondria in cancer cells: what is so special about them? *Trends Cell Biol* 18: 165–173, 2008.
26. Guy CT, Webster MA, Schaller M, Parsons TJ, Cardiff RD, and Muller WJ. Expression of the neu protooncogene in the mammary epithelium of transgenic mice induces metastatic disease. *Proc Natl Acad Sci U S A* 89: 10578–10582, 1992.
27. Hanahan D and Weinberg RA. Hallmarks of cancer: the next generation. *Cell* 144: 646–674, 2011.
28. Holt IJ, He J, Mao CC, Boyd-Kirkup JD, Martinsson P, Sembongi H, Reyes A, and Spelbrink JN. Mammalian mitochondrial nucleoids: organizing an independently minded genome. *Mitochondrion* 7: 311–321, 2007.

29. Jones S, Zhang X, Parsons DW, Lin JC, Leary RJ, Angenendt P, Mankoo P, Carter H, Kamiyama H, Jimeno A, Hong SM, Fu B, Lin MT, Calhoun ES, Kamiyama M, Walter K, Nikolskaya T, Nikolsky Y, Hartigan J, Smith DR, Hidalgo M, Leach SD, Klein AP, Jaffee EM, Goggins M, Maitra A, Iacobuzio-Donahue C, Eshleman JR, Kern SE, Hruban RH, Karchin R, Papadopoulos N, Parmigiani G, Vogelstein B, Velculescu VE, and Kinzler KW. Core signaling pathways in human pancreatic cancers revealed by global genomic analyses. *Science* 321: 1801–1806, 2008.
30. Kelso GF, Porteous CM, Coulter CV, Hughes G, Porteous WK, Ledgerwood EC, Smith RA, and Murphy MP. Selective targeting of a redox-active ubiquinone to mitochondria within cells: antioxidant and antiapoptotic properties. *J Biol Chem* 276: 4588–4596, 2001.
31. Ksenzenko M, Konstantinov AA, Khomutov GB, Tikhonov AN, and Ruuge EK. Relationships between the effects of redox potential, alpha-thenoyltrifluoroacetone and malonate on O(2) and H_2O_2 generation by submitochondrial particles in the presence of succinate and antimycin. *FEBS Lett* 175: 105–108, 1984.
32. Kucej M and Butow RA. Evolutionary tinkering with mitochondrial nucleoids. *Trends Cell Biol* 17: 586–592, 2007.
33. Lemarie A and Grimm S. Mitochondrial respiratory chain complexes: apoptosis sensors mutated in cancer? *Oncogene* 30: 3985–4003, 2011.
34. Lewis W, Levine ES, Griniuviene B, Tankersley KO, Colacino JM, Sommadossi JP, Watanabe KA, and Perrino FW. Fialuridine and its metabolites inhibit DNA polymerase gamma at sites of multiple adjacent analog incorporation, decrease mtDNA abundance, and cause mitochondrial structural defects in cultured hepatoblasts. *Proc Natl Acad Sci U S A* 93: 3592–3597, 1996.
35. Liberman EA, Topaly VP, Tsofina LM, Jasaitis AA, and Skulachev VP. Mechanism of coupling of oxidative phosphorylation and the membrane potential of mitochondria. *Nature* 222: 1076–1078, 1969.
36. Litonin D, Sologub M, Shi Y, Savkina M, Anikin M, Falkenberg M, Gustafsson CM, and Temiakov D. Human mitochondrial transcription revisited: only TFAM and TFB2M are required for transcription of the mitochondrial genes *in vitro*. *J Biol Chem* 285: 18129–18133, 2010.
37. Martin-Montalvo A, Villalba JM, Navas P, and de Cabo R. NRF2, cancer and calorie restriction. *Oncogene* 30: 505–520, 2011.
38. Mattarei A, Biasutto L, Marotta E, De MU, Sassi N, Garbisa S, Zoratti M, and Paradisi C. A mitochondriotropic derivative of quercetin: a strategy to increase the effectiveness of polyphenols. *Chembiochem* 9: 2633–2642, 2008.
39. Miyako K, Kai Y, Irie T, Takeshige K, and Kang D. The content of intracellular mitochondrial DNA is decreased by 1-methyl-4-phenylpyridinium ion (MPP+). *J Biol Chem* 272: 9605–9608, 1997.
40. Murphy MP. How mitochondria produce reactive oxygen species. *Biochem J* 417: 1–13, 2009.
41. Murphy MP and Smith RA. Targeting antioxidants to mitochondria by conjugation to lipophilic cations. *Annu Rev Pharmacol Toxicol* 47: 629–656, 2007.
42. Neuzil J, Dong LF, Rohlena J, Truksa J, and Ralph SJ. Classification of mitocans, anti-cancer drugs acting on mitochondria. *Mitochondrion* 13: 199–208, 2013.
43. Neuzil J, Dyason JC, Freeman R, Dong LF, Prochazka L, Wang XF, Scheffler I, and Ralph SJ. Mitocans as anticancer agents targeting mitochondria: lessons from studies with vitamin E analogues, inhibitors of complex II. *J Bioenerg Biomembr* 39: 65–72, 2007.
44. Neuzil J, Wang XF, Dong LF, Low P, and Ralph SJ. Molecular mechanism of 'mitocan'-induced apoptosis in cancer cells epitomizes the multiple roles of reactive oxygen species and Bcl-2 family proteins. *FEBS Lett* 580: 5125–5129, 2006.
45. Neuzil J, Weber T, Gellert N, and Weber C. Selective cancer cell killing by alpha-tocopheryl succinate. *Br J Cancer* 84: 87–89, 2001.
46. Neuzil J, Weber T, Schroder A, Lu M, Ostermann G, Gellert N, Mayne GC, Olejnicka B, Negre-Salvayre A, Sticha M, Coffey RJ, and Weber C. Induction of cancer cell apoptosis by alpha-tocopheryl succinate: molecular pathways and structural requirements. *FASEB J* 15: 403–415, 2001.
47. Ngo HB, Kaiser JT, and Chan DC. The mitochondrial transcription and packaging factor Tfam imposes a U-turn on mitochondrial DNA. *Nat Struct Mol Biol* 18: 1290–1296, 2011.
48. Oostveen FG, Au HC, Meijer PJ, and Scheffler IE. A Chinese hamster mutant cell line with a defect in the integral membrane protein CII-3 of complex II of the mitochondrial electron transport chain. *J Biol Chem* 270: 26104–26108, 1995.
49. Parsons DW, Jones S, Zhang X, Lin JC, Leary RJ, Angenendt P, Mankoo P, Carter H, Siu IM, Gallia GL, Olivi A, McLendon R, Rasheed BA, Keir S, Nikolskaya T, Nikolsky Y, Busam DA, Tekleab H, Diaz LA, Jr., Hartigan J, Smith DR, Strausberg RL, Marie SK, Shinjo SM, Yan H, Riggins GJ, Bigner DD, Karchin R, Papadopoulos N, Parmigiani G, Vogelstein B, Velculescu VE, and Kinzler KW. An integrated genomic analysis of human glioblastoma multiforme. *Science* 321: 1807–1812, 2008.
50. Ralph SJ, Rodriguez-Enriquez S, Neuzil J, and Moreno-Sanchez R. Bioenergetic pathways in tumor mitochondria as targets for cancer therapy and the importance of the ROS-induced apoptotic trigger. *Mol Aspects Med* 31: 29–59, 2010.
51. Rodriguez-Enriquez S, Hernandez-Esquivel L, Marin-Hernandez A, Dong LF, Akporiaye ET, Neuzil J, Ralph SJ, and Moreno-Sanchez R. Molecular mechanism for the selective impairment of cancer mitochondrial function by a mitochondrially targeted vitamin E analogue. *Biochim Biophys Acta* 1817: 1597–1607, 2012.
52. Rodriguez-Enriquez S, Marin-Hernandez A, Gallardo-Perez JC, Carreno-Fuentes L, and Moreno-Sanchez R. Targeting of cancer energy metabolism. *Mol Nutr Food Res* 53: 29–48, 2009.
53. Rohlena J, Dong LF, Kluckova K, Zobalova R, Goodwin J, Tilly D, Stursa J, Pecinova A, Philimonenko A, Hozak P, Banerjee J, Ledvina M, Sen CK, Houstek J, Coster MJ, and Neuzil J. Mitochondrially targeted alpha-tocopheryl succinate is antiangiogenic: potential benefit against tumor angiogenesis but caution against wound healing. *Antioxid Redox Signal* 15: 2923–2935, 2011.
54. Rohlena J, Dong LF, Ralph SJ, and Neuzil J. Anticancer drugs targeting the mitochondrial electron transport chain. *Antioxid Redox Signal* 15: 2951–2974, 2011.
55. Ross MF, Prime TA, Abakumova I, James AM, Porteous CM, Smith RA, and Murphy MP. Rapid and extensive uptake and activation of hydrophobic triphenylphosphonium cations within cells. *Biochem J* 411: 633–645, 2008.
56. Sasaki R, Suzuki Y, Yonezawa Y, Ota Y, Okamoto Y, Demizu Y, Huang P, Yoshida H, Sugimura K, and Mizushina Y. DNA polymerase gamma inhibition by vitamin K3 induces mitochondria-mediated cytotoxicity in human cancer cells. *Cancer Sci* 99: 1040–1048, 2008.

57. Scarpulla RC. Transcriptional paradigms in mammalian mitochondrial biogenesis and function. *Physiol Rev* 88: 611–638, 2008.
58. Scheffler IE. Mitochondria. 2008.
59. Shi Y, Dierckx A, Wanrooij PH, Wanrooij S, Larsson NG, Wilhelmsson LM, Falkenberg M, and Gustafsson CM. Mammalian transcription factor A is a core component of the mitochondrial transcription machinery. *Proc Natl Acad Sci U S A* 109: 16510–16515, 2012.
60. Smith RA, Porteous CM, Gane AM, and Murphy MP. Delivery of bioactive molecules to mitochondria *in vivo*. *Proc Natl Acad Sci U S A* 100: 5407–5412, 2003.
61. Stern RG, Milestone BN, and Gatenby RA. Carcinogenesis and the plasma membrane. *Med Hypotheses* 52: 367–372, 1999.
62. Sun F, Huo X, Zhai Y, Wang A, Xu J, Su D, Bartlam M, and Rao Z. Crystal structure of mitochondrial respiratory membrane protein complex II. *Cell* 121: 1043–1057, 2005.
63. Trachootham D, Alexandre J, and Huang P. Targeting cancer cells by ROS-mediated mechanisms: a radical therapeutic approach? *Nat Rev Drug Discov* 8: 579–591, 2009.
64. Umeda S, Muta T, Ohsato T, Takamatsu C, Hamasaki N, and Kang D. The D-loop structure of human mtDNA is destabilized directly by 1-methyl-4-phenylpyridinium ion (MPP+), a parkinsonism-causing toxin. *Eur J Biochem* 267: 200–206, 2000.
65. Vander Heiden MG, Cantley LC, and Thompson CB. Understanding the Warburg effect: the metabolic requirements of cell proliferation. *Science* 324: 1029–1033, 2009.
66. Wallace DC. A mitochondrial paradigm of metabolic and degenerative diseases, aging, and cancer: a dawn for evolutionary medicine. *Annu Rev Genet* 39: 359–407, 2005.
67. Wang XF, Birringer M, Dong LF, Veprek P, Low P, Swettenham E, Stantic M, Yuan LH, Zobalova R, Wu K, Ledvina M, Ralph SJ, and Neuzil J. A peptide conjugate of vitamin E succinate targets breast cancer cells with high ErbB2 expression. *Cancer Res* 67: 3337–3344, 2007.
68. Weber T, Dalen H, Andera L, Negre-Salvayre A, Auge N, Sticha M, Lloret A, Terman A, Witting PK, Higuchi M, Plasilova M, Zivny J, Gellert N, Weber C, and Neuzil J. Mitochondria play a central role in apoptosis induced by alpha-tocopheryl succinate, an agent with antineoplastic activity: comparison with receptor-mediated pro-apoptotic signaling. *Biochemistry* 42: 4277–4291, 2003.
69. Wu Z, Puigserver P, Andersson U, Zhang C, Adelmant G, Mootha V, Troy A, Cinti S, Lowell B, Scarpulla RC, and Spiegelman BM. Mechanisms controlling mitochondrial biogenesis and respiration through the thermogenic coactivator PGC-1. *Cell* 98: 115–124, 1999.

Address correspondence to:
Dr. Jiri Neuzil
Apoptosis Research Group
School of Medical Science
and the Griffith Institute of Health
Griffith University
Southport, Qld 4222
Australia

E-mail: j.neuzil@griffith.edu.au

Dr. Jaroslav Truksa
Molecular Therapy Group
Institute of Molecular Genetics
Academy of Sciences of the Czech Republic
Prague 142 20
Czech Republic

E-mail: truksaj@img.cas.cz

Dr. Lan-Feng Dong
Apoptosis Research Group
School of Medical Science
and the Griffith Institute of Health
Griffith University
Southport, Qld 4222
Australia

E-mail: l.dong@griffith.edu.au

Date of first submission to ARS Central, August 16, 2014; date of final revised submission, December 16, 2014; date of acceptance, January 1, 2015.

Abbreviations Used

CCCP = 4-(trifluoromethoxy)phenylhydrazone
CII = complex II
COX1 = cytochrome *c* oxidase 1 protein
DCF = 2′,7′-dichlorodihydrofluorescein diacetate
DHE = dihydroethidium
D-LOOP = displacement loop
EC = endothelial cell
EDTA = ethylenediaminetetraaceticacid
ETC = electron transport chain
FCS = fetal calf serum
GFP = green fluorescent protein
HER2 = human epidermal growth factor receptor 2
MIM = mitochondrial inner membrane
MitoC11 = mitochondrially targeted undecyl
MitoC7 = mitochondrially targeted heptyl
MitoQ7B = mitochondrially targeted quercetin-7-butyl
MitoR3B = mitochondrially targeted resveratrol-7-butyl
MitoVES = mitochondrially targeted vitamin E succinate
mtDNA = mitochondrial DNA
mTF = mitochondrial transcription factor
NAC = *N*-acetyl cysteine
NBE = native blue electrophoresis
nDNA = nuclear DNA
POLG = DNA polymerase γ
qPCR = quantitative polymerase chain reaction
ROS = reactive oxygen species
SQR = succinate quinone reductase
TMRM = tetramethylrhodamine
TPP^+ = triphenylphosphonium
UbQ = ubiquinone
USI = ultrasound imaging
VE = vitamin E
α-TEA = α-tocopheryl acetic acid ether
α-TOS = α-tocopheryl succinate

Evaluation of Respiration of Mitochondria in Cancer Cells Exposed to Mitochondria-Targeted Agents

Katarina Kluckova, Lan-Feng Dong, Martina Bajzikova, Jakub Rohlena, and Jiri Neuzil

Abstract

Respiration is one of the major functions of mitochondria, whereby these vital organelles use oxygen to produce energy. Many agents that may be of potential clinical relevance act by targeting mitochondria, where they may suppress mitochondrial respiration. It is therefore important to evaluate this process and understand how this is modulated by small molecules. Here, we describe the general methodology to assess respiration in cultured cells, followed by the evaluation of the effect of one anticancer agent targeted to mitochondria on this process, and also how to assess this in tumor tissue.

Key words Mitochondrial respiration, Cultured cells, Tumors, Mitochondria-targeted anticancer agents

1 Introduction

Mitochondria are organelles central to the maintenance of cellular metabolism and biosynthetic functions, as well as to cell death induction [1]. To supply the cell with ATP, mitochondria consume large amounts of oxygen in the electron transport chain (ETC), and electron leakage from the ETC makes mitochondria the major cellular site of reactive oxygen species (ROS) production [2]. All these aspects are deregulated in cancer, where metabolic reprograming, increased oxidative load and resistance to apoptosis are important features [3–5]. For these reasons, it has been suggested that mitochondria constitute a prospective target for anticancer treatment, and the agents that eliminate cancer cells by direct mitochondrial destabilization have been termed "mitocans" [6, 7].

A prominent position within this group is occupied by agents (so called class 5 of mitocans) that initiate cell death by ETC blockade, which results in the stimulation of ROS production and initiation of apoptosis [8]. This ETC inhibition will also have a

Volkmar Weissig and Marvin Edeas (eds.), *Mitochondrial Medicine: Volume II, Manipulating Mitochondrial Function*, Methods in Molecular Biology, vol. 1265, DOI 10.1007/978-1-4939-2288-8_14,

direct effect on the oxygen consumption by mitochondria, and changes in this parameter upon treatment may therefore help to pinpoint specific target sites for particular agents within the ETC. Several approaches are available to assess mitochondrial respiration, perhaps the most common being the monitoring of residual oxygen level in the assay medium by polarography-based measurements. High-resolution respirometry (HRR) is a development of this technique, using instrumentation, such as Oroboros Oxygraph, which allows for direct assessment of oxygen changes in small samples of cells and tissues [9]. As excellent and detailed protocols are available to the user interested in the general application of HRR [9, 10], this methodology chapter focuses on the specific issue of modulation of mitochondrial oxygen consumption in vitro and in vivo by mitocans and similar agents.

Several approaches are available to the user, and each of these approaches answers a somewhat different question. To assess the effect of a particular compound on mitochondrial respiration in more or less "native" conditions such as those encountered during in vitro cell culture experiments, protocols using intact cells (Subheading 3.1) should be chosen. On the other hand, if the goal is to determine the approximate site of action of the given compound within the ETC, then the use of permeabilized cells is mandatory (Subheading 3.2). Even though the cell membrane permeabilization in this protocol may not be very "native," it allows for the application of specific cell membrane-impermeable respiratory substrates that are required to assess the contribution of individual ETC complexes. Finally, the investigation of tumor tissue obtained directly from experimental animals is also possible, as described in Subheading 3.3. One has to be aware, however, that whereas the first two approaches allow the real time assessment of the compounds effect on the ETC, when the compound is administered to the animals before the collection of material, only a relatively long term effect (in the range of tens of minutes/hours) will be determined and no true inhibitory curves can be achieved. However, the user will gain information whether the tested compound is able to affect respiration when administered in vivo.

2 Materials

1. Oxygraph-2k high-resolution respirometry (HRR) instrument (Oroboros Instruments).
2. PBI tissue shredder SG3 (Oroboros Instruments).
3. Mitochondrial respiration medium Mir05:
   Weigh 0.190 g EGTA, 0.610 g $MgCl_2 \cdot 6H_2O$, 21.5 g Lactobionic acid, 2.502 g taurine, 1.361 g KH_2PO_4, 4.77 g

HEPES and 37.65 g sucrose . Add water to cca 900 mL, mix, warm to 30 °C and adjust pH to 7.1 with saturated KOH solution. Add 1 g essentially fatty acid free BSA and water to 1 L. Divide into 40 mL portions in 50 mL Falcon tubes and store frozen at –20 °C.

4. Mir06 medium (=Mir05+catalase): Add 125 µL catalase stock solution 112,000 U/mL, dissolve in Mir05 medium to 50 mL Mir05 medium, mix well (gently), store at –20 °C. Alternatively, Mir06 medium can be prepared by adding 5 µL catalase stock solution directly into the Oxygraph chamber filled with the cell sample in 2 mL of Mir05 medium at the beginning of experiment. The final working concentration of catalase is 280 U/mL.
5. Glutamate: For 2 M glumatate dissolve 7.48 g L-glutamic acid sodium salt in 20 mL water and neutralize with KOH. Aliquot and store at –20 °C.
6. Malate: For 0.8 M malate stock solution dissolve 2.146 g L-malic acid in 20 mL water. Neutralize with KOH. Aliquot and store at –20 °C.
7. Pyruvate: For 2 M stock solution weigh 44 mg of pyruvic acid sodium salt into a 1 mL Eppendorf tube and add 200 µL H_2O. Prepare fresh every day.
8. Succinate: For 1 M stock solution dissolve 5.4 g succinate disodium salt hexahydrate in 20 mL water and adjust pH to 7 with HCl. Aliquot and store at –20 °C.
9. ADP: For 200 mM stock solution dissolve 1 g of adenosine 5′-diphosphate monopotassium salt dihydrate in 10 mL of water. Adjust pH to 7 with KOH.
10. FCCP: For 1 mM stock solution dissolve 2.54 mg carbonyl cyanide p-(trifluoro-methoxy) phenyl-hydrazone (Sigma C2920) in 10 mL ethanol. Aliquot into 0.3 mL portions and store at –20 °C. Also the cheaper alternative CCCP may be used.
11. Rotenone: For 1 mM stock solution dissolve 1.97 mg rotenone in 5 mL ethanol. Aliquot and store at –20 °C. It is light-sensitive and therefore should be shielded from direct light.
12. Malonate (Mna): For 1 M stock solution dissolve 2.602 g of malonic acid in 25 mL of water and adjust pH to 7 with KOH. Aliquot and store frozen at –20 °C.
13. Antimycin A (Ama): For 5 mM solution dissolve 11 mg antimycine A in 4 mL ethanol. Aliquot and store at –20 °C.
14. Digitonin: Dissolve 10 mg digitonin in 1 mL DMSO, aliquot and store at –20 °C.
15. Cytochrome c: For 4 mM stock solution dissolve 50 mg cytochrome c in 1 mL water. Aliquot and store frozen at –20 °C.

16. Hydrogen peroxide—Reoxygenation. Pipette 11.4 μL of 17.6 M H_2O_2 into 1 mL tube, add H_2O to the final volume of 1 mL to obtain 200 mM stock solution. Wrap the tube with aluminum foil and store in fridge. Titrate 3 μL of hydrogen peroxide (200 mM) to the chamber when oxygen level is below 50 nmol/mL.

3 Methods

These methods are useful to understand whether mitochondrially targeted compounds suppress respiration. As an example, we use mitochondrially targeted vitamin E succinate (MitoVES) that we synthesized and found to be very efficient in suppressing cancer by means of accumulating in mitochondria and acting via complex II [11–13]. For the structure of MitoVES and the parental untargeted α-tocopheryl succinate (α-TOS) as well as the non-apoptogenic vitamin E (α-tocopherol, α-TOH), *see* Fig. 1.

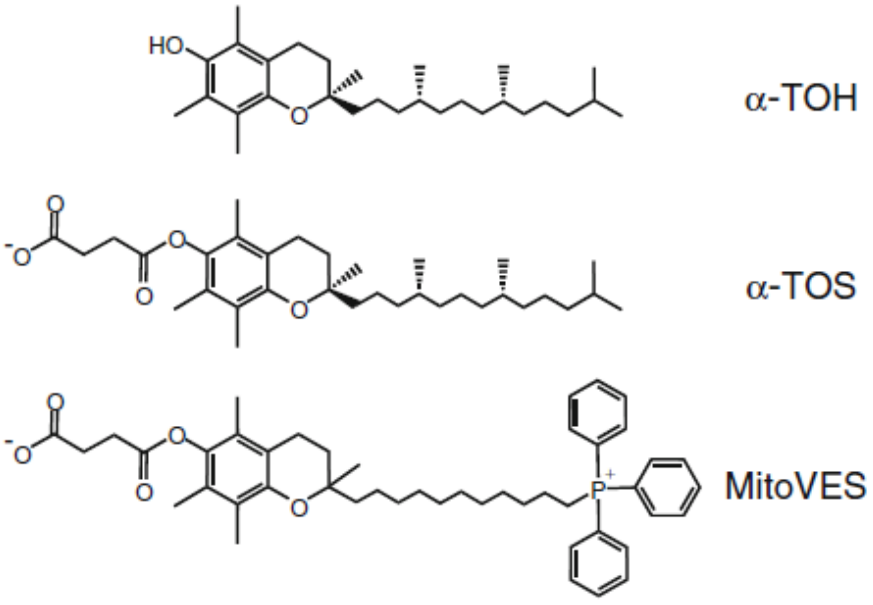

Fig. 1 Structures of vitamin E (α-tocopherol, α-TOH), α-tocopheryl succinate (α-TOS), and mitochondrially targeted vitamin E succinate (MitoVES). The figure shows the structure of the non-apoptogenic α-TOH, of α-TOS that is derived from α-TOS by succinylation of its hydroxyl group and that has a strong apoptogenic activity, and that of MitoVES derived from α-TOS by tagging its aliphatic C-11 chain (without the branched methyl groups) with the delocalized cationic triphenylphosphonium group. MitoVES has additional 1–2 orders of magnitude gain in apoptogenic and anticancer activity compared to α-TOS [11–13, 15]

3.1 Inhibition of Respiration of Intact Cells with Mitochondrially Targeted Compounds

1. Harvest the cells by trypsinization, collect about 5×10^6 of cells (*see* **Notes 1** and **2**).
   Spin cells down for 5 min at $300 \times g$, wash the pellet once with PBS and spin down again and resuspend the cells immediately in 4.5–5 mL of the appropriate medium. Place the resuspended cells in the oxygraph chamber calibrated to 2.1 mL and let them stir for a short while. Then take an aliquot to count the precise number of cells, slowly close the chamber and siphon off the excess liquid that comes out through the stopper. Lift the stopper again as in the calibration protocol and let the signal stabilize for a few minutes. During this time count the cells and type the exact amount in the DatLab software.
2. After signal stabilization close the chamber. The oxygen consumption starts to rise; when it is stable again, start to add increasing concentrations of the tested compounds (*see* **Note 3**). After each step mark the stabilized area of the signal (*see* **Note 4**).
3. When the oxygen consumption is inhibited almost to zero or is not decreasing any further, terminate the measurement.
4. Add 1 µL of 5 mM antimycin to fully inhibit mitochondrial respiration. This inhibits the oxygen consumption completely and is referred to as ROX (residual oxygen consumption). This value should be subtracted from all the values measured when performing final evaluation and data plotting in order to discount non-mitochondrial sources of oxygen consumption (normally these are quite small compared to the contribution of mitochondria) and obtain mitochondria-specific effect.
5. An example of respiration evaluation in intact cells is presented in Fig. 2.

3.2 Inhibition of Specific Substrate-Driven Respiration in Permeabilized Cells

1. Harvest cells by tripsinization as in the case of measurement of intact cells.
2. Close the chamber, after which the oxygen consumption starts to rise. Wait until the signal is stabilized and add 1 µL of digitonin solution per 10^6 cells (*see* **Note 5**). Wait 5–10 min until the oxygen consumption drops significantly and becomes stabilized. For complex I assessment, proceed to **step 3**. When complex II study is planned, however, add 1 µL of rotenone solution to inhibit respiration through complex I, which prevents formation of oxaloacetate, a powerful complex II inhibitor. Oxygen consumption drops almost to zero at this point.
3. Add 25 µL of ADP solution followed by 10 µL glutamate plus 5 µL malate or 5 µL pyruvate plus malate for complex I measurements, or 20 µL succinate solution for complex II measurements. Oxygen consumption will rise, and therefore wait for stabilization of the signal and check for additional increase with 5 µL ADP and 5 µL cytochrome c solutions (*see* **Note 6**).

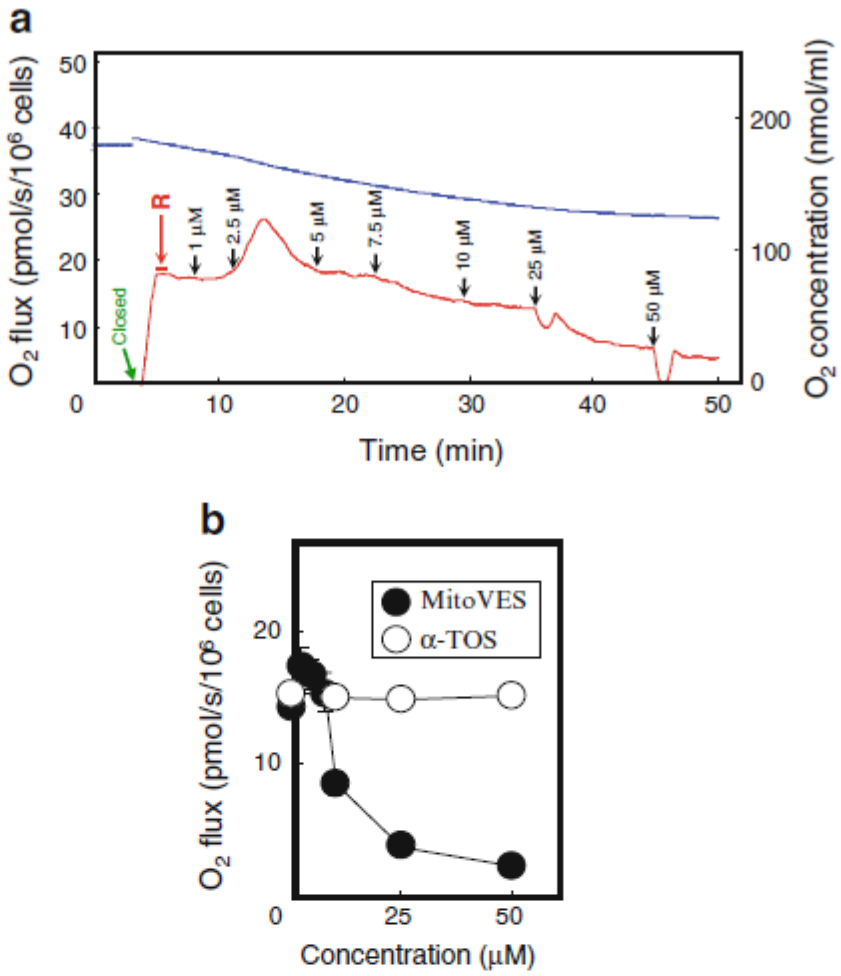

Fig. 2 Evaluation of the effect of MitoVES on respiration of non-permeabilized cells. (**a**) Mouse mesothelioma tumor cells (AE17) were harvested and placed in the chamber of the Oxygraph 2 k instrument at 10^6 per mL in the original medium. After closing of chamber, the system was allowed for oxygen consumption to stabilize to "routine" respiration®. After this, MitoVES was added at increasing concentrations (1–50 µM) and oxygen consumption read at each point. (**b**) Using the experimental approach described in panel (**a**), the effects of MitoVES and α-TOS on respiration of AE17 cells was assessed. Adapted from ref. 15

4. If you wish to inhibit coupled respiration, start adding the inhibitor in small steps at this point. In case of inhibiting the uncoupled state, add FCCP solution in 1–2 µL steps until there is no additional rise in the respiration and then start adding your inhibitor (*see* **Notes 3**, **4** and 7).
5. When the respiration is inhibited almost to zero or is not decreasing any further, finalize the experiment by adding 1 µL of antimycine solution.
6. When evaluating the data, you can plot the exact amount of oxygen consumption recorded after each titration, or you can set the maximal respiration to 100 % and plot it against increasing concentration of the inhibitor. This will allow you

to compare different inhibitors or different cell lines and determine the IC_{50} value. If both respiration via complex I and complex II is inhibited, this means that the site of action for the given inhibitor may be further downstream, for example at complex III. Alternatively, both complex I and CII may be inhibited by such compound.

7. An example of respiration evaluation in permeabilized cells and its inhibition by mitochondrially targeted anticancer agents in shown in Fig. 3.

3.3 Evaluation of Respiration of Tumor Tissue After Treatment of Animals with Experimental Carcinomas with Mitochondrially Targeted Agents

Treat the animals with your desired compound according to your protocol of choice. Use appropriate solvent controls.

1. After excision from the animal, place the tumor quickly in a 50 mL tube containing 30 mL cold Mir05 and store on ice for as short time as possible.
2. Transfer the tumor into a petri dish (on ice) containing ice-cold Mir05.
3. Cut the tumor with a cold blade using cold forceps on the petri dish, then withdraw a small piece of the tissue (of the wet weight around 15–20 mg) from the solid region of the tumor.
4. Dry the water on the surface of the tumor specimen with filter paper.
5. Cut the tumor tissue quickly into small pieces and transfer them into the shredder ram tube (pre-rinsed with 100 µL Mir05 medium). Quickly insert the shredder ram using the shredder tube tool with a twisting motion until the sample is pressed between the serrated surface and the lysis disk.
6. Add 700 µL of ice-cold Mir05 into the cap side of the tube, and cap the tube with the shredder screw cap using the shredder tube tool.
7. Place the shredder tube with the tissue into the shredder base with the ram side down. Then place the SG3 driver onto the cap.
8. Shred the tumor tissue at gear 1 (position 1) for 8 s plus gear 2 (position 2) for 6 s (*see* **Note 8**).
9. Open the shredder tube using the shredder tube tool, transfer the tumor homogenate into a micro-centrifuge tube, dilute with proper volume of the Mir05 medium to obtain the concentration of 2–3 mg protein/mL (*see* **Note 9**).
10. Transfer 2.3 mL of tumor tissue homogenate to each chamber of the Oxygraph, keep the chambers open and incubate the samples for 3 min with the stirrer on to saturate with oxygen before closing the chambers. After the oxygen consumption level is stabilized, substrates or inhibitors are titrated to each chamber according to the following protocol. Oxygen consumption levels are evaluated.

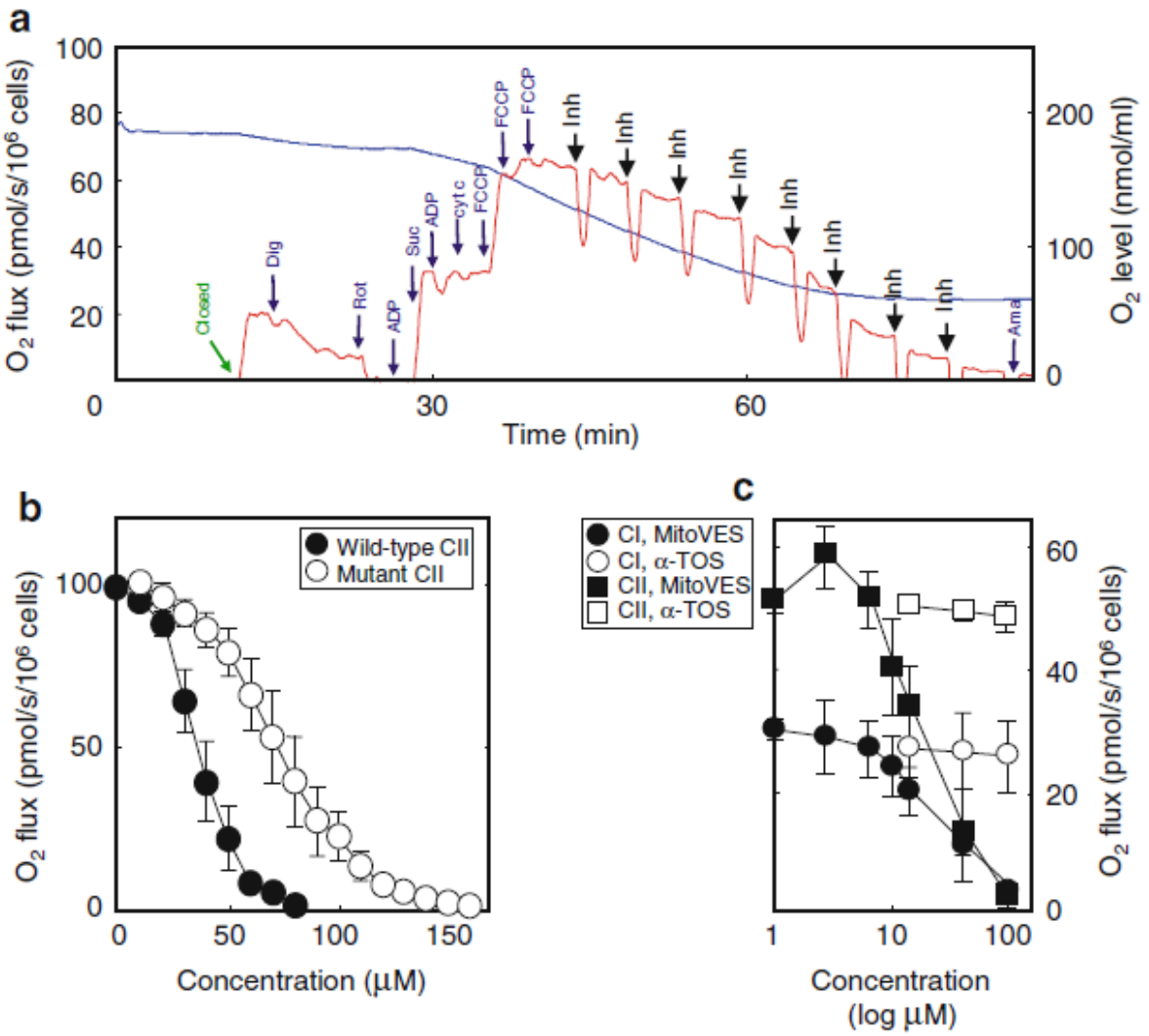

Fig. 3 Evaluation of respiration of permeabilized cells and the effect of mitochondrially targeted vitamin E succinate. (**a**) The experiment was performed as described in Subheading 3.2. After closing the oxygraph chamber and stabilization of the signal, digitonin (dig) was added to permeabilize the plasma membrane of the cells. Rotenone (Rot), ADP, succinate (Suc) and cytochrome c (Cyt c) were added subsequently. FCCP was titrated in the chamber until there was no additional increase in oxygen consumption. At this point the stepwise titration of the inhibitor (MitoVES shown here) started. The experiment was terminated by the addition of antimycine (Ama). (**b**) Example of the final evaluation and presentation of the recorded data (experiments performed as shown in panel (**a**)) showing that the inhibitor was less effective in cells with mutated CII. The calculated corresponding IC_{50} vaules were 35.01 and 66.22 μM. (**c**) Human mesothelioma cells were evaluated after permeabilization with digitonin and in the presence of increasing concentrations of α-TOS or MitoVES for respiration via complex I or complex II using the method described in Subheading 3.2. The results document that the cells respire some 40 % more via CII, which is also more sensitive to the inhibitory activity of MitoVES, while α-TOS does not possess almost any inhibitory activity towards complex I and complex II. Panels (**a**) and (**b**), unpublished data, panel (**c**), adapted from ref. 15

3.4 Protocol for Titrating Substrates or Inhibitors to Oxygraph Chambers

1. PMG: pyruvate + malate + glutamate—substrates of CI, showing CI-linked LEAK state (GM_L): Add 5 µL pyruvate, 5 µL malate and 10 µL glutamate to each chamber. The oxygen consumption level indicates the non-phosphorylating resting state with substrates for complex I.
2. D: Add 10 µL ADP to each chamber, repeat this step until saturated respiration is reached. This indicates CI-linked OXPHOS capacity (GM-P): The respiration is stimulated by saturating level of ADP.
3. C: cytochrome c test for quality control (GM_cP): Addition of 5 µL cytochrome c provides a test for the integrity of the outer mitochondrial membrane: Loss of cytochrome c would be indicated by a stimulation of respiration (*see* the discussion on cytochrome c in **Note 6**).
4. S: succinate—substrate of CII: Add 20 µL of succinate to stimulate the convergent electron flow from CI + CII at the Q-junction, as an estimate of physiological OXPHOS, which indicates CI + CII-linked OXPHOS capacity (GMS_P).
5. F: Titrate 1 µL of the uncoupler FCCP in several consecutive steps until the maximum respiration level is reached, indicating the maximum oxygen flux in the non-coupled state as a test for the limitation of OXPHOS by the phosphorylation system relative to ETS capacity. This indicates maximum reachable (CI + CII)-linked electron transfer system (ETS) capacity (GMS_E).
6. Rot: rotenone—inhibitor of CI: Add 1 µL of rotenone, indicating CII-linked ETS capacity (S(Rot)_E). After blocking CI, ETS capacity is supported only by succinate (respiration via uncoupled complex II).
7. Mna: malonate—inhibitor of CII. Add 5 µL of malonic acid; Ama: antimycin A—inhibitor of CIII: Add 1 µL of antimycin A: After complete inhibition of respiration by malonate and antimycin, it is possible in this way estimate the oxidative "side reactions" referred to as residual oxygen consumption (ROX).

Figure 4 shows an example of acquired data and their analysis.

3.5 Summary and Conclusions

The methodology described here uses the HRR approach with the Oroboros oxygraph as the primary instrument and focuses on the assessment of ETC inhibition. Even though this is not a high throughput method, the possibility to measure the increasing concentrations of an inhibitor in one oxygraph chamber is quite advantageous. In addition, the measurement of ex vivo material is relatively easy in this setup. It should be emphasized at this point that the user has the possibility, when in possession of an optional O2k—Fluorescence LED2 module, to follow simultaneously with

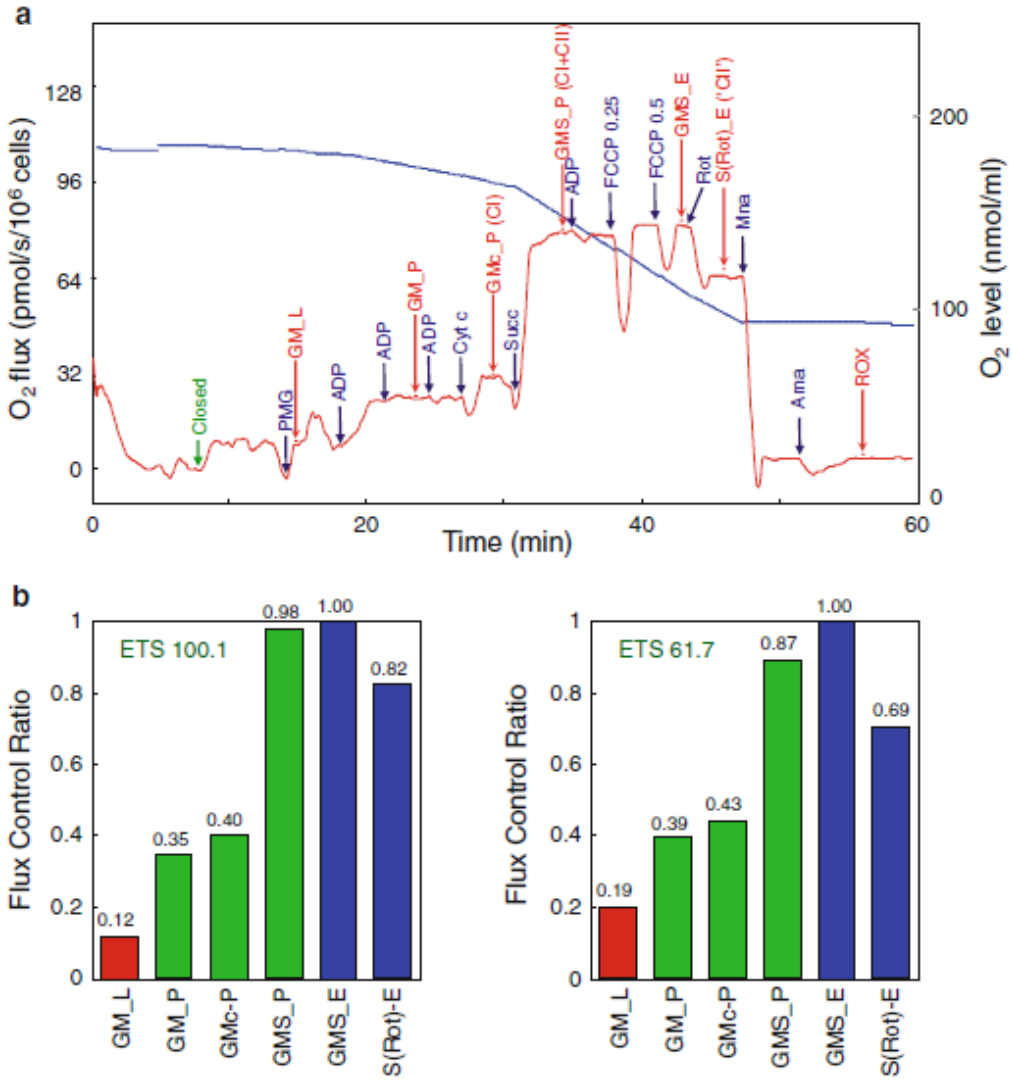

Fig. 4 MitoVES suppresses respiration via complex II but not complex I in experimental breast carcinomas. (**a**) Transgenic FVB/N *c-neu* mouse with spontaneous formation of $HER2^{high}$ breast carcinoma was allowed to develop a tumor (approximately within 7 months of age). When the tumor reached about 250 mm^3, the mouse was sacrificed and the tumor excised. The tissue was processed and respiration assessed as described in the text above (Subheading 3.3). (**b**) Respiration was evaluated for LEAK (GM_L), CI (GM_P), CI (cyt c) (GMc_P), CI + CII (GMS_P), ETS (GMS_E) and "CII" (uncoupled CII) (S(rot)-E) in a control tumor (*left panel*) and a tumor from a mouse treated with MitoVES (*right panel*), as follows: the animal was injected intraperitoneally with 1 μmol MitoVES dissolved in corn oil (control mouse with the excipient) five times on every third or fourth day before the tumor was harvested. The data indicate that the contribution of respiration via complex II was lower in the MitoVES-treated animal (comparing CI and CI + CII for the control and treated mice) and that respiration via uncoupled control II ("CII") was suppressed for the MitoVES-treated animal compared to the control one. These data indicate that MitoVES suppresses tumor respiration in vivo primarily by acting on complex II, the documented molecular target of its activity [11–13]. Panels (**a**) and (**b**), unpublished data

the measurement of respiration also the associated level of ROS generation. This approach allows for quantification of hydrogen peroxide produced during respiration using the Amplex Red probe and peroxidase, and couples the ROS response to the degree of ETC inhibition. Even though only isolated mitochondria can be

used at present (with permeabilized cells the fluorescent signal for hydrogen peroxide is too unstable), this provides an elegant method for coupling respiratory measurements to, for example, apoptotic efficiency of a given compound, which is often related to the level of ROS generated and determines the overall efficacy of the anticancer effect.

4 Notes

1. To compare the effects of different compounds, it is recommended to use similar conditions such as:
   (a) Number of cells—Cell number will influence the efficacy of the tested compounds. It is also important to take into consideration the rate of respiration of the used cell lines in order not to run out of oxygen in the chamber during the experiment.
   (b) Confluency—Passage the cells 1 day before respiration assessment to use the cells in the same phase of the cell cycle and when approximately 60–70 % confluent.
   (c) Media—The media used for evaluation of respiration should be as close to the cultivation media as possible, since different types of media may differ in the level of substrates and oxygen solubility, especially when comparing media with fetal calf serum and serum-free media. The concentration of simple saccharides such as glucose in the medium will also substantially affect the observed respiration (the so called Crabtree effect).
   (d) Concentration of the tested compound and the type of solvent—It is recommended to use the same stock solution of the tested compound and the same solvent in order not to confound the acquired data.
2. The number of cells that should be placed in the chamber for the experiment depends on how much they respire and how pronounced the inhibition of respiration using the compounds of interest is. In case the cells feature low level of respiration, more cells will be needed to achieve sufficiently strong and stable signal. In case respiration of a particular cell line is very high and you wish to observe inhibition of respiration in small steps, it is better to use lower number of cells so that they will not run out of oxygen during the experiment. For example, when working with cells respiring around 40 pmol/s per one million cells when starting the inhibition, 2×10^6 cells per chamber should be optimal for a 1 h evaluation.
3. After addition of low concentration of MitoVES (1–2 μM), we observed a rapid initial increase in respiration, most likely due to mitochondrial uncoupling.

4. It is likely that when adding the inhibitor, the signal of oxygen consumption will not stabilize and there will be a very slow decrease of the signal during the measurement. You will need to define time intervals at which you add the inhibitor rather than wait for stabilization of the signal. Try to finish the experiment in less than 1 h. If you want to plot your graph on the basis of more points, choose shorter intervals (2–4 min). Ideally use the second oxygraph chamber as a control chamber with the same sample and add only the solvent with each inhibitor addition to the first chamber. In this case you can correct for decreasing respiration that might occur in time and that is not linked to the specific inhibition, and subtract the difference when evaluating the data. Also, the potential effect of solvent is accounted for in this way [14].
5. The concentration of digitonin should be optimized before performing any experiments depending on cell lines. Even though for most cell lines the concentration of 5 μg of digitonine per million cells will probably work well, the user is encouraged to titrate the evaluated cells with digitonin in the presence of rotenone (0.5 μM; rotenone stops endogenous respiration in intact cells by inhibiting NADH removal) and succinate (10 mM—cannot pass the intact cell membrane). Add digitonin in small steps in several minute intervals, until the rate of respiration starts to rise. This means that the cell membrane starts to dissolve and succinate is getting inside the cells. Optimal digitonin concentration is the one after which another addition of digitonin does not raise the respiration rate any more. Do not use higher concentrations, as this could destabilize also mitochondrial outer membrane and inhibit respiration. For this reasons it is better not to prolong the time of permeabilization and wait only for signal stabilization even if the oxygen consumption is not inhibited almost to zero. Alternatively, saponin may be used as a permeabilization agent.
6. The first addition of ADP should be sufficient to saturate the system; however, it is better to check if there is no increase in the oxygen consumption after another addition of ADP. Cytochrome c is added to make sure that the outer mitochondrial membrane is intact, as documented by no additional increase in oxygen consumption. This is the ideal case, but with some cells a small increase can occur. You might try handling cells with more care (shorter preparation time before the actual experiment or adding less digitonin); in case nothing works, you can still go on with the experiment as long as you add sufficient amount of cytochrome c solution. Even if there is no increase in oxygen consumption after cytochrome c addition, be sure to add at least 5 μL, because during longer experiments mitochondria will lose their integrity (and endogenous

cytochrome c), thus the data you record in this system can confound your results.

7. Here are two options. You can measure inhibition of a particular complex under conditions of respiration coupled to ATP synthesis (closer to the physiological state). Alternatively, you can uncouple the system from the synthesis of ATP using FCCP or alternatively CCCP, and observe the effect of the inhibitor when the respiratory chain is operating at its maximal capacity.
8. The harder the tissue is, the higher gear and longer times are required for shredding.
9. When tissue has higher respiration activity, for example liver, lower the tissue amount in each chamber.

Acknowledgements

This work was supported in part by grants from the National and Health Medical Research Council and the Australian Research Council, and by BIOCEV European Regional Development Fund CZ.1.05/1.1.00/02.0109 and Czech Science Foundation grant no. P301-12-1851.

References

1. Galluzzi L, Kepp O, Trojel-Hansen C, Kroemer G (2012) Mitochondrial control of cellular life, stress, and death. Circ Res 111: 1198–1207
2. Murphy MP (2009) How mitochondria produce reactive oxygen species. Biochem J 417:1–13
3. Hanahan D, Weinberg RA (2011) Hallmarks of cancer: the next generation. Cell 144:646–674
4. Trachootham D, Alexandre J, Huang P (2009) Targeting cancer cells by ROS-mediated mechanisms: a radical therapeutic approach? Nat Rev Drug Discov 8:579–591
5. Vander Heiden MG, Cantley LC, Thompson CB (2009) Understanding the Warburg effect: the metabolic requirements of cell proliferation. Science 324:1029–1033
6. Fulda S, Galluzzi L, Kroemer G (2010) Targeting mitochondria for cancer therapy. Nat Rev Drug Discov 9:447–464
7. Neuzil J, Dong LF, Rohlena J, Truksa J, Ralph SJ (2013) Classification of mitocans, anti-cancer drugs acting on mitochondria. Mitochondrion 13:199–208
8. Rohlena J, Dong LF, Ralph SJ, Neuzil J (2011) Anticancer drugs targeting the mitochondrial electron transport chain. Antioxid Redox Signal 15:2951–2974
9. Pesta D, Gnaiger E (2012) High-resolution respirometry: OXPHOS protocols for human cells and permeabilized fibers from small biopsies of human muscle. Methods Mol Biol 810: 25–58
10. Kuznetsov AV, Veksler V, Gellerich FN, Saks V, Margreiter R, Kunz WS (2008) Analysis of mitochondrial function in situ in permeabilized muscle fibers, tissues and cells. Nat Protoc 3:965–976
11. Dong LF, Jameson VJ, Tilly D, Cerny J, Mahdavian E, Marin-Hernandez A, Hernandez-Esquivel L, Rodriguez-Enriquez S, Stursa J, Witting PK, Stantic B, Rohlena J, Truksa J, Kluckova K, Dyason JC, Ledvina M, Salvatore BA, Moreno-Sanchez R, Coster MJ, Ralph SJ, Smith RA, Neuzil J (2011) Mitochondrial targeting of vitamin E succinate enhances its pro-apoptotic and anti-cancer activity via mitochondrial complex II. J Biol Chem 286:3717–3728

12. Dong LF, Jameson VJ, Tilly D, Prochazka L, Rohlena J, Valis K, Truksa J, Zobalova R, Mahdavian E, Kluckova K, Stantic M, Stursa J, Freeman R, Witting PK, Norberg E, Goodwin J, Salvatore BA, Novotna J, Turanek J, Ledvina M, Hozak P, Zhivotovsky B, Coster MJ, Ralph SJ, Smith RA, Neuzil J (2011) Mitochondrial targeting of α-tocopheryl succinate enhances its pro-apoptotic efficacy: a new paradigm for effective cancer therapy. Free Radic Biol Med 50:1546–1555
13. Rohlena J, Dong LF, Kluckova K, Zobalova R, Goodwin J, Tilly D, Stursa J, Pecinova A, Philimonenko A, Hozak P, Banerjee J, Ledvina M, Sen CK, Houstek J, Coster MJ, Neuzil J (2011) Mitochondrially targeted α-tocopheryl succinate is antiangiogenic: potential benefit against tumor angiogenesis but caution against wound healing. Antioxid Redox Signal 15: 2923–2935
14. Hroudova J, Fisar Z (2012) In vitro inhibition of mitochondrial respiratory rate by antidepressants. Toxicol Lett 213:345–352
15. Kovarova J, Bajzikova M, Vondrusova M, Stursa J, Goodwin J, Nguyen M, Zobalova R, Pesdar EA, Truksa J, Tomasetti M, Dong LF, Neuzil J (2014) Mitochondrial targeting of α-tocopheryl succinate enhances its anti-mesothelioma efficacy. Redox Rep 19:16–25

Ubiquinone-binding site mutagenesis reveals the role of mitochondrial complex II in cell death initiation

Running title: Mechanism of cell death initiation by complex II

K Kluckova,[1] M Sticha,[5] J Cerny,[1] T Mracek,[2] L Dong,[3] Z Drahota,[2] E Gottlieb,[4] J Neuzil,[1,3,*] and J Rohlena[1,*]

[1]Institute of Biotechnology and [2]Institute of Physiology, Academy of Sciences of the Czech Republic, Prague, Czech Republic, [3]School of Medical Science, Griffith University, Southport, Qld, Australia, [4]The Beatson Institute for Cancer Research, Glasgow, United Kingdom, [5]Faculty of Sciences, Charles University, Prague, Czech Republic

Correspondence: Jiri Neuzil, Mitochondria, Apoptosis and Cancer Research Group, School of Medical Science and Griffith Health Institute, Griffith University, Southport, Qld 4222, Australia; e-mail: j.neuzil@griffith.edu.au; or Jakub Rohlena, Molecular Therapy Group, Institute of Biotechnology, Academy of Sciences of the Czech Republic, 142 20 Prague 4, Czech Republic; email: jakub.rohlena@ibt.cas.cz.

ABSTRACT
Respiratory complex II (CII, succinate dehydrogenase, SDH) inhibition can induce cell death, but the mechanistic details need clarification. To elucidate the role of reactive oxygen species (ROS) formation upon the ubiquinone binding (Q_p) site blockade, we substituted CII subunit C (SDHC) residues lining the Q_p site by site-directed mutagenesis. Cell lines carrying these mutations were characterized on the bases of CII activity and exposed to Q_p site inhibitors MitoVES, TTFA and Atpenin A5. We found that I56F and S68A SDHC variants, which support succinate-mediated respiration and maintain low intracellular succinate, were less efficiently inhibited by MitoVES than the wild-type variant. Importantly, associated ROS generation and cell death induction was also impaired, and cell death in the wild-type cells was malonate- and catalase-sensitive. In contrast, the S68A variant was much more susceptible to TTFA inhibition than the I56F variant or the wild-type CII, which was again reflected by enhanced ROS formation and increased malonate- and catalase-sensitive cell death induction. The R72C variant that accumulates intracellular succinate due to compromised CII activity was resistant to MitoVES and TTFA treatment and did not increase ROS, even though TTFA efficiently generated ROS at low succinate in mitochondria isolated from R72C cells. Similarly, the high affinity Q_p site inhibitor Atpenin A5 rapidly increased intracellular succinate in wild-type cells but did not induce ROS or cell death, unlike MitoVES and TTFA that upregulated succinate only moderately. These results demonstrate that cell death initiation upon CII inhibition depends on ROS and that the extent of cell death correlates with the potency of inhibition at the Q_p site unless intracellular succinate is high. In addition, this validates the Q_p site of CII as a target for cell death induction with relevance to cancer therapy.

Keywords
Complex II, succinate dehydrogenase, ubiquinone-binding site, cell death, reactive oxygen species, mitochondria, electron transport chain.

INTRODUCTION

Mitochondrial respiratory complex II (CII), aka succinate dehydrogenase (SDH), directly links the tricarboxylic acid (TCA) cycle to the electron transport chain (ETC) by mediating electron transfer from the TCA cycle metabolite succinate to ubiquinone (UbQ).[1] For this reason, CII is subjected to a high electron flux between the succinate-binding dicarboxylate site in the matrix-exposed SDHA subunit and the proximal UbQ-binding (Q_p) site, formed by the SDHC and SDHD subunits embedded in the mitochondrial inner membrane (Fig. 1B).[2-5] Disruption of electron transfer to UbQ, for example by Q_p site inhibition, leads to ROS generation from CII due to the leakage of 'stalled' electrons to molecular oxygen at the reduced flavin adenine dinucleotide (FAD) prosthetic group. However, ROS production from reduced FAD is only possible when the adjacent dicarboxylate site is neither occupied by its substrate succinate, typically at low succinate conditions, nor inhibited by other dicarboxylates, for example by malonate. [6-10]

Beyond bioenergetics, CII has emerged as an important factor in cell death induction.[11, 12] On the one hand, it has been proposed that increased ROS production from CII, resulting from changes in matrix pH and calcium status, amplifies cell death signals originating at other sites.[12-15] On the other hand, inhibition of CII may also directly initiate cell death, as suggested by our previous results with vitamin E (VE) analogues such as the mitochondrially targeted vitamin E succinate (MitoVES). This compound inhibits CII activity leading to ROS generation and cell death induction in cancer cells, as evidenced by the suppression of tumour growth in experimental animal models. [16-20] The efficacy of MitoVES is greatly reduced in the absence of functional CII, and computer modelling along with other corroborative evidence suggests that MitoVES binds to the Q_p site of CII.[16] However, this is only circumstantial evidence with respect to cell death induction, as cells lacking electron flux within CII due to a structural defect should not be able to produce CII-derived ROS. Accordingly, not only the direct cell death initiation upon CII inhibition will be compromised in this situation, but also the indirect signal amplification mentioned above will be affected.

In the present study, we combined site-directed mutagenesis of Q_p site amino acid residues with the use of Q_p site inhibitors MitoVES, thenoyltrifluoroacetone (TTFA) and Atpenin A5 to assess the link between Q_p site inhibition and cell death initiation. We show that for MitoVES and TTFA, the potency of Q_p site inhibition correlates with the extent of ROS production and cell death induction in respiration-competent CII variants, and that the induced cell death is dependent on CII-derived ROS.

Atpenin, however, did not induce cell death, possibly due to rapid accumulation of succinate in intact cells, incompatible with ROS generation from CII. These results provide evidence for the role of CII in cell death initiation and establish the Q_p site as a target for cell death induction.

RESULTS

CII Q_p site mutagenesis and the experimental model. To explore the role of CII in cell death induction, we performed site-directed mutagenesis within SDHC, a CII subunit that contributes to Q_p site formation.[3] We concentrated on SDHC residues predicted to be in close contact with bound MitoVES. Serine 68 was mutated to alanine, arginine 72 was replaced by cysteine, and isoleucine 56 was substituted by phenylalanine (Fig. 1). Recent data indicate reduced cell death induction by MitoVES in the S68A variant,[16] but the functional consequences of this mutation for CII activity have not been studied. Nevertheless, substitutions of S68 as well as of R72 are expected to compromise CII activity, based on analogy with *E.coli* and *S. cerevisiae* SDH.[21-24] The I56 residue is further away from the Q_p site, and its role in CII function is unknown. To evaluate these substitutions, we utilized a mammalian model of SDHC deficiency, the Chinese hamster lung fibroblast cell line B9.[25] These cells lack the functional CII due to a nonsense mutation in the SDHC subunit and fail to assemble CII. In consequence they do not respire on succinate and are completely devoid of CII enzymatic activity. Stable transfectants of human wild-type (WT) and variant SDHC cDNA were prepared in B9 cells, and clones with similar level of SDHC were selected. These cells were further transformed by H-Ras fused to GFP, making them plausible models to study the effect of MitoVES and other Q_p site inhibitors on

transformed cells (Fig. S1). Transformants with similar level of H-Ras were selected to control for H-Ras level.

Q_p site mutations differentially affect CII assembly and enzymatic function. The selected clones did not significantly differ in their mitochondrial content, as evidenced by similar citrate synthase activity and mitochondrial protein levels (Fig. 2A, B). Mitochondrial morphology and membrane potential were also similar for all tested cell lines (Fig. 2C, D). To verify CII assembly, mitochondrial fractions were subjected to blue native gel electrophoresis and western blotting using an anti-SDHA antibody. As expected, parental B9 cells did not assemble CII. In contrast, CII was fully assembled in WT and most of the SDHC variant cells (Fig. 2E), with a minor assembly defect found for R72C variant. These results were confirmed using an in-gel SDH activity assay (Fig. 2E), which documented assembled CII with functional dicarboxylate site in all variants except for B9 cells. To assess the condition of the Q_p site and its functional coupling to the dicarboxylate site, succinate-ubiquinone reductase (SQR) activity in the mitochondrial fraction was determined. While no SQR activity was measurable in B9 cells (Fig. 2F), it was high in WT and I56F clones. For S68A and R72C variants the SQR activity was significantly reduced yet remained above the level of parental B9 cells. This suggests that while CII assembles properly in all tested variants, there is a defect in electron transfer to ubiquinone in the S68A and R72C variants.

Q_p site mutations differentially affect basal CII-driven respiration under native conditions. As the CII activity assays described above were done on solubilized enzyme, we also examined the effect of Q_p site mutations on CII-mediated respiration in a more natural environment of permeabilized cells. In this setup respiratory substrates can reach mitochondria, but the mitochondrial outer and inner membranes remain intact in their 'native', undisturbed condition.[26] In the presence of the CII substrate succinate, WT, S68A and, in particular, I56F cells efficiently consumed oxygen. In contrast, R72C and parental B9 cells showed little or no respiration (Fig. 3A). The uncoupler FCCP significantly increased oxygen consumption in WT and I56F, but not in S68A, R72C or B9 cells (Fig. 3A). Hence, the S68A mutation only affects the reserve capacity of this mutant and may not be limiting in intact cells. In contrast, a severe defect in R72C CII substantially compromises its ability to support respiration. To confirm these findings in intact cells, we determined the steady state levels of intracellular succinate, a proxy for CII activity.[27] As shown in Fig. 3B, succinate concentration in WT, I56F and S68A cells was low, consistent with fully functional CII. On the other hand, in B9 and R72C cells the succinate levels were considerably increased. These data demonstrate that whereas B9 and R72C cells cannot utilize succinate for respiration due to the absent or dysfunctional CII, WT, I56F and S68A cells maintain CII respiration under coupled conditions expected to occur in a physiological situation.

Q_p site mutations compromise the efficacy of cell death induction by MitoVES. Should cell death induction by the VE analogue MitoVES be dependent on its binding to the Q_p site of CII as our previous work suggested,[16] then the efficacy of this agent would be compromised in Q_p site mutants. Hence, the variant cell lines were exposed to MitoVES, a compound previously described to induce apoptosis,[17] and the percentage of annexin V-positive cells quantified. The induced cell death displayed signs typical for apoptosis (Fig. S2A, B), and was significantly reduced in all tested variant cell lines compared to WT cells (Fig. 4A). In fact, all substitutions in the Q_p site reduced MitoVES-induced cell death nearly to the level observed in parental B9 cells. Given the absence of assembled CII in B9 cells, this basal level of cell death must be CII-independent and possibly related to the direct effect of MitoVES on cytochrome c.[28]

As ROS generation is the pivotal, early event in the cell death-initiating cascade induced by MitoVES,[16, 17] we assessed ROS production in cultured cells upon MitoVES treatment with dihydroethidium (DHE), a fluorescent probe responsive to superoxide. Compared to WT, all Q_p site variant cells showed reduced ROS formation, which remained at the level similar to that of parental B9 cells (Fig. 4B). In addition, catalase overexpression and co-treatment with the dicarboxylate site inhibitor malonate reduced cell

death and ROS production in WT cells to the level found in the mutants (Fig. 4C, D, E). These data indicate that the Q_p site mutations decrease the efficacy of MitoVES-induced ROS generation and that the induced cell death depends on CII-derived ROS.
Mitochondrial glycerophosphate dehydrogenase (GPD2) feeds electrons into the mitochondrial UbQ pool similarly to CII and can also produce ROS. It has recently been shown that alpha tocopheryl succinate (αTOS), an untargeted analogue of MitoVES, inhibits GPD2 activity in brown adipose tissue (BAT).[29] However, it is unlikely that GPD2 is responsible for the observed ROS and cell death induction upon MitoVES treatment in our experimental model, as the GPD2 levels are much lower than in BAT (Fig. S2D). In addition, GPD2 inhibition by αTOS decreases, rather than increases, GPD2-derived ROS[29], and MitoVES accumulation at the inner mitochondrial membrane/matrix interface[16] owing to the mitochondria-targeting triphenyl phosphonium group will keep it physically separated from the intermembrane space-localised GPD2. The role of the reverse electron flow from GPD2 to FAD[6] in CII and subsequent ROS generation from that site can also be discounted, as this would be inhibited, not stimulated, by MitoVES bound to the Q_p site. Therefore, CII functioning in the forward manner is the likely source of ROS observed upon MitoVES treatment of intact cells.

Sensitivity to Q_p site inhibition correlates with efficacy of cell death induction unless succinate is rapidly accumulated. If the attenuated ROS and cell death induction described above resulted from reduced displacement of UbQ by MitoVES at the Q_p site of variant CII, then these variants should display resistance to inhibition by MitoVES. For this reason, we assessed the effect of increasing concentrations of MitoVES on CII-driven respiration at high succinate (10 mM). Only respiration-competent variants, i.e. WT, I56F and S68A lines were used in this experiment. As shown in Fig. 5A, the efficacy of respiration inhibition was reduced for I56F and S68A variants compared to WT cells, in direct correlation with the observed decrease in ROS levels and cell death induction (c.f. Fig. 4A, B). In contrast to MitoVES, malonate suppressed oxygen consumption similarly for all CII variants tested (Fig. 5B), confirming that the mutations introduced do not substantially affect the dicarboxylate site.
To better understand this phenomenon, we performed *in silico* molecular docking simulation of MitoVES and UbQ with the Q_p site of WT and variant CII. These simulations support the assumption that steric hindrance and differences in affinity can explain less efficient inhibition by MitoVES in S68A and I56F CII (Fig. S3B, C). Since MitoVES is a relatively large molecule (Fig. S3A), we also examined the much smaller Q_p site inhibitor TTFA using the same methodology. Surprisingly, the highest TTFA binding affinity was calculated for the Q_p site of the S68A variant (Fig. S3C). We therefore evaluated oxygen consumption in the presence of increasing concentrations of this smaller Q_p site inhibitor (Fig. 5C) and found that while for the I56F variant the inhibition by TTFA was similar to WT cells, the S68A variant was inhibited much more efficiently. For this reason we speculated that the S68A mutation could also lead to enhanced cell death induction by TTFA, which is known to induce apoptosis.[14] Indeed, while ROS and cell death were significantly increased in S68A cells, only limited ROS and cell death induction were observed in B9, I56F, R72C and WT cells upon TTFA treatment (Figs. 5D, E). Features typical of apoptotic cell death were observed (Fig. S2A, C), and catalase overexpression or malonate treatment reduced cell death and ROS in S68A cells more than in WT cells (Fig. 5F, G, H). These results suggest a direct correlation between the potency of Q_p site inhibition, CII-mediated ROS production, and the extent of ensuing cell death for MitoVES as well as TTFA.
Surprisingly, the CII Q_p site inhibitor Atpenin A5,[24, 30] despite efficient suppression of respiration in WT and I56F cells (Fig. 5I), did not induce cell death or ROS production (Fig. 5 J, K). In contrast to MitoVES and TTFA, Atpenin caused rapid increase of intracellular succinate in intact cells (Fig. 5L), which is incompatible with ROS generation from CII. Hence, CII inhibition results in cell death only when succinate accumulation is not too rapid and ROS can efficiently be produced.

ROS generation in isolated mitochondria correlates with effective Q_p site inhibition at low succinate. To establish the link between ROS production and CII inhibition, we assessed these two parameters simultaneously in isolated mitochondria by combining the Amplex Red method of ROS

detection with oxygen consumption measurements. We used 0.5 mM succinate, because this concentration closely reflects its non-pathological intracellular levels (c.f. Fig. 3B) and favours direct ROS production from CII.[6, 7] Exposure of WT cell mitochondria to increasing concentrations of MitoVES resulted in considerable stimulation of ROS production. In contrast, ROS generation was limited in S68A and I56F mitochondria (Fig. 6A). A modest level of ROS production was also observed in R72C mitochondria, indicating that the low respiration rate of this mutant can still support ROS generation in response to its inhibition. As expected, no ROS increase upon MitoVES treatment was detected in mitochondria from parental B9 cells, which do not assemble CII (Fig. 6B). In addition, induction of ROS by MitoVES was malonate-sensitive, confirming the involvement of CII (Fig. 6C). Evaluation of oxygen consumption revealed reduced sensitivity of CII variants to inhibition compared to WT mitochondria. This effect was visible at higher concentrations of the inhibitor (Fig. 6D), which, importantly, is within the concentration range where ROS induction becomes apparent (c.f. Fig. 6A). Finally, no stimulation of ROS production by MitoVES could be detected at high succinate concentration (10 mM) for any of the variants tested (Fig. 6E), which was confirmed by their insensitivity to malonate (Fig. 6F).

Compared to MitoVES, ROS induction by TTFA followed a different pattern. While for the I56F variant it was similar to WT, much more ROS were generated by S68A cell mitochondria (Fig. 7A). This is in agreement with the very high sensitivity of this mutant to the inhibition by TTFA (Fig. 5C). Surprisingly, induction of ROS in R72C mitochondria was also increased, which is supported by computer modelling and is expected to occur only at low succinate not encountered in intact R72C cells (see Discussion for details; c.f. Figs. 3B, 5E, S3C). In contrast, no ROS production was induced in B9 cell mitochondria (Fig. 7B). Similarly to MitoVES, TTFA-induced ROS generation was suppressed by malonate (Fig. 7C), directly implicating CII.

With non-saturating concentrations of succinate, the build-up of oxaloacetate may lead to CII inhibition at the dicarboxylate site,[6, 7, 31] complicating interpretation of the results. Oxaloacetate accumulation is prevented in the presence of the CI inhibitor rotenone, which at the same time limits reverse electron transfer to CI.[8, 32] The inclusion of rotenone in experiments did not substantially alter the response to either MitoVES (Fig. S4) or TTFA (Fig. S5), excluding these additional factors. In summary, these results demonstrate that MitoVES and TTFA induce ROS from CII in direct proportion to their ability to achieve Q_p site inhibition at low, physiological succinate, which in turn correlates with the efficacy of cell death induction.

DISCUSSION

In the last decade it has become clear that various complexes of the mitochondrial ETC play a multifaceted role in the execution of cell death.[33-35] CII has received particular attention as a target of experimental anti-cancer agents, and the inhibition of the Q_p site of CII was shown to induce cell death in cancer cells *in vitro* and *in vivo*.[16, 36, 37] Clear evidence was missing, however, because the potential function of CII as an amplifier of pro-death signals originating elsewhere should also be considered.[13, 14] In principle, it cannot be excluded that a given compound, anticipated to engage the Q_p site of CII, triggers a pro-death signal further upstream, followed by indirect amplification of this signal at CII. It is impossible to distinguish between these two scenarios using cellular models where CII is not assembled, or is inhibited at the dicarboxylate site. Hence, to demonstrate the autonomous role of CII in cell death induction, functional CII is required.

The CII Q_p site variants I56F and S68A employed in this report respire on succinate similarly to WT under native conditions, yet display alterations in cell death induction upon Q_p site ligation with MitoVES and TTFA. The level of cell death induction directly correlates with the efficacy of inhibition of succinate-driven respiration by these agents. Accordingly, both variants were relatively resistant to the inhibition by MitoVES and to cell death induced by this agent, whereas the S68A variant, which is more efficiently inhibited by TTFA, underwent proportionally higher level of cell death upon TTFA treatment. This likely stems from altered ability of the two inhibitors to displace UbQ at the Q_p site of the individual variant proteins. Indeed, experimental data could be explained by different binding

affinities and various degrees of steric hindrance computationally predicted for variant Q_p sites (Fig. S3). These observations are consistent with the direct, autonomous role of CII in cell death initiation by these agents, and cannot be reconciled with the role of CII as a mere amplifier of upstream effects originating at other sites. The engagement of cell death induction pathways unrelated to CII can be also discounted. In the latter scenarios, all variants retaining CII activity would behave similarly, which is clearly not the case. Compared to WT cells, the variant cell lines show lower response to MitoVES but higher (or similar) level of cell death upon TTFA treatment. This indicates that the mutations are not associated with non-specific defects in cell death induction in our system, and excludes CII-unrelated ROS sources such as GPD2. Accordingly, this study establishes, for the first time, a direct connection between CII inhibition at the Q_p site and initiation of cell death.

In sub-mitochondrial particles, it has been previously established that CII can produce ROS upon Q_p site inhibition only when FAD is reduced and the dicarboxylate site is unoccupied. [7, 38] In intact cells, this introduces an additional level of complexity, because the lack of enzymatically active CII will result in the accumulation of its substrate succinate due to the poor membrane permeability of this metabolite.[27] Succinate then might block the dicarboxylate site and restrict oxygen access to FAD, attenuating ROS production.[6] Indeed, the R72C mutation associated with low residual enzymatic activity of CII did not reduce TTFA-dependent induction of ROS in isolated mitochondria where succinate is low (Fig 7B, S5B), but suppressed TTFA-induced ROS and cell death in intact cells where succinate is high (Figs. 3B, 5D, E). Similarly, Atpenin A5, a high affinity Q_p site inhibitor,[24, 30] did not induce ROS and cell death in intact cells (Fig. 5J, K) in this and an unrelated[39] study, even though it had been previously shown to efficiently generate ROS from CII in sub-mitochondrial particles, where succinate cannot accumulate.[7] We propose that in intact cells the blockade of the dicarboxylate site of Atpenin-inhibited CII, possibly by oxaloacetate as reported[6] or by the rapidly accumulated succinate (Fig. 5L), is the likely reason for this discrepancy. This is consistent with the known behaviour of CII and suggests that CII is the bona fide source of ROS in intact cells upon Q_p site inhibition. Furthermore, co-treatment with dicarboxylate site inhibitor malonate suppressed ROS generation and cell death upon MitoVES and TTFA administration in responsive cell lines, and MitoVES/TTFA-induced cell death was catalase-sensitive (Figs. 4C, D, E and 5F, G, H). We therefore suggest that cell death will be induced only when the Q_p site is inhibited in a manner that allows ROS to be generated (Fig. 8). Accordingly, Q_p site inhibition that is too efficient or rapid, such as with Atpenin, will suppress all CII activity and reduce FAD, but at the same time block the dicarboxylate site by succinate (or other dicarboxylate), quenching ROS formation. Slower, less efficient inhibition, such as with MitoVES or TTFA, will leave some CII molecules unoccupied, slowing down succinate accumulation such that the Q_p site-blocked CII molecules can produce ROS and induce cell death. Reduction of Q_p site inhibition by mutations that do not reduce CII activity will then leave insufficient number of Q_p site-blocked CII molecules to generate ROS, whereas mutations that compromise CII activity will upregulate succinate, limiting ROS production from FAD.

In conclusion, the data presented in this study provide support for the direct role of CII in cell death initiation by demonstrating a clear correlation between the efficacy of inhibition at the Q_p site of CII and the magnitude of cell death in respiration-proficient CII variants for Q_p site inhibitors that do not excessively upregulate succinate. Despite being focused on CII, our results may also be relevant for other ETC complexes, as many ETC inhibitors reported to promote cell death also modulate cell death pathways independent of the ETC. For example, the CI inhibitor rotenone destabilizes microtubules,[40, 41] and the CII inhibitor α-TOS as well as the complex III inhibitor antimycin act as BH3 mimetics.[42, 43] To our knowledge, it has never been unequivocally shown for any of these compounds that ETC inhibition is instrumental in cell death induction by correlating ETC inhibitory efficacy of a single compound at any of the ETC complexes with the extent of cell death. Hence, this report defines the Q_p site of CII as a suitable target for cytotoxic agents and demonstrates that ETC targeting may present a potential clinically relevant approach to cancer treatment.[44]

MATERIALS AND METHODS

Chemicals and reagents. All chemicals and reagents were from Sigma, unless otherwise stated. MitoVES was synthesized in house as described earlier.[16] Atpenin A5 was from Enzo Life Sciences.

Cell culture. Parental cells and variant cell lines were cultured in high glucose (4.5g/L) DMEM medium (Lonza) supplemented with 10% FCS, non-essential amino acids (both Life Technologies) and antibiotics at 37 ºC and 5% CO_2. Eahy926 cells were cultured as described.[18]

Q_p site mutagenesis and the generation of variant cell lines. Generation of the S68A variant was described earlier.[16] For other variants, site-directed mutagenesis of human wt SDHC cDNA was performed in the pEF-IRES-PURO expression vector using the QuickChange Lightening mutagenesis kit (Stratagene) and the following mutagenesis primers: I56F, 5'-gtcctctgtctccccactttactatctacagttgg-3' (forward), 5'-ccaactgtagatagtaaagtggggagacagaggac-3' (reverse), R72C, 5'-gatgtccatctgccactgtggcactggtattgc-3' (forward), 5'-gcaataccagtgccacagtggcagatggacatc-3' (reverse). The sequences were confirmed by DNA sequencing and used to transfect the SDHC-deficient B9 fibroblasts using the Attractene reagent (Qiagen), followed by incubation with 2-4 μg/ml puromycin for two weeks. Clones were analyzed for the expression of human SDHC by RT-PCR and those selected were stably transfected with pEGFP-C3-H-Ras as described with the exception of using Attractene for transfections,[36] after which transfectants with similar level of GFP-H-Ras expression were selected. Total RNA was collected, and the presence of the variant transcript was verified by cDNA sequencing.

Quantitative Real time-PCR. Was performed essentially as described.[16] Primers for human SDHC detection were 5'-cacttccgtccagaccggaac-3' (forward) and 5'-atgctgggagcctcctttcttca-3' (reverse).

Western blotting. Cells were lysed in RIPA buffer (150 mM NaCl, 1.0% Nonidet NP-40, 1% sodium deoxycholate, 0.1% SDS, 50 mM Tris, pH 8.0) supplemented with protease and phosphatase inhbibitors for 30 minutes with shaking on ice. Protein content was determined by the BCA assay (Pierce). Samples were boiled for 5 min in reducing loading buffer before separation on SDS-PAGE gels. Wet blotting was used to transfer the separated samples to nitrocellulose membranes (Whatman). Immunoblotting was done in TBS/tween supplemented with 5% non-fat dried milk overnight at 4 ºC. Following antibodies were used: anti-H-Ras (Santa Cruz sc-520), anti-actin HRP labeled (Cell Signaling, 5125), unlabeled actin (Millipore, MAB1501, used for Fig. 2B), anti-cleaved caspase 3 (Cell Signaling, 9664), anti-catalase (Abcam, Ab1877), Anti-Vdac1/porin (Abcam, ab15895), anti-SDHA (Abcam, ab14715), anti-ATPase alpha subunit (Abcam, ab14748). Rabbit polyclonal antibody to GPD2 was custom prepared.[45] HRP-conjugated secondary antibodies were used in TBS/tween with 5% non-fat dried milk for 1 h at room temperature. WB signals were quantified using the Aida 3.21 Image Analyzer software (Raytest).

Mitochondria isolation. Mitochondria isolation was performed according to a recently described method, with some adaptations.[46] Cells were released by trypsin, washed in PBS, and 40-50x10^6 cells were transferred to 5mL of mitochondria isolation buffer (200 mM sucrose, 1mM EGTA, 10 mM Tris/Mops pH 7.4). The cell suspension was homogenized by three passes through a cell homogenizer (Isobiotec) set to 10 μm clearance using 5 mL syringe (SGE, 5MDF-LL-GT) at 0.5 mL/min flow at 4 ºC. The homogenate was centrifuged (at 4 ºC) at 800g for 8 min, supernatant was collected and pre-cleared at 3000g for 5 min. The final collection of mitochondrial pellet was done at 10000g for 15 min. Protein content was determined by the BCA assay. The mitochondria were undamaged, viable and well coupled, as determined by respirometry (see below) from their reaction to the addition of ADP (about 5x increase in respiration), FCCP (substantial increase of respiration) and cytochrome c (no or very little increase in respiration).

Blue native electrophoresis. Isolated mitochondria were solubilized in the extraction buffer (1.5 M aminocaproic acid, 50 mM Bis-Tris, 0.5M EDTA, and pH 7) containing 1.3% lauryl maltoside or 8 g digitonin / g protein. Samples comprising 20-30 μg of protein were then mixed with the sample buffer (0.75 M aminocaproic acid, 50 mM Bis-Tris, 0.5M EDTA, pH 7, 5% Serva-Blue G-250, and 12% glycerol) and loaded on the precast NativePAGE Novex 4–16% Bis-Tris gels (Life Technologies) and run overnight at a constant voltage of 25 V. Separated protein complexes were then transferred to the PVDF membrane (Millipore), using the Trans-Blot Turbo transfer system (Biorad). CII was detected with the anti-SDHA (2E3) antibody (Abcam, AB14715-200).

In-gel SDH activity. 20-30 μg of lauryl maltoside or digitonine solubilized mitochondria (see above) were mixed with sample buffer containing 50 % glycerol with 0.1 % Ponceau dye and run on the precast NativePAGE Novex 4–16% Bis-Tris gel at constant voltage of 100 V, which was raised to 500 V after the samples entered the separation gel. 0.05 % deoxycholate and 0.01 % lauryl maltoside were added to the cathode buffer for higher resolution as described.[47] Gels with separated protein complexes were incubated for 30 min in assay buffer containing 20 mM sodium succinate, 0.2 mM phenazine methosulfate and 0.25 % nitro tetrazolium blue in 5 mM Tris/HCl, pH 7.4. The reaction was stopped using solution of 50 % methanol and 10 % acetic acid and gels were immediately photographed.

SQR activity measurement. 25 μg of mitochondria were incubated in 200 μL of 25mM phosphate potassium buffer (pH 7.4) containing 0.1 % Triton X-100, 20 mM succinate, 2μM antimycine, 5μM rotenone, 10mM sodium azide, 50 μM decylubiquinone for 3-5 min in 96 well plate. After 30 s recording of the measurement at 600 nm, 10 μl of 2,6-dichlorphenol indophenol (0.015% w/v) was added and the reaction was recorded for another 2-3 minutes. Identical measurements were performed in the presence of 20 mM malonate, and the net SQR activity was obtained by subtracting malonate-insensitive rates.

Mitochondrial membrane potential measurements. Cells were seeded in 12-well plates a day before the experiment. On the day of experiment, one well was used to determine total cellular protein by BCA. The rest of the cells were collected by trypsin, washed with PBS, and resuspended in Mir05 medium (see below) at 0.5 mg/mL concentration with 10 mM succinate, 2 mM malate, 10 mM glutamate, 3 mM ADP and 20 nM TMRM. Next, 60 uL of this cell suspension was permeabilized with 0.1 μg digitonin per μg protein for 5 min at room temperature, and immediately measured on LSR-II flow cytometer (Beckton-Dickinson) for the TMRM fluorescence signal. Finally, 0.2 uL of 1mM CCCP was added and the TMRM signal after uncoupling was assessed. The relative mitochondrial membrane potential was determined as the ratio of TMRM signal before and after the addition of CCCP (f/f_0).

Confocal microscopy. Live confocal images were obtained basically as described[48] with minor modifications. The cells in complete medium in microscopy glass bottom dishes were incubated with 250 ng/ml Hoechst 33342 nuclear stain and 10 nM TMRM for 15 minutes and imaged with 63x oil immersion lens at the heated stage of an SP5 confocal microscope (Leica Microsystems). 2 μm thick stacks were obtained, deconvoluted with the Huygens Professional software (SVI) and presented as maximal intensity projections.

Determination of intracellular succinate. Cells were cultured for 24 h, washed with PBS, scrapped and extracted in 96% ethanol in a cold methanol bath. Extracts corresponding to equal number of cells were used in further analysis (10^6 cells per 1.6 mL). After addition of the internal standard the extracts were dried under argon stream. Afterwards, 50 μL of benzyl alcohol and 30 μL of TMS-chloride were added to the dried samples, and the closed Eppendorf tubes were placed in the ultrasonic bath (room temperature, 45 min) and in an oven (80 °C, 45 min). A final volume of 500 μL was adjusted by adding acetonitrile. Quantification of the derivatized acids was performed with an LC–ESI/MS system (Bruker Esquire 3000), in positive ionization mode. The mass spectrometer was connected to a liquid chromatography system of the 1100/1200 series from Agilent Technologies. Reversed-phase separation of the derivatives was performed on a Supelcosil 150 × 4.6 mm column with a silica-based C-18 stationary phase (5-μm particle diameter). The mobile Phase A was acetonitrile and Phase B was H_2O, 0.1% formic acid. Agilent ChemStation for LC 3D systems B01.03 was used to control the instruments and for data processing. The gradient program was 0 min 50% B, from 0 to 8 min to 5% B and at 20 min back to the initial conditions of 50% B. The injection volume was 10 μL. The LC separation and the ESI settings of the Esquire instrument were optimized utilizing a dibenzyl oxalate as an internal standard. Intracellular succinate concentration was calculated using average cell diameter of 14 μm.

Measurement of CII respiration in permeabilized cells. Cells were collected by trypsinization, washed in PBS, resuspended in Mir05 medium (0.5 mM EGTA, 3mM $MgCl_2$, 60 mM K-lactobionate, 20 mM taurine, 10 mM KH_2PO_4, 110 mM sucrose, 1 g/L essentially fatty acid-free BSA, 20 mM Hepes, pH 7.1 at 30 ºC) and transferred to the chamber of the Oroboros Oxygraph-2k (Oroboros Instruments) for respiration measurements at 37 ºC. The chamber was closed when the oxygen signal became stable,

and after recording the routine respiration on intracellular substrates the plasma membrane was permeabilized by 10 μg digitonin per million cells. The CII respiration was determined in the presence of 0.5 μM rotenone, 10 mM succinate, 3 mM ADP and 10 μM cytochrome c. The maximal respiration in the uncoupled state was then achieved by FCCP titration in 0.5 μM steps. 2.5 μM antimycin A was added at the end to inhibit ETC, and the residual oxygen consumption after antimycin addition was subtracted from all results to obtain the mitochondria-specific rates.

Inhibition of CII respiration. Cells were permeabilized as above, and the effect of CII inhibitors was assessed in the presence of 10 mM succinate, 3 mM ADP, 0.5 μM rotenone, 10 μM cytochrome c and FCCP. The inhibitors (MitoVES, TTFA, Atpenin A5 or malonate) were titrated to the chamber in regular intervals (5 min) and the rate of oxygen consumption was assessed after each addition.[49] Solvent only was titrated into control chambers in parallel to check for non-specific effects and cell deterioration, but the respiration rates remained virtually unaffected (less than 10% decrease at the end of the experiment). Respiration rates after 2.5 μM antimycin A addition were subtracted to obtain mitochondria-specific rates.

Simultaneous measurements of ROS production and oxygen consumption in isolated mitochondria. The chambers of the Oroboros Oxygraph instrument equipped with the O2k-Fluorescence LED2-Module (Oroboros Instruments) were calibrated at 37 ºC with the Budapest-modified respiration medium (120 mM KCl, 20 mM HEPES, 10 mM KH_2PO_4, 2.86 mM $MgCl_2$, 0.2 mM EGTA, 0.025 % BSA, pH 7). After closing the chambers, Amplex Ultra Red (Life Technologies) and peroxidase were injected (at final concentrations 5 μM and 1 U/mL, respectively), followed by the addition of 200 μg of isolated mitochondria, 0.5 μM rotenone (where indicated), 0.5 or 10 mM succinate and 3 mM ADP. The tested inhibitors were titrated as above, and the amount of hydrogen peroxide generated was determined based on the conversion of Amplex Ultra Red to the highly fluorescent product resorufin[50] using excitation LED 525 nm equipped with the Amplex red filter set. Oxygen consumption was recorded simultaneously in the same chamber. 5 mM malonate was added at the end of the titration experiment to confirm that the signal is succinate-dependent. After this, hydrogen peroxide of known concentration was titrated to the chamber in several steps to calibrate the fluorescence signal. Finally, 2.5 μM antimycin A was added to subtract non-specific respiration rates.

ROS measurement in intact cells. The cells were seeded in 12 well culture plates and grown for 24 h. To start the experiment, tested compounds were added to the culture medium and after 15 min, dihydroethidium was added to the final concentration of 20 μM. After another 15 min, the cells were harvested by trypsin, and oxidized ethidium fluorescence was measured on a LSR-II flow cytometer (Becton Dickenson) and expressed as mean fluorescence intensity.

Cell death measurements. Cells were seeded in 12 well culture plates and grown for 24 h. After that, tested compounds were added as indicated. Medium was collected after the required incubation time, the adherent cells were washed by PBS and harvested by trypsin. All these fractions were combined, washed by PBS and incubated with PE- or Dy647-labelled annexin V (Beckton Dickinson, Apronex) in the supplied binding buffer for at least 10 minutes. Hoechst 33258 was added to mark the cells with ruptured cell membrane. Annexin V-positive fraction was measured by flow cytometry. The results were expressed as the percentage of annexin V-positive cells. For the catalase experiments, cells were transfected two days before the experiment with a control or catalase-containing vector (a kind gift of Dr. S Lortz)[51] using the Fugene transfection reagent (Promega) according to manufacturer's instruction.

Computer modelling. The structure of wild type human mitochondrial complex II was obtained as a homology model based on the highly homologous template of the porcine CII[3] (pdb id 1zoy, sequence identity 95, 96, 92, and 88% for SDHA to SDHD) using the Modeller suite of programs.[52] The single point SDHC mutations (I56F, S68A, R72C) were then introduced using the FoldX program,[53] which was also used to optimize the side chain rotamers within the WT as well as mutated structures. All the structures were further subjected to a short (10 ns, implicit solvation) molecular dynamics (MD) run in order to relax the potentially non-equilibrium structures. The MD was prepared and performed using the GPU version of the GROMACS suite of programs[54] as implemented in the OpenMM Zephyr package.[55] Average structures from second half of the simulations were further used for the docking study. The

docking study of the MitoVES, TTFA, and ubiquinone ligands/inhibitors to a series of mutated mitochondrial complex II structures was performed using the autodock suite of programs.[56] The ligands were docked into the homology model of human CII and its single point mutants using Python Molecular Viewer version 1.5.6rc3.[57] Each ligand was allowed to sample docking poses in a box (70x70x70 grid points with 0.375 Å spacing) centered at the level of the ubiquinone binding site (based on the crystal structure). The side chains of residues surrounding the binding site were considered flexible. A series of four separate "local search" runs of 50 cycles each was performed and results combined to find the most stable poses.

Statistical analysis. Statistical analysis was performed using GraphPad Prism 6 software. Statistical significance was determined by oneway ANOVA followed by Dunnett's post test. For pair-wise comparisons (Figs. 3A, 4C,D,E, 5F,G,H, 6C, 7C, S4C, S5C) we used unpaired t-test. $p \leq 0.05$ was considered statistically significant. The value of n indicates the number of independent experiments.

Acknowledgements

The authors are grateful to Dr. Christian Frezza (MRC, Cambridge, UK) for critically reading the manusript, to Dr. Stephan Lortz (Hannover Medical School, Hannover, Germany) for the gift of the catalase overexpression vector and to Dr. Lydie Plecita-Hlavata for consultations. This work was supported by Czech Science Foundation grant no. P301-12-1851 and EMBO travel fellowship to JR, National and Health Medical Research Council of Australia and the Australian Research Council to JN and LFD, Czech Science Foundation grant 14-36804G to TM as well as by BIOCEV European Regional Development Fund CZ.1.05/1.1.00/02.0109

Conflict of interest.

The authors declare no conflict of interest.

Abbreviations

αTOS - alpha tocopheryl succinate, CII - respiratory complex II = SDH - succinate dehydrogenase, CCCP - Carbonyl cyanide 3-chlorophenylhydrazone, DHE – dihydroethidium, ETC – electron transport chain, FAD - flavin adenine dinucleotide, FCCP - carbonyl cyanide 4-(trifluoromethoxy)phenylhydrazone, GFP – green fluorescence protein, GPD2 – mitochondrial glycerophosphate dehydrogenase, MitoVES – mitochondrially-targeted vitamine E succinate, Q_p site – proximal ubiquionone binding site , ROS – reactive oxygen species, SDHC – subunit C of SDH, SQR - succinate-ubiquinone reductase, TCA - tricarboxylic acid, TTFA – thenoyltrifluoroacetone, TMRM - tetramethylrhodamine methyl ester, UbQ – ubiquinone, VE – vitamin E

Supplementary information

Supplementary information is available at Cell Death and Disease's website

References

1. Cecchini G. Function and structure of complex II of the respiratory chain. *Annu Rev Biochem* 2003; **72:** 77-109.
2. Maklashina E, Cecchini G. The quinone-binding and catalytic site of complex II. *Biochim Biophys Acta* 2010 Dec; **1797**(12)**:** 1877-1882.
3. Sun F, Huo X, Zhai Y, Wang A, Xu J, Su D, *et al.* Crystal structure of mitochondrial respiratory membrane protein complex II. *Cell* 2005 Jul 1; **121**(7)**:** 1043-1057.
4. Iverson TM. Catalytic mechanisms of complex II enzymes: a structural perspective. *Biochim Biophys Acta* 2013 May; **1827**(5)**:** 648-657.
5. Huang LS, Sun G, Cobessi D, Wang AC, Shen JT, Tung EY, *et al.* 3-nitropropionic acid is a suicide inhibitor of mitochondrial respiration that, upon oxidation by complex II, forms a

covalent adduct with a catalytic base arginine in the active site of the enzyme. *J Biol Chem* 2006 Mar 3; **281**(9)**:** 5965-5972.
6. Quinlan CL, Orr AL, Perevoshchikova IV, Treberg JR, Ackrell BA, Brand MD. Mitochondrial complex II can generate reactive oxygen species at high rates in both the forward and reverse reactions. *J Biol Chem* 2012 Aug 3; **287**(32)**:** 27255-27264.
7. Siebels I, Drose S. Q-site inhibitor induced ROS production of mitochondrial complex II is attenuated by TCA cycle dicarboxylates. *Biochim Biophys Acta* 2013 Oct; **1827**(10)**:** 1156-1164.
8. Moreno-Sanchez R, Hernandez-Esquivel L, Rivero-Segura NA, Marin-Hernandez A, Neuzil J, Ralph SJ, *et al.* Reactive oxygen species are generated by the respiratory complex II--evidence for lack of contribution of the reverse electron flow in complex I. *FEBS J* 2013 Feb; **280**(3)**:** 927-938.
9. Messner KR, Imlay JA. Mechanism of superoxide and hydrogen peroxide formation by fumarate reductase, succinate dehydrogenase, and aspartate oxidase. *J Biol Chem* 2002 Nov 8; **277**(45)**:** 42563-42571.
10. Zhang L, Yu L, Yu CA. Generation of superoxide anion by succinate-cytochrome c reductase from bovine heart mitochondria. *J Biol Chem* 1998 Dec 18; **273**(51)**:** 33972-33976.
11. Kluckova K, Bezawork-Geleta A, Rohlena J, Dong L, Neuzil J. Mitochondrial complex II, a novel target for anti-cancer agents. *Biochim Biophys Acta* 2013 May; **1827**(5)**:** 552-564.
12. Grimm S. Respiratory chain complex II as general sensor for apoptosis. *Biochim Biophys Acta* 2013 May; **1827**(5)**:** 565-572.
13. Hwang MS, Schwall CT, Pazarentzos E, Datler C, Alder NN, Grimm S. Mitochondrial Ca influx targets cardiolipin to disintegrate respiratory chain complex II for cell death induction. *Cell Death Differ* 2014 Jun 20.
14. Lemarie A, Huc L, Pazarentzos E, Mahul-Mellier AL, Grimm S. Specific disintegration of complex II succinate:ubiquinone oxidoreductase links pH changes to oxidative stress for apoptosis induction. *Cell Death Differ* 2011 Feb; **18**(2)**:** 338-349.
15. Hwang MS, Rohlena J, Dong LF, Neuzil J, Grimm S. Powerhouse down: Complex II dissociation in the respiratory chain. *Mitochondrion* 2014 Nov; **19 Pt A:** 20-28.
16. Dong LF, Jameson VJ, Tilly D, Cerny J, Mahdavian E, Marin-Hernandez A, *et al.* Mitochondrial targeting of vitamin E succinate enhances its pro-apoptotic and anti-cancer activity via mitochondrial complex II. *J Biol Chem* 2011 Feb 4; **286**(5)**:** 3717-3728.
17. Dong LF, Jameson VJ, Tilly D, Prochazka L, Rohlena J, Valis K, *et al.* Mitochondrial targeting of alpha-tocopheryl succinate enhances its pro-apoptotic efficacy: a new paradigm for effective cancer therapy. *Free Radic Biol Med* 2011 Jun 1; **50**(11)**:** 1546-1555.
18. Rohlena J, Dong LF, Kluckova K, Zobalova R, Goodwin J, Tilly D, *et al.* Mitochondrially targeted alpha-tocopheryl succinate is antiangiogenic: potential benefit against tumor angiogenesis but caution against wound healing. *Antioxid Redox Signal* 2011 Dec 15; **15**(12)**:** 2923-2935.
19. Rodriguez-Enriquez S, Hernandez-Esquivel L, Marin-Hernandez A, Dong LF, Akporiaye ET, Neuzil J, *et al.* Molecular mechanism for the selective impairment of cancer mitochondrial function by a mitochondrially targeted vitamin E analogue. *Biochim Biophys Acta* 2012 Sep; **1817**(9)**:** 1597-1607.
20. Neuzil J, Dong LF, Rohlena J, Truksa J, Ralph SJ. Classification of mitocans, anti-cancer drugs acting on mitochondria. *Mitochondrion* 2013 May; **13**(3)**:** 199-208.
21. Szeto SS, Reinke SN, Sykes BD, Lemire BD. Ubiquinone-binding site mutations in the Saccharomyces cerevisiae succinate dehydrogenase generate superoxide and lead to the accumulation of succinate. *J Biol Chem* 2007 Sep 14; **282**(37)**:** 27518-27526.
22. Tran QM, Rothery RA, Maklashina E, Cecchini G, Weiner JH. The quinone binding site in Escherichia coli succinate dehydrogenase is required for electron transfer to the heme b. *J Biol Chem* 2006 Oct 27; **281**(43)**:** 32310-32317.

23. Yang X, Yu L, He D, Yu CA. The Quinone-binding Site in Succinate-ubiquinone Reductase fromEscherichia coli: QUINONE-BINDING DOMAIN AND AMINO ACID RESIDUES INVOLVED IN QUINONE BINDING. *J Biol Chem* 1998 November 27, 1998; **273**(48)**:** 31916-31923.
24. Horsefield R, Yankovskaya V, Sexton G, Whittingham W, Shiomi K, Omura S, *et al.* Structural and computational analysis of the quinone-binding site of complex II (succinate-ubiquinone oxidoreductase): a mechanism of electron transfer and proton conduction during ubiquinone reduction. *J Biol Chem* 2006 Mar 17; **281**(11)**:** 7309-7316.
25. Oostveen FG, Au HC, Meijer PJ, Scheffler IE. A Chinese hamster mutant cell line with a defect in the integral membrane protein CII-3 of complex II of the mitochondrial electron transport chain. *J Biol Chem* 1995 Nov 3; **270**(44)**:** 26104-26108.
26. Pesta D, Gnaiger E. High-resolution respirometry: OXPHOS protocols for human cells and permeabilized fibers from small biopsies of human muscle. *Methods Mol Biol* 2012; **810:** 25-58.
27. Selak MA, Armour SM, MacKenzie ED, Boulahbel H, Watson DG, Mansfield KD, *et al.* Succinate links TCA cycle dysfunction to oncogenesis by inhibiting HIF-alpha prolyl hydroxylase. *Cancer Cell* 2005 Jan; **7**(1)**:** 77-85.
28. Yanamala N, Kapralov AA, Djukic M, Peterson J, Mao G, Klein-Seetharaman J, *et al.* Structural re-arrangement and peroxidase activation of cytochrome c by anionic analogues of vitamin E, tocopherol succinate and tocopherol phosphate. *J Biol Chem* 2014 Nov 21; **289**(47)**:** 32488-32498.
29. Rauchova H, Vokurkova M, Drahota Z. Inhibition of mitochondrial glycerol-3-phosphate dehydrogenase by alpha-tocopheryl succinate. *Int J Biochem Cell Biol* 2014 Aug; **53**(0)**:** 409-413.
30. Miyadera H, Shiomi K, Ui H, Yamaguchi Y, Masuma R, Tomoda H, *et al.* Atpenins, potent and specific inhibitors of mitochondrial complex II (succinate-ubiquinone oxidoreductase). *Proc Natl Acad Sci U S A* 2003 Jan 21; **100**(2)**:** 473-477.
31. Kearney EB, Ackrell BA, Mayr M. Tightly bound oxalacetate and the activation of succinate dehydrogenase. *Biochem Biophys Res Commun* 1972 Nov 15; **49**(4)**:** 1115-1121.
32. Muller FL, Liu Y, Abdul-Ghani MA, Lustgarten MS, Bhattacharya A, Jang YC, *et al.* High rates of superoxide production in skeletal-muscle mitochondria respiring on both complex I- and complex II-linked substrates. *Biochem J* 2008 Jan 15; **409**(2)**:** 491-499.
33. Lemarie A, Grimm S. Mitochondrial respiratory chain complexes: apoptosis sensors mutated in cancer? *Oncogene* 2011 Sep 22; **30**(38)**:** 3985-4003.
34. Ricci JE, Gottlieb RA, Green DR. Caspase-mediated loss of mitochondrial function and generation of reactive oxygen species during apoptosis. *J Cell Biol* 2003 Jan 6; **160**(1)**:** 65-75.
35. Kwong JQ, Henning MS, Starkov AA, Manfredi G. The mitochondrial respiratory chain is a modulator of apoptosis. *J Cell Biol* 2007 Dec 17; **179**(6)**:** 1163-1177.
36. Dong LF, Freeman R, Liu J, Zobalova R, Marin-Hernandez A, Stantic M, *et al.* Suppression of tumor growth in vivo by the mitocan alpha-tocopheryl succinate requires respiratory complex II. *Clin Cancer Res* 2009 Mar 1; **15**(5)**:** 1593-1600.
37. Dong LF, Low P, Dyason JC, Wang XF, Prochazka L, Witting PK, *et al.* Alpha-tocopheryl succinate induces apoptosis by targeting ubiquinone-binding sites in mitochondrial respiratory complex II. *Oncogene* 2008 Jul 17; **27**(31)**:** 4324-4335.
38. Drose S. Differential effects of complex II on mitochondrial ROS production and their relation to cardioprotective pre- and postconditioning. *Biochim Biophys Acta* 2013 May; **1827**(5)**:** 578-587.
39. Mbaya E, Oules B, Caspersen C, Tacine R, Massinet H, Pennuto M, *et al.* Calcium signalling-dependent mitochondrial dysfunction and bioenergetics regulation in respiratory chain Complex II deficiency. *Cell Death Differ* 2010 Dec; **17**(12)**:** 1855-1866.

40. Choi WS, Palmiter RD, Xia Z. Loss of mitochondrial complex I activity potentiates dopamine neuron death induced by microtubule dysfunction in a Parkinson's disease model. *J Cell Biol* 2011 Mar 7; **192**(5)**:** 873-882.
41. Ren Y, Feng J. Rotenone selectively kills serotonergic neurons through a microtubule-dependent mechanism. *J Neurochem* 2007 Oct; **103**(1)**:** 303-311.
42. Tzung SP, Kim KM, Basanez G, Giedt CD, Simon J, Zimmerberg J, *et al.* Antimycin A mimics a cell-death-inducing Bcl-2 homology domain 3. *Nat Cell Biol* 2001 Feb; **3**(2)**:** 183-191.
43. Shiau CW, Huang JW, Wang DS, Weng JR, Yang CC, Lin CH, *et al.* alpha-Tocopheryl succinate induces apoptosis in prostate cancer cells in part through inhibition of Bcl-xL/Bcl-2 function. *J Biol Chem* 2006 Apr 28; **281**(17)**:** 11819-11825.
44. Rohlena J, Dong LF, Ralph SJ, Neuzil J. Anticancer drugs targeting the mitochondrial electron transport chain. *Antioxid Redox Signal* 2011 Dec 15; **15**(12)**:** 2951-2974.
45. Mracek T, Jesina P, Krivakova P, Bolehovska R, Cervinkova Z, Drahota Z, *et al.* Time-course of hormonal induction of mitochondrial glycerophosphate dehydrogenase biogenesis in rat liver. *Biochim Biophys Acta* 2005 Nov 15; **1726**(2)**:** 217-223.
46. Schmitt S, Saathoff F, Meissner L, Schropp EM, Lichtmannegger J, Schulz S, *et al.* A semi-automated method for isolating functionally intact mitochondria from cultured cells and tissue biopsies. *Anal Biochem* 2013 Dec 1; **443**(1)**:** 66-74.
47. Wittig I, Karas M, Schagger H. High resolution clear native electrophoresis for in-gel functional assays and fluorescence studies of membrane protein complexes. *Mol Cell Proteomics* 2007 Jul; **6**(7)**:** 1215-1225.
48. Truksa J, Dong L, Rohlena J, Stursa J, Vondrusova M, Goodwin J, *et al.* Mitochondrially targeted vitamin E succinate modulates expression of mitochondrial DNA transcripts and mitochondrial biogenesis. *Antioxid Redox Signal* 2015 Jan 10.
49. Hroudova J, Fisar Z. In vitro inhibition of mitochondrial respiratory rate by antidepressants. *Toxicol Lett* 2012 Sep 18; **213**(3)**:** 345-352.
50. Zhou M, Diwu Z, Panchuk-Voloshina N, Haugland RP. A stable nonfluorescent derivative of resorufin for the fluorometric determination of trace hydrogen peroxide: applications in detecting the activity of phagocyte NADPH oxidase and other oxidases. *Anal Biochem* 1997 Nov 15; **253**(2)**:** 162-168.
51. Lortz S, Gurgul-Convey E, Naujok O, Lenzen S. Overexpression of the antioxidant enzyme catalase does not interfere with the glucose responsiveness of insulin-secreting INS-1E cells and rat islets. *Diabetologia* 2013 Apr; **56**(4)**:** 774-782.
52. Webb B, Sali A. Protein Structure Modeling with MODELLER. *Protein Structure Prediction, 3rd Edition* 2014; **1137:** 1-15.
53. Schymkowitz J, Borg J, Stricher F, Nys R, Rousseau F, Serrano L. The FoldX web server: an online force field. *Nucleic Acids Res* 2005 Jul 1; **33**(Web Server issue)**:** W382-388.
54. Hess B, Kutzner C, van der Spoel D, Lindahl E. GROMACS 4: Algorithms for highly efficient, load-balanced, and scalable molecular simulation. *Journal of Chemical Theory and Computation* 2008 Mar; **4**(3)**:** 435-447.
55. Eastman P, Friedrichs MS, Chodera JD, Radmer RJ, Bruns CM, Ku JP, *et al.* OpenMM 4: A Reusable, Extensible, Hardware Independent Library for High Performance Molecular Simulation. *J Chem Theory Comput* 2013 Jan 8; **9**(1)**:** 461-469.
56. Morris GM, Huey R, Lindstrom W, Sanner MF, Belew RK, Goodsell DS, *et al.* AutoDock4 and AutoDockTools4: Automated docking with selective receptor flexibility. *J Comput Chem* 2009 Dec; **30**(16)**:** 2785-2791.
57. Sanner MF. Python: a programming language for software integration and development. *J Mol Graph Model* 1999 Feb; **17**(1)**:** 57-61.

Figures

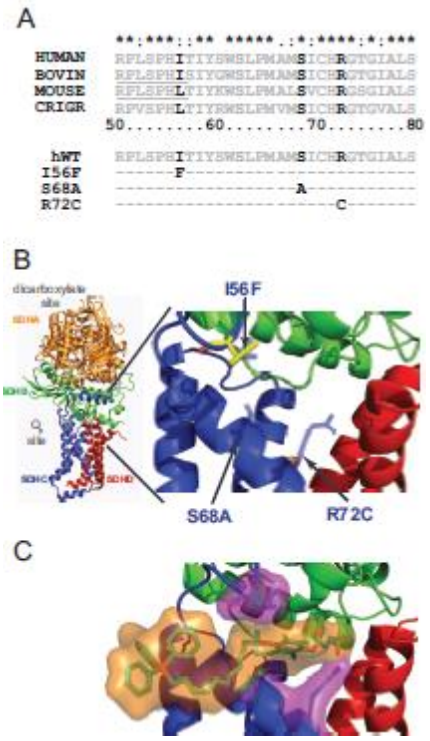

Figure 1. Amino acid substitutions in the Q_p site of CII. (a) Multiple species alignment of the SDHC region bordering the Q_p site shows a high level of conservation. Amino acid substitutions prepared for this study are indicated in human SDHC. (b) Three dimensional representation of CII and the topology of the Q_p site. SDHC residues mutated in this study are indicated by arrows. Displayed is the humanized crystal structure of porcine CII.[8] (c) A snapshot from molecular dynamics simulation of MitoVES interaction with the Q_p site of CII in the presence of phospholipid bilayer.[133] One of the possible conformations of MitoVES is shown in orange, substituted SDHC residues are depicted in magenta.

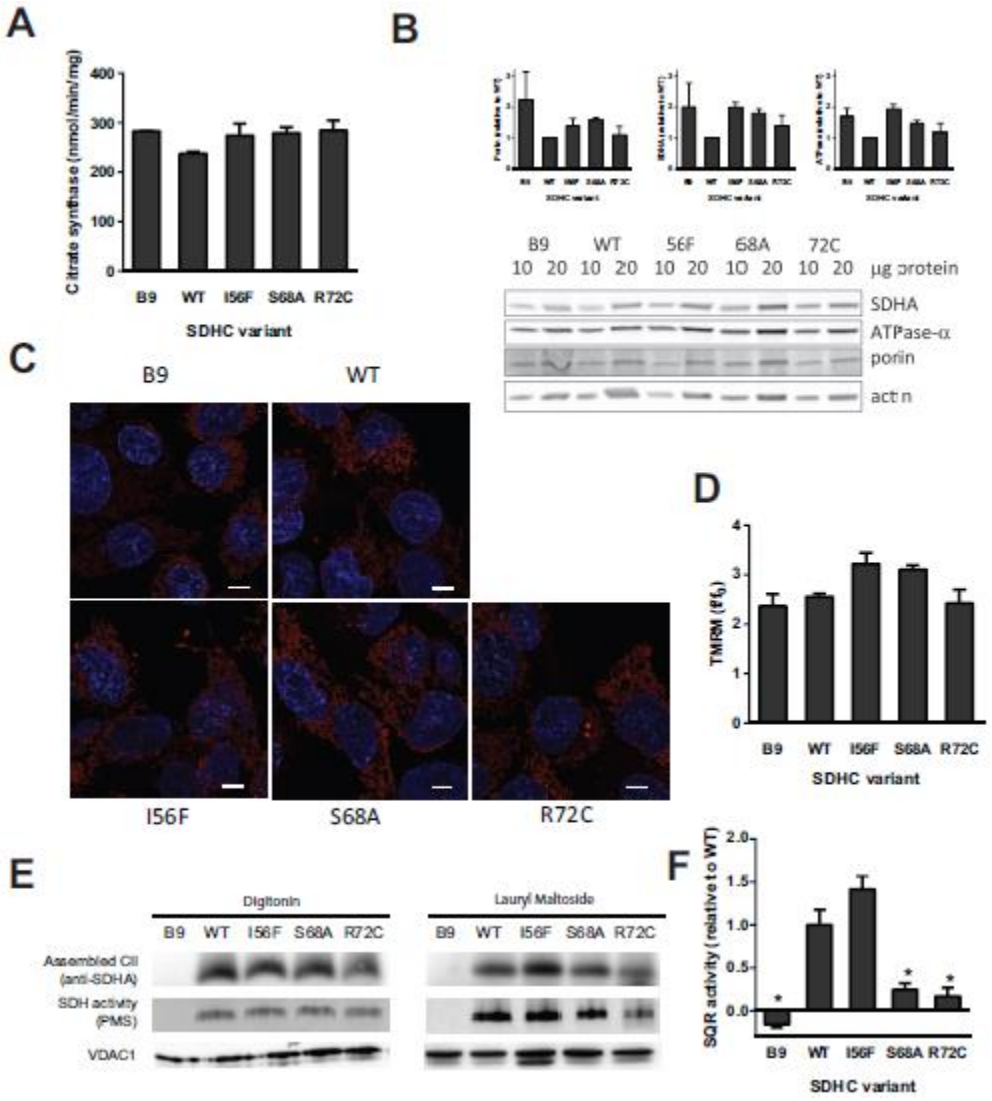

Figure 2. Q_p site substitutions do not decrease mitochondrial content, membrane potential or CII assembly, but can compromise CII activity in the presence of detergents. (a) Citrate synthase was measured in the whole cell lysates and corrected to protein content. (b) Selected mitochondrial proteins were analyzed by western blotting using 10 and 20 µg of whole cell protein. A representative blot is shown along with quantifications based on 3 independent experiments (c) Mitochondria were visualized by live confocal microscopy using TMRM, the nuclei were counterstained by Hoechst 33342. Scale bar, 5 µm. (d) Mitochondrial membrane potential was determined as a ratio of TMRM loading in the presence and absence of FCCP, n = 3, mean ± SEM. (e) Native blue gel electrophoresis of either digitonin- or lauryl maltoside-solubilized mitochondrial fraction isolated from CII variant cell lines. Assembled CII was detected by anti-SDHA antibody, or by in-gel SDH activity assay using phenazine methosulfate (PMS). Representative experiments are shown (f) SQR activity measurement in isolated mitochondrial fraction in the presence of 0.1% Triton-X100 indicates activity impairment for amino acid

substitutions in position S68 and R72. Data represent mean values ± SEM of 3 independent experiments. The symbol * indicates values significantly different from WT.

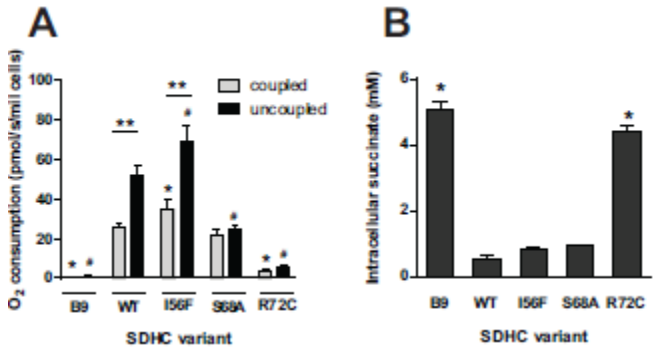

Figure 3. Substitutions in the Q_p site affect CII activity less severely in the native environment. (a) Oxygen consumption of digitonin-permeabilized cells respiring on 10 mM succinate in the presence of rotenone and ADP (coupled) and the maximal rate after addition of FCCP (uncoupled). While I56F and S68A variants support the respiration on succinate, B9 and R72C cells are deficient. The S68A defect is apparent only upon uncoupling. Mean ± SEM of 3-4 independent experiments. The symbol * indicates values significantly different from WT in the coupled state (oneway Anova), the symbol # values significantly different from WT in the uncoupled state (oneway Anova), and the symbol ** values significantly increased after FCCP addition (t-test). (b) Intracellular succinate measured by mass spectroscopy in extracts from an equal number of cells indicates functional CII in the WT, I56F and S68A. Mean ± SEM of 2 independent experiments, the symbol * indicates values significantly different from WT.

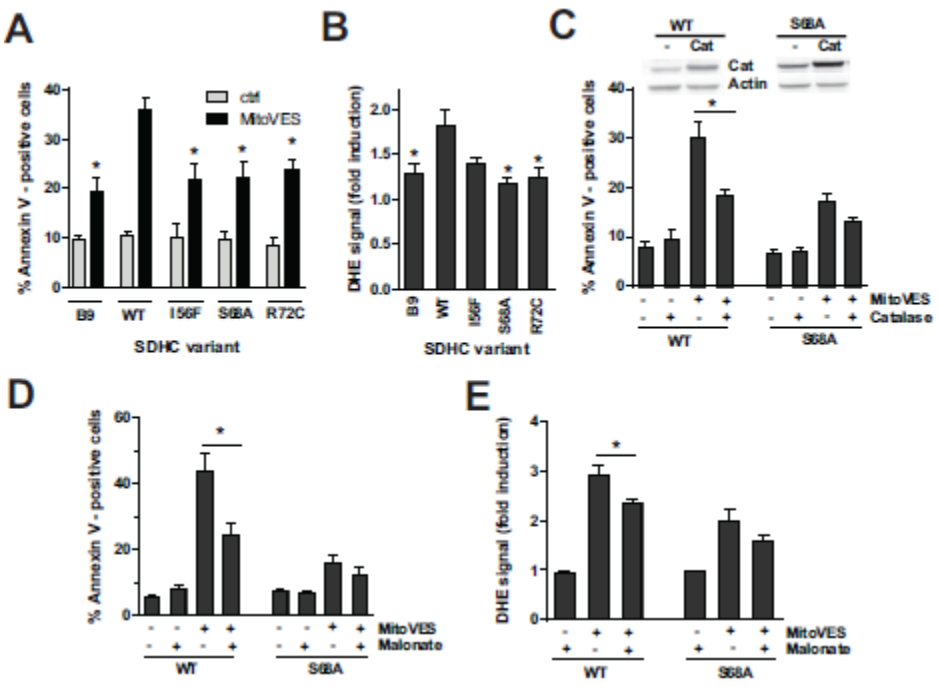

Figure 4. Q_p site substitutions lead to reduced cell death induction and ROS generation in response to MitoVES, and the induced cell death is dependent on CII-derived ROS. (a) Variant cell lines were exposed to 20 µM MitoVES for 24 h and the percentage of annexin V-positive cells was determined by flow cytometry. n ≥ 5, mean ± SEM, * values significantly different from WT. (b) Variant cell lines were exposed to 2 µM MitoVES for 30 minutes and the level of ROS was determined by DHE staining and flow cytometry. n ≥ 5, mean ± SEM, * values significantly different from WT. (c) Cells were transfected with catalase-coding or control vector, exposed to 20 µM MitoVES for 20 h, and the percentage of annexin V-positive cells was determined by flow cytometry. n ≥ 4, mean ± SEM, * values significantly different between catalase and mock-transfected cells. Inset, catalase overexpression verified by western blot. (d) Cells were exposed to 30 µM MitoVES for 12 h in the presence or absence of 20 mM malonate (30 min pre-treatment). The percentage of annexin V-positive cells was determined by flow cytometry. n ≥ 3, mean ± SEM, * values significantly different in the presence and absence of malonate. (e) Cells were exposed to 5 µM MitoVES for 30 min in the presence or absence of 50 mM malonate (30 min pre-treatment) and the level of ROS was determined by DHE staining and flow cytometry. n = 5, mean ± SEM, * values significantly different in the presence and absence of malonate.

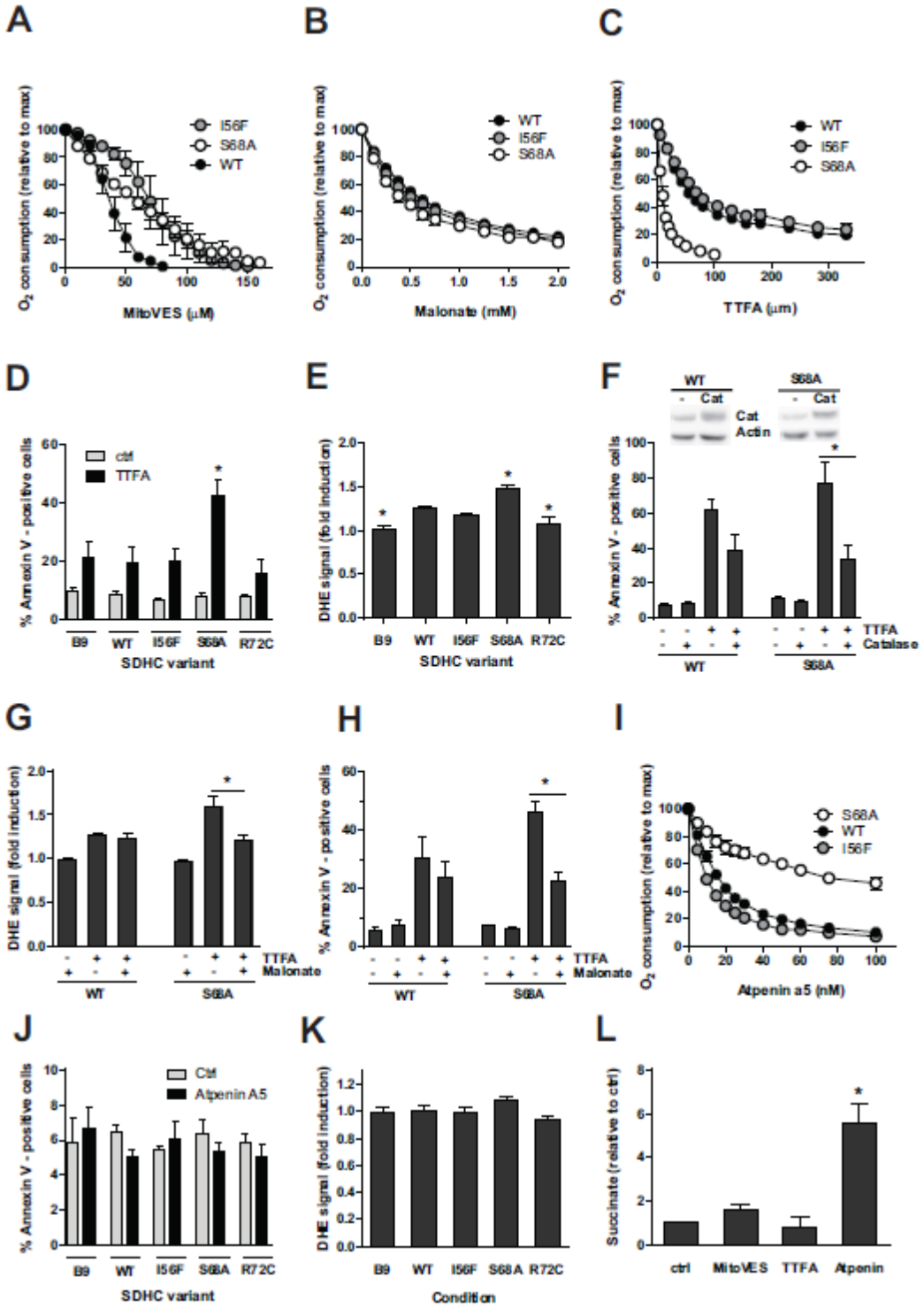

Figure 5. Suppression of CII-driven respiration correlates with cell death for Q_p site inhibitors that do not rapidly increase succinate level. (a) Digitonin-permeabilized respiration-competent variant cell lines respiring on 10mM succinate in the presence of 0.5 μM rotenone and FCCP were exposed to increasing

concentrations of MitoVES. The variants show reduced inhibition compared to WT. (b) Inhibition by the dicarboxylate binding site inhibitor malonate in the same experimental setup shows similar efficiency for all Q_p site substitutions. (c) Similar to a and b, but the Q_p site inhibitor TTFA was used. (a-c) The data represent the mean ± SEM of 3-4 independent experiments. (d) Variant cell lines were exposed to 0.5 mM TTFA for 24 h and the percentage of annexin V-positive cells was determined by flow cytometry. n = 5, mean ± SEM, * values significantly different from WT. (e) Cells were exposed to 250 µM TTFA for 30 min and the level of ROS was determined by DHE staining and flow cytometry. n = 5, mean ± SEM, * values significantly different from WT. (f) Cells were transfected with catalase-coding or control vector, exposed to 2 mM TTFA for 20 h, and the percentage of annexin V-positive cells was determined by flow cytometry. n = 4, mean ± SEM, * values significantly different between catalase and mock-transfected cells. Inset, catalase overexpression verified by western blot. (g) Cells were exposed to 250 µM TTFA for 30 min in the presence or absence of 50 mM malonate (30 min pre-treatment), and the level of ROS was determined by DHE staining and flow cytometry. n = 4, mean ± SEM, * values significantly different in the presence and absence of malonate. (h) Cells were exposed to 1.5 mM TTFA for 12 h in the presence or absence of 20 mM malonate (30 min pre-treatment). The percentage of annexin V-positive cells was determined by flow cytometry. n = 4, mean ± SEM , * values significantly different in the presence and absence of malonate. (i) Atpenin A5-induced inhibition of respiration of permeabilized cells as described in panel a. n ≥ 3, mean ± SEM. (j) Cells were exposed to 1 µM Atpenin A5 for 24 h and the percentage of annexin V-positive cells was determined by flow cytometry. n = 3, mean ± SEM. (k) Cells were exposed to 0.5 µM Atpenin A5 for 30 min and the level of ROS was determined by DHE staining and flow cytometry. n = 5, mean ± SEM. (l) Succinate levels were determined in WT cells exposed to 20 µM MitoVES, 1 mM TTFA or 1 µM Atpenin A5 for 30 minutes. n = 3, mean ± SEM, * values significantly different from control.

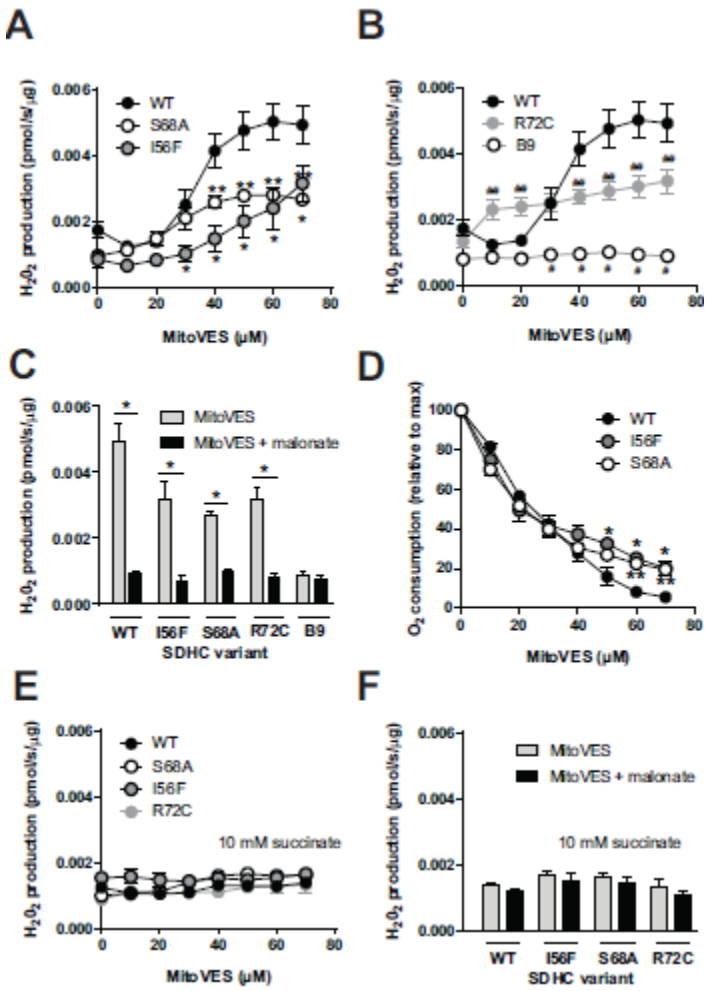

Figure 6. ROS induction by MitoVES correlates with CII inhibition in isolated mitochondria at low succinate. (a-b) Mitochondria isolated from variant cells respiring on 500 µM succinate in an oxygraph chamber were exposed to increasing concentrations of MitoVES, and ROS production was followed in real time in the presence of Amplex Ultra Red and peroxidase. (a) shows reduced ROS production for I56F and S68A variants compared to WT, (b) shows the same for R72C and B9 cells. The same WT data are used in a-b, the panels are separated for clarity only. (c) Under the same conditions, 5 mM malonate inhibits ROS generation by 70 µM MitoVES in all cell lines except for B9 cells. (d) Respiratory data extracted from the experiments shown in panel a reveal that the respiration of WT cells is inhibited by MitoVES most efficiently. (e) ROS were measured as in a-b, but at 10 mM succinate. No increase in ROS generation was detected. (f) At 10 mM succinate there is no effect of 5 mM malonate on ROS at 70 µM MitoVES. Data represent the mean ± SEM of 3-5 independent experiments. Significant differences from WT: * I56F, ** S68A, # B9, ## R72C. Panel c: * denotes a significant decrease after the addition of malonate.

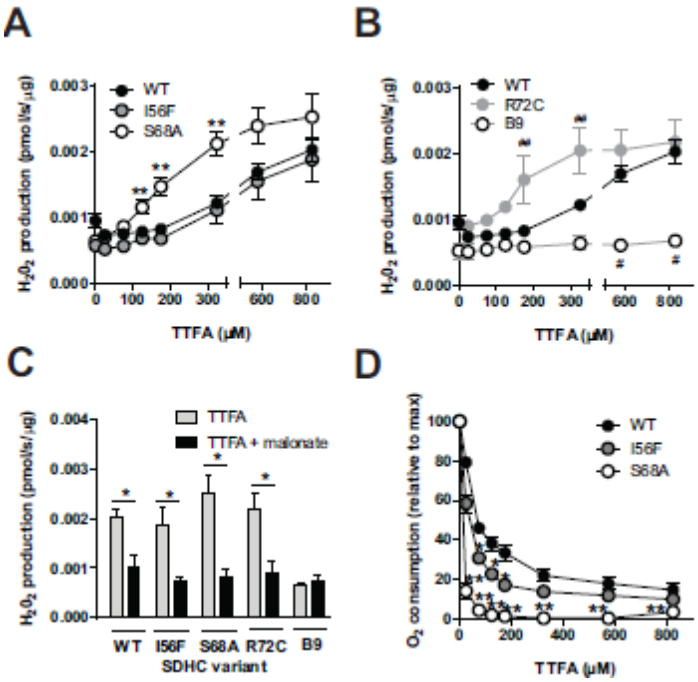

Figure 7. ROS induction by TTFA also correlates with CII inhibition in isolated mitochondria at low succinate. (a-b) Mitochondria isolated from variant cells respiring on 500 µM succinate in an oxygraph chamber were exposed to increasing concentrations of TTFA, and ROS production was followed in real time in the presence of Amplex Ultra Red and peroxidase. (a) shows increased ROS production for S68A variant compared to WT, (b) shows the higher ROS for R72C and no ROS for B9 cells. The same WT data are used in a-b, the panels are separated for clarity only. (c) Under the same conditions, 5 mM malonate inhibits ROS generation by 825 µM TTFA in all cell lines except for B9 cells. (d) Respiratory data extracted from the experiments shown in panel a reveal that the respiration of S68A cells is inhibited by TTFA most efficiently. Data represent mean ± SEM of 4-5 independent experiments. Significant differences from WT: * I56F, ** S68A, # B9, ## R72C. Panel c: * denotes a significant decrease after the addition of malonate.

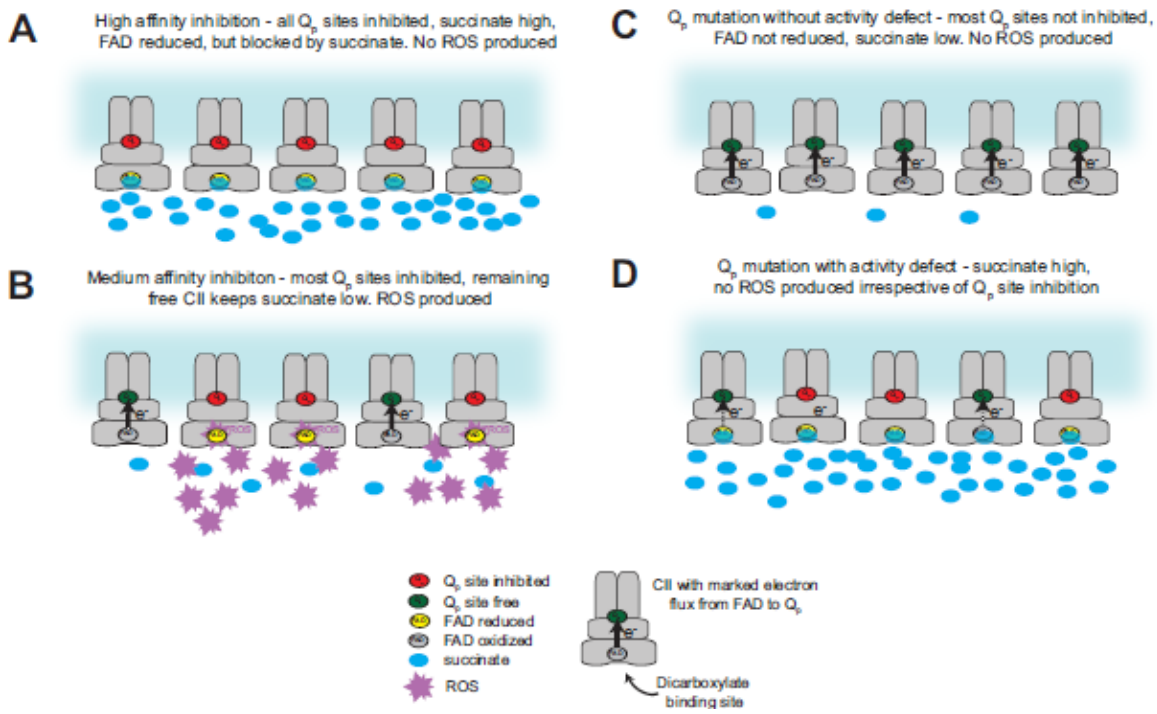

Figure 8. A proposed model of cell death initiation at CII explaining the regulation of ROS production from reduced FAD group in intact cells. (a) High affinity Q_p site inhibitors, such as Atpenin A5, will immediately block most of the available Q_p sites in a cell and rapidly upregulate intracellular succinate. CII will be inhibited and FAD reduced, but no ROS will be produced, because succinate in the dicarboxylate site will block oxygen access. (b) Medium affinity inhibition such as with MitoVES or TTFA will not immediately block all available Q_p sites, and some free CII will be left to keep succinate levels from rising rapidly. Because of the free dicarboxylate site, the reduced FAD in Q_p-inhibited CII molecules will be able to produce cell death-inducing ROS. (c) Mutation in the Q_p site that do not affect CII activity will lower the ability of an inhibitor such as MitoVES to displace ubiquinone, and despite low intracellular succinate FAD will not be reduced and therefore unable to produce ROS. (d) Q_p site mutations that affect CII activity will upregulate succinate, blocking dicarboxylate site and preventing ROS generation from FAD. Additional Q_p site inhibition will not generate ROS under these conditions.

Contribution of Katarína Kľučková to individual publications

Mitochondrial targeting of vitamin E succinate enhances its pro-apoptotic and anti-cancer activity via mitochondrial complex II. J Biol Chem. 2011

Flow cytometry experiments for apoptosis detection in Jurkat cells exposed to α-TOS/MitoVES and analogous experiments including uncoupler FCCP.

Mitochondrial targeting of α-tocopheryl succinate enhances its pro-apoptotic efficacy: A new paradigm for effective cancer therapy. Free Radic Biol Med. 2011

Preparation of Jurakt cells silenced for *BAK* and subsequent flow cytometry for apoptosis after MitoVES exposure in the established cell line deficient in Bak and parental cells as well as $Bax^{-/-}/Bak^{-/-}$ Jurkat cells.

Mitochondrially targeted α-tocopheryl succinate is antiangiogenic: Potential benefit against tumor angiogenesis but caution against wound healing. Antioxid Redox Signal. 2011

Flow cytometry for apoptosis in cells exposed to MitoVES/α-TOS with or without the uncoupler FCCP and relative determination of $\Delta\Psi$. Isolation of mitochondria and subsequent BNE.

Mitochondrial targeting overcomes ABCA1-dependent resistance of lung carcinoma to α-tocopheryl succinate. Apoptosis. 2013

Respiratory measurements with parental and α-TOS resistant H1299 cells.

Mitochondrially Targeted Vitamin E Succinate Modulates Expression of Mitochondrial DNA Transcripts and Mitochondrial Biogenesis. Antioxid Redox Signal. 2015

Isolation of mitochondria and subsequent BNE and CII SQR activity determination in the parental B9 cells and mutant cell lines derived from them.

Evaluation of respiration of mitochondria in cancer cells exposed to mitochondria-targeted agents. Methods Mol Biol. 2015

Respirometry experiments with permeabilised cells and partially with nonpermeabilised cells.

Ubiquinone-binding site mutagenesis reveals the role of mitochondrial complex II in cell death initiation. Cell Death Dis. 2015

All experiments except: assessement of CS activity, mass spectrometry, computer modelling, site-directed mutagenesis and some SDS-PAGE experiments. Confocal microscopy only partly.